OPTIMIZING GREEN ROOF DESIGN PARAMETERS AND THEIR EFFECTS ON THERMAL PERFORMANCE UNDER CURRENT AND FUTURE CLIMATES IN THE CITY OF TORONTO

BITA YOUSEFI PIHANI

A THESIS SUBMITTED TO
THE FACULTY OF GRADUATE STUDIES
IN PARTIAL FULFILLMENT OF THE REQUIREMENTS
FOR THE DEGREE OF
MASTER OF SCIENCE

GRADUATE PROGRAMME IN CIVIL ENGINEERING
YORK UNIVERSITY
TORONTO, ONTARIO

AUGUST 2021

ABSTRACT

Buildings contribute 30% of total energy consumption worldwide and account for 28% of CO2 emissions. Green roofs (GRs) have shown potential in reducing cooling and heating loads of buildings, and thus, the related carbon emissions. This research aimed to analyse the thermal performance of extensive GRs compared to conventional roofs using three design parameters: GR growing media (GM) depth, Leaf Area Index (LAI) and thermal insulation thickness under current and future climates in Toronto, Canada. EnergyPlus was used to model the GR for three building archetypes of secondary school, office, and hospital. In addition, precipitation data for current and future climates was generated to account for GR moisture input. Results show higher GM depth, and LAI provides the highest annual energy savings for uninsulated GRs. However, at highly insulated roofs, the GR thermal performance is impacted and depending on the building type, the GR may require higher energy consumption.

ACKNOWLEDGEMENTS

Throughout the writing of this dissertation, I have received a great deal of support and assistance.

I would first like to thank my supervisors, Dr. Usman Khan and Dr. Magdalena Krol whose expertise's were invaluable in formulating the research questions and methodology. Your insightful feedback pushed me to improve my thinking and brought my work to a higher level.

I would also like to thank my colleagues for their help and guidance throughout my studies. You provided me with the support I needed to choose the right direction and successfully complete my dissertation.

In addition, I would like to thank my parents for their wise counsel and sympathetic ear. You are always there for me. Finally, I could not have completed this dissertation without the support of my brother Ali, my sister Kimia and my two best friends Rahma and Donia, who provided stimulating discussions as well as happy distractions to rest my mind outside of my research, love you all.

TABLE OF CONTENTS

LIST OF TABLES

LIST OF FIGURES

LIST OF ABBREVIATIONS

C_e^g - bulk transfer coefficient for latent heat near ground
C_h^g - bulk transfer coefficient for sensible heat
C_f - bulk transfer coefficient
$c_{p,a}$- specific heat of air at constant pressure (J/kg K)
H_f - foliage sensible heat flux (W/m^2)
H_g - ground sensible heat flux (W/m^2)
$I_{ir}^{\downarrow}$ - total incoming long-wave radiation (W/m^2)
$I_s^{\downarrow}$ - total incoming short-wave radiation (W/m^2)
L_f - foliage latent heat flux (W/m^2)
L_g - ground latent heat flux (W/m^2)
LAI - Leaf Area Index
l_f - latent heat of vaporization at foliage temperature (J/kg)
l_g - latent heat of vaporization at ground surface temperature (J/kg)
q_{af} - mixing ratio of air at foliage interface
$q_{f,sat}$ - saturated foliage mixing ratio
q_g - mixing ratio of air at ground surfacer
$r^{"}$ - foliage surface wetness
T_{af} - air temperature in foliage (K)
T_f - foliage temperature (K)
α_f - albedo (short-wave reflectivity) of the canopy
T_g - ground surface temperature (K)
W_{af} - wind speed at air-foliage interface (m/s)
z - height or depth (m
α_g - albedo (short-wave reflectivity) of ground surface
ε_f - emissivity of canopy
α_g - emissivity of the ground surface
$\varepsilon_g{+}\varepsilon_f = \varepsilon_g\varepsilon_f$
ρ_{af} - air density in foliage near atmosphere-foliage inter-face (kg/m^3)_
ρ_{ag} - air density near foliage-ground interface (kg/m^3)_
σ - Stefan-Boltzmann constant (W m−2K^{-4})
σ_f - fractional vegetation coverage
κ - soil thermal conductivity of the surface (W/m K)
GM - Growing Media
CON - Conventional Roof

Chapter One: Introduction

This chapter provides an overview to the thesis and identifies the key points of this research. The role of global energy demand and the impact of climate change on the building sector is explained. Green roofs as a sustainable solution in mitigating the impact of climate and reducing building energy consumption is described. Lastly, a list of research objectives and the thesis layout is presented.

1.1 Building and Energy Demand

Based on the International Energy Agency (IEA), the global primary energy (unconverted original fuels) demand grew by 2.3% in 2018, which was the largest increase since 2010 (IEA 2019). Fossil fuels account for 70% of the growth in global primary energy demand with gas, oil and coal comprising 46%, 15%, and 9% respectively (IEA 2019). Burning of coal generates steam that is used to turn turbines and generate electricity. Natural gas is another fossil fuel used in heating systems after being processed. Both fossil fuels are the main source of carbon dioxide (CO_2) production which is considered the primary source of greenhouse gas emission (GHG) (Hemed et al. 2020). The recent increase in global energy demand, mainly due to the high proportion of fossil fuels in the energy mix, has led to an increase in GHG emissions reaching a historic high of over 33 billion tons of carbon dioxide (IEA 2017). The final energy demand has also increased by 2.2%, and of this increase, the strongest growth was due to gas, and electricity consumption driven mainly by its use in the buildings and industry sector (United Nations Environment Programme 2019).

According to the 2019 Report on Global Status for Building and Construction, buildings and construction sector accounted for the largest share of both global final energy use (36%) and energy-related CO_2 emissions (39%) in 2018. This indicates the primary target for the reduction of GHGs emissions should be the building and construction sectors. In 2020, it was reported that building heating and cooling was mainly provided by electricity, natural gas, and traditional biomass, however, the use of electricity to heat buildings has increased in recent years leading to further increase CO_2 emissions (United Nations Environment Programme. 2019). Buildings'

energy consumption is based on energy used for space heating, space cooling, water heating, lighting, cooking, and appliances. Due to technological improvements, there has been a reduction in the overall energy intensity (increase in energy efficiency) for most of these applications however, space cooling energy intensity has increased because of higher cooling demand in hot regions (United Nations Environment Programme. 2019).

Factors influencing increase in global energy demand include change in population, floor area, climate variation, building construction and energy service demand like household appliances and cooling equipment. Nonetheless, improvements in building envelope, building performance and the components have helped in neutralizing the demand in energy growth. Although, as floor areas have been expanding at a higher rate in hot regions, cooling space demand is increasing. Up to present day, space heating, water heating, and cooking continues to be a major end use energy demand in buildings; however, the fastest growing end use energy demand is space cooling and appliances (United Nations Environment Programme. 2019). Therefore, it is important to invest and consider improving design strategies for all building energy usage components to limit the increase in total energy demand.

Climate Change and Impact on Building Energy Usage

The world temperature has been rising since the Industrial Revolution. Based on an ongoing temperature analysis, the Earth's average global temperature has increased about 0.8 ℃ since 1880 (Al-Ghussain 2019). The increase in Earth temperature is due to the amount of trapped heat in the Earth's atmosphere because of GHG emissions. The global temperature depends on how much energy the planet is receiving from the sun and how much energy is radiated back into space; usually, there is little change in these heat exchange quantities. However, the amount of energy radiated by Earth significantly depends on the chemical composition of the atmosphere, which has changed due to the heat-trapping capability of GHGs (Al-Ghussain 2019). Based on the yearly temperature anomalies from 1880 to 2019 recorded by NASA (National Aeronautics and Space Administration), NOAA (National Oceanic and Atmospheric Administration), Japan Meteorological Agency and the Met Office Hadley Centre in United Kingdom, it is concluded that rapid warming has occurred in the past few decades, with the highest warming occurring in the

last decade (Al-Ghussain 2019). Therefore, mitigation of climate change is necessary to limit the effects of GHGs emissions on global warming.

Since the building and construction sector account for most of the global energy consumption and CO_2 emission, it should be the primary target for the reduction of GHGs emissions. Energy-efficient building systems and envelopes continue to limit energy use growth in both residential and non-residential buildings, however, continued effort is needed to reduce energy intensity and account for the impact of climate change (United Nations Environment Programme 2019). The change in global temperature patterns is causing an increase in the cooling demand of buildings and this trend will continue to increase in future years (Wilde and Coley 2012). Therefore, building energy system design plays an important role in the amount of GHG emissions in future years (Robert and Kummert 2012). Climate change driving forces such as changes in temperature, precipitation, humidity, solar irradiation, and wind condition, affects the environmental conditions and leads to change in frequency, severity and geography of weather events (Wilde and Coley 2012). Environmental effects then impact building performance and its occupants. The building envelope, components, and performance would be significantly affected by climate change and the resulting shifts in weather patterns. Eventually, if buildings are not designed to be efficient under the future climate, they may experience reduced performance, structural failure and potentially pose risks to human health (Wilde and Coley 2012). Therefore, the use of any new building elements that incorporate sustainable and environmentally responsive energy-efficient technologies to reduce building energy consumption needs to be analysed by accounting the impacts caused by climate change.

1.2 Green Roofs: A Method to Manage Building Energy Demand

Among various eco-technologies, energy-efficient systems, and renewable energy sources, green roofs are considered a valuable strategy for making buildings more sustainable (Berardi et al. 2014; la Roche and Berardi 2014). Green roofs offer many benefits. The most cited benefit of green roofs is reduction of stormwater runoff (Czemiel Berndtsson 2010). Studies have shown green roofs can reduce stormwater runoff by more than 50% (Mentens et al. 2006). Recently, green roofs have also been found to decrease building energy use. Green roofs have the potential to alter the heat

flux through the roof, thereby affecting the building heating and cooling loads. Additional benefits include urban island effect mitigation and ecology preservation.

The origin of green roofs goes back to the fifth century Babylon, where they were used as structures called hanging gardens (Berardi et al. 2014). Other ancient empires such as Mesopotamia and Roman used roof gardens in their Villas for improving aesthetic value and roof life. Modern uptake of green roofs started in the 1970s in German-speaking countries and gained more popularity in France and Switzerland around the same time. In the last fifteen years, the installation of green roofs has increased significantly. Based on a recent survey by the German Professional Green Roof Association (FBB), there has been approximately 8 million m^2 of new green roofs installed every year in Germany (Berardi et al. 2014). In other European countries, such as the United Kingdom and Austria, the installation of green roofs is also becoming widespread. The City of Toronto implemented a bylaw that requires green roofs to be installed on new buildings with flat roofs and areas over 2,000 m^2 (City of Toronto 2012) and since the new policy, the city's total green roof area has reached approximately 232,000 m^2 between the years of 2010 and 2015 (Berardi et al. 2014). In recent years, Japan has indicated that green roofs are a prime technology in decreasing the urban heat island (UHI) effect and promoting more sustainability to buildings (Berardi et al. 2014).

Modern green roofs are constructed on the outer layer of the building's roof area and typically consist of four construction layers: a protection layer directly above the roof to alleviate moisture and includes waterproof membranes and root barriers; filter and drainage layer to release excess moisture out of the green roof; and the growing media layers (the soil layer) and the vegetation area (Figure 1-1).

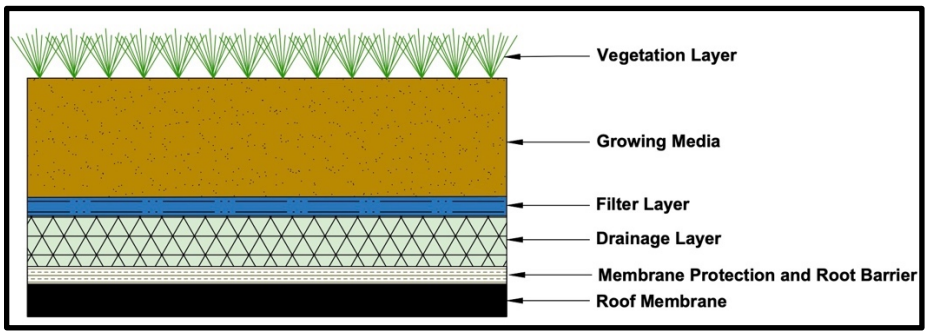

Figure 1-1: Green roof structural components.

Green roofs have been shown to be effective for reducing stormwater runoff and to augment green spaces in urbanized areas (Berardi, GhaffarianHoseini, and GhaffarianHoseini 2014), but their energy-related performance stands to be the most adopted benefit worldwide (D'Orazio, di Perna, and di Giuseppe 2012; Eksi et al. 2017; Squier and Davidson 2016; Tang and Qu 2016). Green roofs can absorb solar heat, shade building components, and reduce roof surface temperature fluctuations, making them extremely suitable for improving the thermal performance of buildings (MacIvor et al. 2016). However, all benefits offered by green roof are extremely climate-dependent (Cascone et al. 2018), therefore it is important to evaluate thermal performance of green roof specific to the climate they have been installed in.

1.3 Research Objectives and Layout

Green roofs have shown potential in reducing the cooling and heating loads of buildings globally. Given the implementation of the City of Toronto's new green roof bylaw, an investigation on their impact in decreasing building energy consumption and optimizing green roof design is important.

Moreover, due to green roofs performance being climate-dependent, the thermal energy performance will be impacted due to the rise in global temperature and shift in weather patterns in future climate. Therefore, assessing green roof performance under both current and future climate is crucial.

In general, there are two types of green roofs: extensive (shallow layer of growing media) and intensive (deeper layer of growing media). This research aims to investigate the thermal energy performance of extensive green roofs on building energy consumption, in the City of Toronto, under both current and future climate conditions. In the first part of this research, the green roof

thermal performance of a specific building type, secondary school, will be evaluated based on three design parameters: growing media depth, leaf area index (LAI) and added thermal insulation thickness. The growing media layer and the LAI have shown in past studies to be the most effective green roof design parameters in reducing the total cooling and heating loads (Zeng et al. 2017; Sailor et al. 2012; Gomes et al. 2019; Vera et al. 2015; Mahmoodzadeh et al. 2020). The added thermal insulation layer thickness is also investigated in combination with the green roof design parameters due to the insulation layer being a requirement in the green roof structure in the City of Toronto. A sensitivity analysis is performed to determine the impact of selected design parameters on green roof thermal performance. Lastly, an optimal green roof design based on three variables of growing media depth, LAI and thermal insulation thickness is suggested. This is done using EnergyPlus, a building energy modelling software. In the second part, the green roof thermal impact on other building types is evaluated, under current and future climate, to determine whether the green roof energy performance behaves similarly for buildings with different characteristics. Lastly, the water retention performance of the green roof is evaluated for all three archetypes to display other green roof benefits.

Thesis Objectives

1. Evaluate green roof thermal performance for a secondary school building, under current and future conditions, through three design parameters: growing media depth of 100 mm, 150 mm, and 200 mm; LAI of 1, 2 and 3; and the thermal insulation thickness of 50 mm, 80 mm, 100 mm, 120 mm, 150 mm, 200 mm, 250 mm and 300 mm. Suggest an optimal green roof design based on the three variables of growing media depth, LAI and thermal insulation thickness.

2. Evaluate the green roof thermal performance under current and future climate on two other archetype buildings: office and hospital building. Measure the impact of growing media depth of 100 mm, 150 mm and 200 mm; LAI of 1, 2 and 3; and thermal insulation thickness of low (50 mm), medium (120 mm), and high (300 mm) on green roof energy performance. Determine optimal green roof design for the two building types. Compare the green roof

thermal performance and optimal designs for buildings of office and hospital to the secondary school.

3. Evaluate the green roof runoff reduction on three building types of secondary school, office, and hospital under current and future climate to showcase other green roof benefits.

Thesis Layout

Chapter One focuses on the introduction and background knowledge regarding the research. This chapter provides information regarding building and their energy consumption globally. The impact and role of building on GHGs and the cause of climate change are also discussed. Green roofs are introduced as a potential solution in building energy savings. Lastly, the thesis goal, objectives and layout are presented.

Chapter Two discusses the green roof design, types, components, and benefits. This chapter also presents an overview of green roof modelling and building simulation tools used to evaluate the energy saving impacts of green roofs. Additionally, weather climate data and approaches on generating future hourly weather files for building simulation tools are explained. This chapter also covers the research gaps and objectives.

Chapter Three describes the methodology and approach used to accomplish the goals and objectives of the research. This chapter covers information regarding EnergyPlus software, the Ecoroof model and archetypes used. Type of current climate data used, the method chosen to generate future climate data, and precipitation data for both current and future climate is explained.

Chapter Four discusses the results and analysis of green roof thermal performance on a secondary school building under current and future climate. In this chapter, the impact of LAI, growing media depth and insulation thickness on green roof thermal performance are explained. Seasonal analysis of the green roof energy consumption compared to the conventional roof are presented. The annual energy savings of the green roof and the Dynamic Benefit of Green Roof (DBGR) of each green roof design are reported, and the green roof benefits compared to the conventional roof are explained.

Chapter Five analyses the impact of green roof thermal performance on office and hospital buildings under current and future climate. The annual energy consumption, energy savings and seasonal energy analysis of green roof designs compared to the conventional roof are discussed. In this chapter, the DBGR of each green roof design is also presented. Lastly, the chapter presents the results for the retention performance of the green roof for all building archetypes.

Chapter Six summarizes the conclusions of the research and recommendations for future works.

Chapter Two: Literature Review

Chapter two focuses on providing information regarding literature studies on green roofs and describing their types, benefits, and design components. Additionally, this chapter explains the area of study in modelling green roofs using building simulation tools and different methods to generate the weather data files necessary to model green roofs.

2.1 Introduction to Green Roofs: Types, Benefits and Components

2.1.1 Classification and Types

In general, green roofs can be classified into two main groups: extensive and intensive, however, some use semi-intensive classification as well (Berardi et al. 2014). Intensive green roofs have a deeper growing media depth, usually ranging between 20 - 200 cm, compared to the extensive green roof where a thinner growing media layer of 5 - 20 cm is used (Cascone et al. 2018). Intensive green roofs also require more care, maintenance, and irrigation; therefore, they have higher construction costs (Cascone et al. 2018). Intensive and extensive roofs are also classified based on the type of vegetation used; since the survival of plants highly depends on the depth of the growing media layer used (Montressor et al. 2005). In extensive green roofs, the most common plants used are sedums, since they do not require a thick growing media layer for growth and can survive without the use of irrigation (Montressor et al. 2005). On the other hand, intensive green roofs can grow plants with deeper roots therefore there is a higher variety of plants that can be used and depending on the depth of the growing media layer, even shrubs and small trees can be planted on intensive roofs (Cascone et al. 2018). Usually, the installation of intensive green roofs highly depends on the building's bearing structural load, since their weight will add at least 300 kg/m^2 to the building structure (Berardi et al. 2014). In addition, intensive green roofs, due to their deeper growing media depth, have a higher potential in improving insulation, enhancing stormwater management, and energy performances of buildings, however the type of vegetation used plays an important role (Cascone et al. 2018). In Table 2-1, the classification of green roofs has been summarized.

Table 2-1: Green Roof Classification

Green Roof Type	Extensive Green Roof	Intensive Green Roof
Depth	5 – 20 cm	20 – 200 cm
Vegetation	Low diversity (sedum, herbs, grass)	High diversity (shrubs, trees)
Irrigation	Mainly not required; optional	Required
Accessibility	Inaccessible to public	Accessible to public; used for recreation purposes
Weight	60 – 150 kg/m2	Above 300 kg/m2
Maintenance	Low	High
Installation	Easy	Complex
Cost	Low	High

2.1.2 Benefits

The primary focus of this research is the energy performance of green roofs and their effect on reducing the energy consumption of buildings. However, green roofs offer other benefits such as reduction of stormwater runoff, reduction of Urban heat Island (UHI) effect and ecological preservation due to the greenery area they provide. These benefits are summarized below.

Green Roof Reduction on Energy Consumption

The main goal of green roofs in urbanized cities is the thermal benefit they offer, which is considered of great importance to local municipal authorities (Ghaffarianhoseini et al. 2013). Green roofs have been proven to be highly efficient in decreasing indoor temperature, heat flux through and out of the roof, surface roof temperature fluctuations, and the overall energy consumption of buildings in various climates (Maiolo et al. 2020; D'Orazio et al. 2012; Mahmoodzadeh et al. 2020). Many parameters affect thermal green roof performance. The green roof design variables such as growing media (composition and thickness), vegetation type, and irrigation all affect the energy performance of green roofs (Maiolo et al. 2020; Bevilacqua et al. 2016). As mentioned previously, the performance of the green roof is extremely climate dependent hence most design variables vary based on the climate zones the green roof is located in. For this reason, the implementation of the green roof has created an obstacle for policymakers and designers. Building characteristics such as the building type (e.g. office, school, hotel, supermarket or an apartment), building size, and the material used in the building such as type of insulation, all

affect the green roof thermal performance and building energy consumption (Karachaliou et al. 2016). In older buildings, due to poor insulation the impact of green roofs is proven to be higher in reducing building total energy consumption compared to newer improved insulated buildings, where the contribution of the green roof in energy reduction has been much lower; however, these conclusions are highly climate-dependent (Mahmoodzadeh et al. 2020; Berardi 2016). One way of understanding the green roof contribution to the reduction of energy consumption of buildings is through the building heating and cooling loads. The building heating load is the amount of heat energy needed to be added to the indoor environment to maintain a suitable temperature. The cooling load is the amount of heat energy needed to be removed from the indoor environment, or cool the space, to maintain a suitable temperature. The suggested thermostat heating setpoint in winter and cooling setpoint in the summer according to the United States Environmental Protection Agency (EPA) is 21 °C and 25.5 °C, respectively (Maiolo et al. 2020). Other than the reduction in heating and cooling loads, there have been studies where the thermal performance of the green roof is evaluated through roof surface temperature and roof heat flux (Maiolo et al. 2020; D'Orazio et al. 2012; He et al. 2020). Green roofs have shown to reduce surface roof temperature and daily temperature fluctuations in all types of climates (D'Orazio et al. 2012). Additionally, the insulation provided by the green roof reduces heat transfer and improves the indoor temperature. Therefore, both heat flux and roof surface temperature have been considered as a valuable strategy for measuring the thermal performance of green roofs (Maiolo et al. 2020).

Stormwater Reduction

The second most important environmental benefit of the green roof next to the reduction in energy consumption of buildings is the reduction of stormwater runoff (Cascone et al. 2018; Mentens et al. 2006). Studies have emphasized that green roofs' reduction of runoff depends on the water availability in green roofs design, its roof plants, and the plant types in climates with low water availability (Czemiel Berndtsson 2010). The roof slopes have also been an affecting factor in reducing and retaining runoff water; retention values decrease as slope increases (Getter et al. 2007a). Runoff mitigation of green roofs, for extensive green roofs could reduce the runoff water up to 60% and for intensive green roofs up to 100% (Berardi et al. 2014); however, results may vary depending on climate, roof structure, and plant type. In another study, three different roof

surfaces, a standard commercial roof with gravel ballast, an extensive green roof system without vegetation, and a typical extensive green roof with vegetation, were used to quantify the differences in stormwater retention. Overall, the results showed the mean percentage rainfall retention was between 48.7% for gravel and 82.8% for the vegetated roof (VanWoert et al. 2005). Talebi et al. (2019) investigated the retention performance of a green roof through modelling in six Canadian climates. Results showed a reduction of runoff varies from 17% to 50% depending on climate for low water use plants. Both Toronto and London had the highest volume in water retention performance for low water use plants. Sensitivity analysis showed vegetation type had a more significant impact on reducing runoff than an increase in growing media storage capacity in all climates (Talebi et al. 2019). The impact of climate on four Canadian cities on water retention performance of green roofs in Sims et al. (2016) showed antecedent moisture condition (AMC) had the largest impact for medium-sized storms. Optimizing the AMC through growing media design by changing field capacity, plant type, and higher stormwater retention could be achieved (Sims et al. 2016). A study by Zhang et al. (2019) found species with higher evapotranspiration (ET) not only result in replenishing storage between rainfall events more effectively, but they can also reduce maximum growing media storage capacity due to the creation of preferential flow caused by their rooting system. The preferential flow is the fast transport of water and other compounds in a small portion of the pore system. This finding suggested that plant selection first needs to be based on their effect on growing media storage capacity since plants with high ET can reduce the storage capacity and reduce water retention performance. Therefore, green roofs are valuable designs in reducing stormwater runoff.

Urban Heat Island (UHI) Mitigation

Increase in urbanization, especially in developed countries, has caused many negative environmental impacts, including the urban heat island effect (UHI). In urbanized environments, due to higher human activity, the heat generated in the atmosphere is greater; therefore, the temperature in these environments is typically higher than in non-urbanized areas. Green roofs could contribute to solving the problem of rising urbanized temperatures through the cooling effect they provide. The albedo of green roofs is much higher (0.7 to 0.85) than the albedo of conventional roofs such as bitumen, tar, and gravel roofs, ranging from 0.1 to 0.2 (Berardi et al.

2014). Past studies show green roofs reduce the ambient temperature from 0.3 to 3 ℃, and they have been considered effective technologies in reducing the UHI effect (Santamouris 2014). Additionally, in a comparison study between cool roofs and green roofs, it was concluded, the green roof had a higher cooling effect during the daytime, while the cooling effect of the cool roof was better at nighttime (He et al. 2020). Berardi et al. (2014) findings concluded the highest impact of green roofs in reducing the UHI effect is in dry and hot climate conditions by 1.5 to 2 ℃ on average.

Ecological preservation

Green roofs can increase biodiversity and habitat wildlife. The greenery environment provided by the green roof enhances the quality of the environment and ecological preservation. The green roof plays an essential role in urban ecology; however, measuring these benefits is challenging. Many studies show that green roofs help reduce the loss of habitat in urbanized areas (Shafique et al. 2018; Francis and Lorimer 2011). In addition, green roofs promote wildlife habitat by the greenery area they provide and promote recreational activities in urban environments. In one study, the life-cycle analysis on the environmental benefit of green roofs compared the emissions produced through green roof material manufacturing processes such as polymers against the capacity of the pollution removal of the green roof such as NO_2, SO_2, and PM_{10}. In the long term, the study concluded that green roofs are sustainable products to use since the air pollution produced by the polymer process can be balanced by green roofs in 13 years (Berardi et al. 2014).

2.1.3 Climate Dependency

Green roofs generally impact the building energy demand through two mechanisms. The first mechanism is the change of heat flow through the roof, also called the direct effect. The second mechanism is altering the surrounding air temperature that is assumed to be entrained into the building and providing fresh air for occupants, called the indirect effect (Virk et al. 2015). These green roof mechanics are affected in three ways: first, the growing media layer acts as an insulation layer; second, the plant canopy shades the roof surface; third, the evapotranspiration process has a cooling effect (Eksi et al. 2017). Evapotranspiration is evaporation from the growing media layer and the transpiration from the vegetation area (Sailor 2008). The evapotranspiration effect cools

down the air temperature around the building and provides a lower surface temperature at roof level. The thermal mechanism of the green roof is climate-dependent since the magnitude of its influence is affected by weather variables such as solar radiation, ambient air temperature, precipitation, snow cover and thus growing media moisture (Eksi et al. 2017).

Both experimental and numerical studies have evaluated the effect of green roofs on the energy consumption of buildings in different climates. Generally, the impact of green roofs in warm climates is significant on cooling loads; however, their reduction in heating loads has been marginal (la Roche and Berardi 2014). In subtropical regions, intense rainfall levels and high temperatures create a great potential for extensive roofs (Simmons et al. 2008). An experimental study in Greece found that an extensive green roof reduced the cooling loads between 2% to 48% depending on the green roof covered area (Ghaffarianhoseini et al. 2013). Another study in a Mediterranean coastal climate showed that due to the increase in green roof vegetation density, the cooling load reduction was 60% compared to a conventional roof (Olivieri et al. 2013). The energy performance of a conventional roof with an extensive green roof in Italy showed the green roof reduced 100% of heat flux entering the roof in the summer, while only 30% to 37% of heat loss was prevented in winter (Bevilacqua et al. 2016). Another experimental study on green roof thermal performance in a Mediterranean climate located at Calabria University concluded the benefit of green roofs in the summer is much higher than winter when compared to a conventional roof (Maiolo et al. 2020). Green roofs with no insulation layer showed better overall thermal performance than added insulation layers in Mediterranean climates (Maiolo et al. 2020). The effect of the green roof on the reduction of heating and cooling load in three different European climates of hot, temperate, and cold was investigated through modelling by Jaffal et al. (2012). The cooling reduction loads were impacted significantly in the hot and temperate climates of Athens and La Rochelle, respectively. In Stockholm, a cold climate, the reduction in cooling loads was negligible. However, the insulation effect of green roof growing media caused a decrease of 8% in heating loads during the winter for Stockholm. Overall, green roofs in all three different climates decreased the total building energy demand (Jaffal et al. 2012). In one study in the Midwestern U.S. with hot and humid summers and cold and snowy winters, the impact of the green roof on surface temperature and heat flux was significantly higher in summer compared to winter

(Getter et al. 2011b). Another experimental study in Toronto, Canada, showed the reduction of heat flow through the roof was more in summer (70% - 90%) and less in winter (10% - 30%); however, the use of extra insulation significant impact in lowering heat flow through the roof in winter (Liu and Minor 2005). Hence, the thermal performance of green roofs varies on cooling and heating reduction depending on the climate.

Most research studies evaluate green roof influence on building energy performance based on the green roof design variables and climate (Mahmoodzadeh et al. 2020; Eksi et al. 2017; MacIvor et al. 2016; Sailor et al. 2012). The most common green roof design parameters considered in research studies are the vegetation characteristics such as leaf area index (LAI), plant height, stomatal resistance, leaf albedo, and emissivity; and growing media characteristics such as growing media thickness, thermal properties, and moisture content (Mahmoodzadeh et al. 2020). Eksi et al. (2017) evaluated the thermal properties of an extensive green roof, through experiment, based on the effect of growing media depth and vegetation type (sedum compared to herbaceous perennials and grasses) in Michigan. Based on the result, the herbaceous roof, compared to the sedum, experienced more heat entering the building during the summer and less heat escaping the building during the winter. Therefore, during the winter months, the herbaceous roof would reduce heating costs, while in the summer, it increased cooling costs. Thus, the study concluded that results go against conventional logic that plants with high transpiration rates are superior. During the summer months, the sedum roof outperformed the herbaceous roof due to the herbaceous roof displaying more heat flux entering the building (Eksi et al. 2017). Another experimental study in Toronto, Canada, evaluated the impact of plants and growing media type using irrigation on extensive green roof surface temperature (MacIvor et al. 2016). Two types of plants, sedum and meadow mix of wildflowers, were used. Sedum roof cooled the roof significantly more than meadow vegetation due to the sedum capability of storing a significant amount of water. The irrigated meadow mix of wildflowers performed as well as unirrigated sedum vegetation. Findings concluded that the sedum promoted improving green roof cooling due to constant, near 100% vegetative cover; however, additional benefits might come from combining sedum and other suitable wildflowers and grasses to improve green roof functions (MacIvor et al. 2016).

In one study, green roof thermal performance was analysed through modelling using EnergyPlus software, based on different LAI and growing media thickness in four U.S. cities. Results showed that in colder cities, a thicker growing media layer impacts the reduction in heating loads. While increase in LAI reduces the cooling load for warm cities through a combination of evapotranspiration and shading effect (Sailor et al. 2012). Vera et al. (2015) used EnergyPlus to evaluate the effect of irrigation, growing media density, plant height and LAI of a green roof on the cooling and heating load in Santiago of Chile. Based on the results, change in plant height was negligible in affecting the building cooling and heating loads with various growing media densities and LAI. An increase in the amount of irrigation showed an increase in the reduction of cooling loads for heavy growing media due to higher moisture content and higher thermal conductivity; however, it also generated higher heating loads. As for the influence of LAI, higher LAI decreased the cooling loads and increased the heating loads; however, the increase in heating loads was less significant than the reduction in cooling loads. The study also concluded LAI is the most important parameter in reducing the energy consumption of supermarket buildings in semiarid climates (Vera et al. 2015).

Gomes et al. (2019) used EnergyPlus to evaluate the effect of growing media density, LAI, plant height, growing media depth, and irrigation on the energy performance of green roofs in Portugal. Results showed that irrigation was more effective in reducing the cooling loads than heating loads since the use of irrigation increased the building heating consumption. The heating loads reduced as the growing media depth increased due to higher thermal resistance. The cooling loads are reduced by increasing LAI and plant height due to higher evapotranspiration and shading effects. Sensitivity analysis performed assessed the influence of each parameter, growing media depth, plant height, and LAI on the cooling and heating loads' magnitude. The growing media depth had the highest impact on energy variation, followed by LAI and plant height. The findings concluded that irrigation is more important in reducing the cooling loads than the volume of water irrigated since the use of irrigation with a flow rate of 3 mm/day was more effective than the use of 6 mm/day (Gomes et al. 2019). In Sailor (2008), the variation of growing media thickness, LAI, and use of irrigation on the thermal performance of green roofs in two cities of Chicago and Houston were analysed through modelling using EnergyPlus. The results suggested the growing media

thickness layer has the highest effect due to its insulation, and higher thickness would decrease heating and cooling loads.

The effect on reduction of heating loads was more in cold climates. Increasing LAI reduced the cooling loads in summer; however, the heating loads increased due to the shading effect. An increase in irrigation was effective in the summer and reduced cooling loads; however, it was most effective in less humid climates (Sailor 2008). Another study in Toronto, Canada, used EnergyPlus to investigate the benefits of green roof retrofits on a university campus. An extensive green roof was modelled by considering LAI and growing media depth as design parameters. Results indicated an increase in growing media depth caused an increase in energy savings in the winter. In contrast, green roofs with higher LAI and growing media thickness in the summer resulted in higher energy savings. Based on the parametric analysis, increasing the growing media depth is more effective than increasing the LAI in green roof energy savings performance (Berardi 2016).

Ascione et al. (2013) used EnergyPlus to analyse the thermal performance of the green roof against a cool roof and conventional roof in six European climates of Tenerife, Sevilla, Rome, Amsterdam, London, and Oslo. The study considered influencing parameters such as rainfall intensity, different types of vegetation (different plants, height, and LAI), and irrigation needs on an office building. Results showed in warm climates such as Tenerife, Sevilla, and Rome using cool roofs was better in the energy reduction of the building than the green roof in the summer. However, during winter, the green roof with the most vegetated area (highest LAI and plant height) had the lowest heating demand. Results concluded that due to the lower heating degree days of warm climates, a cool roof is the better choice than a green roof since the annual energy consumption of a cool roof is lower. On the other hand, for cold climates such as Amsterdam, London and Oslo use green roofs to reduce the annual energy demand compared to cool and conventional roofs due to higher heating degree days for these climates. The study also concluded that if enough precipitation is not available in warm climates, there is a need for irrigation for green roofs to perform well (Ascione et al. 2013). He et al. (2020) evaluated the thermal performance of five green roofs designed with a different combination of growing media depth and vegetation compared to a cool roof and a conventional roof in Shanghai through modelling. Simulation results showed that a green roof could reduce the cooling and heating loads of the top floor by 3.6% and 6.2%, respectively. The

cool roof could reduce the cooling load by 3.6% and increase the heating load by 10.4%. The parametric analysis showed LAI is most effective in summer due to the reduction of cooling loads than in winter since an increase in LAI would increase the heating loads due to higher evapotranspiration and shading effect. The effect of growing media depth is more in the winter as it acts as an insulator; the analysis showed as the growing media depth passes 10 cm, the decrease in cooling loads becomes negligible. An increase in the insulation layer reduced the heating loads in winter but increased cooling loads in summer. The overall use of both cool roofs and green roofs was much more effective in reducing the energy consumption of buildings (He et al. 2020).

The thermal performance of green roofs on buildings with a high level of thermal transmittance, meaning added insulation layer with the green roof, is also studied (D'Orazio et al. 2012; Maiolo et al. 2020). D'Orazio et al. (2012) compared the thermal performance of insulated green roofs in summer and winter periods under temperate climates with various strongly insulated conventional roofs. Results showed the green roof heat loss and the delay of roof heat flux rate during summer are higher than a conventional roof. Additionally, in winter, green roofs provided the insulation needed and reduced the heat loss through the roof (D'Orazio et al. 2012). Maiolo et al. (2020) analysed the thermal impact of insulated and non-insulated green roofs in summer and winter in southern Italy climate. Results showed that green roofs without insulation have a higher difference in temperature compared to the insulated green roof, indicating green roofs without insulation performed better in summer seasons. On the other hand, in winter the green roof with insulation showed a higher difference in temperature (difference with referenced roof) compared with a green roof without insulation. Overall, the study concluded in Mediterranean climates, no use of insulation improves green roof performance in summer, and this effect prevails despite the negative effects on heating loads in winter (Maiolo et al. 2020).

Various studies under different climate conditions concluded that the growing media depth and LAI have the most impact on decreasing building overall energy consumption. However, based on design parameters, the reduction of green roofs on heating and cooling loads may vary depending on the climate conditions. Studies have also shown that in warmer climates cooling load reduction is higher compared to heating. On the other hand, in cold climates, green roofs are more effective in reducing heating loads. Some research studies also concluded that green roofs increase heating

loads during summer and limit the overall energy benefits. Furthermore, few studies on the impact of added insulation layer on green roof thermal performance have shown that the reduction of heating and cooling loads by insulated green roofs is significantly dependent on the climate. Hence, findings by other research studies highlight the importance of green roof design parameters and their thermal performance dependency based on climate conditions.

2.1.4 Design Components

The main design parameters that the thermal performance of the green roof is affected by are the growing media and vegetation layer. The characteristics of the parameters of each layer affect the thermal performance of the green roof differently, and therefore understanding the effect of each parameter helps to evaluate the green functioning better.

Vegetated Area

LAI and Fractional Vegetative cover

The LAI represents the type of vegetation density used, or in other terms, it's a representation of the plan-form area coverage of the leaves (Sailor 2008). The LAI is the ratio of one-sided leaf area per unit ground area (1 m^2). LAI is unitless due to being ratio of areas. For example, a canopy with LAI of 1 have a 1:1 ratio of leaf area to ground area; meaning both the leaf area and ground area have area of 1 m^2. A canopy with LAI of 4 would have a 4:1 ratio of leaf area to ground area. The fractional coverage describes the fraction of the roof surface directly covered by at least one leaf. LAI is different from fractional vegetation cover; LAI is the dimensionless ratio of the projected leaf area for a unit ground area. The fractional vegetative cover is the ratio of the shaded ground surface to the total ground surface area. The fractional vegetated cover is the governing parameter in radiative characteristics of growing media. It is related to LAI however; it displays and refers to a different concept. Usually, the larger the LAI, the higher the shading provided by the plants and less of the roof area is exposed to solar radiation, as a result, the roof surface temperature decreases. Other than the shading effect, LAI has a major impact on the evapotranspiration rate. An increase in LAI would increase the evapotranspiration rate as it has a proportional inverse relation to the stomatal resistance of plants (Sailor 2008). Based on various studies, higher LAI has a significant

impact on reducing cooling loads in all climates during summer (Mahmoodzadeh et al. 2020; Sailor 2008; Ascione et al. 2013).

Stomatal Resistance

Stomatal resistance is a biophysical parameter that describes the rate at which the plant can transpire moisture through its leaf stomata (the intercellular openings between epidermal cells on the leaf surfaces) for a given environmental condition. In other words, the diffusion of water vapor from these epidermal cells on the leaf into the atmosphere is called stomatal resistance. The actual stomatal resistance (r_s) at any time is proportional to minimum stomatal resistance ($r_{s,min}$) and inversely proportional to LAI (Equation 1) (Sailor 2008).

$$r_s = \frac{r_{s,min}}{LAI} f_1 f_2 f_3 \qquad \text{Equation 1}$$

The stomatal resistance is modified by fractional multiply factors, $f_1 f_2 f_3$, that depend on incoming solar radiation and atmospheric moisture (Sailor 2008). Other than LAI being an effective factor in the evapotranspiration rate, there are other parameters such as plant height, solar radiation, wind speed, ambient air temperature, relative humidity and growing media moisture that affect the evapotranspiration rate (Mahmoodzadeh et al. 2020).

Plant Height

The plant height like LAI affects the shading of the roof surface and the evapotranspiration rate. In some studies, for short plants, the growing media area on the roof surface is exposed to greater solar radiation than taller plants, therefore, the higher solar radiation increase the growing media temperature and cancels the cooling impact caused by the evapotranspiration (Zeng et al. 2017). The use of taller plants impact the thermal performance of green roofs and reduce the cooling loads (Mahmoodzadeh et al. 2020; Gomes et al. 2019; Ascione et al. 2013; Vera et al. 2015). An increase in plant height causes the wind velocity within the canopy to increase, which leads to higher evapotranspiration; this effect is strongly related to the aerodynamic resistance (Sailor 2008). There are thick boundary layers formed on the leaf surface where air close to the leaf surface has marginal movement, this area is called aerodynamic resistance; it's the resistance to moisture exchange on the leaf surface. When water vapor leaves the stomata, it transfers through this

motionless boundary layer to reach the atmosphere, therefore, the thicker the boundary layer, the slower the transpiration rate. Aerodynamic resistance, measured in units of (s/m) is influenced by wind speed, surface roughness and stability of the atmosphere (MacIvor et al. 2016). The aerodynamic resistance of plants is inversely proportional to wind velocity, meaning the lower the wind velocity, the higher the aerodynamic resistance and thicker the boundary. The combined effect of aerodynamic resistance (r_a) and stomatal resistance (r_s) to vapor diffusion is called surface wetness factor ($r^{"}$) and its the ratio of aerodynamic resistance to total resistance (Equation 2).

$$r^{"} = \frac{r_a}{r_a + r_s} \qquad \text{Equation 2}$$

In tall plants, the aerodynamic resistance is small due to the higher wind velocity effect. When the aerodynamic resistance is small, the wetness factor approaches zero leaving the leaf surface dry as the moisture readily evaporates. However, as the aerodynamic resistance increases relative to stomatal resistance, the wetness factor approaches 1, indicating the moisture readily travels to the leaf surface, and it's not easily evaporated (Sailor 2008). Therefore, an increase in plant height would reduce the aerodynamic resistance, decrease the wetness factor of the leaf surface and allow moisture to evaporate readily, hence a higher rate of evapotranspiration. Therefore, after LAI, plant height has the highest impact on decreasing cooling loads and increasing both LAI and plant height would increase the thermal performance of green roofs in summer (Mahmoodzadeh et al. 2020; Ascione et al. 2013).

Plant Albedo

The albedo is the reflectivity of the leaf surface to the solar energy incident on the surface that is received (Sailor 2008). The lower the plant albedo, the higher the plant surface temperature since more incident solar radiation is absorbed by the plant's surface. He et al. (2020) analysis on green roof optical property showed a green roof with an albedo of 0.13 would reflect 13% of incident global solar radiation and absorb 56%, which indicated the estimated solar radiation entering the roof to be 31% (the green roof had LAI of 4). Higher plant albedo prevents heat from penetrating the roof surface; however, higher plant albedo means higher plant surface temperature. The plant surface temperature affects the energy balance on green roofs; if plant surface temperature is high

(lower albedo), the ambient air temperature increases, reducing the green roof's mitigation effects (Mahmoodzadeh et al. 2020). The plant surface temperature depends on the amount of solar radiation, thermal radiation adsorption, convective heat transfer with ambient air, and the latent heat of the transpiration process. Mahmoodzadeh et al. (2020) found low albedo increases both the plant surface and growing media temperature due to higher solar adsorption. The high plant surface temperature led to a higher evapotranspiration rate; however, this created a tradeoff system and did not affect the energy performance of the green roof. The higher rate of evapotranspiration and its cooling effect is cancelled out by the increase in growing media temperature (Mahmoodzadeh et al. 2020).

Growing Media

Growing media has the highest impact on the green roof, higher than LAI and plant height, in decreasing the energy consumption during summer and winter. Based on several studies, an increase in growing media depth would reduce the heat flux into or out of the building (Sailor 2008; Liu and Minor 2005; Gomes et al. 2019; Berardi 2016; Eksi et al. 2017). Solar radiation heats the growing media faster when the depth is shallower. However, one study concluded the use of a growing media with a depth of 7.5 cm or 15 cm had no impact on lowering the net heat loss (Lundholm et al. 2014). Various reasons could affect the capability of growing media depth in the reduction of heat flux, such as growing media composition, compact, and the climate condition the green roof is exposed to. Ouldboukhitine et al. (2012) concluded growing media with heat-expanded slate had two to three times higher thermal conductivity than growing media with a silica-based aggregate. In many other studies, such as Sailor and Hagos (2011) and Pianella et al. (2016), both have found differences between the growing media composition. The growing media characteristics such as density, specific heat, thermal conductivity, particle size distribution, and thermal diffusivity affect the heat transfer in the growing media (Mahmoodzadeh et al. 2020; Eksi et al. 2017; Sailor 2008). Generally, as density increases, the growing media's thermal conductivity and heat flux increase (Castleton et al. 2010a). Additionally, the air pockets in the growing media increase the ability to act as an insulator (Saadatian et al. 2013). When the moisture content of growing media increases, the density and thermal conductivity also increases (Ouldboukhitine et al. 2012). The increase in moisture content would fill the pores with water and

increase the specific heat capacity of growing media (the storage heat capacity of water is higher than air) (Mahmoodzadeh et al. 2020). An increase in moisture content also reduces the albedo of growing media due to the surface wetness and causes higher absorption of solar radiation. Thermal diffusivity is another factor that is affected by an increase in the moisture content of the growing media. The ability of materials to conduct the energy relative to their thermal capacity is called thermal diffusivity, and it plays an important role in the heat transfer of growing media. Therefore, all the thermal properties are affected when the moisture content of growing media increases (Mahmoodzadeh et al. 2020).

The thermal conductivity and thermal diffusivity of growing media affect the thermal performance of the green roof differently in terms of the reduction of heat flow in or out of the roof. During winter, the thermal conductivity becomes of great importance since the higher the conductivity of growing media, the higher the heat flux out of the roof surface and more heat is lost through the roof. On the other hand, the thermal diffusivity of growing media plays a key role in the summer due to the temperature oscillations occurring, which are higher than in winter. As mentioned before, thermal diffusivity is the ability of growing media material conducting energy and due to the higher temperature difference between day and night in the summer, the thermal diffusivity has a higher effect on heat transfer than thermal conductivity (Mahmoodzadeh et al. 2020). The thermal performance of the green roof was studied in Mahmoodzadeh et al. (2020) based on different growing media compositions of light and heavy and water content. The light-weight growing media had higher specific heat capacity, lower thermal conductivity, and lower thermal diffusivity than the heavy-weight growing media. The thermal performance of the green roof was higher in terms of reduction of cooling loads in summer due to the higher thermal conductivity of the heavy-weight growing media. However, the lower thermal diffusivity of the light-weight growing media caused the green roof to perform better (Mahmoodzadeh et al. 2020). The study also found that in light-weight growing media, as the moisture content increased, the thermal diffusivity remained almost unchanged, whereas, in heavy-weight growing media, the thermal diffusivity increased as moisture content increased. Therefore, even at the highest moisture content level (100%), the light-weight growing media performed better than heavy-weight growing media. On the other hand, in winter, thermal conductivity impacted the energy performance of the green

roof the most. The thermal conductivity of heavy-weight growing media was twice as light-weight at higher moisture content levels, which led to higher heating loads as more heat was lost through the roof (Mahmoodzadeh et al. 2020). Hence thermal conductivity plays a major role during winter and thermal diffusivity plays a key role during summer. However, the study mentioned the use of growing media characteristics such as density, thermal heat capacity, and thermal conductivity, depends on the climate the green roof is exposed. In cold dominant cities where the heating degree days are higher, the thermal conductivity characteristic of growing media plays a more important role, and the choice of light-weight growing media with lower thermal conductivity would be ideal. On the other hand, in warm climates, the effect of light-weight or heavy-weight growing media on the overall performance (accounting for both heating and cooling loads) of the green roof would be minimal (Mahmoodzadeh et al. 2020). Therefore, it is concluded designing green roof parameters specific to the climate they are installed in is extremely crucial as the thermal performance of green roofs varies in different climate conditions.

2.1.5 Energy Balance

In general, the energy balance system of the green roof is driven by the radiative heat being forced from by the sun. The solar radiation is balanced by the sensible heat (convection heat which is the heat required to change temperature; no change in phase) and by the latent heat flux (the heat required to convert vapour or liquid, without the temperature change) from the growing media and vegetated (Sailor 2008). It's combined with the conduction heat of the growing media and long-wave radiation (radiation gets emitted back to the atmosphere) to and from the growing media and vegetated layer (Sailor 2008). As mentioned before, green roof performance is climate-dependent; however, based on various studies on the thermal performance of green roofs in different regions around the world, the phenomena occurring in the green roof have been summarized in three main principles. First, the growing media is the inertial mass with high heat thermal capacity where it provides a high lag time effect and reduces the dynamic thermal transmittance. Second, the shading effect of the foliage provokes the convection heat transfer as well as the absorption of the thermal energy through the process of photosynthesis. Lastly, the growing media and the vegetative layer cause the evaporative and evapotranspiration cooling effect (Berardi and Jafarpur 2020).

Green roofs have the capability of reflecting the solar radiation and absorb the radiation through the photosynthesis process. An increase in depth of the growing medium and the use of lighter colours would also reduce heat flow and increase the thermal energy performance of the green roof (He et al. 2020). Studies have also shown the thermal performance of the green roof is affected by the thermal resistance layer beneath the green roof, such as insulated roofs. If the green roof is built upon a well-insulated roof, the energy balance would be decoupled from that of the building and have more impact on the urban environment than energy performance. On the other hand, the green roof installed on a poorly insulated roof could maximize the potential benefit of green roofs on thermal energy influences (D'Orazio et al., 2012). For these reasons, understanding the heat fluxes in the green roof is important.

The heat flux is a key process in the heat transfer of green roofs. In a green roof energy balance system, there is the radiative exchange of shortwave and long-wave radiations, the convective thermal flow of the vegetation area, the evapotranspiration through the growing media and the vegetation layer, and the heat transfer through the ground with accounting for the change in growing media thermo-physical properties and moisture content. More on the energy balance system of green roof is explained in section 3.1.

2.2 Green Roof Modelling Using Building Simulation Tools

Simulation tools are needed to help design and evaluate green roofs' potential thermal performance. The thermal behaviour of the green roof needs to be modelled through the study of several interacting phenomena like heat and mass transfer, as well as plant physiology. The main mechanisms of heat and mass transfer in green roofs are based on how vegetation and growing media counterbalance the incident solar radiation on the roof by means of evapotranspiration and shading. These phenomena are based on the canopy and growing media parameters: (1) the plant height; (2) LAI, (3) stomatal resistance for water vapour transport; (4) growing media hygrothermal properties; and (5) growing media thickness (Vera et al. 2015) There have been several studies where field measurements have been used to employ mathematical models on predicting energy performance of green roofs (Kumar and Kaushik 2005; Takakura et al. 2001; Sailor 2008; Jaffal et al. 2012). These models are based on the heat balance system of green roofs,

the decrease in thermal transmittance of the roof, as well as the influencing phenomena such as solar shading by foliage and cooling by evapotranspiration. In Kumar and Kaushik (2005), a mathematical model was developed based on the green roof components: green canopy, growing media, and roof support layer to evaluate cooling potential and solar thermal shading in buildings. The green roof model developed is incorporated in the building simulation code using fast Fourier transform (FFT) techniques in MATLAB. In Takakura et al. (2001), temperature profiles and influencing environmental parameters were used to evaluate the cooling effect of green roofs. The system was constructed and simulated using the Continuous System Modelling Program (CSMP). In Sailor (2008) the energy balance model of the green roof was developed using energy balance equations and integrated into the EnergyPlus program. This model was validated on a green roof building at the University of Florida and used to evaluate the energy consumption of office buildings in the software in the cities of Chicago and Houston. Jaffal et al. (2012) developed a green roof energy balance model using heat balance equations based on Sailor (2008) and Frankenstein et al. (2004), where the model was coupled with Transient System Simulation Program (TRNSYS).

Green roof growing media parameters such as thermal conductivity, specific heat capacity, short-wave reflectivity, and albedo vary depending on the moisture content level (Sailor 2008). Additionally, the shape and the optical properties of the foliage layer varies because of the outdoor conditions, the growing media water content level, mineral deficiencies, etc. (Jaffal, Ouldboukhitine, and Belarbi 2012). In green roof models, these properties are assumed to be constant. Therefore, there is a significant issue in developing coupled heat and mass transfer models with considering properties of vegetation and growing media that need to be studied.

Green building could also be referred to as "the practice of increasing the efficiency of using energy, water, and materials in the building, while reducing the negative impacts on the environment and human health, through better siting, design, construction, maintenance, operation, and removal during the complete life cycle of the building" (Al Ka'bi 2020). Building Information Modelling (BIM) is often used for planning, designing, implementing, and managing green building projects. BIM provides information on how the building functions; detailed information on the building infrastructure and its individual components (floors, walls, doors,

windows, and internal energy systems). BIM gives full flexibility to building designers to achieve the most efficient models for the building. Energy modelling software applications are part of BIM, and they are used to design efficient energy systems in green buildings, such as the use of efficient energy usage resources, increasing usage of natural energy resources, and reducing the negative impacts of fossil fuel on the environment. There are a variety of energy modelling applications available where the design processes of green buildings are at different levels of complexity, and each has a different use of design parameters as well as operating conditions (Al Ka'bi 2020). In general, there are 10 most common energy simulation models used in analyzing energy consumption and the design of green buildings. In one study, the performance of each software was evaluated based on four main objectives: (1) the details of the building geometry, (2) the user interface of the application, (3) the application capability of importing/exporting data from/to other applications, (4) the accuracy of the simulation results, documentation, and the user support. A typical residential building model was created and used by all the energy simulation applications to produce building energy simulation models for the building, and thus, models were analysed, compared and ranked against certain design criteria and operating conditions. It was concluded the best software tool is TRNSYS with a 91% score, followed by Ecotect, Autodesk-Green Building Studio, and EnergyPlus with scores of 85%, 82%, and 79%, respectively. However, the study specified the type of software chosen still depends on the user and the type of application it is being used. TRNSYS software included limitations such as the incapability to connect with AutoCAD software application in terms of importing and exporting files, while in this aspect, EnergyPlus is more suitable to be used (Al Ka'bi 2020). When it comes to coupling green roof modelling with building energy programs, TRNSYS and EnergyPlus have been the most used software (Jaffal et al. 2012; Mahmoodzadeh et al. 2020). The model developed by Sailor (2008) has been the most well-adapted in evaluating the performance of green roof systems, which has been coupled with EnergyPlus software. In Castleton et al. (2010), it is recommended EnergyPlus be used as the thermal software for green roof modelling. In this model, the heat transfer phenomenon of green roofs is considered in a relatively simple way, explained in section 3.1.

2.2.1 EnergyPlus

Green roof models are coupled with building energy programs to evaluate the green roof thermal performance. The model needs to consider both the green roof system (growing media and canopy layer) and the heat transfer in the roof structure to accurately evaluate the thermal impact of the green roof (Jaffal et al. 2012). The model developed by Sailor (2008) has been adaptable well in evaluating the energy performance of green roofs, and it is coupled with the building energy program, EnergyPlus. Most works of literature on evaluating the thermal performance of green roofs have used EnergyPlus as their building energy software program (Berardi 2016a; Gomes et al. 2019; Castleton et al. 2010; Chan and Chow 2013; Scherba et al. 2011; Yang et al. 2018; Mahmoodzadeh, Mukhopadhyaya, and Valeo 2020). There is a study where TRNSYS software is used as the building energy software program for green roof thermal performance (Jaffal et al. 2012), however, EnergyPlus, due to its relatively simple model for heat transfer, is the most well-known energy modelling tool used.

EnergyPlus is an energy and thermal load simulation program model developed by the U.S. Department of Energy (DOE), capable of modelling hourly energy consumption of a building subject to user-specified construction, internal loads, schedules, and weather. It can compute and report hourly heat gain components, including heat conduction and solar radiation, through the building envelope. The heat fluxes are calculated based on the indoor and outdoor environmental conditions of the building surfaces. The heat balance system on the outside surface of the building is calculated based on the absorbed short-wave solar radiation flux, the net long-wave radiation flux exchange, the convective flux, and the conduction heat flux into a wall. The heat Conduction is calculated using the Conduction Transfer Function (CTF) method (U.S. DOE 2010). The most important input parameters are roughness coefficients, wind speed, tilt angle, surface temperature, and the ambient temperature of the environment building is exposed. A typical EnergyPlus used 6 –15-time steps per hour to represent the building operation subject to a typical meteorological year (Scherba et al. 2011). EnergyPlus at its core, relies on two key element programs: BLAST and DOE-2. The Army Construction Engineering Research Laboratory developed the building loads analysis and system thermodynamics tool (BLAST), intended for building designers and architects wishing to size HVAC equipment. The Department of Energy developed another similar building

energy simulation code – DOE-2 – that has become the industry standard for building energy simulation. The developers of EnergyPlus combine the best features from each code in a modular framework that facilitates the development of the new featured software, in which the green roof model is one example (Sailor 2008). EnergyPlus reports the heating, cooling, lighting, ventilation, and other energy flow systems based on indoor and outdoor environmental conditions. Two main input files are required for the simulation to be conducted: a building input data file (IDF) and a weather data file (Scherba et al. 2011).

2.3 Generating Current and Future Weather Files for Building Simulation Tools

To evaluate green roof thermal performance using building simulation tools under current and future climates, hourly weather data files are needed. Building simulation programs require hourly meteorological data to evaluate energy and thermal behaviour of buildings, therefore, providing suitable weather data files representing both current and future conditions is important.

2.3.1 Typical Weather Files Conditions

The building simulation tools are used to evaluate a proposed design of a building under probable climate conditions that the building is exposed during its lifetime. In numerical models, weather data define the external conditions of the building, therefore hourly data is required to describe the dynamic energy behavior of the building. Weather files are based on actual historical weather data however they may come from different baseline observation periods (Moazami et al. 2019). These weather files are based on a year of typical weather data that represents a typical regional climate condition. Typical weather condition files include hourly data on temperature, dew point, global horizontal radiation, diffuse solar radiation, wind speed, and wind direction. These weather data are based on a continuous-time span of 20 to 30 years of historical observed data, depending on the availability of data. The number and weighting of different meteorological variables are considered a feature of weather file type and hence different typical weather files are used around the world. Typical meteorological year (TMY) is one type of typical weather data and it's computed using the Finkelstein–Schafer (FS) statistic (Herrera et al. 2017). The data sets are derived from years of 1961 – 1990, where input variables such as minimum, maximum, and mean

values of dry bulb temperature, dew point temperature, global radiation, direct normal radiation are used. TMY2 and Weather Year for Energy Calculations 2 (WYEC2) are similar to TMY but they have more complex solar models; the weightings for dry bulb and dew point temperature are slightly changed and less emphasis is given to wind speed. The base period for TMY2 is 1961 - 1990 as well. The TMY3 is similar to TMY2 however the baseline is 1976 – 2005. The International Weather for Energy Calculations (IWEC) year is created by the American Society of Heating, Refrigerating, and Air-Conditioning Engineers (ASHRAE). These files are like TMY3 format; however, they contain weather observations of wind speed and direction, sky cover, visibility, ceiling height, dry-bulb temperature, dew-point temperature, atmospheric pressure, and liquid precipitation. IWEC has recently been updated to IWEC2 which contains slightly more cooling degree-days, more variation in the solar radiation, lower weights for global horizontal radiation, and higher weights for direct normal solar radiation than the previous version. The IWEC2 files are available for locations in the USA and Canada as well as some other countries (Herrera et al. 2017).

2.3.2 Future Weather Files Conditions

To generate future weather data files to study the impact of climate change on building energy performance many different approaches have been proposed and used. There are two main approaches in obtaining future weather files in hourly datasets: prediction based on historical data and prediction based on fundamental physical models. Historical models are based on extrapolation of previous datasets and imposed offset methods where a historical pattern is mapped to an average change. Physical models are based on stochastic and global climate models (known as General Circulation Models (GCMs) (Guan 2009). Global climate models consider the energy transfer mechanisms between a three-dimensional turbulent and radiation active atmosphere, ocean, cryosphere, and land surface (Guan 2009). GCM is a type of global climate model that is considered a reliable and most adapted source. The Intergovernmental Panel for Climate Change (IPCC) has studied climatic change using several possible future emissions scenarios. The different scenarios were created by varying the greenhouse gas production rate by using different socio-economic scenarios. Based on the IPCC Fifth Assessment Report (AR5), the emission scenarios have evolved into Representative Concentration Pathways (RCPs), and now provide the input to

GCMs (Herrera et al. 2017; IPCC 2014b). GCMs produce data at a coarse resolution, typical horizontal resolution is 300 km x 300 km and 24-hour temporal resolution (Belcher et al. 2005). To assess the impact of climate change on building performance, local weather data at high temporal resolution is required. For this reason, GCMs need to be downscaled and they are in general two main methods of downscaling: dynamical and statistical downscaling.

Dynamical downscaling

Dynamical downscaling derives local or regional climate using a Regional Climate Model (RCM). RCMs are numerical models that require explicitly specified boundary conditions from a GCM, or an observation-based data set (Moazami et al. 2019). RCMs are finer in both spatial and temporal resolution (climate information at a much finer resolution than GCM), one well known example is UK MetOffice's HadRM3 model (GCM: HadCM3) that produces regional (25 km resolution) projections of future climate (Guan 2009; Roetzel and Tsangrassoulis 2012). An RCM is nested into a GCM; therefore, the overall quality of the outputs is tied to the accuracy of the GCM.

Statistical downscaling

Statistical downscaling derives regional or local climate variables from larger-scale climate data using stochastic or deterministic approaches. Statistical downscaling approach is simpler than dynamical downscaling, however, since more hourly data is available (data can be directly extracted from RCMs), number applications for locations worldwide is going to decrease for statistical downscaling and increase more for dynamical downscaling (Moazami et al. 2019). Statistical downscaling of GCM outputs can be achieved through two methods: stochastic and morphing.

Stochastic

Stochastic weather models are based on a statistical analysis of recorded climate data. These models can derive all weather variables using inputs of few independent weather variables and generate an artificial meteorological database. However, this method due to its stochastic nature needs to generate weather data over many years to be representative of the climatic patterns during the desired time periods (Guan 2009). It has also been proven this method has difficulties in

accurately modelling many climatic variables since it's not meteorologically consistent (Belcher, Hacker, and Powell 2005). Meteronorm is a software used for generating weather files based on Stochastic method (Moazami et al. 2019). Meteronorm uses GCMs under the IPPC fourth assessment report (AR4) and calculates typical years with hourly resolution for any site.

Morphing

The morphing method was proposed by Belcher et al. (2005) and it's considered a deterministic statistical downscaling method. In this method, the 'baseline climate' which is the weather data for a specific location (such as TMY) is used to morph or transform the data. The data morphed uses projections from GCM or RCM models. The morphing method is constructed based on three algorithms that are applied to the hourly values of weather variables. These three algorithms are called Shift, Stretch, and Combination of shift and stretch. Morphed weather files use historical observation to represent the present-day climate, therefore they are meteorologically consistent, but they ignore some aspects of future climate change like change in frequency of heat waves (Herrera et al. 2017). Additionally, the morphing method assumes that the weather patterns will not change in the future, the weather file generated will contain identical patterns of the base year (Herrera et al. 2017). CCWorldWeatherGen and WeatherShift are two available tools, using the morphing method to create climate change weather files starting from EnergyPlus weather files (EPW). CCWorldWeatherGen provides future weather data for different locations around the world. In this weather generator tool output data of HadCM3 with A2 emissions scenario of the IPPC fourth report (AR4) is used and the morphing method is applied to generate EPW files (Moazami et al. 2019). The baseline climates used is for years 1961 – 1990 and generates future weather files for worldwide locations within three-time slices: 2011–2040 (referred as '2020s'), 2041–2070 (referred as '2050s'), and 2071–2100 (referred as '2080s') (CCWorldWeatherGen 2009). WeatherShift tool is based on the representative concentration pathways (RCPs) of 4.5 and 8.5 emission scenarios of the IPPC fifth report (AR5) (Dickinson et al. 2016). In this tool, the morphing method is applied to 14 GCMs and it provides three different time periods of 2026–2045 (referred to as '2035s'), 2056–2075 (referred to as '2065s'), 2081–2100 (referred as '2090s'). The baseline climate used is based on the years 1976 -2005 for both emission scenarios. In this tool, a

cumulative distribution function (CDF) is also constructed to enable users to assign a probability to the projections (the warming percentile of future conditions) (Moazami et al. 2019).

Comparison of Future Weather Data Generation Methods

In (Moazami et al. 2019) the objective of the study was to identify the most reliable future weather generation method to use in building energy simulations. The study first compared the methods of generating future weather files through dynamical and statistical downscaling. The study then, using the two main downscaling methods, generated four different future weather files and investigated the energy performance of buildings under these weather files. The first three weather data generated was based on statistical downscaling using CCWorldWeatherGen, WeatherShift and Meteonorm weather generator tool, and the last weather file generated was based on dynamical downscaling by using RCM (RCA4 model generated by Rossby Centre Regional Atmospheric Climate Model). Based on the results, it was concluded that only those weather files generated based on dynamical downscaling are the most reliable for providing representative boundary conditions to test the energy robustness of buildings under future climate uncertainties (Moazami et al. 2019). In Berardi and Jafarpur (2020) three different weather files based on the statistical and dynamical downscaling method were generated to assess the impact of climate on the energy performance buildings. The two statistical downscaled weather files were generated using WeatherShift and CCWorldWeatherGen tools and a dynamically downscaled weather file was generated using HRM3 (downscaled of HadCM3 GCM model). The results showed the higher spatial resolution of dynamical downscaling (RCMs) compared to the statistical method presents a better picture of the local climate conditions. Therefore, the impacts of climate change on building energy demand were quantified better. Also, the HRM3 projected weather parameters in 3-h time-steps, which were significantly better than the monthly time-steps seen in HadCM3; this reduces the significance of the statistics in data interpolation. Berardi and Jafarpur (2020) concluded that the use of multiple GCMs rather than just a single model for future weather file generation creates statistically significant results. Therefore, a combination of multiple GCMs, like in the WeatherShift tool, as well as RCM, such as HRM3, provides the most accurate climate prediction for the future (Berardi and Jafarpur 2020). In Herrera et al. (2017) various methods on the generation of weather files have been discussed and compared. It was concluded among future

weather files generated through RCMs, morphing, and synthetic (Stochastic), the most suitable to generate future weather files are through RCMs, however, if the hourly temporal resolution is provided. One main limitation of RCMs is that their resolution varies depending on the world region targeted and models employed.

The morphing downscaling method is commonly used to generate future weather files and evaluate the buildings energy performance (Robert and Kummert 2012; Chan and Chow 2013; Moazami et al. 2019; Belcher et al. 2005). In Belcher et al. (2005) where the morphing method was proposed, it has been mentioned the major disadvantage of this method is the future weather file has the variability and character of the present data. In Belcher et al. (2005), the future weather data was generated through the morphing method and compared to UKCIP02, which is a regional climate model to validate the morphing process. The results showed the reduction in heating degree days compared to present-day weather file agreed with the results calculated from the regional climate model, which proved that the morphing method is valid to produce future weather file data (Belcher, Hacker, and Powell 2005). In another study by Robert and Kummert (2012), future weather files were generated through the morphing method to evaluate the impact of future climates on net-zero energy buildings (NZEBs). It was also shown in the study that the data generated using the morphing method matched the average changes of the GCM model HadCM3, indicating again the validation of the morphing method (Robert and Kummert 2012). There have also been studies by (Guan 2009) and (Chan and Chow 2013) which have validated the morphing method and its use on evaluating the energy performance of buildings (Chan and Chow 2013; Guan 2009). In Table 2-2, the advantages and disadvantages of downscaling methods for generating future weather files for building energy simulation tools are summarized. As observed from Table 2-2, the dynamical downscaling method is not constrained by historical data and has high spatial and temporal resolution, however it is computationally intensive. On the other hand, statistical downscaling method is widely available through various software and can be generated in hourly durations. The major disadvantage of statistical downscaling is that future data generated relies strictly on historical observations and could lead to similar historic climate patterns.

Table 2-2: Methods for generating future weather data used in building energy simulation models.

Downscaling method	Advantages	Disadvantages
Dynamical downscaling using RCM	• High spatial resolution • High temporal resolution • Physically consistent data set for different variables • Not constrained by historic data	• Resolution varies globally based on region targeted and models employed; may need temporally downscaling if resolution is too coarse • Computationally intensive
Statistical downscaling: stochastic method	• All weather variables could be driven using few inputs independent weather variables • Hourly data generated through software such as Meteonorm	• Difficulties in accurately modelling climatic variables • Not meteorologically consistent • Relies statistically based on historical observations climate data
Statistical downscaling: morphing method	• Meteorologically consistent and simple method • Accounts for local weather conditions • Available in variety of weather generator tools such as CCWorldWeatherGen and Weather Shift	• Assumes future weather patterns will not change; weather file generate contains identical patterns of the base year • Some future climate change aspects are ignored such as change in heat waves frequency is ignored

2.4 Research Gap and Objectives

Based on future projections, by the end of the 21st century, annual average temperatures across Canada will increase by 1.8 ℃ for a low greenhouse gas emission scenario (RCP 2.6) to 6.3 ℃ for a high emission scenario (RCP 8.5) compared to the reference time-period of 1986–2005. The annual and winter precipitation is projected to increase in all parts of Canada, while there would be a reduction in summer rainfall for southern parts of Canada (Zhang et al., 2019). Climatic extremes are projected to become more intense and frequent because of climate change such that the annual highest daily temperature, which currently occurs every 20 years, will become a once in 5-year event by the mid-century under a low emission scenario and a once in 2-year under a high emission scenario (Berardi and Jafarpur 2020). Therefore, buildings across Canada are expected to be exposed to drastically different annual and seasonal climatic conditions with more frequent and intense extreme events such as rain and heatwaves over their design life. This shows

the importance of evaluating the thermal performance of new buildings under both current and future climate conditions, so a failure in building design would be limited. Additionally, it's as important to measure the energy performance of buildings when effective design elements such as green roofs are used to reduce the environmental impacts caused by climate change.

There have been various studies that have investigated the performance of buildings under future climate conditions. All studies revealed similar conclusions that, in general, buildings in regions with projected increases in temperature would require more energy for cooling space and lower energy for heating space in future (Moazami et al. 2019). Robert and Kummert (2012) analysed building performance under future climate conditions of Massena (NY) for horizon years of the 2020s and 2050s. Results showed the future conditions climate would be warmer, sunnier, and dryer in the months of June to September, while winters are warmer and less sunny compared to current climate conditions. In Roetzel and Tsangrassoulis (2012), the energy performance of a building in Athens was studied under the future climate conditions through modelling using EnergyPlus. As a result, the peak heating loads from the horizon year of the 2050s to 2080s would decrease by 40 to 100%, and the peak cooling loads would increase by a factor ranging from 1.3 to 2.6. In Chan and Chow (2013), the impact of climate change for horizon years of the 2020s, 2050s, and 2080s on an office building using EnergyPlus was studied to evaluate the building's air-cooled and cooled chiller systems. The study concluded 3.9 to 4.2 % extension capacity should be considered to meet the increasing cooling demand. In Canada, studies are performed on the effect of climate change on building heating and cooling loads. In Berardi and Jafarpur (2020), the building energy consumption under the future climate of Toronto city was analysed. The result showed an average decrease of 18%–33% for the heating energy use intensity and an average increase of 15%–126% for the cooling energy use intensity by 2070 (Berardi and Jafarpur 2020).

Although the impact of climate change on building thermal performance is evaluated, up to now, there has been no research on the energy performance of green roof systems on buildings under future climatic conditions in Canada or around the world. Green roofs are considered valuable strategies for making buildings more sustainable and have proven to decrease and improve building energy consumption. In addition, the impact of climate change and shift in weather patterns in future conditions changes the building cooling and heating consumption magnitudes,

which would impact the green roof thermal performance. Designing green roofs based on future climate conditions could offer an opportunity to manage the energy patterns of buildings in the future. Over the years, the green roof thermal performance evaluated globally under different current climate conditions have shown green roof performance varies depending on the climate. Thus, designing and optimizing green roof thermal performance specific to the climate they are installed in is crucial.

In this research, optimizing green roof designs under both current and future climate conditions of the City of Toronto is investigated through modelling. In 2012, the City of Toronto issued a by-law that buildings with areas more than 2000 m^2 require the installation of green roofs. Thus, most new buildings in the City of Toronto are considered to have green roofs, but they all have different design configurations (various growing media and vegetation types). Therefore, it is important to investigate the impact of green roofs in decreasing building energy consumption in the City of Toronto to be able to optimize green roof design and implementation. Furthermore, adding an insulation layer to green roof structures is a design requirement under Toronto climate. The impact of added insulation thickness is not studied extensively, and its effect on various green roof design configurations on building energy performance is unknown. Hence, this research aims to evaluate the impact of added insulation thickness with various green roof design parameters on building thermal performance.

Three design parameters of growing media depth, LAI and insulation thickness on green roof thermal performance are considered. The growing media depth and LAI are selected due to being the most effective green roof parameters in decreasing heating and cooling loads. The objective is to determine optimal green roof design using varied ranges of growing media depth, LAI, and thermal insulation thickness. The influence and importance of each parameter on green roof thermal performance are quantified. The research is performed through modelling using EnergyPlus software, which is a well-accepted simulation tool for modelling green roof thermal performance on building energy consumption. Archetype benchmarks available by DOE on the EnergyPlus simulation tool are used as reference buildings, and a green roof is defined in the software with suggested design parameters. The current climate weather data is based on the Canadian Weather Year for Energy Calculation (CWEC) file that is available in hourly durations.

For future climate data, the CCWorldWeatherGen tool is used to generate future climate conditions for the time frame of the 2080s using CWEC current climate as the baseline year. In this research, precipitation is also considered as the moisture input source of green roofs; however, due to the unavailability of hourly precipitation data under both current and future conditions, the precipitation data is generated using a different approach explained in Chapter 3 section 3.2.3.

The primary stage of this research determines optimal green roof design parameters in the City of Toronto that would be most effective in decreasing the energy consumption of a secondary school building compared to the conventional roof (no green roof installed). According to (NRCan 2013), primary/secondary school buildings are considered the largest energy consumers in Canada. Hence, the secondary school building is chosen as the reference building for evaluating the green roof thermal performance and energy savings.

In the secondary stage, the green roof energy savings are analysed based on two other building archetypes. The second stage aims to determine if building type and characteristic would impact the green roof performance on building energy savings and compare the difference for the green roof optimal design in the first and second stage. An office and a hospital building archetype are considered in the second stage of this research. These two archetypes are selected due to their different characteristics compared to secondary school. The impact of green roof thermal performance for office and hospital buildings are evaluated under current, and future climate conditions and optimal green roof configuration designs are suggested similar to the secondary school.

Lastly, the green roof water retention performance is analysed for all three archetypes to showcase other green roof benefits. For more details on the objectives of this research, the reader can refer to Chapter one, section 1.3.

Chapter Three: Methodology

The method employed in this research simulates the energy balance for three building archetypes of a secondary school, an office and a hospital using the EnergyPlus building simulation tool with green roof designs under current and future climates in the City of Toronto. In addition, a sensitivity analysis using three design parameters of growing media depth, LAI, and thermal insulation thickness to evaluate the effect of green roof thermal energy performance on building energy consumption is performed.

3.1 EnergyPlus Simulation Tool

In this research, EnergyPlus, a widely accepted simulation tool for modelling annual building energy consumption, is used. EnergyPlus is an energy and thermal load simulation program developed by the United States Department of Energy (DOE). It is used to model the hourly energy consumption to specified building construction layers, internal loads, schedules, and weather (U.S. DOE 2010).

The heat fluxes are calculated based on the indoor and outdoor temperature of building surfaces. EnergyPlus reports the heating, cooling, lighting, ventilation, and other energy flow systems based on indoor and outdoor environmental conditions. The heat flux through the building envelope is calculated using Conduction Heat Transfer (CTF) method (U.S. DOE 2010). Two main input files are required for the conduction simulation: a building input data file (IDF) and a weather data file in EnergyPlus weather (EPW) format. The IDF describes the building characteristics and HVAC system. The weather file includes climatic variables such as wind speed, wind direction, direct and diffuse solar radiation, dew point temperature and dry bulb temperature. EnergyPlus includes a one-dimensional green roof model, called Ecoroof, developed by Sailor (2008). It allows users to specify a green roof as the outer layer of a building rooftop. The user can select various aspects of the green roof design parameters such as growing media depth, the height of plants, LAI, leaf albedo, the depth, density, thermal conductivity, and specific heat of the growing media (referred to as “soil” the software). To account for soil moisture conditions in Ecoroof, irrigation and precipitation schedules can also be implemented in EnergyPlus. The Ecoroof module contains

energy budgets for both the foliage layer and soil surface. The green roof energy balance is dominated by solar radiation and the model accounts for long-wave and short-wave radiative exchange within the plant canopy; effect of plant canopy on sensible heat exchange among the ambient air, leaf, and soil surfaces; thermal and moisture transport in the soil with moisture inputs from precipitation and irrigation; evaporation from the soil surface, and transpiration from the vegetation canopy. In addition, the green roof model is fully coupled with the EnergyPlus building energy simulation code that accounts for the internal and environmental loads on the building, mechanical/HVAC system and models the building system for 8760 hours in a "typical" year (Sailor and Bass 2014).

The solar radiation is balanced by sensible (convection) and latent (evaporative) heat flux from soil and plant surfaces combined with heat conduction into the growing media and long-wave (thermal) radiation to and from the soil and leaf surfaces. The energy budget analysis follows the fast-all-season soil strength (FASST) model developed by Frankenstein and Koenig and the energy and moisture balance (including ice and snow) within vegetated soil is tracked. The green roof model is a one-dimensional model that draws heavily from other plant canopy models (atmospheric modelling communities), the Biosphere-Atmosphere Transfer Scheme (BATS) and the Simple Biosphere Model (SiB). The model adopts a relatively thin soil layer and the sign convention used assumes all heat fluxes are positive when energy is absorbed into the layer (Sailor 2008). The Ecoroof model energy balance in EnergyPlus is shown in Figure 3-1. In Sailor (2008), the model has been validated using soil surface temperature data from a monitored green roof on a building in Florida. Verification of the current model is also discussed in section 3.3.1.

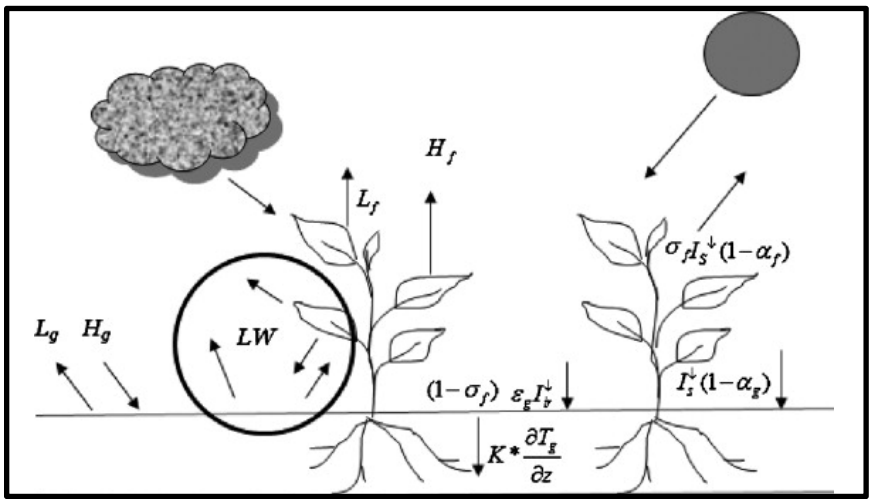

Figure 3-1: Energy Balance of Green Model by Sailor (D. J. Sailor 2008).

The green roof model by Sailor (2008) is a one-dimensional model that contains energy budgets for both the foliage layer (F_f) and ground surface layer (F_g). The foliage energy balance is given by (Equation 3):

$$F_f = \sigma_f\left[I_S^{\downarrow}(1-\alpha_f) + \varepsilon_f I_{ir}^{\downarrow} - \varepsilon_f \sigma T_f^4\right] + \frac{\sigma_f \varepsilon_g \varepsilon_f \sigma}{\varepsilon_1}\left(T_g^4 - T_f^4\right) + H_f + L_f \qquad \text{Equation 3}$$

Where:

$$H_f = 1.1\ LAI\ \rho_{af} C_{p,a} C_f W_{af}\left(T_{af} - T_f\right) \qquad \text{Equation 4}$$

$$L_f = l_f LAI \rho_{af} C_f W_{af}\ r^{"}\left(q_{af} - q_{f,sat}\right) \qquad \text{Equation 5}$$

The energy budget of the foliage layer accounts for short (I_s) and long-wave radiation (I_{ir}) as well as sensible heat flux (H_f) and latent heat flux (L_f) transfer in the vegetation layer, Equation 4 and Equation 5, respectively. The sensible heat transfer between the foliage and near canopy air (H_f) is influenced by the temperature difference between the foliage temperature (T_f) and air temperature within the canopy (T_{af}), wind speed in the canopy (W_{af}), and LAI. In equation 4, constant 1.1 accounts for heat transfer from stems, twigs, and limbs; ρ_{af} the density of air near the foliage; C_f is the bulk transfer coefficient and $C_{p,a}$ is the specific heat of air at constant pressure.

The process of water loss through plant respiration is known as transpiration. It is controlled by opening and closing of the stomata. The resistance to leaf activity (diffusion of water vapour into and out of stomata) or the stomatal resistance depends on light intensity, soil moisture content, and the vapour pressure difference between the leaf interior and the ambient air. The actual stomatal resistance at any time is proportional to this minimum resistance and inversely proportional to LAI (Sailor 2008). Additionally, the boundary layer formed due to aerodynamic resistance; depends on wind speed, surface roughness, and atmospheric stability. The combined effect of aerodynamic and stomatal resistances to vapour diffusion creates the foliage surface wetness factor. The higher the wind speed, the lower the aerodynamic resistance, which would result in a smaller wetness factor, implying that the leaf surface remains dry, and moisture is readily evaporated. However, with low wind speed, the aerodynamic resistance increases, and the wetness factor approaches 1.0. This indicates that moisture readily travels to the leaf surfaces but is not easily evaporated. The latent heat flux transfer of the foliage layer (L_f) is based on the latent heat of vaporization (l_f), the foliage wetness factor ($r^{"}$), the wind speed within the canopy (W_{af}), the difference between the saturation mixing ratio at the foliage surface temperature ($q_{f,sat}$) and the mixing ratio of the air within the canopy (q_{af}). The mixing ratio is the mass of water vapour to mass of dry air. The soil surface energy balance (F_g) is given by (Equation 6):

$$F_g = (1-\sigma_f)\left[I_S^{\downarrow}(1-\alpha_g) + \varepsilon_g I_{ir}^{\downarrow} - \varepsilon_g \sigma T_g^4\right] + \frac{\sigma_f \varepsilon_g \varepsilon_f \sigma}{\varepsilon_1}\left(T_g^4 - T_f^4\right) + H_g + L_g + \kappa * \frac{\partial T_g}{\partial_z} \quad \text{Equation 6}$$

Where the sensible heat (H_g), latent heat flux (L_g) and multiple reflections associated with long-wave and short-wave radiation is presented. The last term on the right side gives the conduction of heat into the soil.

The soil energy budget is mainly influenced by the soil thermal properties, the amount of foliage coverage (σ_f) and the amount of moisture in the soil. The heat released or gained due to phase changes of soil water, precipitation heat flux and heat flux due to vertical water transport in the soil are ignored. The energy equation of the soil combines reflections associated with short and long-wave radiation, sensible heat flux H_g (Equation 7), latent heat flux L_g (Equation 8) and conduction of heat through the soil. Sensible heat flux (H_g) between the soil surface and the air is

dependent on the temperature difference between the ground surface temperature (T_g) and air temperature within the canopy (T_{af}), and the wind speed within the canopy (W_{af}). Equation 7, C_{hg} presents the sensible heat flux bulk transfer coefficient at ground layer.

$$H_g = \rho_{ag} C_{p,a} C_{hg} W_{af} (T_{af} - T_g) \quad \text{Equation 7}$$

$$L_g = C_{e,g} I_g W_{af} \rho_{ag} (q_{af} - q_g) \quad \text{Equation 8}$$

The removal of water vapour from the soil surface depends on the difference between the mixing ratio at the ground surface (q_g) and mixing ratio at the foliage-atmosphere interface (q_{af}), the wind speed within the canopy (W_{af}), and the latent heat vaporization at ground surface temperature (I_g) resulting in latent heat flux (Equation 8). The $C_{e,g}$ is the latent heat flux bulk transfer coefficient at ground layer, presented in Equation 8.

The other elements of the energy balance, heat conduction is assumed to be uniform in the horizontal direction. This one-dimensional heat conduction allows the thermal properties to vary in response to the moisture content of the soil The user specifies albedo values, thermal conductivity, specific heat capacity, and density for dry soil. The green roof module updates these properties based on the current moisture state of the soil and generalised sensitivity functions. This sensitivity function is based on experimental work performed by Sailor (2008). As a rule, it was found that diffusivity and thermal conductivity varied linearly with soil moisture saturation level, with saturated soil having a 40% higher specific heat capacity and twice the thermal conductivity of their dry counterparts. As mentioned previously, EnergyPlus can track precipitation through a user supplied schedule. The precipitation schedule serves as a moisture input for the soil layer. In general, moisture leaves the soil through one of three mechanisms: runoff, evaporation from the soil surface, or evapotranspiration from vegetation surfaces. Runoff results when precipitation occurs when the soil is saturated. Evaporation and evapotranspiration are calculated directly from the latent heat flux calculations for the soil (L_g) and vegetation layers (L_f) and the corresponding values of latent heat of vaporisation of water. Within each time step the soil moisture state is updated based on the net inflow of moisture to the soil layer.

The soil surface (T_g) and foliage (T_f) temperature equations are solved each time step simultaneously, inverting the CTF to extract heat flux information for the energy balance calculation. This model functions as an integral component of the simulation software, performing an energy balance on a vegetated rooftop within each time step. This Ecoroof model in EnergyPlus can simulate and evaluate the thermal and energy performance constructed with a green roof system. Detailed energy balance analysis and resulting equations within the Ecoroof model can be found in Sailor (2008).

3.2 Weather Climate Data

Building energy simulation programs require meteorological data to evaluate buildings' energy and thermal behaviour; therefore, providing suitable weather data files representing both current and future conditions is essential. In this research, hourly weather data files were obtained to assess green roof thermal performance using EnergyPlus software under current and future climate and are described below.

3.2.1 Base Year Current Climate Weather Data

Weather files are based on actual historical weather data; however, they may come from different baseline observation periods (Castleton et al. 2010). These weather files are based on a year of typical weather data that represents a typical regional climate condition. Typical weather condition files include hourly data on temperature, dew point, global horizontal radiation, diffuse solar radiation, wind speed, and wind direction. Typically, depending on data availability, these files are based on continuous-time span (20 to 30 years) of observed historical data. As weather file types differ based on the number and weighting of different meteorological variables, other weather files are used worldwide. In Canada, the Canadian Weather Year for Energy Calculations (CWEC) is a typical weather file available, developed by joining twelve typical meteorological months from the Canadian Weather Energy and Engineering Datasets (CWEEDS). The CWEC months are chosen by statistically comparing individual monthly means with long-term monthly means for daily total global radiation, dry bulb temperature, dew point temperature and wind speed (MSC 2008). The latest CWEEDS update was in 2016 and included 492 Canadian locations for periods between 1998 and 2014. In this research, the current climate data (or base year) was taken to be CWEC

2016 in EPW format (WMO station 716240), which is available publicly by the Government of Canada.

3.2.2 Future Climate Weather Data

Many different approaches have been proposed by others to generate future weather data files to study the impact of climate change on building energy performance. Physical models are based on stochastic and global climate models (Wilde and Coley 2012) that consider the energy transfer mechanisms between a three-dimensional turbulent and radiation active atmosphere, ocean, cryosphere, and land surface (Guan 2009). A General Circulation Model (GCM) is a global climate model that is considered reliable and adapted by many (Guan 2009; Chan and Chow 2013; Berardi and Jafarpur 2020; Robert and Kummert 2012). To assess the impact of climate change on building performance, local weather data at high temporal resolution is also required.

For this reason, GCM has to be downscaled either through dynamical or statistical downscaling methods. In this research, Climate Change World Weather Generator (CCWorldWeatherGen) tool is used to statistically downscale GCMs and generate hourly future weather files (University of Southampton 2009). The CCWorldWeatherGen generates climate change weather files through a statistical downscaling method called morphing.

Building simulation tools require hourly weather data files for various climate variables such as hourly dry bulb temperature, dew point temperature, wet bulb temperature relative humidity, atmospheric pressure, wind speed, wind direction, total sky cover, horizontal infrared radiation, diffuse solar radiation, and direct solar radiation. Additionally, in EnergyPlus, all weather files need to be in EPW format. Accessing downscaled future weather data that includes all weather variables under the same emission scenarios and time periods at hourly resolution can be challenging. Therefore, the CCWorldWeatherGen tool is a suitable method available to generate the future weather data in EPW format using the morphing method. In this research morphing approach was chosen as the statistical downscaling method due to reliable baseline climate (CWEC) since it's the present-day weather series. The spatial downscaling is achieved through morphing due to baseline weather data obtained from observations at a real location. Thus, morphing method technique has been validated in producing future weather files in many research

studies, discussed previously in section 2.3.2. Weather files generated using the morphed method have been shown to match the average changes of the GCM model HadCM3. One limitation of the morphing method is that the generated future weather data has the variability and character of the baseline, present-day weather file; therefore, the future time frames may have different climate characteristics. However, the morphing method is a practical method to generate future weather files and it gives future weather files that are meteorologically consistent. Lastly, the morphing method has been the most widely used approach in literature for generating future weather files to evaluated building energy demand under future years (Berardi and Jafarpur 2020; Moazami et al. 2019; Robert and Kummert 2012; Chan and Chow 2013; Belcher et al. 2005).

The morphing method was proposed by Belcher et al. (2005). It uses the 'baseline climate', which is the typical weather data for a specific location (such as CWEC), to morph or transform data with projections from GCMs. The morphing method produces weather data for building simulations by considering the changes in the climate conditions. The morphing method consists of shifting, stretching, or combination of both of current present-day climatic variables time-series resulting in the generation of new time series that contains the average change in climate conditions. It should be noted that morphed weather data maintains the physical realistic weather sequences of the source (base climate) data. The three main algorithms of shift, stretch, and combination of shift and stretch used in the morphing method are listed in Equation 9 to 12, respectively.

$$x = x_o + \Delta x_m \qquad \text{Equation 9}$$

$$x = \alpha_m x_o \qquad \text{Equation 10}$$

$$x = x_o + \Delta x_m + \alpha_m (x_0 - (x_o)_m) \qquad \text{Equation 11}$$

Where x_o is the hourly present climate variable, Δx_m is the absolute change in monthly mean climate variable for month m, α_m is the fractional change in monthly mean climate variable for month m and $(x_o)_m$ is the climatic variable x_o averaged over month m. The "shift" algorithm (equation 10), adds the monthly mean change to the current (base climate) hourly weather variable data and shifts the baseline data by Δx_m. The second algorithm (equation 11), "stretch" the current

hourly data and scales the data with relative monthly mean change of the weather data. "Stretch" is used when there is change to the mean or variance as a percentage or fractional change rather than an absolute increment. For combined shift and stretch, the current hourly weather data is shifted by adding absolute monthly mean change and stretched by a monthly diurnal variation of the parameter (equation 12). A combination of shift and stretch is applied when there is a change in both mean value and variance. A typical example of the shift approach is adjusting atmospheric pressure while the stretch approach is mainly used for solar irradiance (due to solar irradiance having a value of zero at night). The combined shift and stretch approach is primarily used in adjusting dry bulb temperature to account for changes in daily mean, minimum and maximum daily temperature.

In this research, the CCWorldWeatherGen tool, based on HadCM3 with A2 emission scenario, is selected as the software for generating future climate data. Emission scenario A2 describes a continuous population increase with regionally oriented economic growth and slow technological change (IPCC 2000a). The CCWorldWeatherGen tool is based on Microsoft Excel, and data is transformed from the present climate weather file (EPW format) to future climate conditions in EPW. In this research, to generate the future files using CCWorldWeatherGen, first, the EPW format from CWEC files was uploaded. Then HadCM3, A2 scenario and a future time frame was selected. There are three different future time frames provided by CCWorldWeatherGen, the 2020s, 2050s and 2080s. In this research, the time frame of 2080s was chosen. After choosing the future time frame, the morphing procedure was started to superimpose the future climate data onto the CWEC file. Lastly, the climate change data was generated in the EPW weather file.

It is important to note, in the morphing method, the averaging period used for the baseline, present-day data, should be the same as the period for the baseline used for the climate change scenario. In this research, the CCWorldWeatherGen tool applied the projected changes in 1961-1990 baseline data from 1998-2014 of CWEC. This difference in baseline period would result in higher maximum, and minimum temperatures since baseline 1998-2014 climate have higher temperature values. In statistical downscaling such as the morphing method, the baseline is used to superimpose the future changing climate to create the future climate. Selecting a different historical period for the baseline weather file than the baseline used for the climate change scenario could result in

variations of the projected future climate (Berardi and Jafarpur 2020). In this research, the CCWorldWeatherGen tool generates future climate conditions based on HadCM3, where the baseline used for the climate change scenario is the historical period of 1961-1990. Due to the unavailability of data, CWEC data for averaging periods of 1998-2014 was selected. Hence, the use of different averaging periods for the present day baseline data and baseline periods for climate change scenarios in generating future climate data using the morphing method is a limitation of this research.

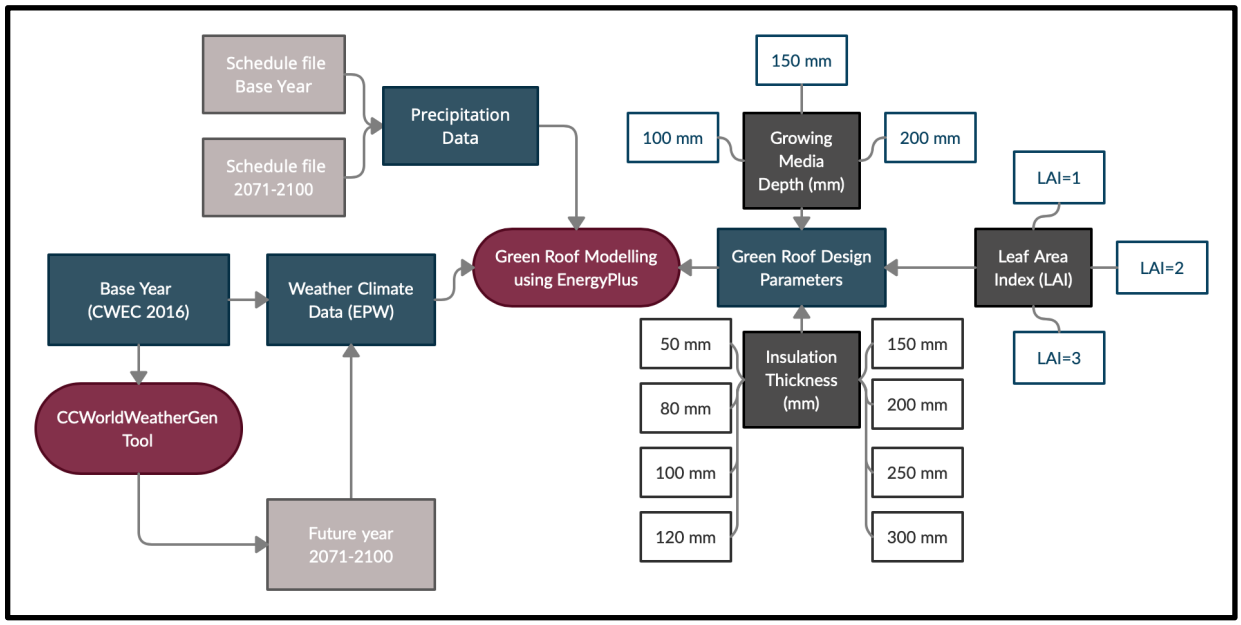

Figure 3-2: Method schematic

In Figure 3-2, the schematic of the method used in this research is presented. There are three fundamental steps involved: the weather files in EPW format; the schedule precipitation data; and the green roof design parameters. There are two weather files for the base year (current climate) and future time horizon of 2080s. The precipitation data is inserted as scheduled files for the two time periods of base year and 2080s; creating precipitation schedule files are explained in section 3.2.3. Lastly, the three design parameters of growing media depth, LAI and insulation thickness, which were used in a sensitivity analysis are explained in section 3.3.

3.2.3 Current and Future Precipitation Weather File Generated

Current Precipitation Data

In this research, precipitation as a source of moisture input is considered in the green roof simulation using EnergyPlus. Precipitation weather data includes rain and equivalent water content of snow; however, most building weather data files do not contain precipitation; if they do, EnergyPlus does not consider it in green roof simulation. The CWEC2016 in EPW includes weather observations for light, moderate and heavy rainfall in meter per hour. The light rainfall is considered to be 0.00083 m/hr, moderate rainfall is 0.0067 m/hr, and heavy rainfall is 0.002 m/hr. However, these values reported as light, moderate and heavy rainfall in weather observations of EPW estimate the intensity of rainfall and not the actual values of precipitation. Hence, new rainfall data needs to be generated that accounts for the rainfall's hourly duration and intensity scale.

In EnnergyPlus, the precipitation data needs to be defined as a schedule separately through the "Site: Precipitation" object in EnergyPlus, used by the "Material: RoofVegetation" object. The "Site: Precipitation" object is often used to define precipitation rates (m/hr) using the "Schedule" object. In this research, the precipitation schedule data was developed using the observation fields from CWEC2016 weather file, EPW format, and the average monthly precipitation for the same CWEC 2016 weather site provided by Canadian Climate Normals (Environment Canada 2013). International Pearson Airport weather station data was used for both CWEC2016 in EPW and Canadian Climate Normals.

Table 3-1: Monthly and total precipitation for EPW observations and Canadian Climate Normals (Toronto Pearson Intl AP Station)

ID		716240	6158733
Climate Data		EPW Observations Precipitation (mm)	Canadian Climate Normals Precipitation (mm)
Precipitation	Jan	92	51.8
	Feb	48	47.7
	Mar	97.2	49.8.5
	Apr	192	68.5
	May	172.8	74.3
	Jun	128	71.5
	Jul	123.2	75.7
	Aug	96.8	78.1
	Sep	108	74.5
	Oct	164	61.1
	Nov	162	75.1
	Dec	116	57.9
	Sum	1500	786

The Canadian Climate Normals provide the average monthly precipitation data in the last 15 years for certain locations. Table 3-1 provides the monthly and sum of precipitation data for both EPW observations and Canadian Climate Normals data. From Table 3-1 it can be observed the annual precipitation from EPW observation precipitation is 1500 mm while the annual precipitation data from Canadian Climate Normals is 786 mm; indicating EPW precipitation data are not presenting realistic values. Therefore, to generate realistic rainfall data for the precipitation schedule in EnergyPlus, the hourly weather observations from the EPW file that indicates the hourly duration of the rainfall were used to sum the monthly observations rainfall and rescaled to meet the average precipitation for the Canadian Climate Normals data. The monthly ratio of Canadian Climate Normals precipitation to weather observation precipitation were used to scale the hourly observation precipitation of EPW to generate an hourly base precipitation weather data, as shown in Equation 12.

$$Ratio = \frac{Monthly\ Canadian\ Climate\ Normals}{Monthly\ Weather\ Observataion\ Precipitation\ (EPW)} \quad \text{Equation 12}$$

To show the step by step process of the method used to generate precipitation, weather observation data for the 24 hour duration of January 18th is chosen as a sample calculation. First, monthly

precipitation from both Canadian Climate Normals and observation weather data (EPW) for month of January given in Table 3-1 is used to calculate the ratio for month of January using Equation 12.

$$Ratio_{Jan} = \frac{51.8}{92} = 0.563$$

Then, the calculated ratio for month of January is used to scale the observation weather precipitation data (EPW) at hourly duration to realistic precipitation data similar to the Canadian Climate Normals. Table 3-2 shows the weather observation data from EPW for light, moderate and heavy precipitation, and the scaled generated data for January 18th.

Table 3-2: Sample of generated precipitation data at hourly duration

Time (Hour)	Weather observation precipitation data (EPW) (m)	Weather observation precipitation (EPW) * Ratio $_{Jan}$	New Generated Precipitation Data (m)
01/18 01:00:00	1.17E-03	1.17E-03 * 0.563	6.57E-04
01/18 02:00:00	2.00E-03	2.00E-03 * 0.563	1.13E-03
01/18 03:00:00	2.00E-03	2.00E-03 * 0.563	1.13E-03
01/18 04:00:00	8.33E-04	8.33E-04 * 0.563	4.69E-04
01/18 05:00:00	0.00E+00	0.00E+00 * 0.563	0.00E+00
01/18 06:00:00	1.17E-03	1.17E-03 * 0.563	6.57E-04
01/18 07:00:00	8.33E-04	8.33E-04 * 0.563	4.69E-04
01/18 08:00:00	1.17E-03	1.17E-03 * 0.563	6.57E-04
01/18 09:00:00	8.33E-04	8.33E-04 * 0.563	4.69E-04
01/18 10:00:00	0	0 * 0.563	0
01/18 11:00:00	0	0 * 0.563	0
01/18 12:00:00	0	0 * 0.563	0
01/18 13:00:00	0	0 * 0.563	0
01/18 14:00:00	1.17E-03	1.17E-03 * 0.563	6.57E-04
01/18 15:00:00	8.33E-04	8.33E-04 * 0.563	4.69E-04
01/18 16:00:00	0	0 * 0.563	0
01/18 17:00:00	0	0 * 0.563	0
01/18 18:00:00	0	0 * 0.563	0
01/18 19:00:00	0	0 * 0.563	0
01/18 20:00:00	0	0 * 0.563	0
01/18 21:00:00	0	0 * 0.563	0
01/18 22:00:00	0	0 * 0.563	0
01/18 23:00:00	0	0 * 0.563	0
01/18 24:00:00	0	0 * 0.563	0

It should be noted that the average climate condition for the precipitation data is based on 1981-2010, and the average climate condition for CWEC2016 (EPW) is 1998-2014; this difference was due to the unavailability of data. The generated hourly precipitation data was inserted in the "Schedule: file "object in EnergyPlus.

Future Precipitation Data

The CCWorldWeatherGen tool downscales all weather variables within the CWEC weather file, however since precipitation data was not included in the CWEC file, future precipitation data was generated using a different approach. The CCWorldWeatherGen tool projections are based on HadCM3 A2 emissions, which is considered to be older version of climate scenarios and the projected precipitation data under these emission scenarios are unavailable. Additionally, projected future precipitation data should match the projections from the HadCM3 A2 emission scenario and use of other GCMs and emission scenarios would create inconsistency in results. Therefore, the precipitable water climate variable which is included in the CWEC (EPW) format was used to generate future precipitation projections. The precipitable water is the amount of water potentially available for precipitation; however, it does not represent the total amount of actual precipitation. While using the CCWorldWeatherGen tool, the precipitable water climate variable is morphed, and the projections for the precipitable water variable is generated. Therefore, the hourly current precipitation data generated in the Current Precipitation Data section with the current precipitable water from the CWEC2016 (EPW) weather file was used to determine the ratio presented in Equation 13. This ratio scales the precipitable water climate of future projection and generates hourly future precipitation data; the precipitable water for each hour time period of 2080s was scaled accordingly.

$$Ratio_{hour} = \frac{Hourly\ Current\ Precipitation\ Data}{Hourly\ Current\ Precipitable\ Water\ Data} \qquad \text{Equation 13}$$

Table 3-3 presents a sample of hourly generated precipitation on January 23rd where equation 14 is used to calculate the ratio for each hour. The precipitable water for each hour of 2080s period is then multiplied by the ratio of each hour to determine the precipitation at each hour. Additionally,

Table 3-4 provides the monthly precipitation from the current climate and generated precipitation data and the percentage change for the future time frame of the 2080s.

Table 3-3: Sample of generated future precipitation data

Time (hour)	Current Precipitation (m)	Current PW* (m)	Ratio $_{hour}$	2080s PW (m)	2080s Precipitation (m): Ratio $_{hour}$ * 2080s PW
01/23 01:00:00	0.0E+00	12	0.0E+00	14	0.0E+00
01/23 02:00:00	0.0E+00	12	0.0E+00	14	0.0E+00
01/23 03:00:00	0.0E+00	13	0.0E+00	15	0.0E+00
01/23 04:00:00	0.0E+00	13	0.0E+00	15	0.0E+00
01/23 05:00:00	6.6E-04	13	5.1E-05	15	7.6E-04
01/23 06:00:00	1.1E-03	13	8.7E-05	15	1.3E-03
01/23 07:00:00	1.1E-03	14	8.0E-05	16	1.3E-03
01/23 08:00:00	1.1E-03	13	8.7E-05	15	1.3E-03
01/23 09:00:00	1.1E-03	15	7.5E-05	18	1.4E-03
01/23 10:00:00	1.1E-03	18	6.3E-05	21	1.3E-03
01/23 11:00:00	1.1E-03	18	6.3E-05	21	1.3E-03
01/23 12:00:00	1.1E-03	18	6.3E-05	21	1.3E-03
01/23 13:00:00	4.7E-04	19	2.5E-05	22	5.4E-04
01/23 14:00:00	0.0E+00	18	0.0E+00	21	0.0E+00
01/23 15:00:00	6.6E-04	17	3.9E-05	20	7.7E-04
01/23 16:00:00	1.1E-03	20	5.6E-05	24	1.4E-03
01/23 17:00:00	1.1E-03	18	6.3E-05	21	1.3E-03
01/23 18:00:00	4.7E-04	18	2.6E-05	21	5.5E-04
01/23 19:00:00	0.0E+00	18	0.0E+00	21	0.0E+00
01/23 20:00:00	0.0E+00	20	0.0E+00	24	0.0E+00
01/23 21:00:00	6.6E-04	20	3.3E-05	24	7.9E-04
01/23 22:00:00	1.1E-03	18	6.3E-05	21	1.3E-03
01/23 23:00:00	1.1E-03	21	5.4E-05	25	1.3E-03
01/23 24:00:00	4.7E-04	18	2.6E-05	21	5.5E-04

*PW: precipitable water

Table 3-4: Baseline (current) and future precipitation for time periods of 2080s with percentage change in precipitation future climates

Month	Precipitation(mm)-Baseline (1989-2014)	Precipitation(mm) -2080s	Precipitation%-2080s
Jan	52	61	15%
Feb	48	62	23%
Mar	50	66	24%
Apr	69	85	19%
May	74	99	25%
Jun	72	67	-7%
Jul	76	57	-33%
Aug	78	61	-28%
Sep	75	71	-6%
Oct	61	73	16%
Nov	75	94	20%
Dec	58	68	15%
Total	786	864	9%

To validate the generated precipitation data for future climates, projections for Toronto climate were compared to projected precipitation data for future time periods in other studies. In Rincon (2020), the projection precipitation data for Toronto climate were presented for three future time periods of the 2020s, 2050s and 2080s. The projections in Rincon (2020) were based on RCP 4.5 and 8.5 instead of emission scenario A2, which was used in this research. The RCPs are more recent climate scenarios developed by the IPPC that have replaced the Special Report Emissions Scenarios (SRES); A2 emission is one of the four scenarios of this report. The SRES was chosen in this research due to constrains in CCWorldWeatherGen and only offering the A2 emission scenario for projections of future climates. The RCP 8.5 is characterized based on a scenario of increasing greenhouse gas emissions, leading to higher greenhouse gas emissions, while RCP 2.5 represents a climate scenario leading to very low greenhouse gas emissions (IPCC 2014b). Therefore, results for RCP 8.5 instead of RCP 2.5 were chosen from Rincon (2020) to compare the precipitation projections for future times. The RCP 8.5 and the A2 emission have a similar scenario basis and both continue to increase greenhouse gases production in future periods (IPCC 2000a; IPCC 2014b). Figure 3-3(a), presents the monthly precipitation for projected future climates from (Rincon 2020), and Figure 3-3(b), shows the monthly precipitation data for projected years generated in this research.

As observed from Figure 3-3, the precipitation projections for both Figure 3-3(a) and (b), show higher annual precipitation compared to baseline (observed) data. Generally, the future precipitation projection in both Figure 3-3(a) and (b) show higher precipitation during spring and lower during winter. It can also be seen that for projections of 2071–2100 both Figure 3-3(a) and (b), show a decrease in precipitation in June and July while having the highest annual precipitation. Overall, similar monthly trends were observed to precipitation projections presented in (Rincon 2020); however, slight variations were expected due to different emission scenarios, downscaling method, and baseline (observed) period data.

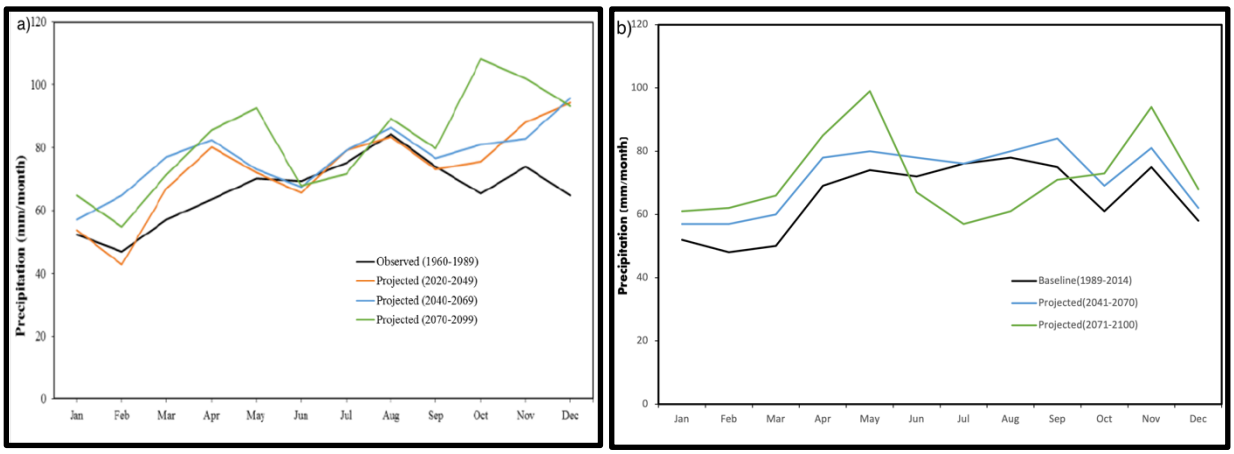

Figure 3-3: Monthly precipitation for projected future climates. Figure 3-3(a) present monthly precipitation for future projected years under RCP 8.5 emission scenario (image reproduced from Rincon 2020). Figure 3-3(b) presents monthly precipitation for future projected years under A2 emissions (this research).

Another study (Zhang et al. 2019) was compared to the projected precipitation data for future periods. In Zhang et al. (2019), the projected precipitation for Canada under emission scenarios RCP 2.5 and RCP 8.5 for two time periods of 2031-2050 and 2081-2100 were presented. It was concluded in Zhang et al. (2019) that under high emissions (RCP 8.5) in the late century (2081-2100), Southern Canada would experience decrease in precipitation during summer (Zhang et al. 2019). Figure 3-4, presents the Canada map for summer precipitation change under emission scenario RCP 8.5 for the two time periods. As observed from the colour shading scale in Figure 3-4, Southern Canada, including Toronto, Ontario, would experience negative percentage precipitation during the 2081-2100 period. Figure 3-5, presents the winter map for Canada changes in precipitation under emissions scenario RCP 8.5 for both periods. Figure 3-5 shows that the Southern Ontario region would experience an increase in precipitation, especially in 2081-2100.

To verify the generated precipitation data in this research, the seasonal precipitation data was compared to the parentage scale coloured map in Zhang et al. (2019).

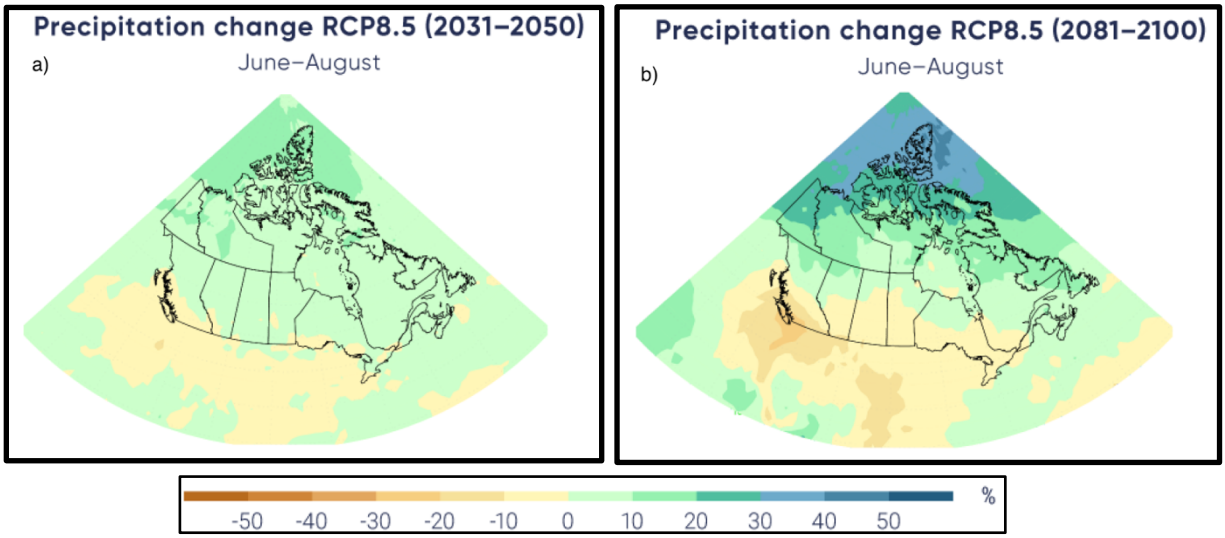

Figure 3-4: Canadian summer precipitation projections under emission RCP 8.5 for periods of 2031-2050 and 2081-2100. Image from (Zhang et al. 2019).

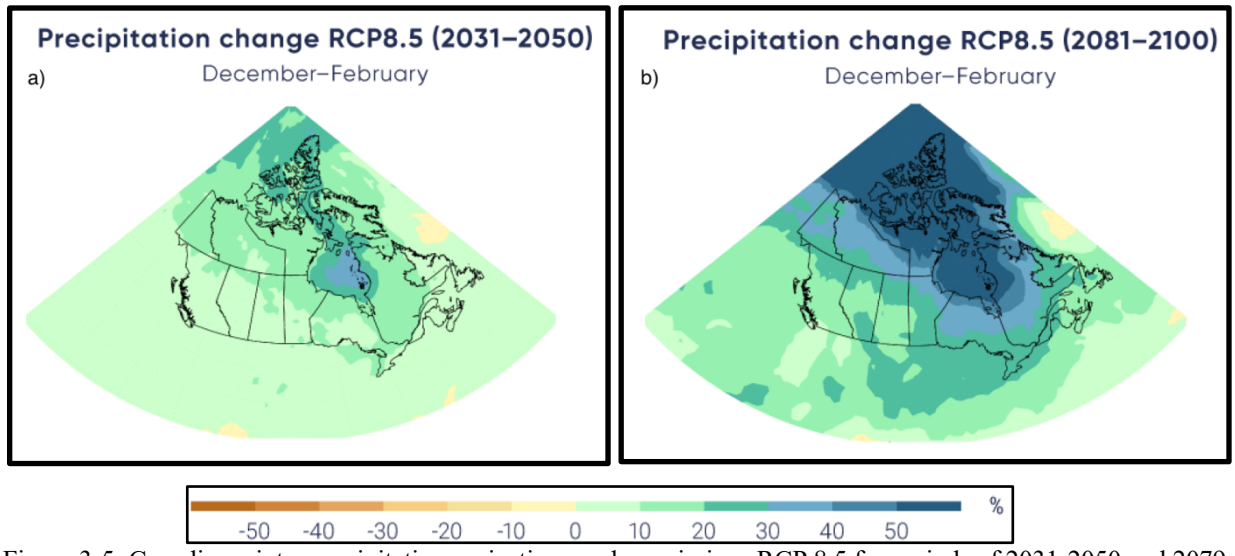

Figure 3-5: Canadian winter precipitation projections under emissions RCP 8.5 for periods of 2031-2050 and 2079-2100. Image from (Zhang et al. 2019).

Table 3-5 presents the seasonal percentage precipitation for the time period of 2071-2100 under A2 emission scenario for the City of Toronto. The seasonal percentage precipitation values in Table 3-5 for the period of 2080s shows negative reduction during the summer season and higher percentage in winter; similar conclusions have also been reported in Zhang et al. (2019).

Additionally, the annual mean percentage precipitation change under emission scenario RCP 8.5 reported in Zhang et al. (2019) for Ontario is 17.3% with 8.5% (25th percentile) and 26.1% (75th percentile) for the period 2080s. The annual mean percentage precipitation for the period of 2080s under the A2 emission scenario generated for the City of Toronto in this research are also presented in Table 3-5. It can be observed based on results in Table 3-5, the annual mean percentage for precipitation for the time period of 2080s is within the findings found in Zhang et al. (2019) for Ontario.

Table 3-5: Seasonal precipitation percentage change for time periods of 2071–2100 under emission scenario A2 (this research).

Season	Precipitation Projected (2071–2100)
Winter	17%
Spring	23%
Summer	-22%
Fall	11%

3.3 Building Archetype and Green Roof Design Parameters

The American Society of Heating and Refrigerating and Air-Conditioning Engineers (ASHRAE), focus on building systems, energy efficiency, indoor air quality, refrigeration, and sustainability of the built environment. ANSI/ASHRAE/IES Standard 90.1 is a globally used benchmark to set minimum energy performance standards (MEPS) and energy codes. It provides minimum requirements for the energy-efficient design of most building types. Standard 90.1 is a crucial reference needed in designing buildings and building simulation tool systems. These reference buildings are supported by DOE and provide complete descriptions for whole-building energy analysis in EnergyPlus software. There are a total of 16 commercial building archetypes available for 19 climate zones, (16 in U.S. cities and three international locations) for Standard 90.1 (DOE 2018). These benchmarks are available for DOE's EnergyPlus simulation software as input files (IDF format). Building archetype models change across various locations, therefore, design and construction of the building needs to be according to the standards and codes of the building location. To comply with the National Energy Code of Canada for Buildings (NECB), ASHRAE Standard 90.1 – 2013 edition was chosen in this research. Each archetype has a designated IDF for each thermal climate zone. The City of Toronto is considered climate zone 5A with cool and humid conditions (Berardi 2020).

In this research, three building archetypes following the ASHRAE standard 90.1-2013 are used. The secondary school archetype is shown in Figure 3-6. The secondary school building model consists of two floors with a roof area of 11,902 m^2 and gross floor area of 19,592 m^2, a window-to-wall ratio of 33%, metal roof albedo of 0.2 and 46 thermal zones.

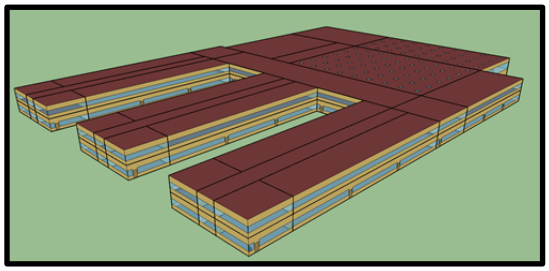

Figure 3-6: Secondary school archetype model from ASHRAE standard 90.1 (DOE 2018).

In addition to the secondary school archetype, two other building types of office and hospital are used to evaluate the thermal energy performance of the green roof. The office building archetype consists of 12 floors with a roof area of 3563 m^2 and a floor area of 46 320 m^2. The window-to-wall ratio of the large office is 37.5%, with a metal roof albedo of 0.2 and 74 thermal zones. The hospital archetype has five floors with a roof area of 3739 m^2 of, floor area of 22,436 m^2, the window-to-wall ratio is 16%, with 162 thermal zones. The layout of both large office and hospital archetypes are provided in Figure 3-7 and Figure 3-8, respectively.

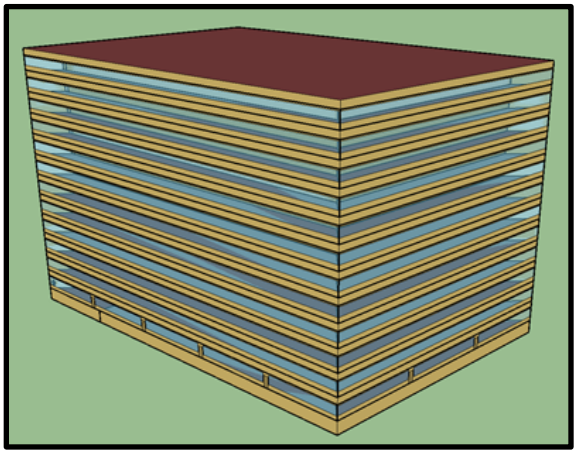

Figure 3-7: Large office archetype model from ASHRAE standard 90.1 (DOE 2018).

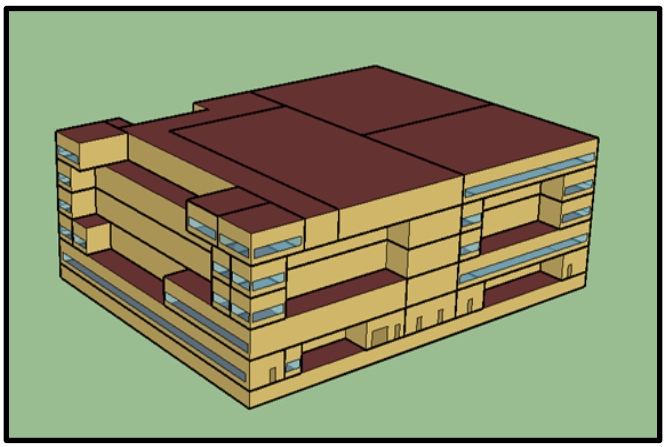

Figure 3-8: Hospital archetype model from ASHRAE standard 90.1 (DOE 2018).

In this research, all building characteristics of the benchmark remained unchanged except for the roof layer structure and the addition of a green roof on the outer roof layer. Three design parameters were examined, through a sensitivity analysis, to determine the effect of green roof thermal performance on building energy reduction: growing media depth, LAI and roof thermal insulation thickness. The purpose was to evaluate thermal performance of extensive green roof types. Therefore, the growing media depths and LAI values were chosen based on extensive green roof design characteristics. As mentioned in section 2.1.1, extensive green roofs, are shallow in growing media depth, are simple to instal, have low cost and maintenance, and are a light load structure compared to intensive green roofs. Hence, extensive green roofs have an advantage over intensive green roofs and can be installed on almost any roof. Therefore, in this research, three growing media depth ranges representing extensive green roofs were selected.

The type of plant selected on green roofs is based on design parameters like LAI, leaf albedo, and plant height. Sedum is a common plant used on extensive green roofs because it can withstand harsh environmental conditions on the roof, and it's also effective in reducing stormwater runoff (Blanusa et al. 2013). Hence, in this research, sedum plant was chosen due to its suitability to the City of Toronto climate. The LAI for sedum reported in studies ranges from 1 to 3 (Ascione et al. 2013; Gomes et al. 2019; Berardi 2016) and therefore these three LAI ranges have been considered in this research.

All green roof parameters (growing media and LAI) and thermal insulation thickness are taken from previous studies (Mahmoodzadeh, Mukhopadhyaya, and Valeo 2020; Berardi 2016). For the

thermal insulation layer, eight different levels of thicknesses were considered. Due to Toronto being located in a heating-dominated region, the thermal insulation layer is required to increase the thermal resistance (R-value) of the roof. Thus, various ranges of thermal insulation thickness were selected from low - high to determine the impact on green roof thermal energy performance. Polyurethane was used as the insulation material with a thermal conductivity, specific heat, and density of 0.04 W/m-K, 1600 J/kg-K and 40 kg/m^3, respectively. A layout of the sensitivity analysis is presented in Figure 3-9 where variations of design parameters for growing media depth, LAI and thermal insulation thickness are provided; in total, there were 72 green roof design simulations for the secondary school building under current climate conditions.

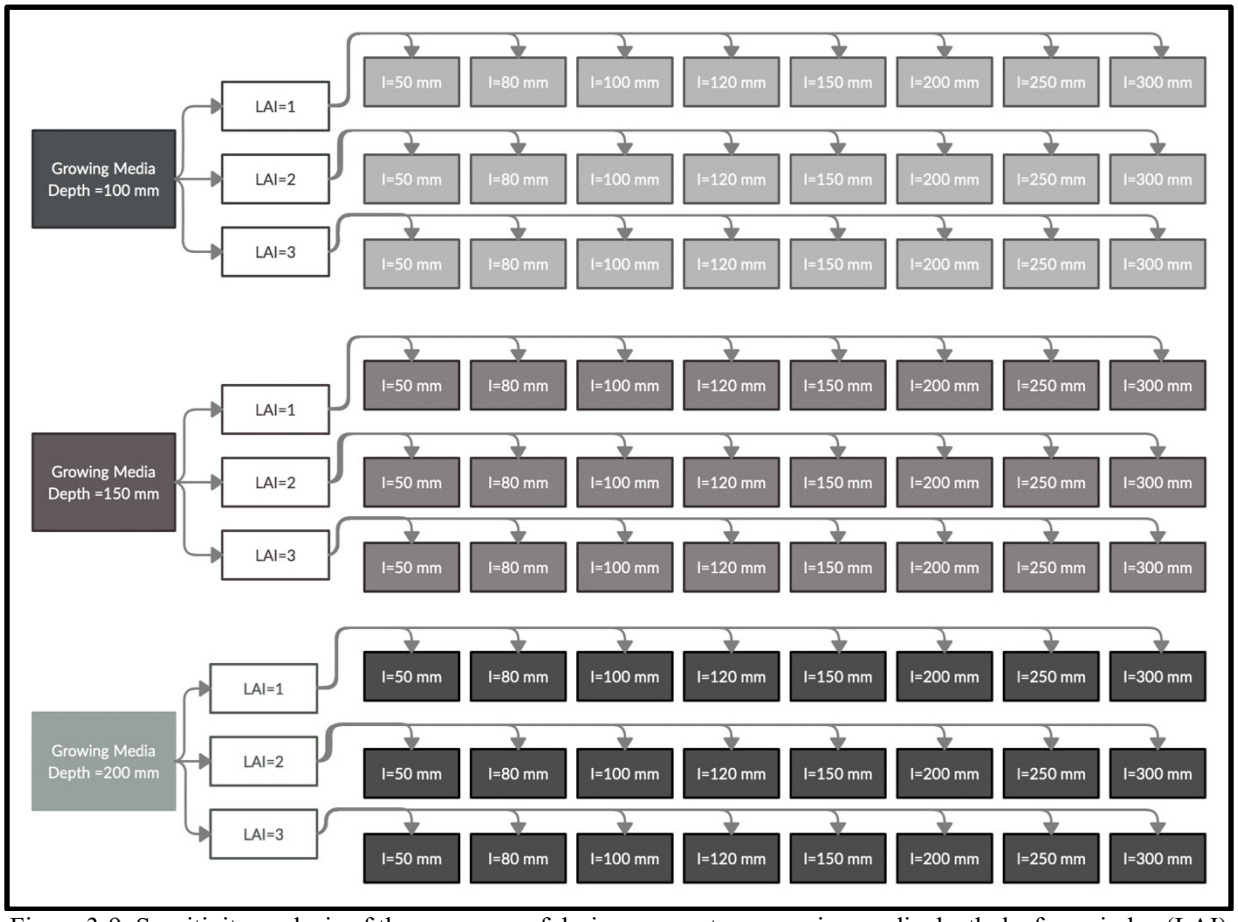

Figure 3-9: Sensitivity analysis of three green roof design parameters: growing media depth, leaf area index (LAI) and insulation (I).

To simulate the green roof on the building roof layer, the design characteristics were defined in the green roof construction element, RoofVegetation (Ecoroof), in EnergyPlus. The input

parameters are height of plant, LAI, leaf reflectivity, leaf emissivity, minimum stomal resistivity and thickness, thermal conductivity, density, specific heat of the growing media layer. In this research, three different growing media depths of 100, 150 and 200 mm and three LAI values of 1, 2 and 3 were chosen to evaluate the thermal performance of green roof through a sensitivity analysis. The remaining green roof parameters remained constant. The list of constant design parameters in the RoofVegetation element of EnergyPlus is provided in Table 3-6. Once input parameters were inserted, the RoofVegetation element was added onto the outer roof layer construction and initializing stage of green roof layer in EnergyPlus was completed.

Table 3-6: Green roof input parameters in EnergyPlus (Ecoroof).

Green Roof Parameter	Input Value
Height of Plants (m)	0.2
Leaf Reflectivity (-)	0.11
Leaf Emissivity (-)	0.95
Minimum Stomatal Resistance (s/m)	300
Roughness	Medium Rough
Conductivity of Dry Soil* (W/m-K)	0.21
Density of Dry Soil* (kg/m3)	765
Specific Heat of Dry Soil* (J/kg-K)	1284
Thermal Absorptance (-)	0.9
Solar Absorptance (-)	0.73
Visible Absorptance (-)	0.75
Saturation Volumetric Moisture Content of the Soil* Layer (-)	0.5
Residual Volumetric Moisture Content of the Soil* Layer (-)	0.01
Initial Volumetric Moisture Content of the Soil* Layer (-)	0.2
Moisture Diffusion Calculation Method	Advance

*Growing media is referred to as soil in EnergyPlus.

The building built-up roof structure in EnergyPlus consists of roof membrane, thermal roof insulation layer, and metal decking (Figure 3-10). The characteristics of the built-up roof structure was defined in the Material construction of the software. The thickness, density, specific heat and thermal conductivity for roof membrane and metal decking remained constant throughout all the simulations using the same characteristic defined in the EnergyPlus construction library tool. The thermal property of the built-up roof structure is provided in Table 3-7. However, to evaluate the thermal insulation thickness effect on green roof thermal performance, variation of insulation

thickness within ranges of 50 to 300 mm were chosen in the sensitivity analysis. The complete roof layer structure is shown in Figure 3-10 where both the built-up roof structure and the added green roof layer are presented.

Table 3-7: Thermal properties of built-up roof structure.

Material	Thickness (m)	Conductivity (W/ m^2.K)	Density (kg/m^3)	Specific Heat (J/kg.K)
Roof Membrane	0.0095	0.16	1120	1460
Insulation Layer	Varies*	0.04	40	1600
Metal Decking	0.008	45.28	7824	500

*Insulation layer thickness varies from ranges of 50 – 300 mm

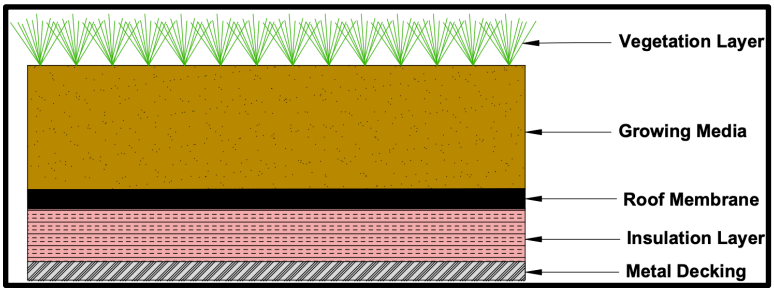

Figure 3-10: Layout of roof structure and green roof layers implemented in EnergyPlus.

Lastly, to add the precipitation data, a schedule file was created using Excel with 8760 hours representing the annual precipitation at hourly duration. There were in total three different schedule files created for each time period of base climate, time horizon 2080s. The created scheduled files were first attached in the Schedule:File object of EnergyPlus, and then the precipitation was defined for each time period using the Site:Precipitation object.

The analysis for the secondary school archetype served as the primary stage, where optimal design criteria for green roof design parameters were established (chapter four). In the secondary stage of the research, office and hospital archetypes were chosen to evaluate the green roof thermal performance with respect to optimal designs outcomes from the primary stage (chapter five). In the second stage, the design parameters selected are mainly influenced by the outcome from the preliminary results, which are discussed in chapter four.

For both office and hospital archetypes only three insulation thicknesses of 50 mm, 120 mm and 300 mm were chosen. The green roof design parameters were growing media depth of 100 mm,

150 mm and 200 mm with LAI of 1, 2 and 3. The impact of thermal insulation thickness was analysed through four levels of no insulation, low insulation (50 mm), medium insulation (120 mm) and high insulation (300 mm). All other design parameters remained the same as in the preliminary stage; this includes green roof constant parameters and the built-up roof structure characteristics.

3.3.1 Modelling Verification

EnergyPlus software is a widely accepted simulation tool in modelling annual building energy consumption. In EnergyPlus, Ecoroof has been implemented to create a representation of green roof energy and water balance. In Sailor (2008), the Ecoroof model was tested successfully using observations from a monitored green roof in Florida. However, to verify the green roof modelling in this research, comparison of results from other studies are used. Various research studies that used EnergyPlus software for either building thermal simulation modelling were chosen and sub-sections of the research results were replicated to verify the correct use of EnergyPlus. Although it was challenging to replicate other studies due to lack of all simulation details, general trends were seen that established confidence in the model and its ability to predict energy consumption of buildings with green roofs. In particular, the following was tested: use of the various archetypes, correct implementation of Ecoroof, impact of green roof on cooling and heating loads, impact of thermal insulation, and implementation of growing media depth and LAI in EnergyPlus.

To test the use of various archetypes, a study using EnergyPlus software to analyse the effect of various roof designs on building energy consumption under four different climates was used. The investigation used two different archetype buildings, office and multi-lodging buildings for each city of New York City, New York; Houston, Texas; Phoenix, Arizona; and Portland, Oregon. The electricity and gas consumption for each archetype in all city climates were presented in Sailor, Elley, and Gibson (2012) . To verify proper use of archetypes and EnergyPlus simulation system, results for two archetype buildings (office and multi-lodging building) were replicated and compared to findings in Sailor et al. (2012). The roof design presented in Sailor et al. (2012) were used to regenerate the building characteristics and simulations using EnergyPlus software were conducted. The annual energy consumption results generated were then compared to findings in

Sailor et al. (2012) and presented in Figure 3-11(a) and (b). The identical weather climate data used in Sailor et al. (2012) was unavailable and the replicated results were generated based on a newer version of climate data with higher cooling degree days (CDD) and lower heating degree days (HDD). The difference in CDD and HDD resulted in a higher electricity consumption due to higher CDD and lower gas consumption due to lower HDD, for both buildings (Figure 3-11). However, the comparison of the annual energy consumption for two building archetypes in the four cities showed a similar trend between the generated results and Sailor et al. (2012). It can be observed that the total energy consumption of the archetypes in the four various climate cities follow a similar trend in both Figure 3-11(a) and (b) and that the multi-lodging building (L) consumes more annual energy than the office building (O). Since the objective of this exercise was to verify that the building archetypes were being used correctly, the results corroborate that this was achieved.

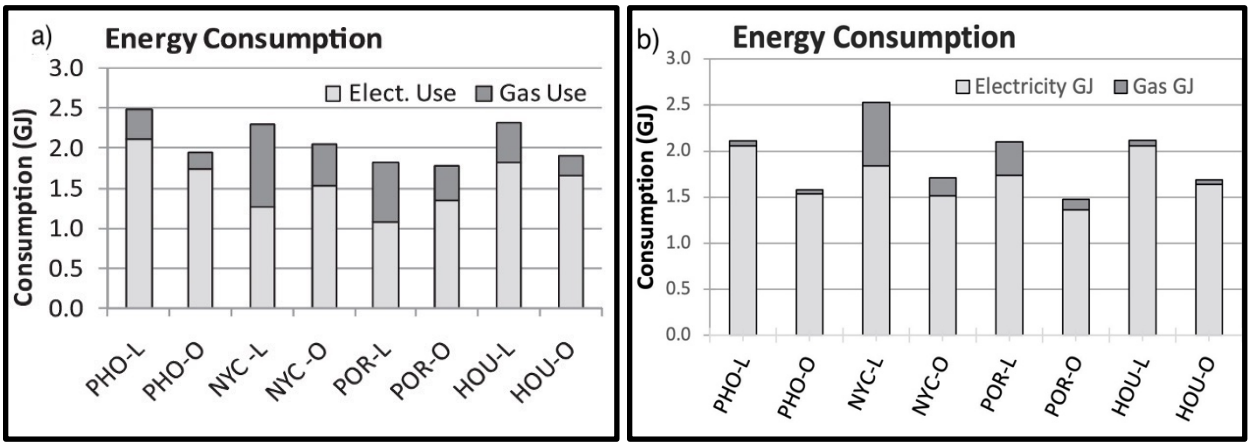

Figure 3-11: Annual energy consumption of multi-lodging (L) and office (O) building in four climates of Phoenix (PHO), New York City (NYC), Portland (POR) and Houston (HOU). Figure 3-11(a) are the plots from (David J. Sailor, Elley, and Gibson 2012) and Figure 3-11 (b).

To ensure that the Ecoroof model in EnergyPlus works properly, a replica of results from Berardi (2016) was selected, where EnergyPlus was used to evaluate the effect of several green roof designs on a retrofit building in Toronto, Canada. In Berardi (2016), local microclimate weather data was used to observe the impact of an extensive green roof on building energy savings at a university campus in Toronto, Canada. EnergyPlus software was used to compare the energy-saving results of four green roof designs. The measured building energy consumption was

compared to the simulated one using EnergyPlus and confirmed the validity of Ecoroof model in Berardi (2016). To verify that the Ecoroof model simulation in this research is executed correctly, results for the four simulated green roof models in Berardi (2016) were replicated and compared. It should be noted that using the identical building model used in (Berardi 2016) was difficult due to a variety of unknown building characteristics; therefore, the secondary school archetype model from ASHARE Standard 90.1-2013, which has the closest building characterises to a university campus, was used instead. The results for the annual energy savings for the four green roof designs from Berardi (2016) and the replicated results are presented in Figure 3-12. It is difficult to verify the whole energy building model when different reference building models are used since the building system, energy usage, equipment, occupant, and characteristics vary. Therefore, variation in magnitude of annual energy savings for the four green roof designs in cooling, heating and fan system was compared. As observed in Figure 3-12(b), the replicated results for cooling loads (cooling load and fan system) are different compared to (Berardi 2016) plots, Figure 3-12(a). The cooling load energy savings are much lower, and fan system energy savings are much higher for Figure 3-12(b) compared to Figure 3-12(a). This shift in the distribution of energy savings in cooling load and fan system in Figure 3-12(a) and (b), could be due to different types of Heating, Ventilation and Air Conditioning (HVAC) systems and the effect on building energy consumption usage on cooling type. Additionally, the trend in energy savings for each roof design for the heating load was different than Berardi (2016) (Figure 3-12). This is due to unavailability of information for green roof characterises such as growing media thermal properties, roof optical properties and roof insulation parameters which all affect the heating saving. Most green roof parameters, as well as roof insulation, were assumed in replicating the plots from Berardi (2016). Another reason for the difference in results was the use of different weather climate data. In Berardi (2016), a local weather station of the City of Toronto was used whereas the replicated results in this research was based on the weather station of Toronto Pearson International airport. Although similar, these two weather data can result in some differences between the two studies.

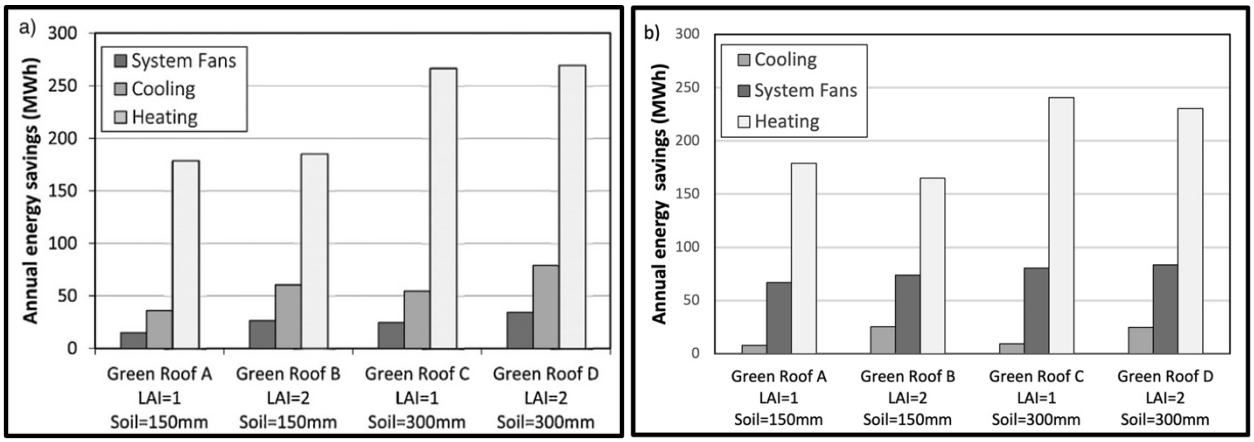

Figure 3-12: Annual energy savings for all green roof designs with divided energy use. Figure 3-12(a) are plots from (Berardi 2016) and Figure 3-12(b) represents the replicated results.

However, once the total annual energy savings of all green roof designs were compared, results followed the same conclusion as found in Berardi (2016), where higher growing media (soil depth) and higher LAI achieved the highest building energy savings. In Figure 3-13, the results for total monthly energy savings for all four green roofs are compared to the findings in Berardi (2016). The trend for the total annual energy savings of the four green roof designs in Figure 3-13(b) is similar to the results found in Berardi (2016), shown in Figure 3-13(a); excluding the slight variations which were due to reasons mentioned previously. The comparison of results of the two studies show that green roof design parameters such as LAI and growing media (soil) depth are behaving similarly, and therefore the implementation of the EcoRoof within EnergyPlus was done correctly.

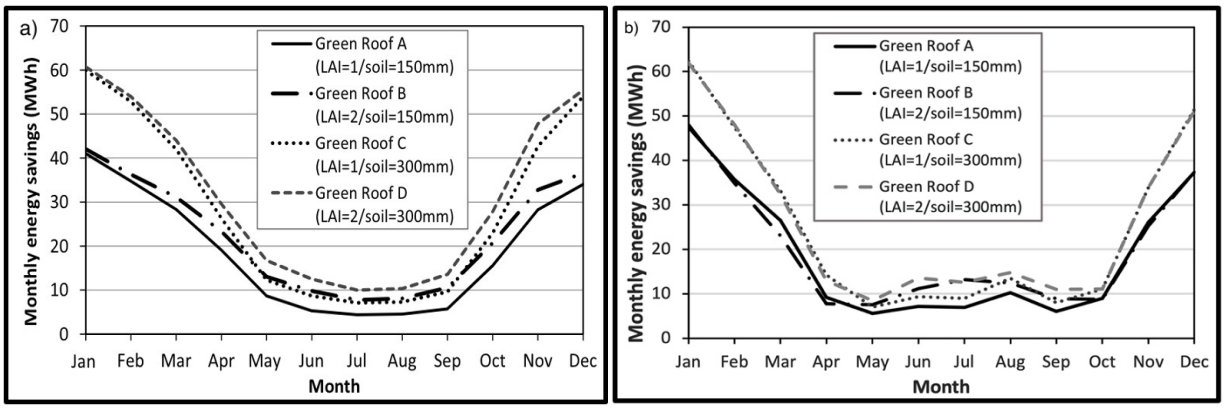

Figure 3-13: Monthly energy savings for four green roof designs. Figure 3-13(a) results from (Berardi 2016) and Figure 3-13(b) represents the replicated plot.

Another study was used to compare cooling and heating results of Ecoroof using EnergyPlus based on Toronto, Canada climate. Mahmoodzadeh et al. (2020) evaluated the influence of green roof parameters on the thermal energy performance of a secondary school building, using EnergyPlus, in four North American climates of Vancouver, BC; Toronto, ON; Las Vegas, NV; and Miami, FL. In Mahmoodzadeh et al. (2020), several green roof design parameters such as LAI, growing media depth, leaf albedo, plant height and thermal insulation were considered in evaluating green roof thermal performance. For comparison purposes, only part of the results reported in Mahmoodzadeh et al. (2020) were used to replicate and verify the impact of green roof on cooling and heating loads under the City of Toronto climate. The same archetype model of secondary school, ASHRAE Standard 90.1-2013, and identical green roof design parameters were used to replicate results. Figure 3-14(a) plots green roof heating loads with LAI variations from Mahmoodzadeh (2020) and Figure 3-14(b) represents the replicated results. As it can be observed, the trend in green roof designs with different LAIs are similar; the only difference is the magnitude of the heating load. The same outcome could be seen in Figure 3-15(a) and (b), where cooling loads for the green roof with variation in LAI are provided. The variation between the two models could be the addition of an insulation layer and the insulation material characterises that were unknown. Comparison results concluded that the green roofs under the City of Toronto climate using EnergyPlus are behaving accordingly with respect to the design parameters used in Mahmoodzadeh (2020). Although the magnitude of the heating and cooling loads were different, the trend and impact of green roof designs were similar.

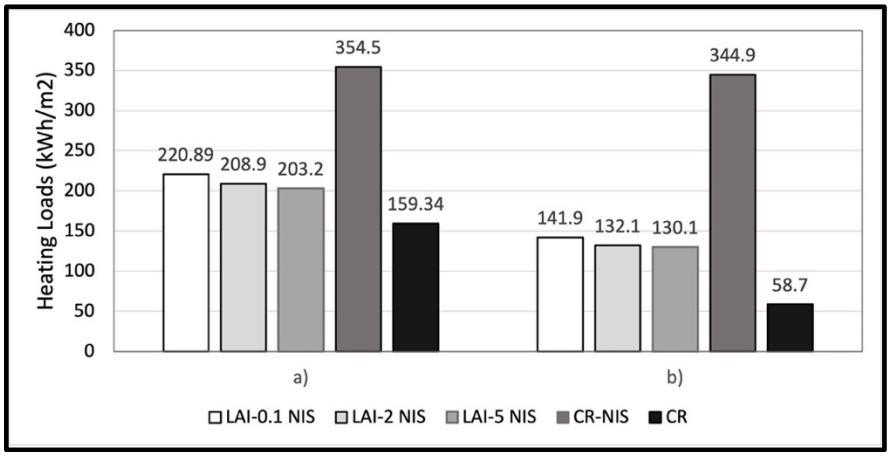

Figure 3-14: Annual heating loads (MWh) for green roof design with three of LAI 1, 2 and 3 no insulation (NIS); insulated conventional roof (CR) and no insulation conventional roof (CR-NIS). Figure 3-14(a) represents results from (Mahmoodzadeh, Mukhopadhyaya, and Valeo 2020) and Figure 3-15(b) are the replicated results.

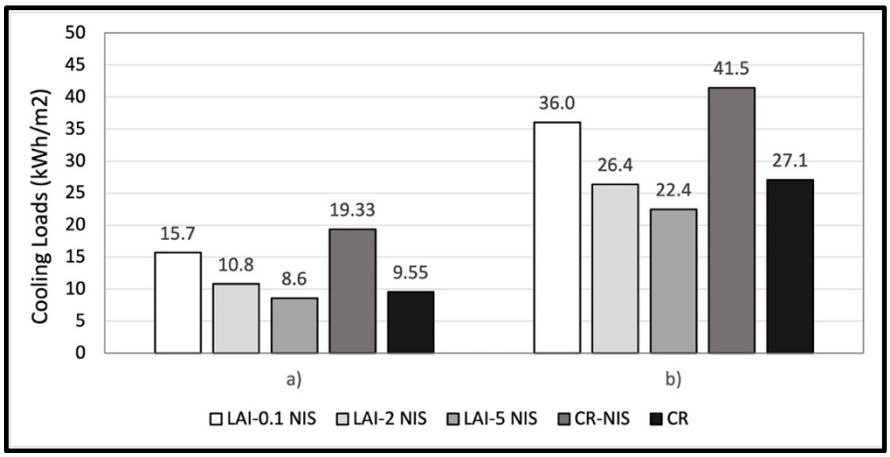

Figure 3-15: Annual heating loads (MWh) for green roof design with three of LAI 1, 2 and 3 no insulation (NIS); insulated conventional roof (CR) and no insulation conventional roof (CR-NIS). Figure 3-15(a) represents results from (Mahmoodzadeh, Mukhopadhyaya, and Valeo 2020) and Figure 3-15(b) are the replicated results.

As mentioned before, it is crucial to verify that the modelling system of Ecoroof in EnergyPlus is correct and results are following the same behaviour established in other research studies. The growing media depth and LAI and their impact on green roof thermal performance have been verified by comparing results to Berardi (2016) and Mahmoodzadeh et al. (2020). However, the impact of thermal insulation thickness layer, which is a design parameter used in this research, and its impact on the energy performance of green roof also needs to be confirmed with other research studies. Therefore, Moody and Sailor (2013) work was used to verify the impact of thermal insulation layer on green roof energy performance using Ecoroof in EnergyPlus. The Dynamic Benefit of Green Roofs (DGBR), which is the ratio of HVAC energy use for a building with a

conventional roof to that of a building with a green roof, was used to evaluate the thermal performance of green roofs in Moody and Sailor (2013). In other words, if the green roof results in lower energy use compared to a conventional roof with the same level of thermal resistance, then the DBGR value would be greater than unity.

In Moody and Sailor (2013), an office building archetype model was used to estimate the DGBR in four climates of Portland, Oregon; Chicago, Illinois; Atlanta, Georgia; and Houston, Texas. To verify the impact of thermal insulation on green roofs using EnergyPlus, part of the results was used to replicate and compare with findings in Moody and Sailor (2013). Variety of thermal resistance (R-values) were used in Moody and Sailor (2013) to observe the effect on HVAC energy usage during summer in Portland. The purpose was to show that adding insulation onto green roof increases the energy use of HVAC as well as showing the HVAC energy consumption curve for the conventional and green roof asymptotically approach each other but do not cross. The same office building archetype with similar green roof design parameters and insulation characteristics were used to simulate building thermal loads under Portland climate using EnergyPlus software. It should be noted, that the green roof design parameters and insulation characteristics used in replicating the results were not identical to Moody and Sailor (2013), due to unavailability of the information; thus, variation in results were anticipated. Figure 3-16 presents the asymptotic behaviour of HVAC energy consumption during summer for the conventional and green roof as insulation was added. It can be observed in Figure 3-16 (a) and (b) that the results from this research follow similar trends to that of Moody and Sailor (2013). Therefore, it was concluded, the Ecoroof model is working correctly, and for different R-values the HVAC system is behaving similarly to results found by others (Moody and Sailor, 2013).

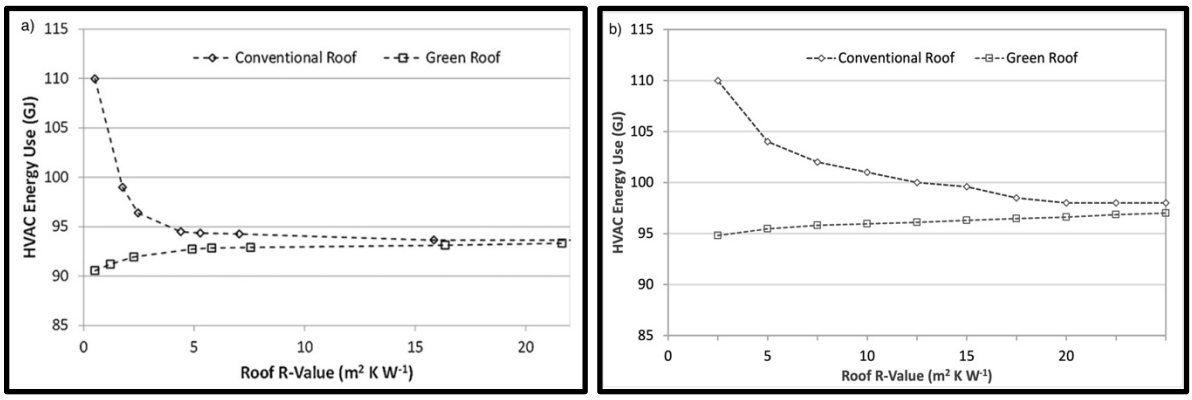

Figure 3-16: Asymptotic behaviour of HVAC energy usage of a conventional and green roof with added insulation layer. Figure 3-16(a) is a plot from (Moody and Sailor 2013) and Figure 3-16(b) is the replicated work.

Other approaches were used to conform to the proper use of EnergyPlus and Ecoroof modelling. EnergyPlus installation comes with example files; "EcoroofOrlando.idf" is one of many examples provided where the use of the "Material: RoofVegetation" object, also known as Ecoroof, is demonstrated. All example files also include an HTML output file, where the results for each example simulations are provided. The "EcoroofOrlando.idf" was used to run the simulation in EnergyPlus and results for the cooling/heating loads (W) for each zone under the "Zone Sizing Information" were compared and verified with the given HTML output in the example files.

Lastly, all results regarding simulations in EnergyPlus and use of Ecoroof were also verified by a source, Bigladder software, which is a Denver-based company, providing software and services for building the energy modelling industry. They specialise in all information related to the EnergyPlus simulation engine and provide consulting services.

3.4 Evaluation

This research analyses the green roof thermal performance on reducing the energy consumption of specific building types under current and future climate conditions in Toronto. Three design parameters, thermal insulation thickness, green roof growing media depth and LAI, are considered. The influence and importance of each parameter on green roof thermal performance are quantified. The overall objective of this research is to determine the optimal green roof design parameter for the City of Toronto that would be most effective in lowering the energy consumption of secondary school, office and hospital buildings.

In chapter four, a sensitivity analysis is performed by varying three design roof configurations, insulation thickness layer, growing media depth and LAI. All design simulations are performed on secondary school buildings, and the annual heating, cooling and total energy consumption for each design is presented for both green roof and reference conventional roof. The reference (conventional) roof in this research is a building with no green roof installed. The building thermal performance is evaluated by comparing the green roof energy consumption to the conventional reference roof. Results are reported in the amount of energy saved (MWh) for annual cooling and heating loads for each design. The growing media surface temperature (℃) and rate of evapotranspiration (mm/day) are also reported to measure the impact of LAI for green roof design on building thermal performance. The building inside surface temperature for both the green roof and reference conventional roof are compared and reported to analyse the effect of green roof designs on roof ceiling temperature. The cooling and heating loads for all designs are evaluated for each season to understand the impact of green roofs on building energy consumption. The green roof energy savings compared to the conventional are also measured. In addition, the Dynamic Benefit of Green Roof (DBGR) for all green roof designs are reported under both current and future climate conditions to evaluate the impact of insulated green roofs with the conventional roof of same insulation thickness.

In chapter five, the annual cooling and heating energy consumption for an office and hospital building design are compared to the conventional roof under current and future climates. In addition, all green roof designs are compared to conventional reference roofs to evaluate the impact of green roof thermal performance; results are presented in the amount of energy saved (MWh) for both heating and cooling loads. The DBGR for all green roof designs are reported. Lastly, the amount and percentage of water captured by the green roof for all three building types are presented.

Chapter Four: Results and Discussion

This chapter presents the results from modelling green roof designs under both current and future climate conditions for a secondary school. The annual total heating and cooling for each green roof designs are compared to the conventional reference roof. The impact of different LAI on green roof thermal performance through growing media surface temperature and evapotranspiration rate are analysed. The influence of different growing media depths and insulation thicknesses on the inside surface temperature of green roofs versus the conventional roof are explained. In addition, the seasonal cooling and heating variation for all green roof designs are compared to the conventional roof to determine the behaviour and performance of green roofs under each season. Furthermore, the green roof energy savings on total annual cooling and heating loads are compared to the conventional roof and reported. Finally, the DBGR values are presented to determine the decrease in building annual energy consumption using green roofs compared to a conventional roof with the same R-value.

4.1 Secondary School - Current Climate

The secondary school building uses electricity for cooling and gas for the heating loads. Figure 4-1, Figure 4-2 and Figure 4-3 show all the roof design combinations for heating, cooling, and total energy consumption (heating and cooling) for the secondary school. Each figure compares the energy consumption of the conventional reference roof and the green roof designs for different growing media (GM) depth and LAI with and without insulation thicknesses. Figure 4-1 and Figure 4-2, illustrate how the secondary school is a heating-dominated building as it uses more heating than cooling load. For example, the heating load for the insulated conventional building with an insulation thickness of 50 mm, was 844 MWh, while the cooling load was only 322 MWh. Comparing the conventional reference uninsulated roof to the different uninsulated green roof configurations showed heating and cooling energy consumption were lowered significantly, shown in Figure 4-1 and Figure 4-2 (NI represents no insulation thickness). However, the conventional and green roof designs with the same insulation thicknesses showed a smaller difference than uninsulated roofs. This indicates that uninsulated green roofs decreased building

cooling and heating loads more effectively than insulated green roofs. Furthermore, the results showed that as the insulation thickness increases, the efficacy of green roofs decreases, and insulation thickness becomes dominant.

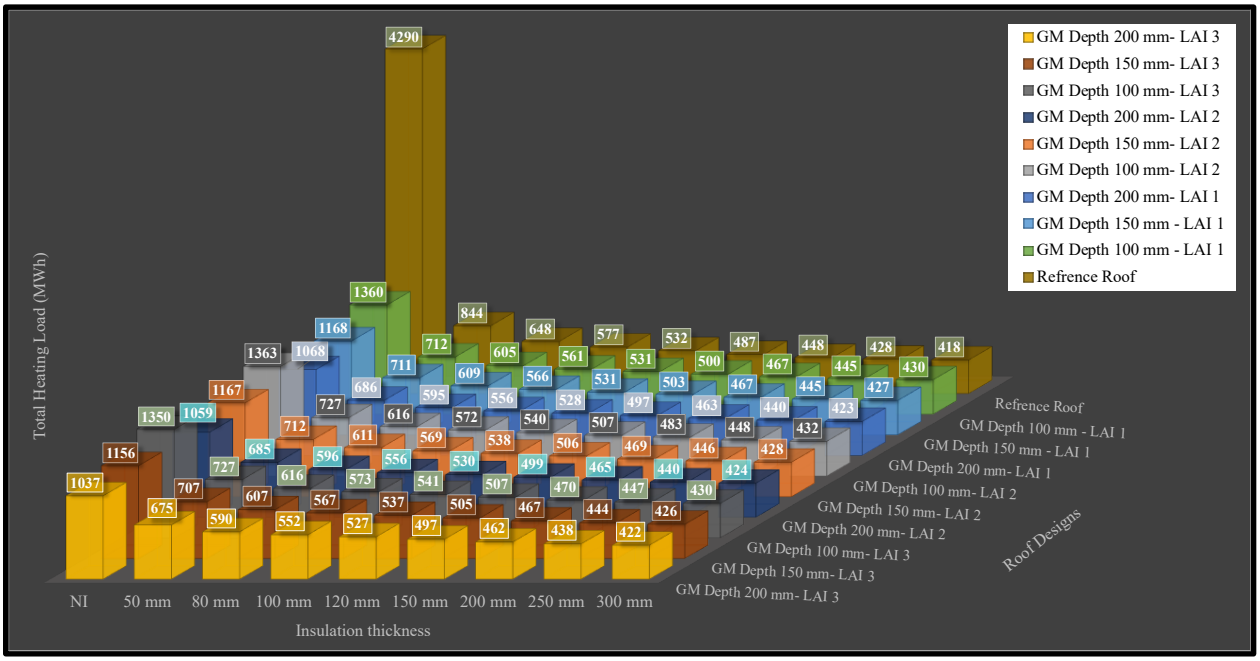

Figure 4-1: Total heating loads for all roof designs; all insulation thickness; LAIs; and growing media depths under current climate conditions – secondary school.

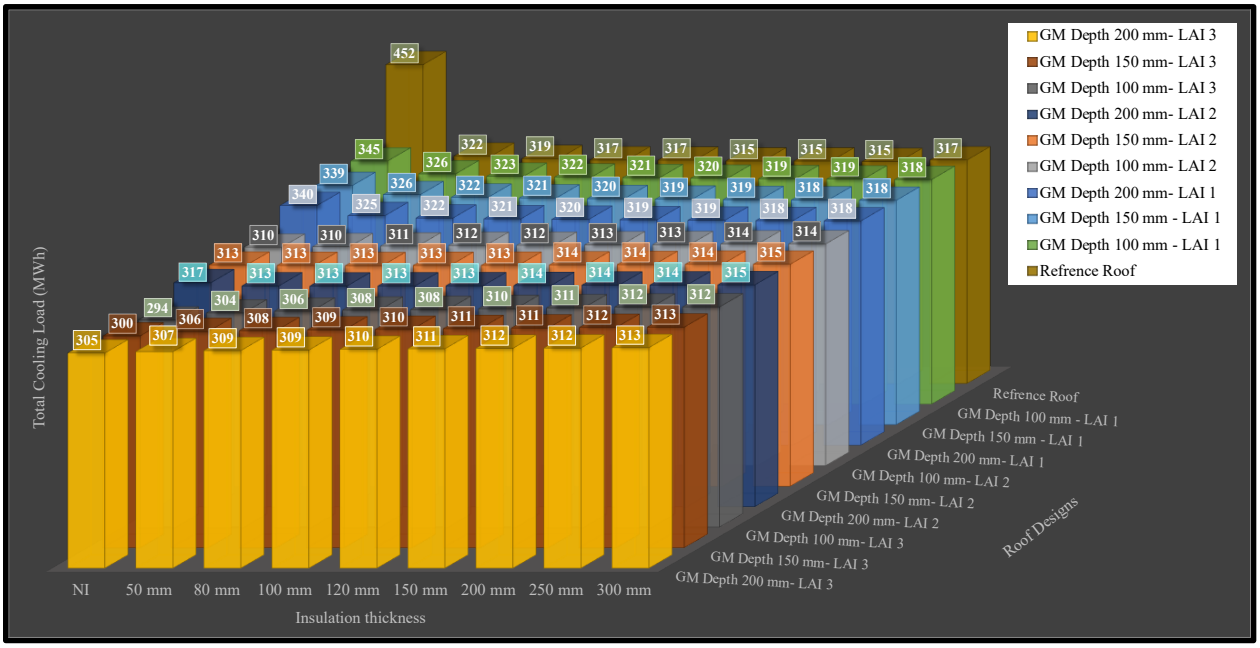

Figure 4-2: Total cooling loads for all roof designs; all insulation thickness; LAIs; and growing media depths under current climate – secondary school.

As seen in Figure 4-1, for each LAI and insulation thickness combination, the 200 mm growing media depth was the most effective in decreasing the heating load compared to the 100 mm and 150 mm depths. This was due to the growing media of the green roof acting as an insulator. Hence, a deeper growing media depth resulted in higher insulation effect on the roof and lowered the building heating load consumption more compared to lower growing media depths. These results align with the findings reported in Berardi (2016) and Mahmoodzadeh et al. (2020), under Toronto climate, where higher growing media depths have shown to decrease the heating loads more compared to lower growing media depths.

In Figure 4-2, it was evident that the use of LAI of 3 led to a lower cooling energy consumption than LAI of 1 and 2 for the same insulation thickness. This is because the green roof vegetated area, through evapotranspiration, provided a cooling effect and caused lower building cooling loads. The higher evapotranspiration rate of larger LAI led to lowering the building cooling loads more than smaller LAIs. The impact of different LAIs on cooling loads were similar to findings in MacIvor et al. (2016), where larger LAI reduced higher cooling loads. However, the added insulation thickness layer impacted the green roof's cooling effect and caused an increase in the building's cooling loads. For example, the green roof design with a growing media depth of 200 mm and LAI of 3 with insulation thickness of 50 mm consumed a cooling load of 307 MWh, while with insulation thickness of 300 mm the green roof cooling load is increased to 315 MWh.

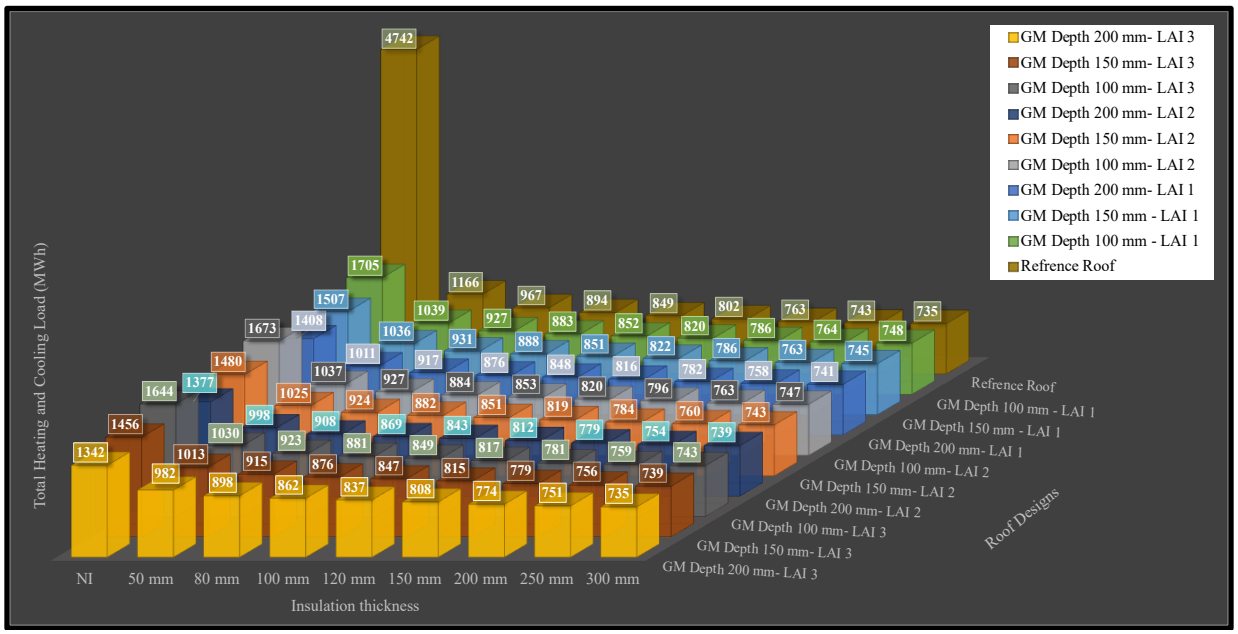

Figure 4-3: Total heating and cooling loads for all roof designs; all insulation thickness; LAIs; and growing media depths under current climate conditions – secondary school.

Figure 4-3 presents the secondary school combined total energy consumption for heating and cooling loads. The growing media depth of 200 mm with an LAI of 3 resulted in the lowest total energy consumption compared to other green roof designs for various insulation thicknesses. Additionally, the uninsulated green roof with growing media depth of 200 mm and LAI of 3 had the highest energy consumption reduction of 71.7% compared to the conventional uninsulated roof, shown in Figure 4-3. This showed that the combined effect of high growing media depth of 200 mm decreased the heating loads and the use of LAI of 3 decreased the cooling loads which resulted in the lowest total energy consumption of the building. Thus, the use of high insulation thickness on green roofs resulted in increased total heating and cooling loads compared to insulated conventional roofs. This can be observed in Figure 4-3, where at insulation thicknesses above 120 mm, green roof designs started to consume more energy than the conventional roof, and green roofs no longer provided any energy benefit. Additionally, the green roof thermal performance became limited when insulation thicknesses were greater than 120 mm since the added insulation took over as the dominant effect.

In this research, the objective was to determine suitable design parameters for green roofs in Toronto. It is essential to understand the behaviour of each green roof design parameter on building

thermal performance to identify an optimal green roof design. Therefore, in the following sections, the impact of LAI, growing media and insulation thickness on green roof thermal performance are defined and evaluated. Additionally, to better understand the behaviour of green roof designs compared to conventional reference roofs, the seasonal heating and cooling loads of the conventional roof and green roof designs are compared as well as the annual energy savings achieved by the green roofs.

4.1.1 Impact of LAI on Evapotranspiration and Growing Media Surface Temperature

The green roof with a larger LAI would provide more coverage on the roof surface and shield the roof from solar radiation exposure. Hence, higher LAI would result in lower growing media surface temperature. Additionally, LAI affects the evapotranspiration rate; a higher LAI would result in a higher evapotranspiration rate, lowering roof surface temperature through cooling.

Growing Media Surface Temperature

This section only considers the uninsulated green roof designs in analysing the impact of LAI values on growing media surface temperature. Figure 4-4 presents the surface temperature during typical summer days for various LAIs with a growing media depth of 200 mm. Figure 4-4 shows that the surface temperature for all green roof designs was generally higher than the ambient temperature due to higher solar radiation absorption. However, the green roof design with LAI of 3 and 2 had lower surface temperatures with an average of 22.6 ℃ and 22 ℃, respectively, compared to LAI of 1 with average surface temperatures of 28.6 ℃. This is because the higher LAI provided more vegetated coverage during summer and decreased the roof surface temperature. The use of larger LAI also led to cooler surface temperature than smaller LAI when growing media depth of 100 mm and 150 mm were used due to more coverage.

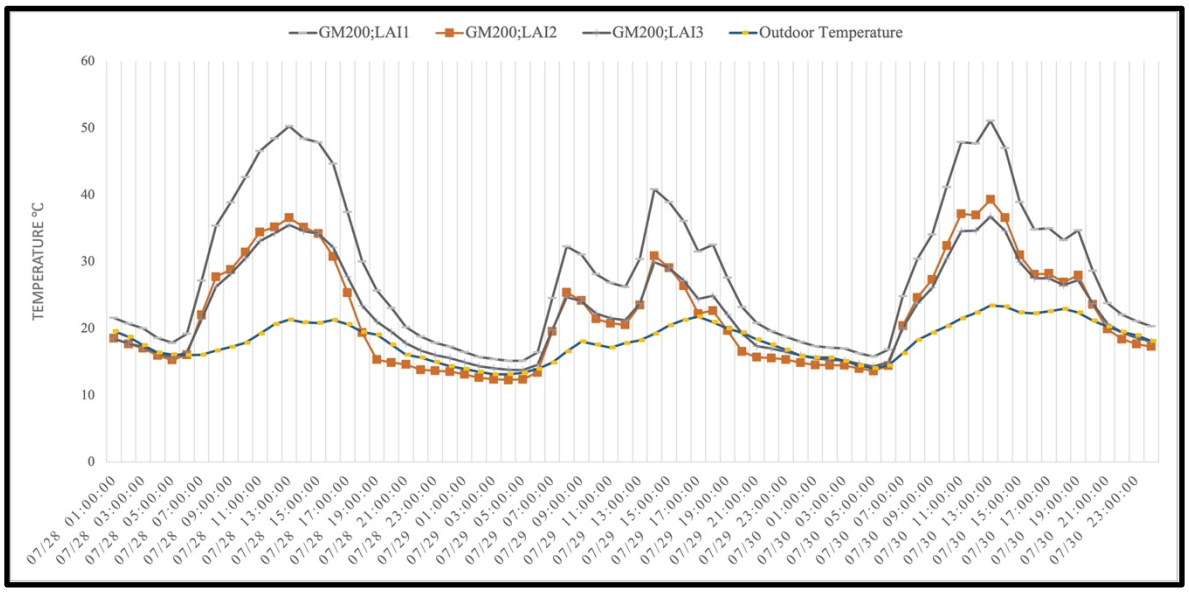

Figure 4-4: Growing media surface temperature for green roof design with growing media depth of 200 mm and LAI of 1, 2 and 3 in typical summer days - no insulation.

Figure 4-5 and Figure 4-6 presents the surface temperature during typical spring and fall day, respectively, for various LAIs with growing media depth of 200 mm. In spring and fall, similar to patterns in summer, the green roof surface temperature was higher than the ambient temperature. However, during spring, due to higher solar absorption compared to fall, the growing media surface temperature was warmer for a more extended period throughout the day. Additionally, LAI of 3 resulted in a lower average surface temperature for spring and fall than LAI of 1 and 2. This is due to evapotranspiration being larger for LAI of 3, leading to higher cooling and decreasing the roof surface temperature. Figure 4-5 presents the roof surface temperature for typical spring days; LAI of 3 resulted in an average roof surface temperature of 14.3 ℃, while LAI of 1 and 2 resulted in an average surface temperature of 15.2 ℃ and 15 ℃, respectively. Similar findings are observed during fall (Figure 4-6), where the average surface temperature for LAI of 3 is 19.8 ℃ while for LAI of 1 and 2, the temperatures are 20.9 ℃ and 20.5 ℃ respectively. In both spring and fall, larger LAI led to cooler surface growing media surface temperatures for 100 mm and 150 mm depths.

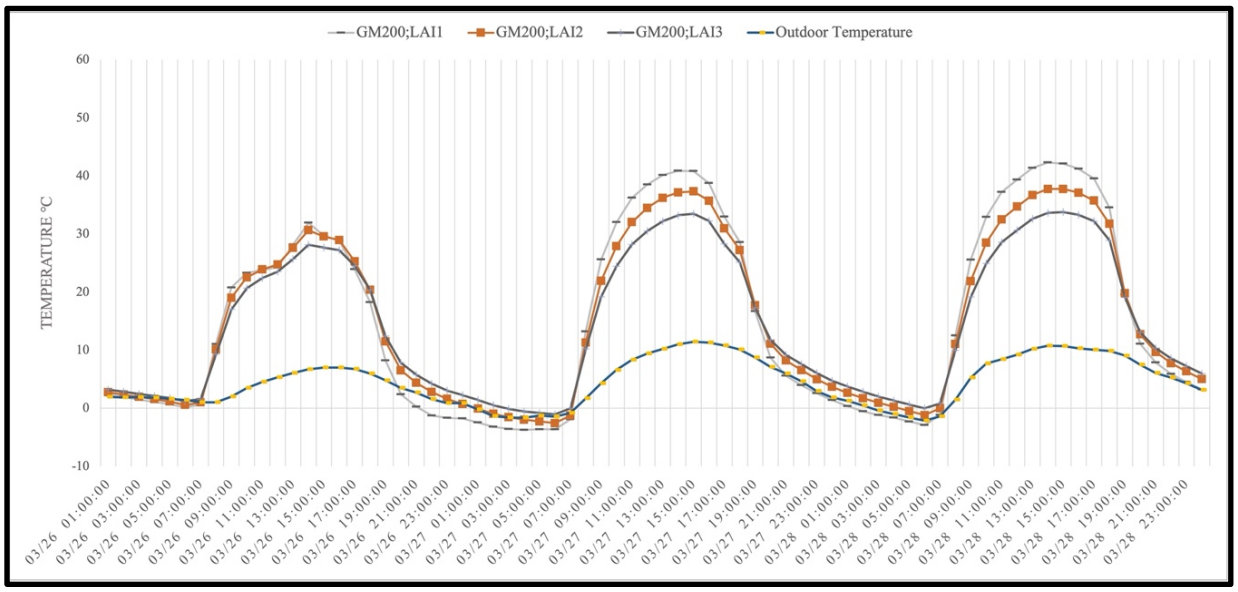

Figure 4-5: Growing media surface temperature for green roof design with growing media depth of 200 mm and LAI of 1, 2 and 3 in typical spring days - no insulation.

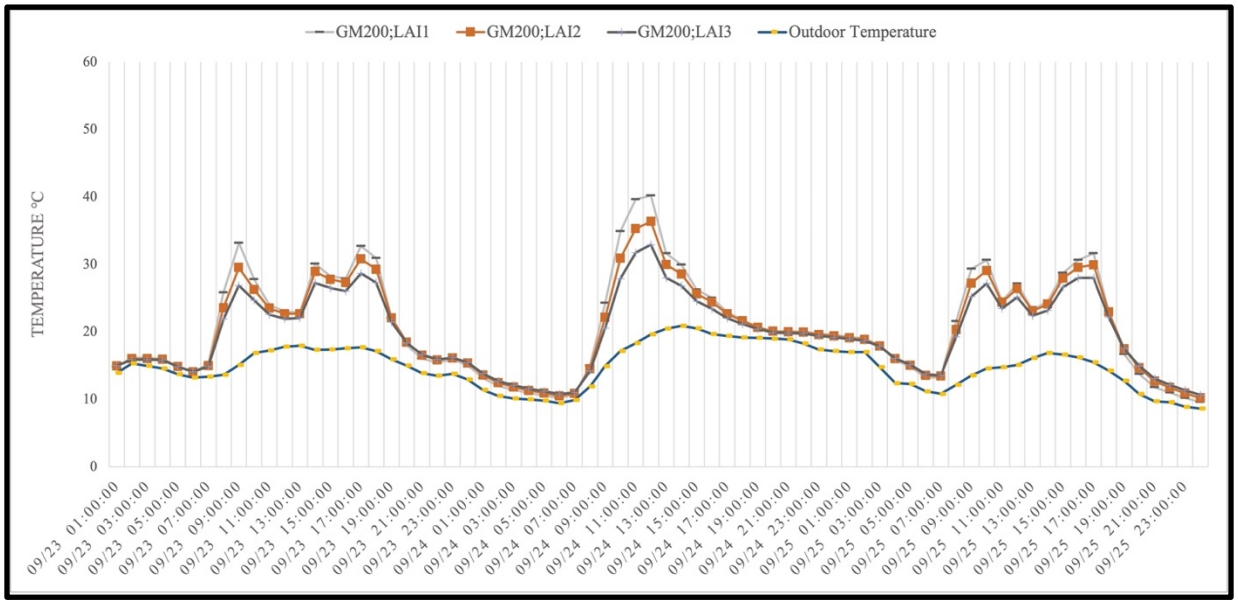

Figure 4-6: Growing media surface temperature for green roof design with growing media depth of 200 mm and LAI of 1, 2 and 3 in typical fall days - no insulation.

During typical winter days, use of green roof designs with LAI of 1, 2 and 3 had an average roof surface temperature of 1.1 ℃, 1.2 ℃ and 1.0 ℃, respectively while the average ambient temperature was -4.7 ℃ for growing media depth of 200 mm (Figure 4-7). All LAI of 1, 2 and 3 acted as insulators and caused warmer roof surface temperatures than the ambient temperature,

shown in Figure 4-7. The growing media surface temperatures were similar for all LAIs when growing media depths of 100 mm and 150 mm were used.

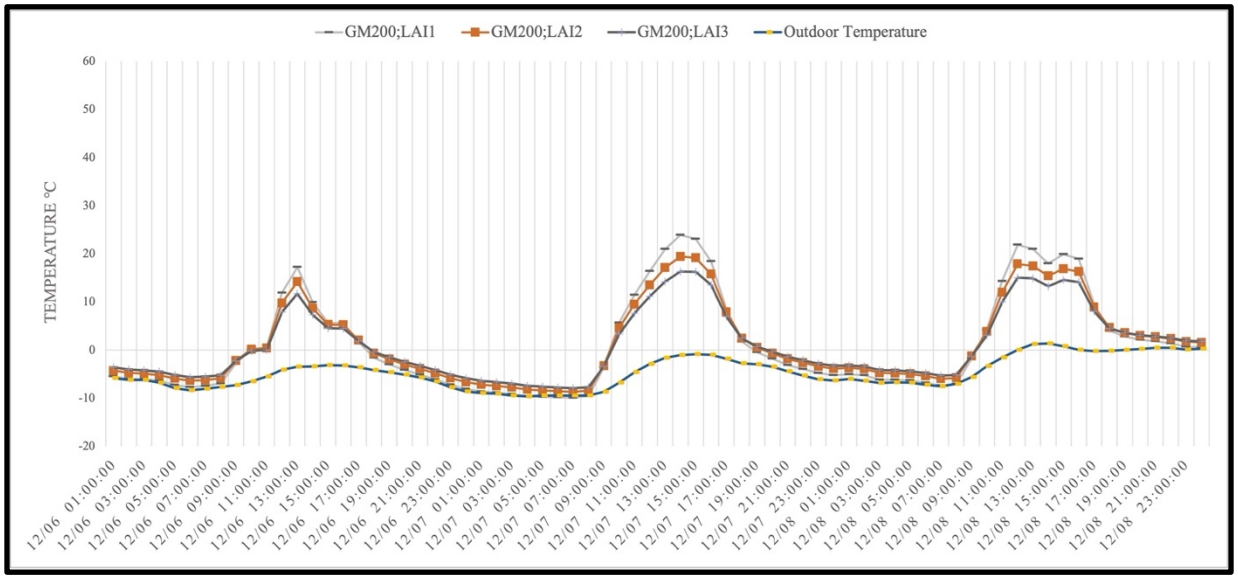

Figure 4-7: Growing media surface temperature for green roof design with growing media depth of 200 mm and LAI of 1, 2 and 3 in typical summer days – no insulation.

Evapotranspiration

The monthly rate of evapotranspiration was analysed to understand the impact of different LAI values. The LAI parameter significantly impacts the evapotranspiration rate, and as the LAI value increases, the rate of evapotranspiration increases. Although, other than LAI, the evapotranspiration process is affected by parameters such as wind speed, solar radiation, relative humidity, ambient temperature, and growing media moisture content. Figure 4-8 presents the monthly evapotranspiration rate (mm/day) for growing media of 200 mm, without insulation, of different LAIs. It should be noted, the evapotranspiration rate in EnergyPlus accounts for both evaporation from the growing media and vegetation. As observed in Figure 4-8, the monthly evapotranspiration is low during the winter months due to lower solar radiation absorption and ambient temperature. During spring, which is considered late March up to late June in this research, the evapotranspiration rate is higher towards the mid-spring (Figure 4-8). During summer, considered from late June onwards up to late September, the evapotranspiration rate increased and peaked in July. The evapotranspiration rate was highest in July for LAI of 2 and 3. However, there was a decrease in evapotranspiration rate using LAI of 1 during July. This decrease was due to low

vegetation density of LAI of 1, high solar radiation and ambient temperature in July. In green roofs with low vegetation density (LAI 1), the amount of solar radiation absorbed by the plants and the coverage provided on the green roof was lower than green roofs with denser vegetation (LAI 2 and 3). Therefore, in a month like July, the green roof with LAI of 1 had limited moisture content and low evapotranspiration rate compared to LAI of 2 and 3. The growing media moisture ratio for LAI of 2 and 3 for July was 0.33 and 0.361, respectively, while for LAI of 1, it was 0.26. The densely vegetated area maintains more moisture content in the growing media, absorbs higher solar radiation and leads to higher evapotranspiration. During the fall season, considered late-September to late-December, lower solar radiation decreased evapotranspiration rate compared to summer. Similar to spring and summer, LAI of 3 maintained a higher evapotranspiration rate than LAI of 2 and 1 during fall (shown in Figure 4-8). As for winter, the evapotranspiration rate was minimum, and all LAIs of 1, 2 and 3 maintained similar evapotranspiration rates.

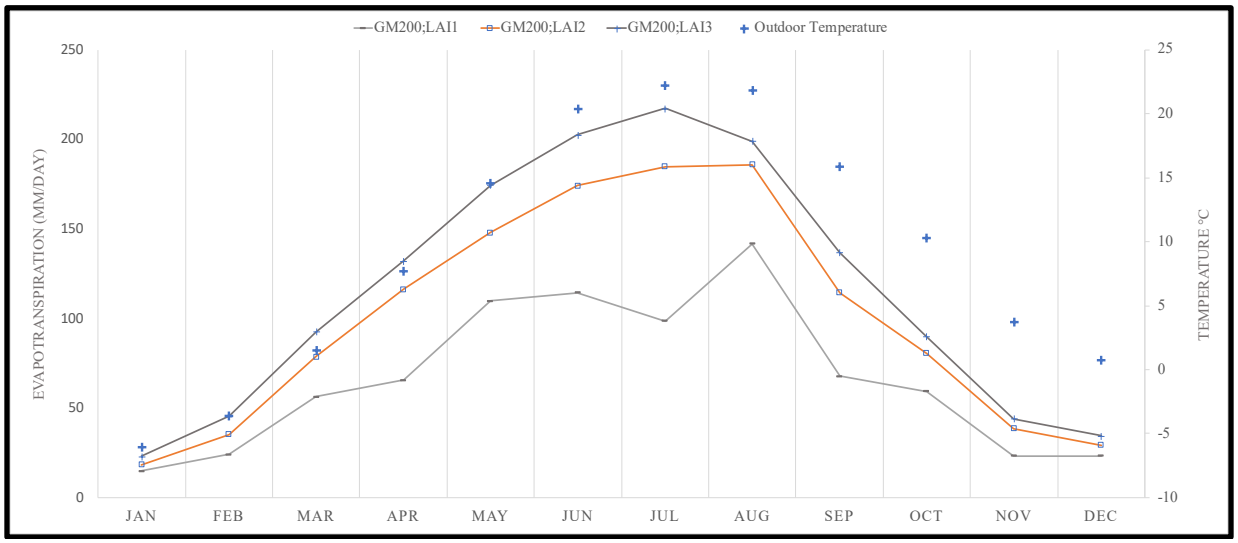

Figure 4-8: Monthly evapotranspiration rate (mm/day) for growing media of 200 mm with LAI of 1, 2 and 3 - without insulation.

Overall, due to higher solar absorption, the evapotranspiration rate was higher during summer and spring compared to fall and winter. Results showed the evapotranspiration rate during summer and spring for LAI of 3 with growing media of 200 mm were 616 mm/day and 473 mm/day, respectively, while for fall, the evapotranspiration rate was only 177 mm/day and even lower during winter with the rate of 132 mm/day. Additionally, results showed that the impact of different growing media depths on evapotranspiration rate with the same LAI was not notable. In

Figure 4-9, all three different growing media depths with LAIs of 2 and 3 are presented. As observed in Figure 4-9, for growing media depths of 100 mm, 150 mm, and 200 mm, there was a limited difference between the monthly evapotranspiration when LAI of 2 and 3 was used.

This section concludes LAI impacts the growing media surface temperature and the rate of evapotranspiration during all seasons. All three LAIs caused the growing media surface temperature to be warmer during spring and fall than the ambient temperature. The higher evapotranspiration rate by LAI of 3 led to the lowest growing media surface temperature among other LAIs due to higher cooling effects during spring and fall. In winter, the vegetated area for all LAIs of 1, 2 and 3 acted as an insulator and increased the growing media surface temperature compared to the ambient temperature. During summer, larger LAI provided more coverage, shielded the roof area from the solar radiation and lowered the roof surface temperature through the evapotranspiration process.

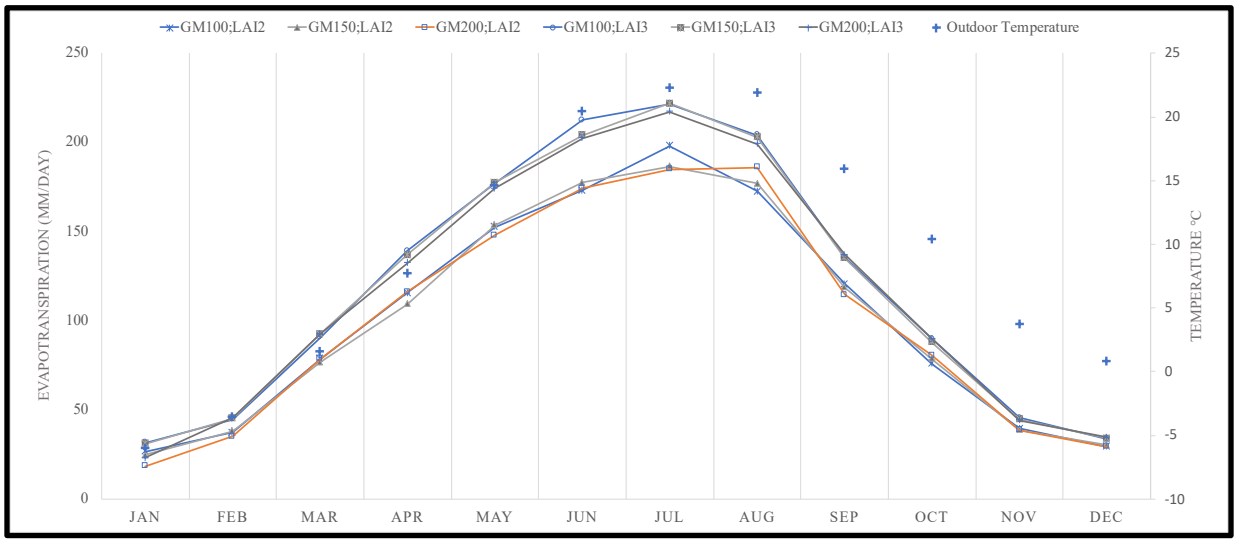

Figure 4-9: Monthly evapotranspiration rate (mm/day) for all growing media of 100 mm, 150 mm and 200 mm with LAI of 1, 2 and 3 - without insulation.

4.1.2 Impact of Insulation Thickness Layer and Growing Media Depth on Inside Surface Temperature

The added thermal insulation layer and green roof growing media depth both act as insulators and impact the building's total energy consumption. The higher the growing media depth and thermal insulation, the higher the insulation effect and reduction of heat flux in and out the roof building.

The inside roof temperatures for the green roof designs and the conventional roof were analysed to measure the thermal performance of growing media depth and insulation thickness on reducing roof heat flux. In this section, the impact of growing media depth on the inside roof surface temperature for designs without insulation and high insulation (300 mm thickness) are compared to the conventional roof for each season. In addition, the green roof design with LAI of 3 was only considered in evaluating the inside roof surface temperature since it had the highest impact on building thermal performance.

Figure 4-10 and Figure 4-11 present the inside roof surface temperature, during a typical spring day, for green roof designs and conventional roofs without insulation and with insulation thickness of 300 mm, respectively. Figure 4-10 shows all growing media depths display warmer temperatures than the outdoor ambient air while maintaining lower temperature and fluctuations than the conventional (CONV) roof. This indicated that the green roof growing media depth provided insulation effect and reduced the temperature fluctuations throughout the day. There is also an average difference of 1 ℃ between the inside surface temperatures for different growing media depths. However, the addition of 300 mm insulation layer caused all growing media depths to maintain similar temperatures (Figure 4-11). This indicated the thermal performance of green roof designs with different growing media depths is affected by the added insulation layer. The added insulation thickness of 300 mm caused the inside roof surface temperature to be the same for all green roof designs and conventional roof, shown in Figure 4-11. The conventional roof displayed no fluctuations at high insulation thicknesses and maintained steady inside temperatures like all green roof designs.

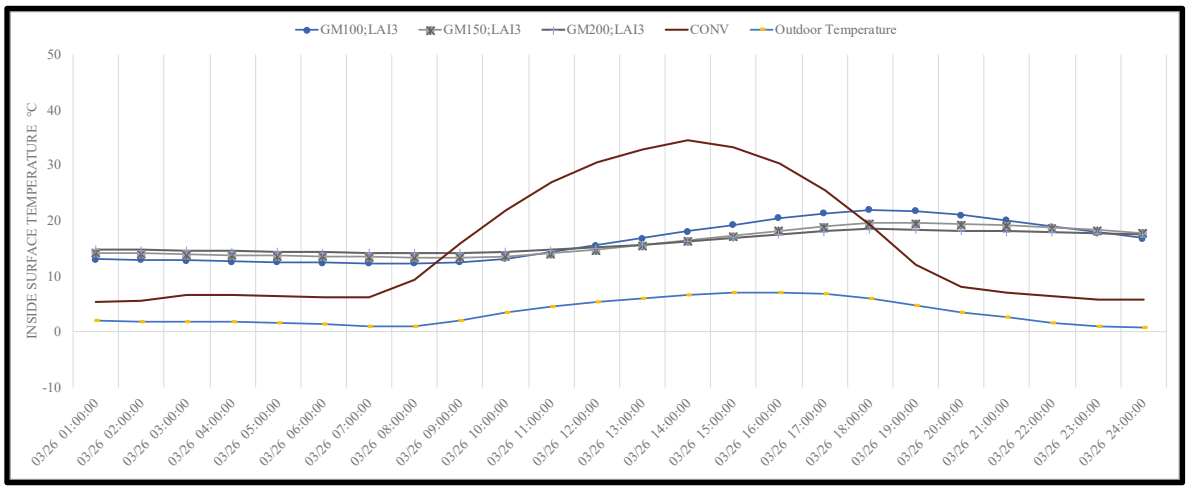

Figure 4-10: Inside roof surface temperature for conventional roof and green roof designs with growing media depths of 100 mm, 150 mm and 200 mm with LAI of 3 without insulation during a typical spring day.

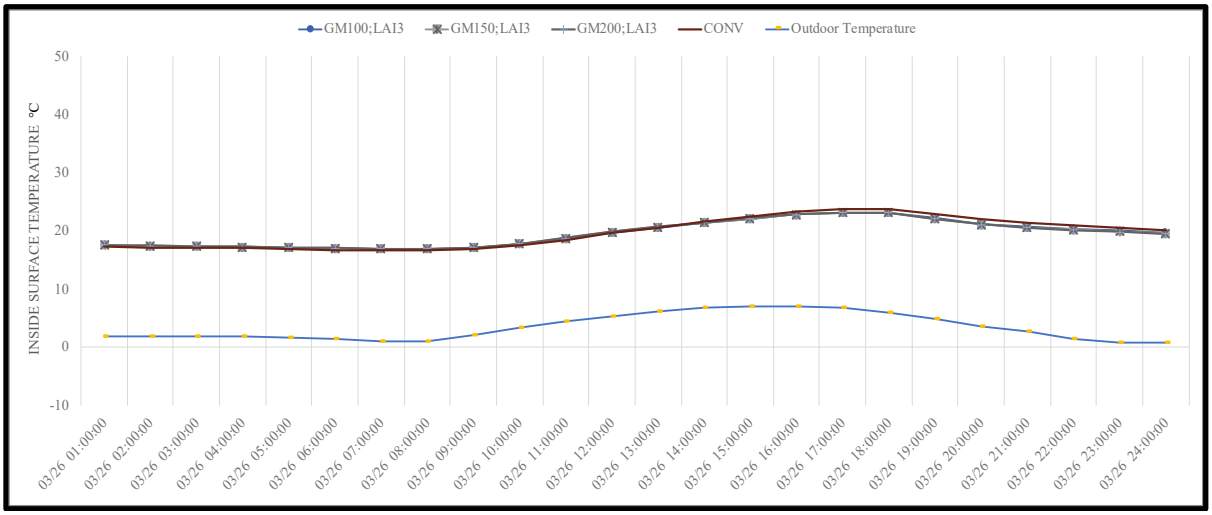

Figure 4-11: Inside roof surface temperature for conventional roof and green roof designs with growing media depths of 100 mm, 150 mm and 200 mm with LAI of 3 with insulation of 300 mm during a typical spring day.

All green roof designs maintained inside surface temperature close to the ambient air temperature during a typical summer day. Figure 4-12 and Figure 4-13 present the inside surface temperature without insulation and 300 mm insulation, respectively, for green roofs and conventional roof design for typical summer days. All green roof growing media depths maintained temperatures close to the ambient air and reduced the daily temperature fluctuations, unlike the conventional roof. However, for insulation thickness of 300 mm, both the conventional roof and green roof designs reached similar inside roof temperatures (Figure 4-13).

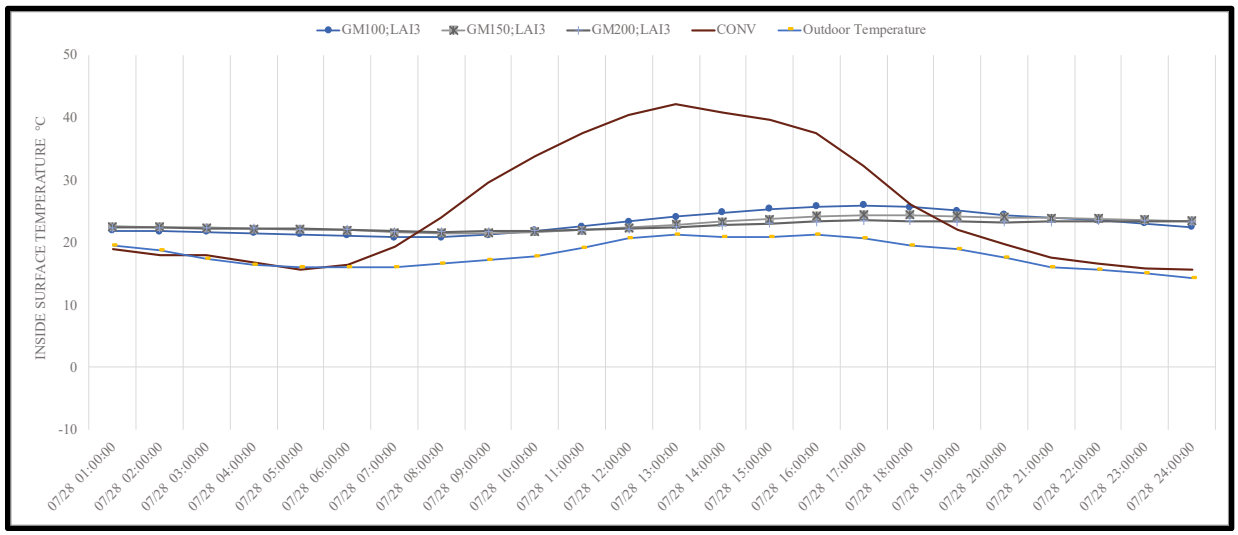

Figure 4-12: Inside roof surface temperature for conventional roof and green roof designs with growing media depths of 100 mm, 150 mm and 200 mm with LAI of 3 without insulation during a typical summer day.

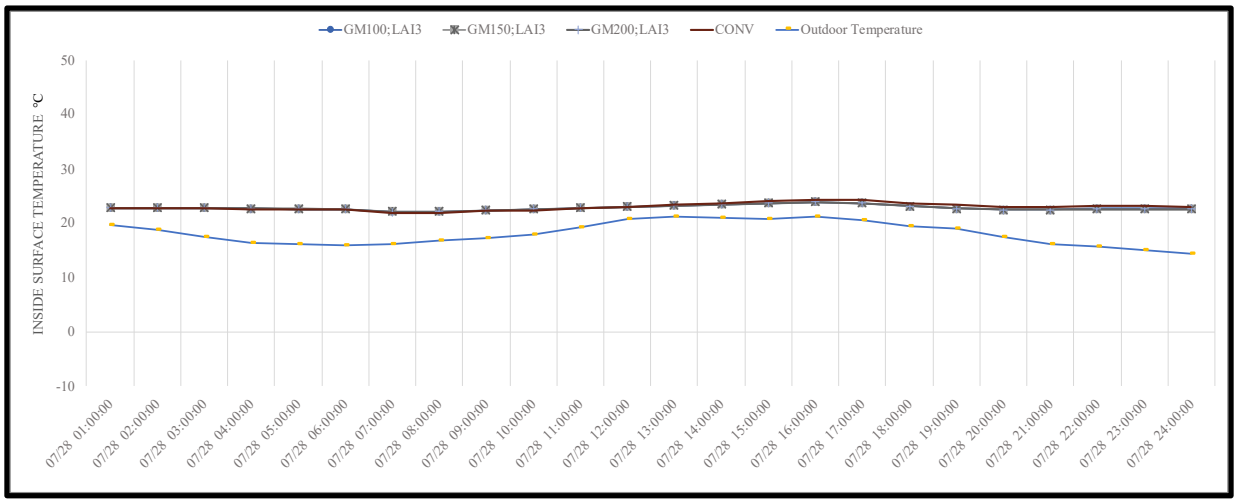

Figure 4-13: Inside roof surface temperature for conventional roof and green roof designs with growing media depths of 100 mm, 150 mm and 200 mm with LAI of 3 with insulation of 300 mm during a typical summer day.

During a typical fall day, the green roof designs had inside surface temperatures higher than the cold ambient temperature in the fall. However, the conventional roof still experienced temperature fluctuations for roof designs without insulation like the spring and summer. This indicated that the uninsulated green roofs, during fall, would perform much better in maintaining steady inside roof temperatures with fewer fluctuations compared to the conventional uninsulated roof (Figure 4-14). The use of 300 mm insulation thickness caused the conventional roof and all green roof designs to behave and maintain the same inside surface temperature in fall, shown in Figure 4-15.

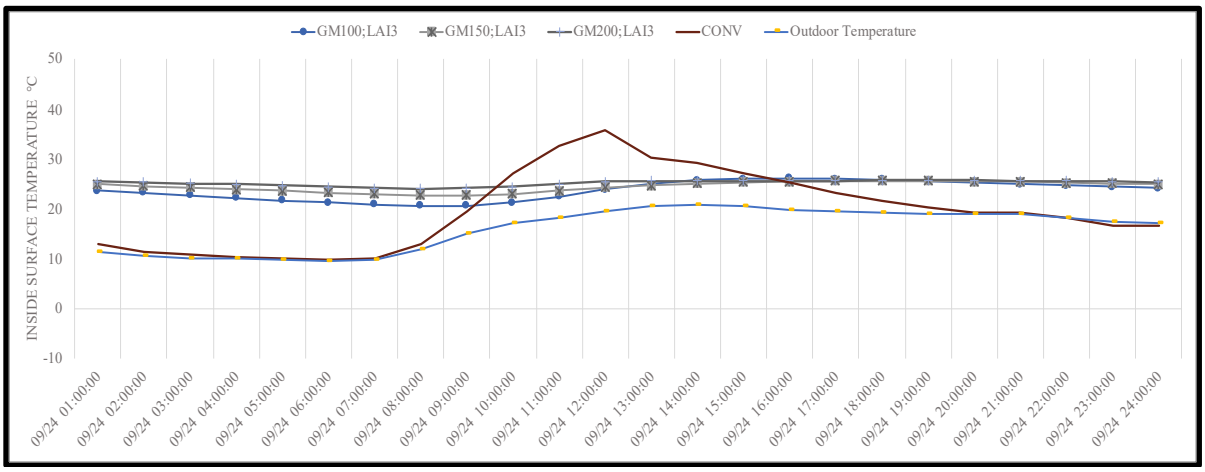

Figure 4-14: Inside roof surface temperature for conventional roof and green roof designs with growing media depths of 100 mm, 150 mm and 200 mm with LAI of 3 without insulation during a typical fall day.

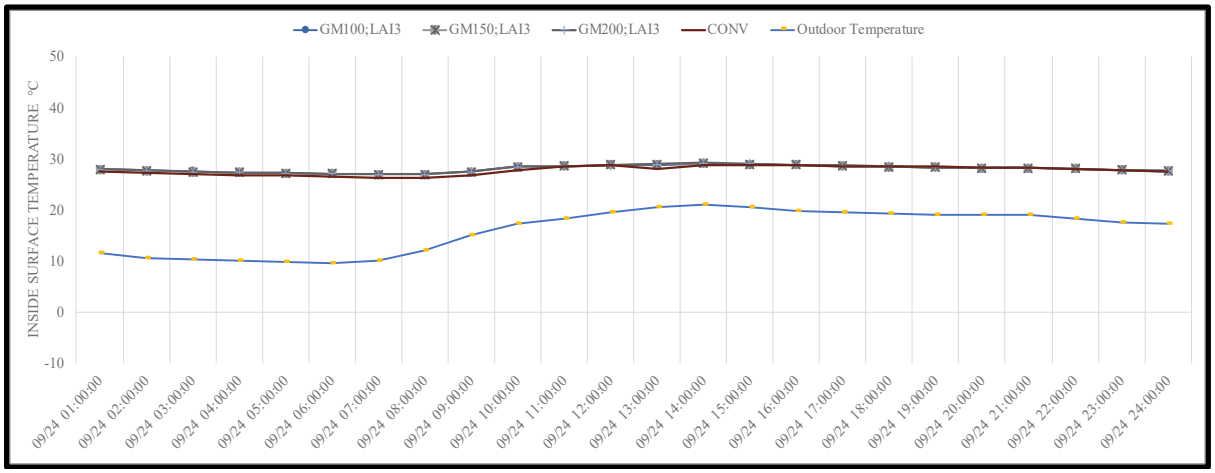

Figure 4-15: Inside roof surface temperature for conventional roof and green roof designs with growing media depths of 100 mm, 150 mm and 200 mm with LAI of 3 with insulation of 300 mm during a typical fall day.

During a typical winter day, green roof growing media depths insulated the building and maintained warmer inside surface temperatures than the cold ambient temperature (Figure 4-16). On the other hand, the conventional uninsulated roof experienced colder inside surface temperatures than uninsulated green roofs, as shown in Figure 4-16. However, once the insulation thickness of 300 mm was used, all green roof designs and the conventional roof maintained the same inside surface temperature (Figure 4-17).

Compared to the conventional roof, the analysis showed that green roof designs provide the most benefit in reducing the inside surface temperature fluctuations when no insulation thickness is used. The inside surface temperature for both the conventional roof and green roof behaved

similarly when the insulation thickness of 300 mm was added for all seasons, indicating a minimal difference in thermal performance of different roof types.

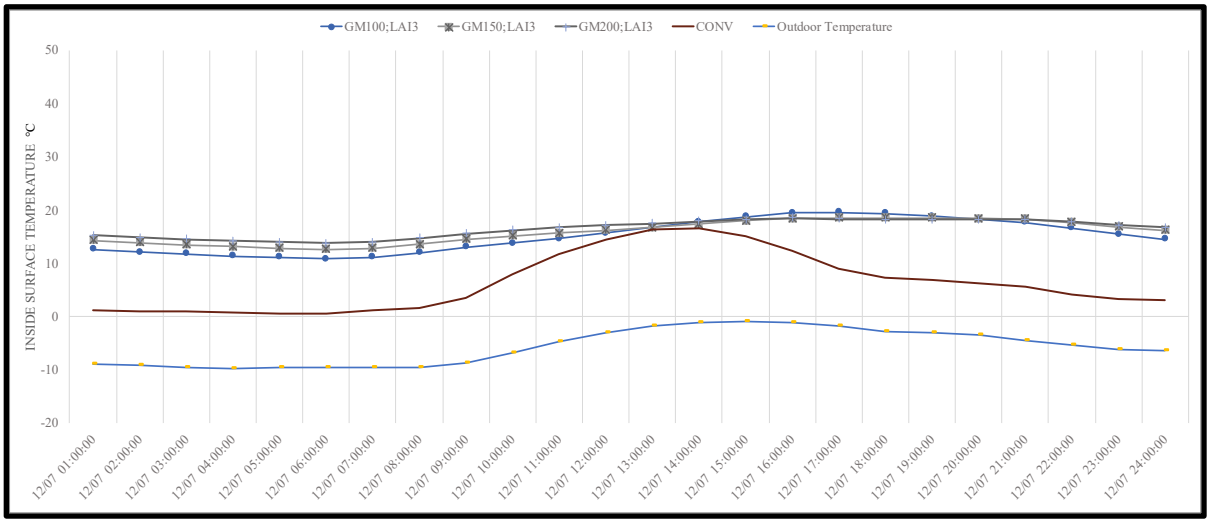

Figure 4-16: Inside roof surface temperature for conventional roof and green roof designs with growing media depths of 100 mm, 150 mm and 200 mm with LAI of 3 without insulation during a typical winter day.

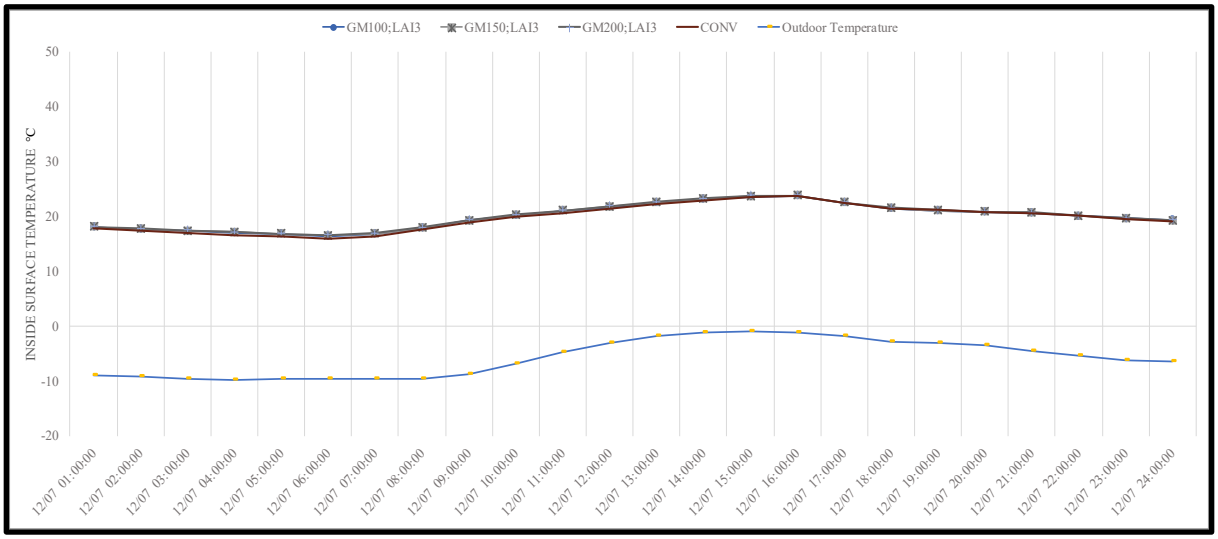

Figure 4-17: Inside roof surface temperature for conventional roof and green roof designs with growing media depths of 100 mm, 150 mm and 200 mm with LAI of 3 with insulation of 300 mm during a typical winter day.

4.1.3 Seasonal Heating and Cooling Loads

The LAI and growing media depth impact the building cooling and heating loads. The LAI provides a cooling effect through evapotranspiration, while the growing media depth insulates the building by reducing the heat flux in and out of the building. Green roof thermal performance is

dependent on the climate conditions; therefore, it is important to evaluate the impact of LAI and growing media depth on cooling and heating loads based on each season.

As mentioned previously, the increase in added insulation thickness limits the green roof performance in decreasing the cooling and heating loads. Hence, in this section, the impact of LAI and growing media depth with insulation thicknesses of low (50 mm), medium (120 mm) and high (300 mm) on seasonal cooling and heating loads are analysed. Table 4-1 is an identification table for the design names used in the seasonal cooling and heating plots. The green roof designs for seasonal cooling and heating loads have been compared to the conventional roof with three insulation layer thicknesses in each plot.

Table 4-1: Identification labels for seasonal heating and cooling plots

Design Name Tags: **Conventional Reference Roof + Insulation Thickness** **Growing Media Depth + LAI + Insulation Thickness**	
ID	**Description**
CON	Conventional Reference roof
A	Growing Media Depth: 100 mm
B	Growing Media Depth: 150 mm
C	Growing Media Depth: 200 mm
1	LAI: 1
2	LAI: 2
3	LAI: 3
50	Insulation Thickness: 50 mm
120	Insulation Thickness: 120 mm
300	Insulation Thickness: 300 mm

Impact of LAI on Cooling and Heating Loads

The insulated green roof designs for growing media depth of 100 mm and LAI of 1 showed no benefit in decreasing the cooling loads compared to the conventional roof during spring and summer. This indicated that the cooling effect provided by the small LAI through evapotranspiration was limited and caused the green roof to provide no benefit in decreasing the cooling loads during spring and summer. Due to the limited cooling effect provided by an LAI of 1, the impact of growing media was dominant, and the green roof consumed more cooling loads than the conventional roof. The secondary school building uses both cooling and heating loads

throughout the year; hence, small magnitudes of the cooling load were consumed by the building during the fall and winter. However, the impact of LAI of 1 on decreasing the cooling loads compared to the conventional roof for all insulation thicknesses with growing media of 100 mm was negligible during fall and winter. At an insulation thickness of 300 mm, both the conventional roof and green roof consumed similar cooling loads in all seasons, indicating the insulation thickness layer takes over the dominant effect on building thermal performance.

The green roof design with LAI of 2 and growing media depth of 100 mm showed decreased cooling loads compared to the conventional roof during spring and summer. The impact of LAI of 2 on decreasing cooling loads was higher when low insulation thickness (50 mm) was used. As the added thermal insulation thickness increased, the green roof performance on cooling saving loads compared to the conventional roof was inhibited. In summer, the green roof with insulation thickness of 50 mm consumed 209 MWh of cooling load, and the conventional roof consumed 217 MWh, while with insulation thickness of 300 mm, green roof and conventional roof consumed cooling loads of 205 MWh and 206 MWh, respectively. Due to high evapotranspiration rates in summer, the cooling loads were decreased more in summer than spring. During fall and winter, minimal impact on lowering the cooling loads compared to the conventional roof were observed.

Results for growing media of 100 mm with LAI of 3 showed a relatively larger decrease in cooling loads than LAI of 1 and 2 during the spring and summer season, shown in Figure 4-18. However, at higher insulation thicknesses of 120 mm and 300 mm, the green roof performance was impacted, and the cooling consumption was less reduced. In fall and winter, similarly to LAI of 1 and 2, minimal impact on cooling loads was observed between the conventional roof and green roof design with growing media depth of 100 mm and LAI of 3.

The use of LAI of 1, 2 and 3 with the same growing media depth showed that the impact on cooling loads are more significant during spring and summer. The green roof design with LAI of 1 had no impact on cooling reduction, while the use of LAI of 3, due to a higher evapotranspiration rate, had the highest reduction of cooling loads during summer and spring. In addition, the green roof performance was inhibited on cooling reduction when high insulation thicknesses were used.

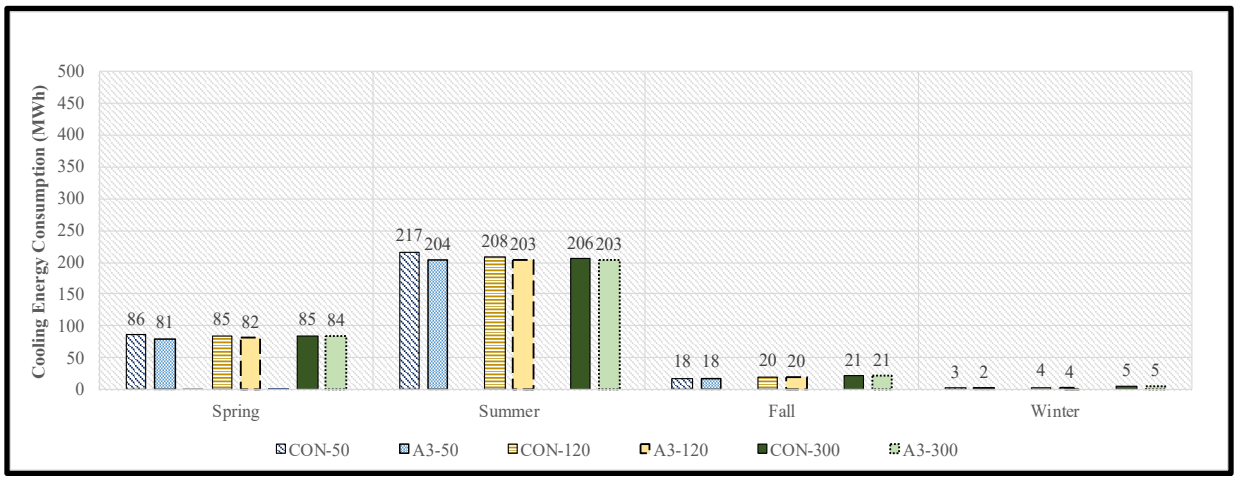

Figure 4-18: Seasonal cooling loads for conventional roof (CON) and green roof with design of growing media of 100 mm and LAI of 3 for insulation thicknesses 50 mm, 120 mm and 300 mm – current climate (secondary school).

The magnitude of the secondary school heating loads was higher during fall and winter compared to spring and summer. The insulated green roof consumed lower heating loads than conventional insulated roofs during fall and winter due to the higher insulation effect of green roofs. However, during spring and summer, the green roof required higher heating loads than the conventional roof. This is observed in Figure 4-19, where the green roof for growing media depth of 100 mm and LAI of 1 consumes more heating loads than the conventional roof. One reason for the increase in heating loads during spring and summer is the growing media insulation effect. Another reason for the increase in green roof heating loads during spring and summer is the evapotranspiration effect; the green roof vegetated layer provides a cooling effect and indirectly causes higher heating loads compared to the conventional roof. This is observed in Figure 4-20, where the green roof with LAI of 3 and growing media depth of 100 mm requires higher heating loads compared to the conventional roof and the green roof design with LAI of 1 (shown in Figure 4-19). Therefore, the increase in heating loads during spring and summer compared to the conventional roof is due to the combined effect of the added growing media depth and the cooling mechanism provided through evapotranspiration. However, at higher insulation thicknesses, the impact of evapotranspiration by LAI and the growing media on increasing the building heating loads decreased due to the insulation layer acting as the dominant effect. As shown in Figure 4-20, the heating loads during summer for LAI of 3 with insulation thickness of 50 mm is 102 MWh, while with insulation thickness of 300 mm, the green roof heating load decreased to 99 MWh. Similar behaviour was observed during spring where at insulation thickness of 50 mm with LAI of 3, the

green roof consumed 92 MWh of heating loads, while with added insulation thickness of 300 mm, only 57 MWh was consumed.

The use of different LAIs for the same growing media depth showed limited impact on heating loads during fall and winter, observed in Figure 4-19 and Figure 4-20. This is due to low evapotranspiration rates during fall and winter that cause a minimum impact on the building heating consumption when different LAIs with the same growing media depth is used.

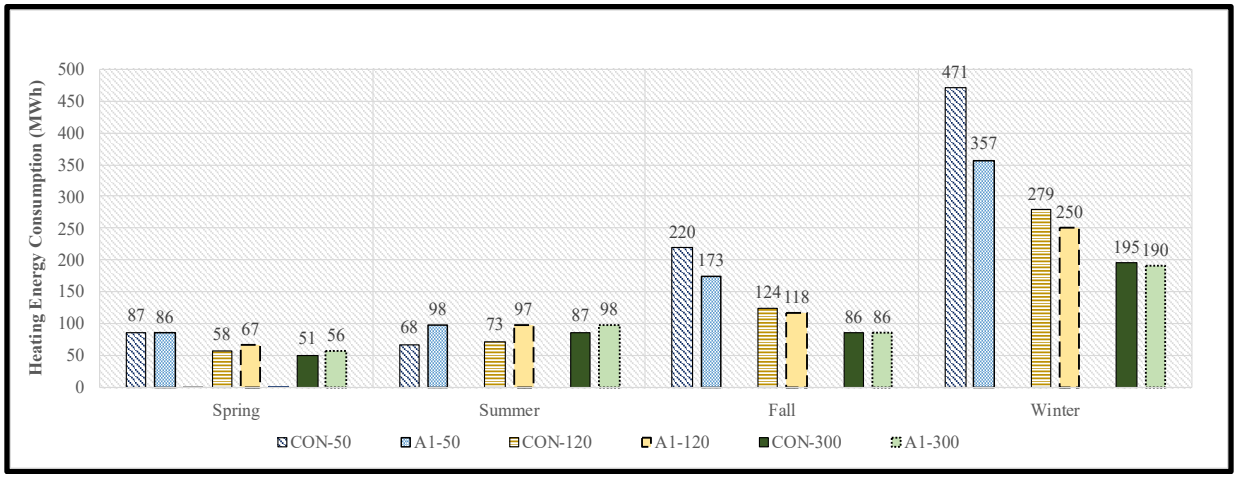

Figure 4-19: Seasonal heating loads for conventional roof (CON) and green roof with design of growing media of 100 mm and LAI of 1 for insulation thicknesses 50 mm, 120 mm and 300 mm – current climate (secondary school).

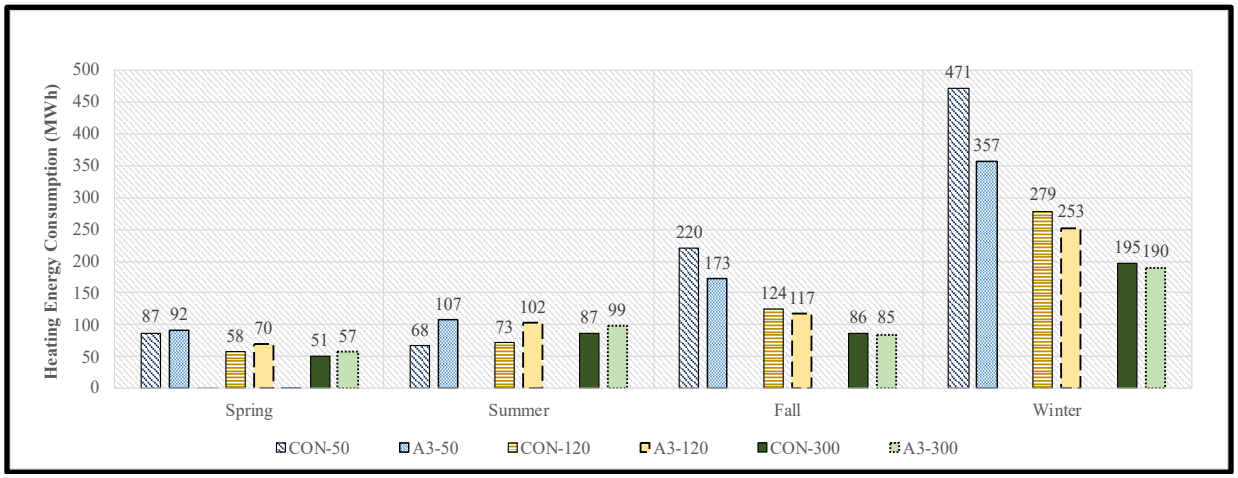

Figure 4-20: Seasonal heating loads for conventional roof (CON) and green roof with design of growing media of 100 mm and LAI of 3 for insulation thicknesses 50 mm, 120 mm and 300 mm – current climate (secondary school).

The combined total seasonal heating and cooling loads showed during spring and summer, the green roof required higher total energy than the conventional roof. This is because the total energy

benefit provided by the green roof cooling effect during spring and summer was cancelled off by the increase in heating loads during these seasons. As observed in Figure 4-21 and Figure 4-22 the green roof consumes higher total energy than the conventional roof during spring and summer when different LAIs of 2 and 3 with the same growing media is used. On the other hand, since the LAI impact on cooling and heating loads was minimal during fall and winter, the total energy consumption of the green roof and conventional building stayed the same for different LAIs.

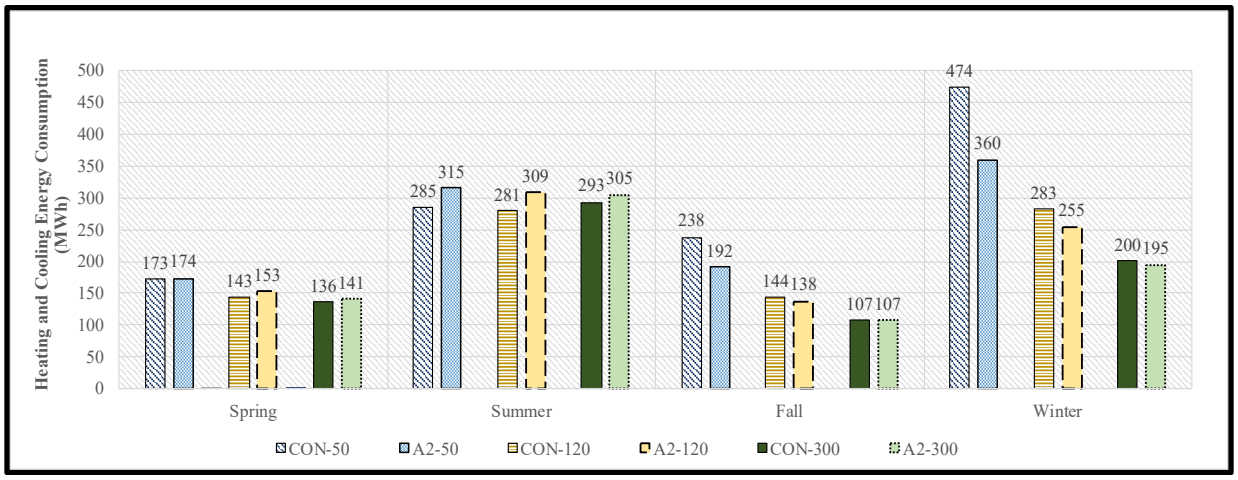

Figure 4-21: Seasonal total heating and cooling loads for conventional roof (CON) and green roof with design of growing media of 100 mm and LAI of 2 for insulation thicknesses 50 mm, 120 mm and 300 mm – current climate (secondary school).

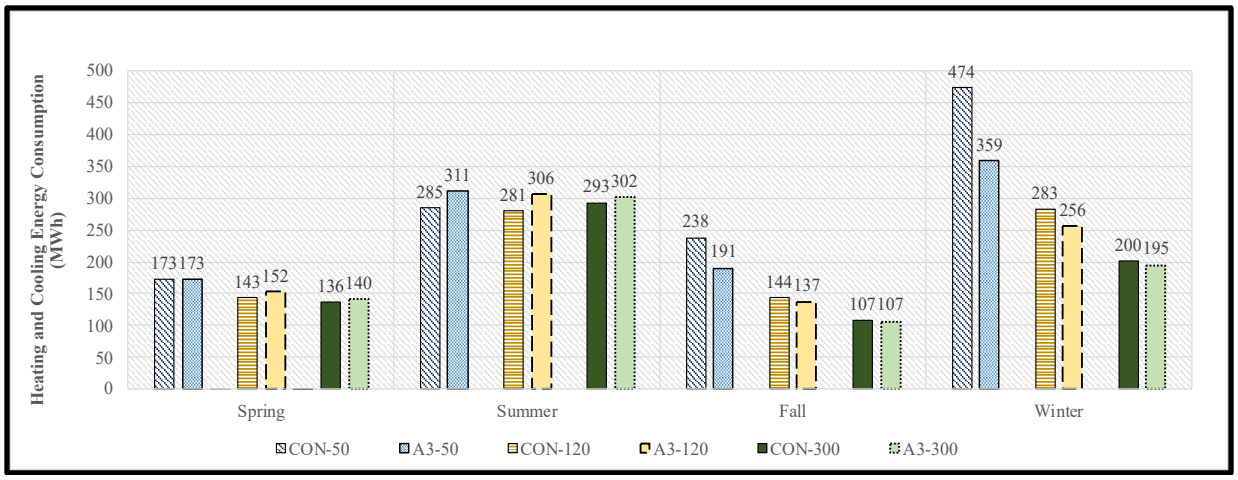

Figure 4-22: Seasonal total heating and cooling loads for conventional roof (CON) and green roof with design of growing media of 100 mm and LAI of 3 for insulation thicknesses 50 mm, 120 mm and 300 mm – current climate (secondary school).

Results for the impact of LAI on total cooling and heating consumption conclude that LAI's highest effect is first during summer and then spring. For cooling consumption, the use of larger LAI

resulted in a higher reduction of cooling load during spring and summer. However, the cooling benefit provided by the green roof was cancelled out due to the rise in heating loads during spring and summer, leading to the higher green roof total energy consumption compared to the conventional roof. Results also showed that as the insulation thickness increased, the green roof cooling effect was impacted and inhibited.

Impact of Growing Media Depth on Cooling and Heating Loads

Different growing media depths with the same LAI impacted the heating loads during fall and winter while having a minimum effect on cooling loads. As the growing media depth increased, the green roof experienced lower heating loads for all insulation thickness in fall and winter than the conventional roof; this was due to a greater insulation effect provided by the green roof than the conventional roof. However, at low insulation thicknesses during summer, the increase in growing media depth and greater insulation effect caused a small increase in green roof cooling and heating loads for the same LAI values. The increase in growing media depth with the same LAI value decreased the green roof cooling and heating loads compared to the conventional roof; however, the impact was low. Figure 4-22, Figure 4-23 and Figure 4-24 present the total seasonal heating and cooling consumption for growing media depths of 100 mm, 150 mm and 200 mm, respectively, with LAI of 3. Total seasonal cooling and heating consumption showed higher growing media depth lowers the green roof energy consumption than the conventional roof during fall and winter. For example, the use of a higher growing media depth of 200 mm lowered the total energy consumption to 321 MWh in winter for insulation thickness of 50 mm, while lower growing media depth of 150 mm and 100 mm with the same insulation thickness consumed 359 MWh and 340 MWh, respectively.

For growing media depths of 100 mm, 150 mm, and 200 mm with LAI 1 and 2, results generally followed the same pattern; higher growing media depth provided more insulation effect and resulted in a higher reduction of total energy consumption during winter and fall seasons for all insulation thickness. In addition, for both LAI of 1 and 2, the increase in growing media depth had a small impact on cooling and heating loads during spring and summer.

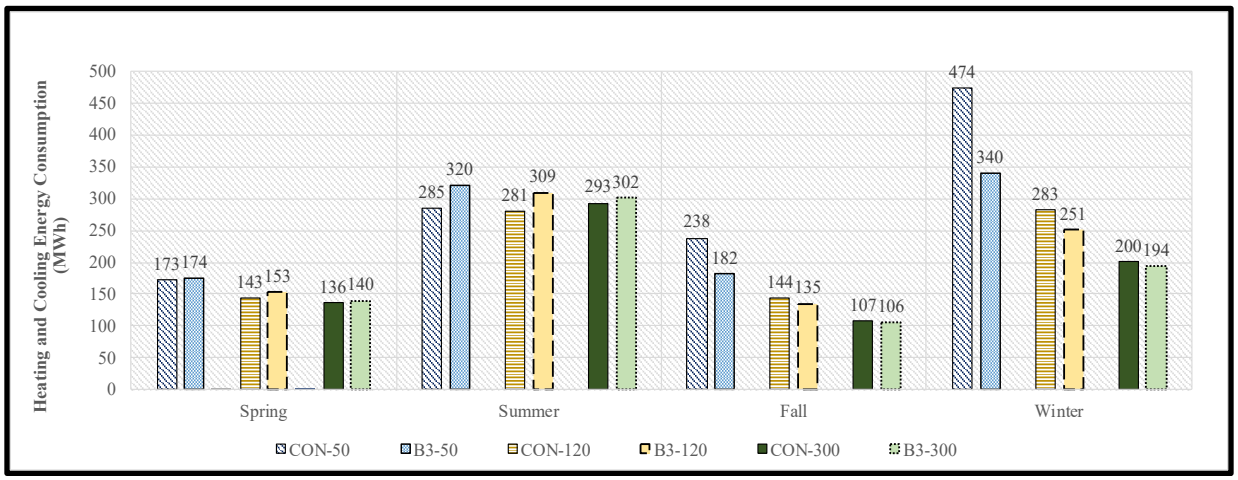

Figure 4-23: Seasonal total heating and cooling loads for conventional roof (CON) and green roof with design of growing media of 150 mm and LAI of 3 for insulation thicknesses 50 mm, 120 mm and 300 mm – current climate (secondary school).

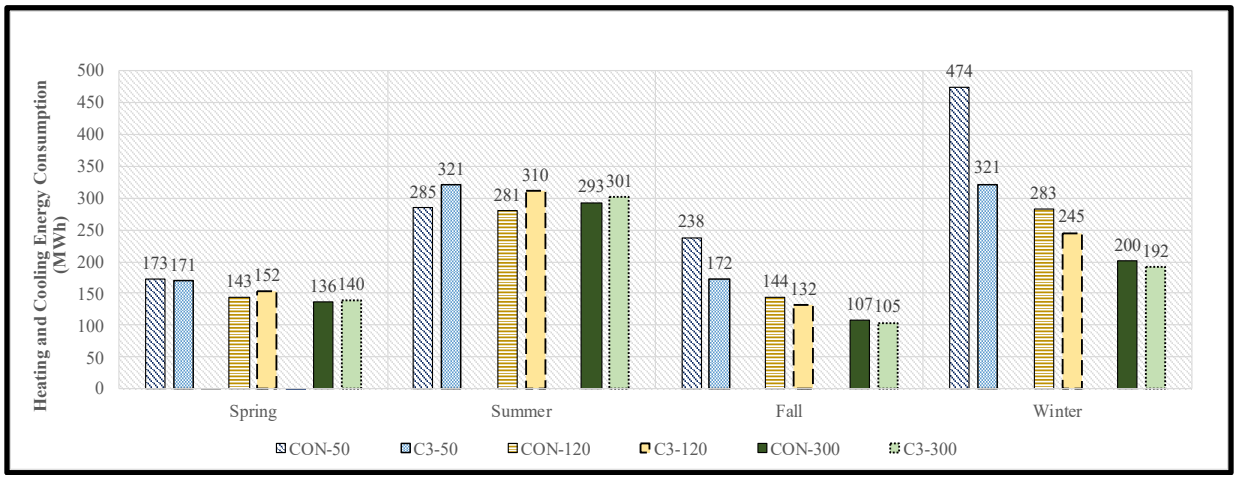

Figure 4-24: Seasonal total heating and cooling loads for conventional roof (CON) and green roof with design of growing media of 200 mm and LAI of 3 for insulation thicknesses 50 mm, 120 mm and 300 mm – current climate (secondary school).

Generally, the seasonal impact of growing media and LAI on cooling and heating loads showed that in fall and winter, due to the heating-dominance of these seasons, the growing media depth has the highest impact on green roof thermal performance. On the other hand, for spring and summer that are considered cooling-dominant seasons, the LAI has the highest impact on green roof thermal performance.

The combined effect of a higher growing media depth of 200 mm and large LAI of 3 resulted in the lowest total annual energy consumption of all seasons combined compared to other green roof designs. A growing media depth of 200 mm resulted in the lowest heating loads during winter and

fall for all insulation thicknesses compared to the conventional roof. The LAI of 3 caused higher evapotranspiration, provided the highest cooling effect and lowered the cooling loads during spring and summer compared to a conventional roof. Therefore, the combination of LAI 3 and growing media depth of 200 mm, used the advantage of each green roof parameter and lowered the total annual cooling and heating consumption the most compared to all other green roof designs. However, no green roof design maintained total energy consumption lower than the conventional roof all season. In fall and winter, the higher insulation effect provided by the growing media depth and the thermal insulation thickness helped reduce energy consumption compared to the conventional roof (for all green roof designs). On the other hand, during spring and summer, the total energy consumption of the green roof always remained higher than the conventional roof. This is due to heating loads being used during spring and summer and causing the green roof to always maintain higher heating loads than the conventional roof. Hence, no green roof design could have lower energy consumption than the conventional roof in all seasons. All plots for the seasonal cooling and heating loads for various roof designs with insulation thicknesses of 50 mm, 120 mm and 300 mm for the secondary school under current climate are provided in Appendix A.

4.1.4 Annual Cooling and Heating Energy Savings

The impact of LAI and growing media depth were determined in the previous sections based on seasonal analysis for low, medium, and high insulation thicknesses. However, to evaluate the thermal performance of green roofs compared to the conventional roof on building energy consumption, the total cooling and heating energy savings achieved by the green roof for each design is analysed. This section discusses the impact of all green roof designs with and without thermal insulation on building energy savings. The energy savings are the amount of energy consumption reduced by the green roof compared to the conventional reference roof.

Figure 4-25 presents the total heating and cooling energy savings (MWh) for all growing media depths and LAIs for uninsulated green roof designs. All uninsulated green roof designs provide positive energy savings for cooling and heating loads. Based on Figure 4-25, growing media depth of 200 mm with LAI of 3 had the highest annual total energy savings compared to all other green roof designs. This is due to the thick growing media depth of 200 mm providing a higher insulation

effect than growing media of 100 mm and 150 mm and having more energy savings. In addition, the large LAI of 3 provided a higher cooling effect through evapotranspiration and vegetation coverage compared to LAI of 1 and 2, resulting in higher cooling savings.

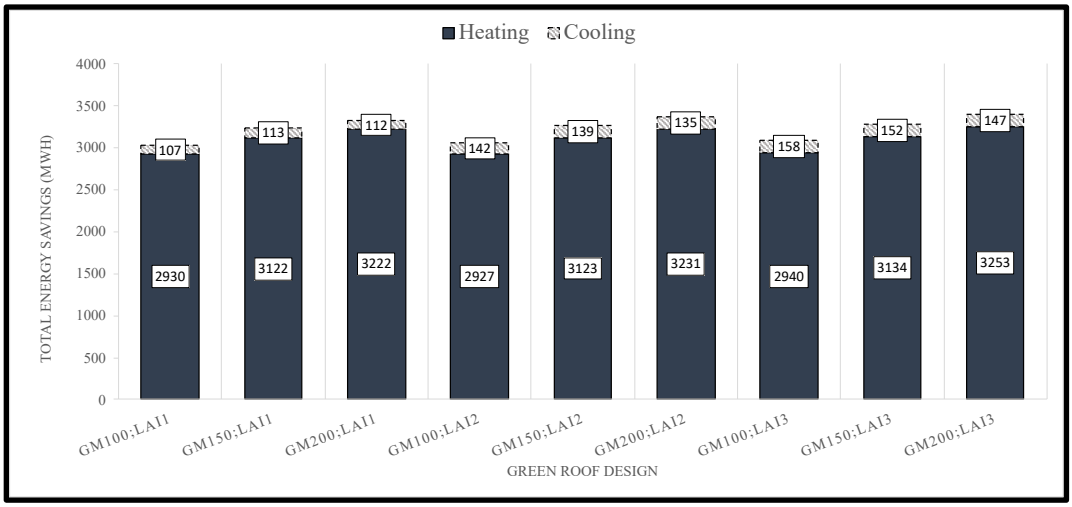

Figure 4-25: Total heating and cooling energy savings (MWh) of green roof compared to conventional roof for all growing media (GM) depths and LAIs; without insulation layer -current climate (secondary school).

Green roof energy savings, however, changed significantly once the thermal insulation layer was added. Figure 4-26 presented the energy savings for cooling and heating loads for all green roof designs with an insulation thickness of 50 mm. The added thermal insulation layer impacted the green roof thermal performance and lowered the energy savings for cooling and heating loads compared to uninsulated green roofs without insulation. It is observed in Figure 4-26 designs with an LAI of 1 experienced negative savings in cooling loads, indicating the conventional roof consumed less cooling energy compared to the green roof designs. The evapotranspiration rate is limited for green roofs with an LAI of 1, and once the insulation layer is added, any benefit provided by the green roof on cooling load savings is inhibited due to the high insulation effect. The cooling energy savings are positive for green roof designs with LAI of 2 and 3 due to the higher evapotranspiration rate for these designs (Figure 4-26). However, the added insulation layer of 50 mm thickness lowered the cooling energy savings of green roofs with LAI of 2 and 3 by a magnitude of more than 100 MWh compared to uninsulated green roofs.

The heating energy savings with insulation thickness of 50 mm were lowered significantly compared to uninsulated green roof designs. However, all designs maintained positive total energy

savings, indicating that the green roofs with insulation thickness of 50 mm could lower building total energy than the conventional roof. The results for cooling and heating energy savings with insulation thickness of 50 mm showed the added thermal insulation impacts the performance of the green roof and lowers the green roof energy savings compared to uninsulated green roofs.

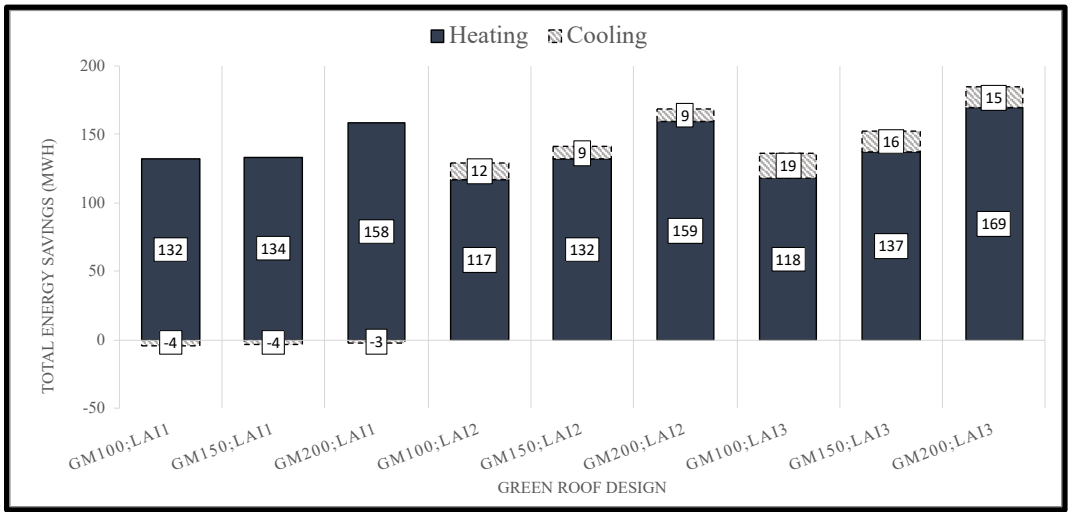

Figure 4-26: Total heating and cooling energy savings (MWh) of green roof compared to conventional roof for all growing media (GM) depths and LAIs; with 50 mm insulation layer – current climate (secondary school).

Green roof designs with added thermal insulation thickness of 120 mm showed even lower energy savings for all green roof designs. Figure 4-27 shows the growing media depth of 200 mm with LAI of 2 and 3 are the only green roofs with total energy savings of 6 MWh and 11 MWh, respectively, and all other designs experienced negative energy savings in cooling and heating loads. Furthermore, the added thermal insulation thickness of 120 mm caused a decrease in green roof energy savings on heating loads compared to green roofs with 50 mm insulation thickness. Green roof negative heating energy savings are due to the cooling effect provided by the green roof during spring and summer, causing the green roof to consume more heating loads than the conventional roof. However, the cooling energy savings for LAIs of 2 and 3 maintained positive for green roofs with insulation thickness of 120 mm, indicating that the green roof always provides cooling benefits even at high thermal insulation thickness.

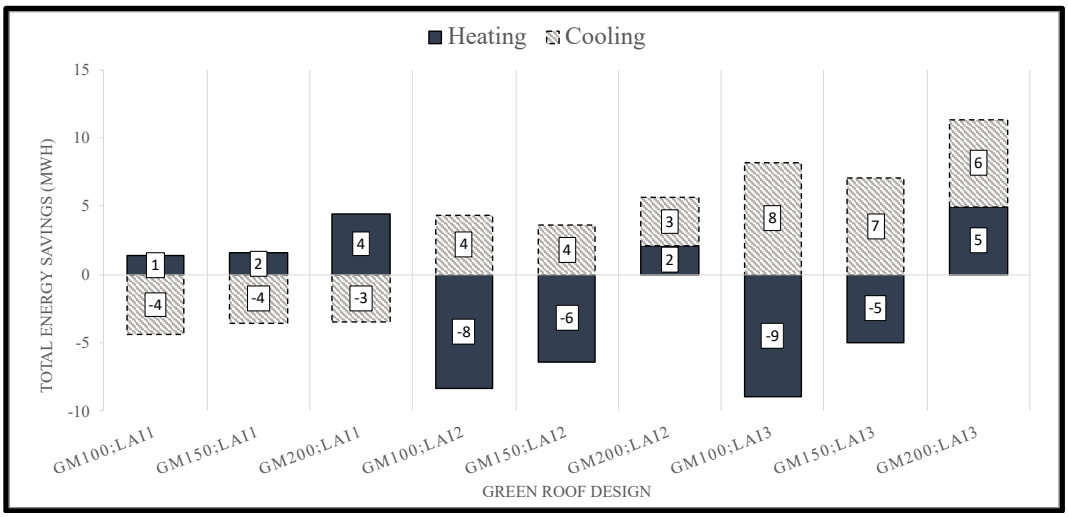

Figure 4-27: Total heating and cooling energy savings (MWh) of green roof compared to conventional roof for all growing media (GM) depths and LAIs; with 120 mm insulation layer – current climate (secondary school).

Similar to insulation thickness of 120 mm, the cooling energy savings for LAI of 2 and 3 were positive for green roof designs with insulation thicknesses of 300 mm (Figure 4-28). Although green roofs with insulation thickness of 300 mm had lower cooling savings than green roof designs with insulation thicknesses of 50 mm and 120 mm. The heating loads for all green roof designs at thermal insulation thickness of 300 mm continued to have negative heating energy savings, shown in Figure 4-28. Therefore, at high thermal insulation thickness of 300 mm, no benefit on total annual energy savings was provided by the green roof designs, and the conventional roof consumed less total energy. Overall, the negative heating energy savings cancelled any cooling benefit provided and resulted in negative total energy savings for all green roof designs. For all plots on green roofs' heating and cooling energy savings compared to the conventional roof for all insulation thicknesses for the secondary school under the current climate conditions, refer to Appendix A.

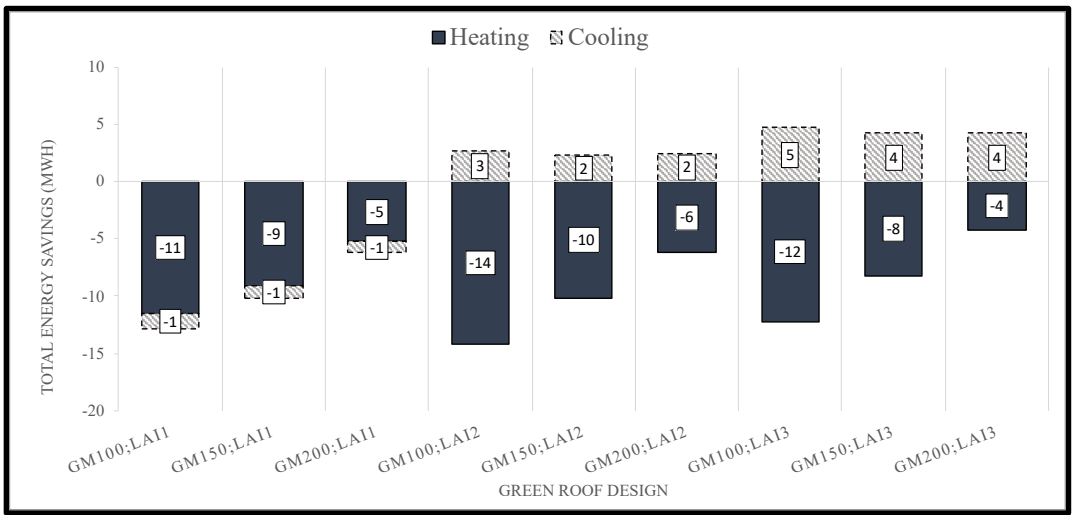

Figure 4-28: Total heating and cooling energy savings (MWh) of green roof compared to conventional roof for all growing media (GM) depths and LAIs; without insulation layer – current climate (secondary school).

The added thermal insulation layer, even at low thicknesses, impacted the total energy savings of the green roof. As the insulation thickness layer increased, the energy savings provided by the green roof decreased until at high insulation thickness of 300 mm, the green roof provided no total energy benefit compared to the conventional roof. Therefore, the use of added thermal insulation thickness with green roofs inhibits their energy performance, and once the thermal insulation thickness above a specific range is reached, the green roof starts to require more energy than the conventional roof. Consequently, to identify optimal thermal insulation thickness range for green roof designs that lower the building energy consumption and provide energy benefit compared to the conventional roof, the ratio of DBGR is determined and discussed in the next section.

4.1.5 Dynamic Benefit of Green Roof (DBGR)

In this research, different green roof designs with added thermal insulation thickness are compared with the conventional roof of the same added thermal insulation. The objective is to determine whether the green roof can reduce the building's annual energy consumption compared to the conventional roof with the same R-value (thermal resistance). The R-value measures roof building insulation; a higher R-value means higher roof insulation. The thermal resistance is calculated using the thickness of the insulation layer and its thermal conductivity. Thus, having different thermal conductivities for the growing media and the added thermal insulation causes the conventional and green roofs to have different R-values.

The Dynamic Benefit of Green Roof (DBGR), Equation 14, is the annual energy use for a conventional membrane roof with an R-value equal to the measured R-value of the green roof construction (Moody and Sailor 2013).

$$DBGR = \frac{E_{CR}}{E_{GR}} \qquad \text{Equation 14}$$

E_{GR} represents the annual heating and cooling consumption of the green roof and E_{Conv} is the annual heating and cooling consumption of the conventional roof. The DBGR greater than unity indicates that the green roof membrane performs better than the conventional roof with the same R-value.

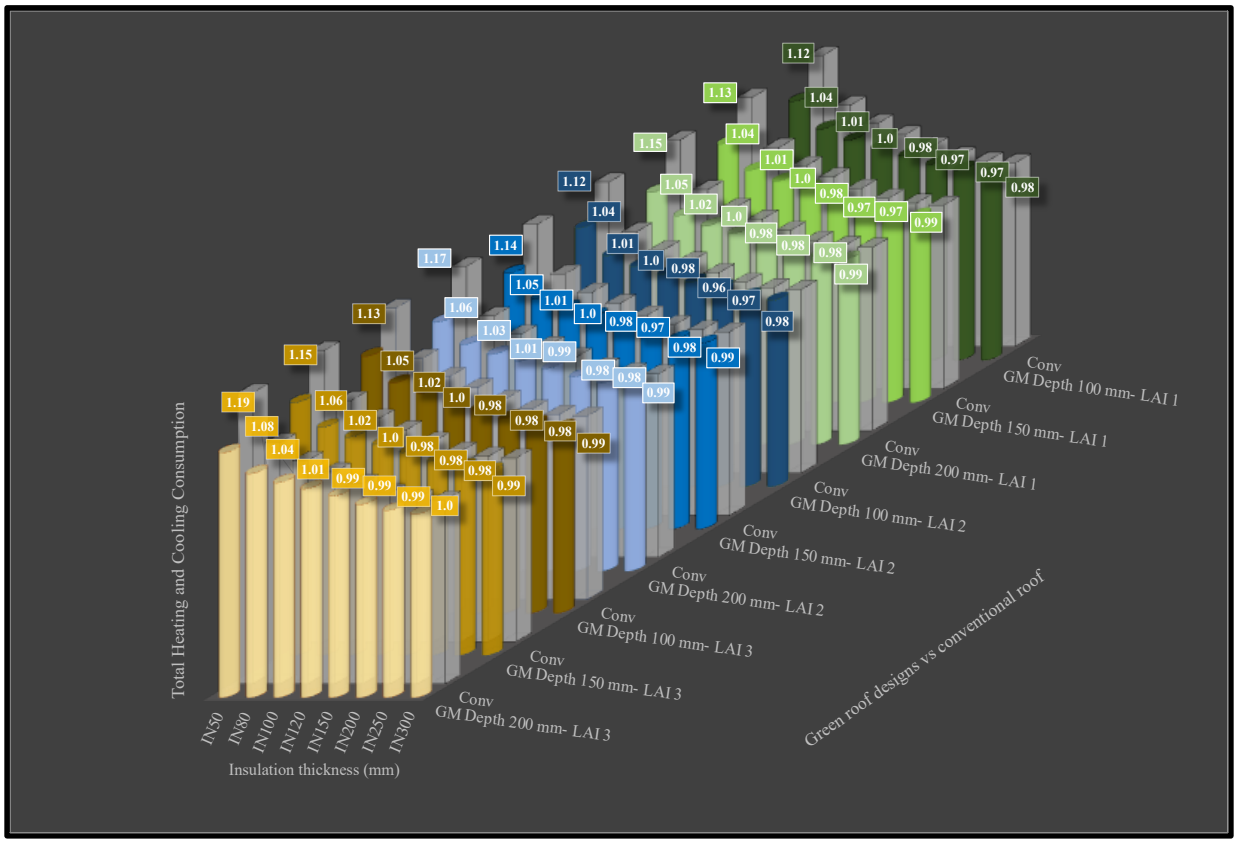

Figure 4-29: DBGR of all green roof designs under current climate (grey colour bars represent conventional roof) – secondary school.

Figure 4-29 includes the DBGR for all roof designs; as the insulation thickness increases, the DBGR for all green roof designs reach values below 1, indicating the green roof designs require

more energy than the conventional (Conv) roof. On the other hand, at low insulation levels, the green roof designs required lower energy compared to the conventional roofs and maintained a DGBR value higher than 1. The green roof with growing media of 200 mm, and LAI of 3 had the highest DBGR than all green roof designs with the same insulation thickness. For insulation thickness of 50 mm, the green roof with growing media depth of 200 mm and LAI of 3 had a DBGR of 1.08, while all other green roof designs with the same insulation thickness had DBGR values of 1.06 and lower. The high growing media depth of 200 mm and larger LAI of 3 caused the green roof to perform better in lowering the total heating and cooling loads compared to other green roof designs. Figure 4-29 shows above certain insulation thickness; all green roof designs start to consume more energy than the conventional roof and reach DBGR values less than 1. All green roof designs at insulation thickness of 120 mm and below maintain DBGR equal or greater than 1 (Figure 4-29). Among green roof designs with insulation thickness of 120 mm, the growing media depth of 200 mm with an LAI of 3 has the highest DBGR of 1.01. However, once insulation thicknesses were above 120 mm, all green roof designs required higher energy than the conventional roof and had a DBGR less than 1, shown in Figure 4-29. The green roof thermal performance was studied in Moody and Sailor (2013) using the DBGR ratio. Similar findings were reported where a highly insulated green roof, depending on the climate, could require higher energy than insulated conventional roofs.

The added thermal insulation layer is essential for building roof designs since it lowers the building total energy consumption by providing a higher roof R-value. In all roof designs, as the added insulation thickness increased, R-value increased, and thus, the total building energy consumption decreased (Figure 4-3). For example, green roof designs with a growing media depth of 200 mm, LAI of 3 and insulation thickness of 250 mm required less total energy than the same green roof design with an insulation thickness of 200 mm. The same applied to conventional roofs, where the increase in insulation thickness reduced the building's total energy consumption. However, when green roof designs were compared to conventional roofs with the same R-value, the outcome differed. Green roofs thermal performance was impacted as the insulation thickness increased, this indicated the total energy savings provided by the green roof was reduced as the insulation thickness increased. Additionally, increase in insulation thickness caused the green roof to require

more heating loads than the conventional roof. The green roof seasonal analysis for cooling and heating loads showed that the cooling effect by the green roof during spring and summer caused the building to require more heating loads compared to conventional roof and cancel any benefit provided by the green roof on total energy savings. However, the thermal performance of conventional roof was only affected by the added thermal insulation layer and as the insulation thickness increased, the energy consumption of the building decreased. Therefore, when the energy consumption for the conventional and green roof at insulation thicknesses above 120 mm were compared, the green roof due to higher required heating loads during spring and summer performed worse than conventional roof.

This research aims to determine optimal design parameters of extensive green roofs in the City of Toronto. According to the Green Vegetative Roof Building Standard for the City of Toronto (City of Toronto 2007), the roof thermal resistance for non-residential buildings must be a minimum of R-3.91. Therefore, in the City of Toronto, it is a requirement for green roofs to maintain a certain R-value. Table 4-2 presents the thermal resistance (R-value) provided by the conventional roof and the green roof with added insulation thicknesses for all building designs.

Table 4-2: Thermal resistance (R) provided by each insulation thickness for the reference roof and green roof growing media depths of 100 mm, 150 mm and 200 mm. Highlighted values are above the City of Toronto R-value requirements.

Insulation Thickness (mm)	**Conventional roof ($K.m^2/W$)**	**Green roof growing media depth 100 mm ($K.m^2/W$)**	**Green roof growing media depth 150 mm ($K.m^2/W$)**	**Green roof growing media depth 200 mm ($K.m^2/W$)**
No insulation	-	0.5	0.7	1.0
50	1.25	1.7	2.0	2.2
80	2	2.5	2.7	3.0
100	2.5	3.0	3.2	3.5
120	3	3.5	3.7	4.0
150	3.8	4.2	4.5	4.7
200	5.0	5.5	5.7	6.0
250	6.3	6.7	7.0	7.2
300	7.5	8.0	8.2	8.5

The R-values for all insulated green roof designs within standards limits are designed with insulation thicknesses above 120 mm (bolded values in Table 4-2), except green roof with growing media depth of 200 mm that maintain standards with 120 mm insulation thickness. Results from the DBGR suggested that green roofs with insulation thicknesses greater than 120 mm would result

in higher energy consumption and reach DBGR values less than 1. Therefore, the use of green roof designs with insulation thickness greater than 120 mm is not recommended. Instead, using conventional roofs would provide more benefit in reducing the total building energy consumption than green roofs.

Therefore, the recommended optimal design that could be used for extensive green roofs in the City of Toronto under current climate conditions for the secondary school buildings is the green roof with growing media depth of 200 mm, LAI of 3 and insulation thickness of 120 mm. This design provides the highest total heating and cooling energy savings compared to all other green roof designs with 120 mm insulation thickness and maintains DBGR higher than 1.

4.2 Secondary School - Future Climate

The energy consumption for green roof designs with different insulation thicknesses was different under future climate conditions than current due to changes in weather patterns. Figure 4-30 presents the average monthly temperatures under current and future climate conditions in the City of Toronto. The average monthly temperatures are predicted to rise in future conditions, and warmer temperatures will be experienced. Figure 4-31 and Figure 4-32 presents the heating and cooling loads of the secondary building for all roof designs under future climate conditions. Results showed that the heating loads required yearly by buildings decreased, and the cooling loads increased in future conditions.

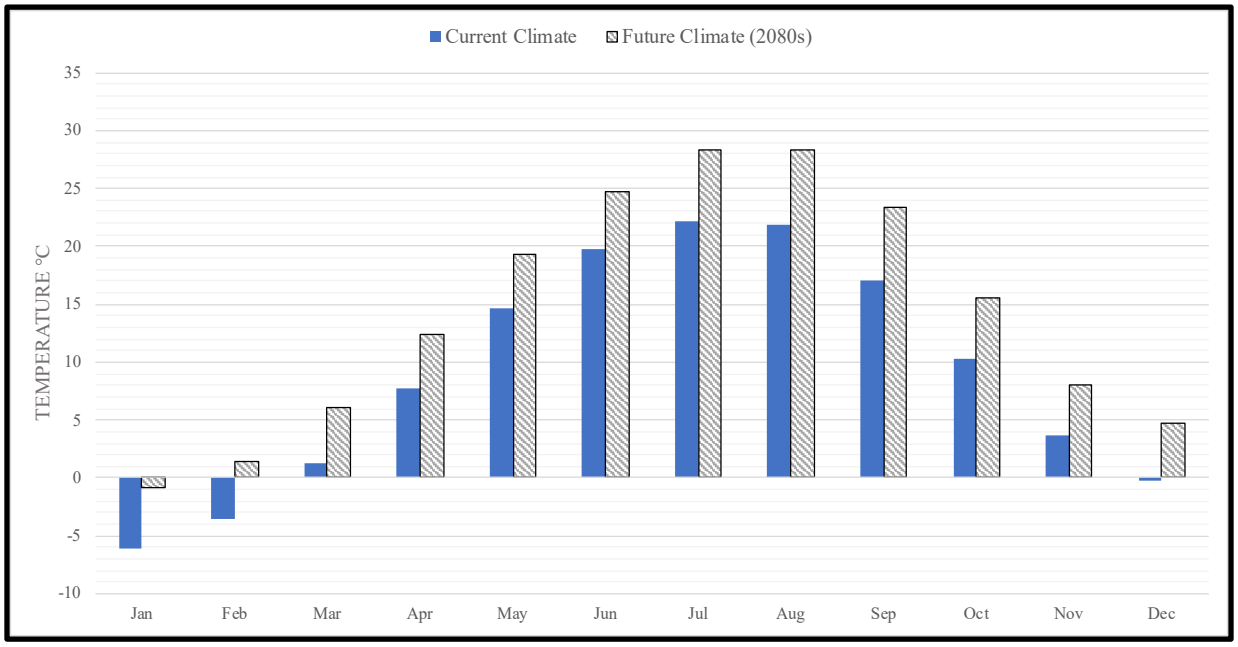

Figure 4-30: Monthly mean temperatures for current and future climate of 2080s – Toronto, ON.

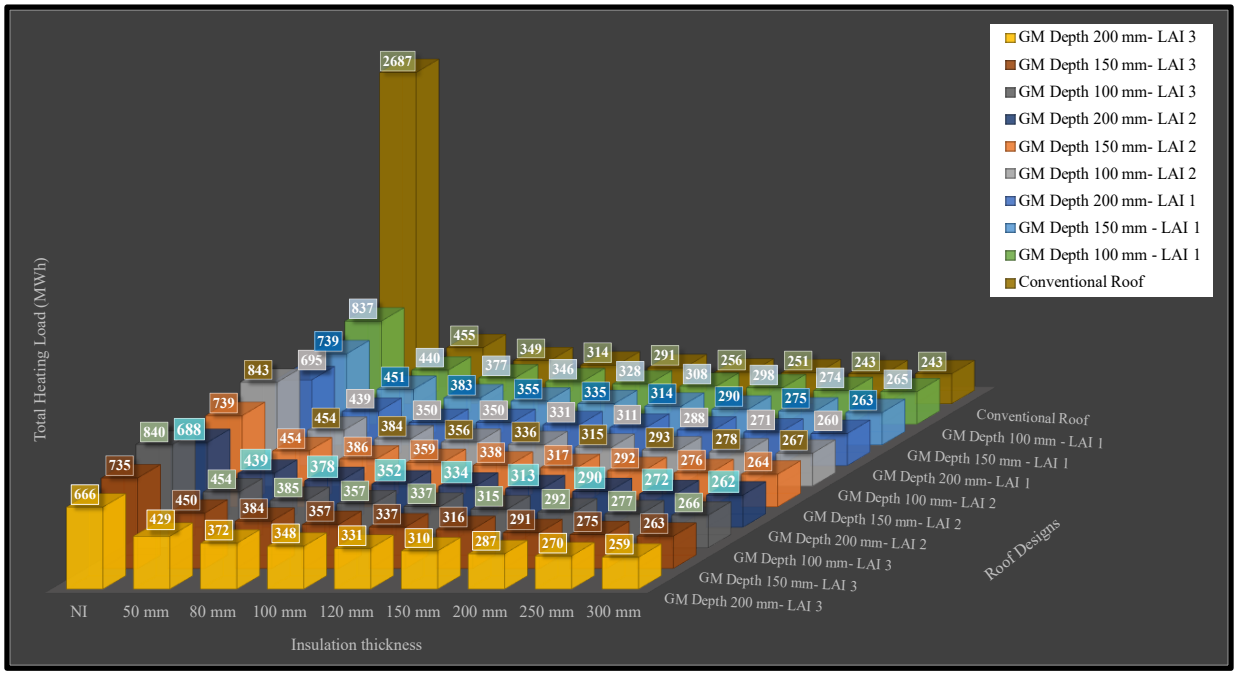

Figure 4-31: Total heating loads for all roof designs; all insulation thickness; LAIs; and growing media depths under future climate of 2080s – secondary school.

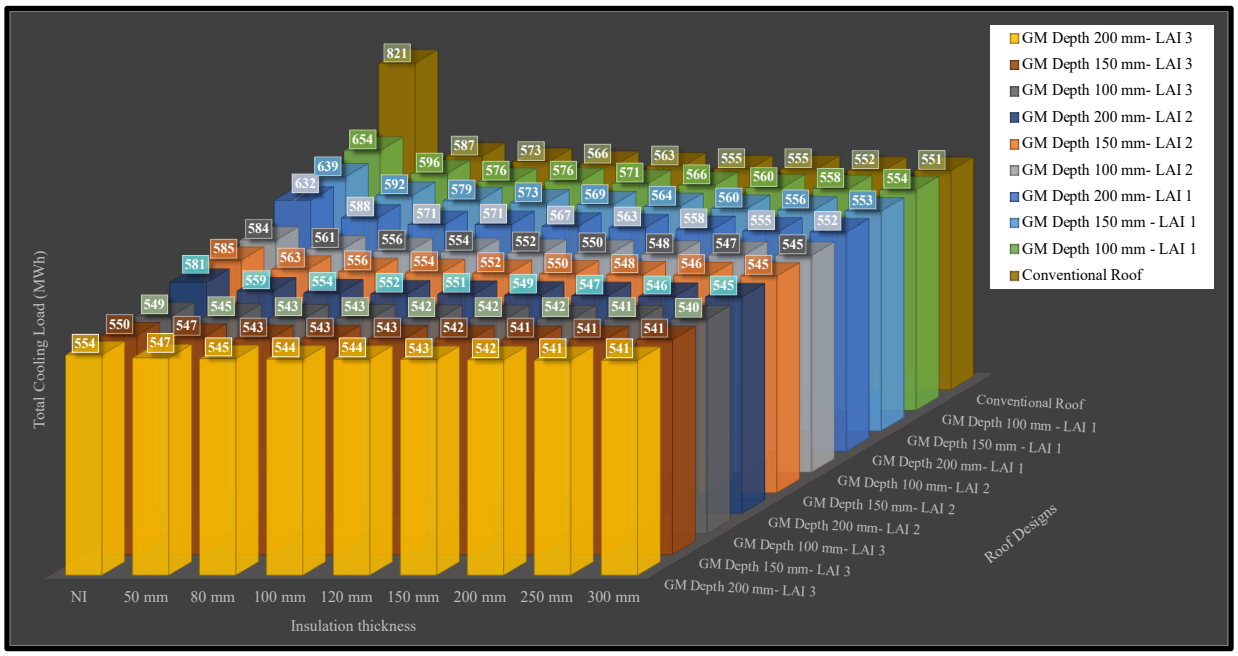

Figure 4-32: Total cooling loads for all roof designs; all insulation thickness; LAIs; and growing media depths under future climate of 2080s – secondary school.

Under future climate conditions, the uninsulated green roof designs decreased the building cooling and heating loads compared to the conventional uninsulated roof. In Figure 4-33, uninsulated green roof with growing media depth of 200 mm and LAI of 3 reduced 65% of total energy consumption compared to the conventional uninsulated roof. However, for insulated green roofs, the added insulation layer affected the thermal performance and lowered the energy savings provided by the green roof. The growing media depth of 200 mm with an LAI of 3 had the best overall performance in reducing the heating and cooling loads compared to other green roof designs with the same insulation thickness.

However, when green roof designs for total heating and cooling loads were compared to a conventional roof with the same insulation thickness, the green roof designs with insulation thicknesses of more than 80 mm consumed more energy than the conventional roof, shown in Figure 4-33. This suggested that the green roof provides minimum benefit in terms of energy under future climates compared to conventional roofs with insulation thicknesses more than 80 mm.

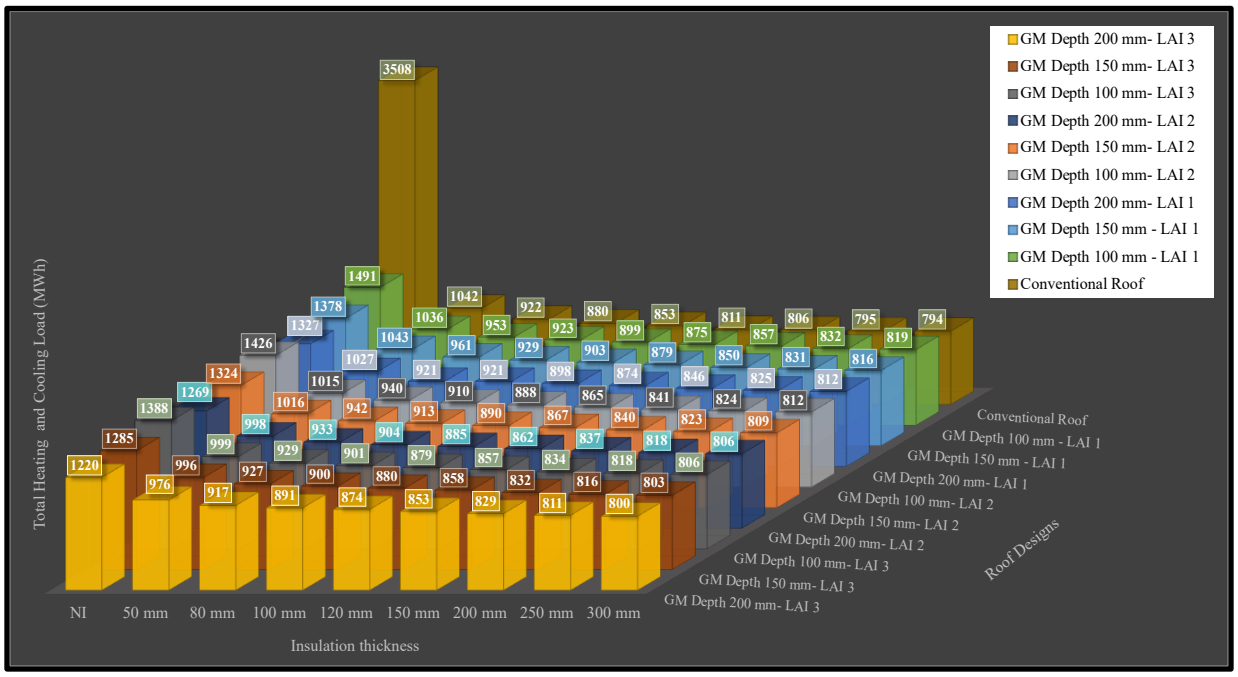

Figure 4-33: Total heating and cooling loads for all roof designs; all insulation thickness; LAIs; and growing media depths under future climate of 2080s – secondary school.

To explain the reason for the increase of energy consumption of green roofs with higher insulation thickness layers under future climate, the seasonal behaviour of the green roof is analysed. In the future conditions, similar to the current climate, using a green roof was beneficial in reducing the cooling loads during summer and spring for different insulation thicknesses (Figure 4-35). However, the seasonal heating loads were different in future compared to the current climate conditions. During fall and winter, the difference between the green roof heating loads and the conventional roof was smaller, indicating that a green roof would provide a lower benefit in decreasing the heating loads compared to the conventional roof. This is observed in Figure 4-34 when at insulation thickness of 80 mm during the fall season, the conventional and green roofs have similar heating loads. Hence, the total benefit of the green roof during winter and fall on decreasing the heating loads with different insulation thicknesses compared to the conventional roof was much lower than the current climate. Additionally, like the current climate, the cooling effect provided by the green roof during spring and summer caused the green roof to consume higher heating loads during these seasons compared to the conventional roof, as shown in Figure 4-34. Therefore, the small benefit provided by the green roof on heating loads and the rise in

heating loads (during spring and summer) led the green roof to require higher total energy compared to the conventional roof (shown in Figure 4-36).

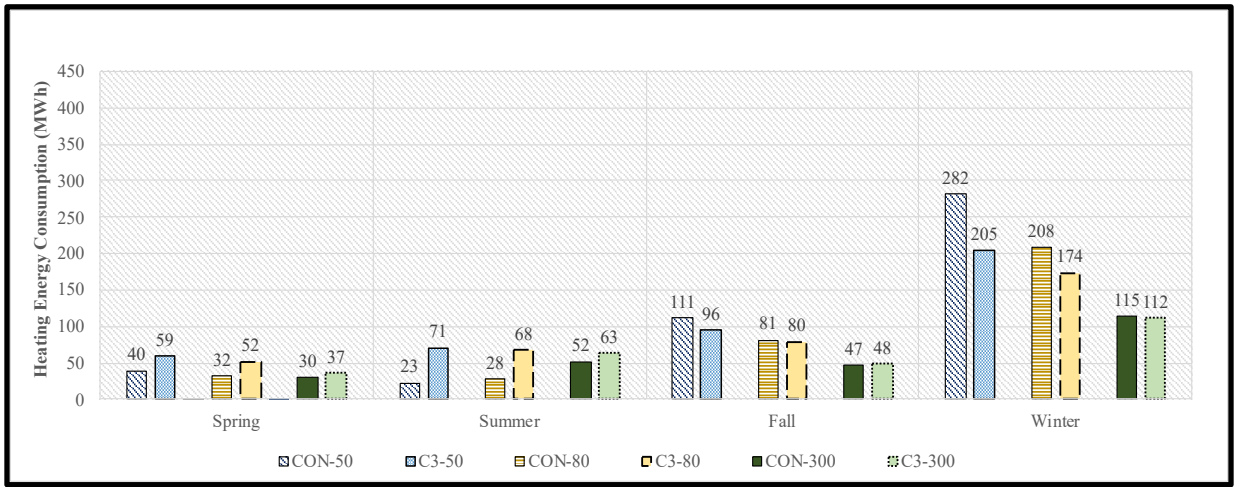

Figure 4-34: Seasonal heating loads for conventional roof (CON) and green roof with design of growing media of 200 mm and LAI of 3 for insulation thicknesses 50 mm, 80 mm and 300 mm – future climate (secondary school).

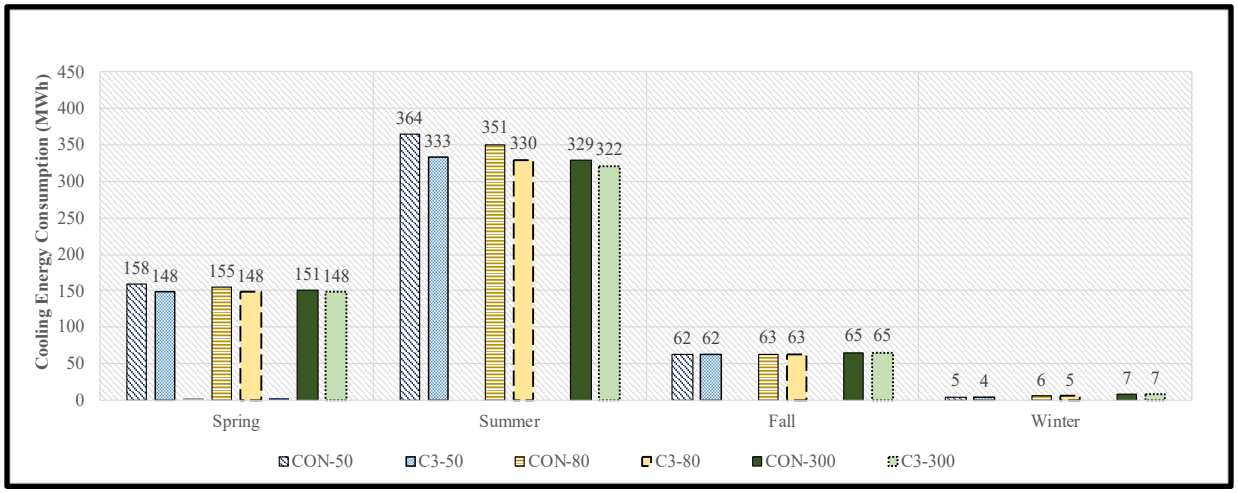

Figure 4-35: Seasonal cooling loads for conventional roof (CON) and green roof with design of growing media of 200 mm and LAI of 3 for insulation thicknesses 50 mm, 80 mm and 300 mm – future climate (secondary school).

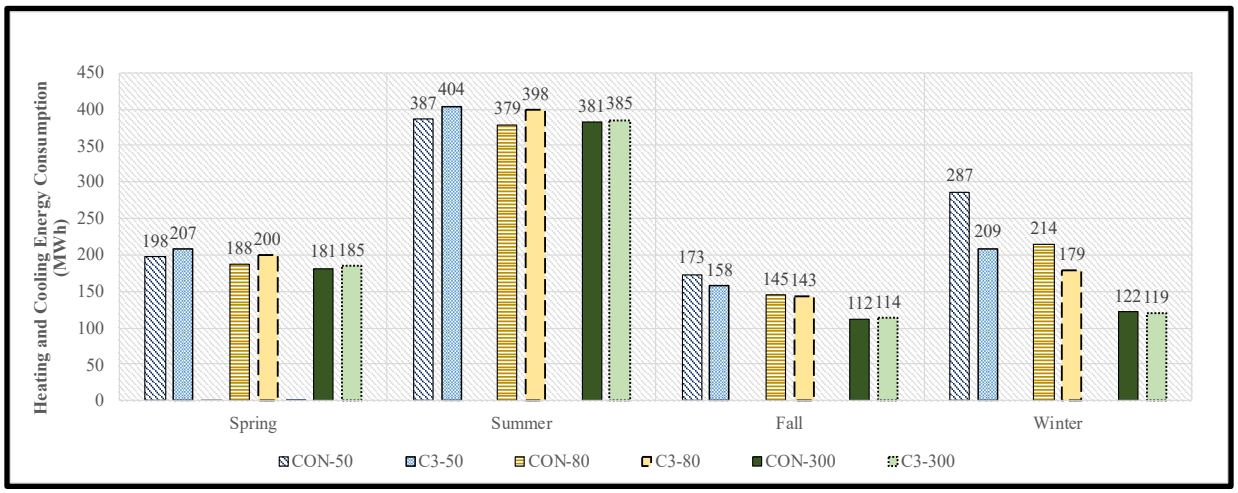

Figure 4-36: Seasonal total heating and cooling loads for conventional roof (CON) and green roof with design of growing media of 200 mm and LAI of 3 for insulation thicknesses 50 mm, 80 mm and 300 mm – future climate (secondary school).

The results for annual energy savings showed green roofs with insulation thickness of 80 mm caused higher annual heating loads compared to the conventional roof. Hence all green roof designs experienced negative heating energy savings, shown in Figure 4-37. On the other hand, the green roofs with LAI of 2 and 3, due to high evapotranspiration and the cooling effect, caused positive cooling savings. This led to positive total heating and cooling energy savings for all green roof designs with LAI of 2 and 3. Figure 4-37 shows for growing media of 200 mm and LAI of 3, the total energy saved by the green roof design is 6 MWh, indicating the green roof consumed lower total energy compared to the conventional roof. Although, for insulation thicknesses of 100 mm and above, the total energy savings reached a negative value due to the insulation layer inhibiting green roof thermal performance. This is shown in Figure 4-38 where with an insulation thickness of 100 mm, all green roof designs have negative total energy savings.

All plots for the energy savings and seasonal cooling and heating loads for different roof designs with insulation thicknesses of 50 mm, 80 mm and 300 mm for the secondary school under future climate are provided in Appendix B.

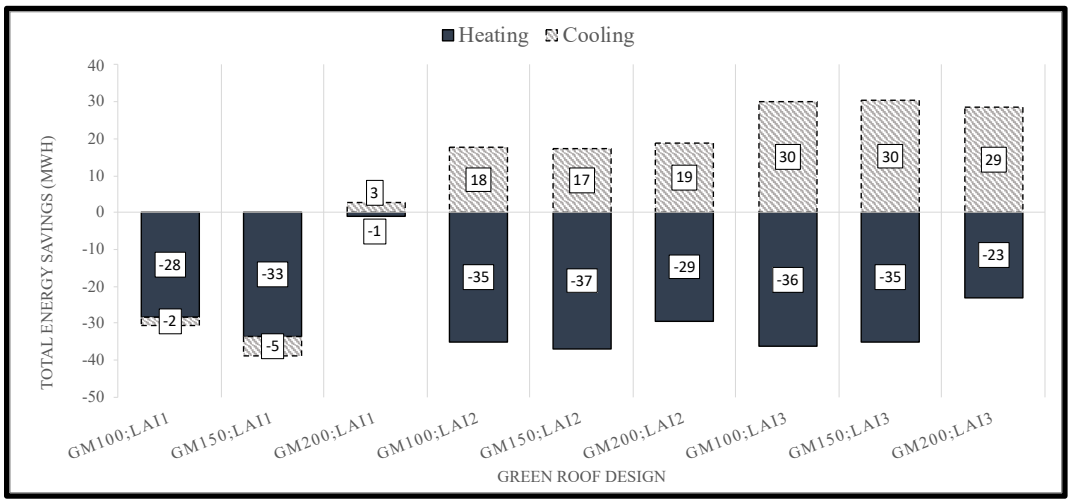

Figure 4-37: Total heating and cooling energy savings (MWh) of green roof compared to conventional roof for all growing media (GM) depths and LAIs; with 80 mm insulation layer – future climate (secondary school).

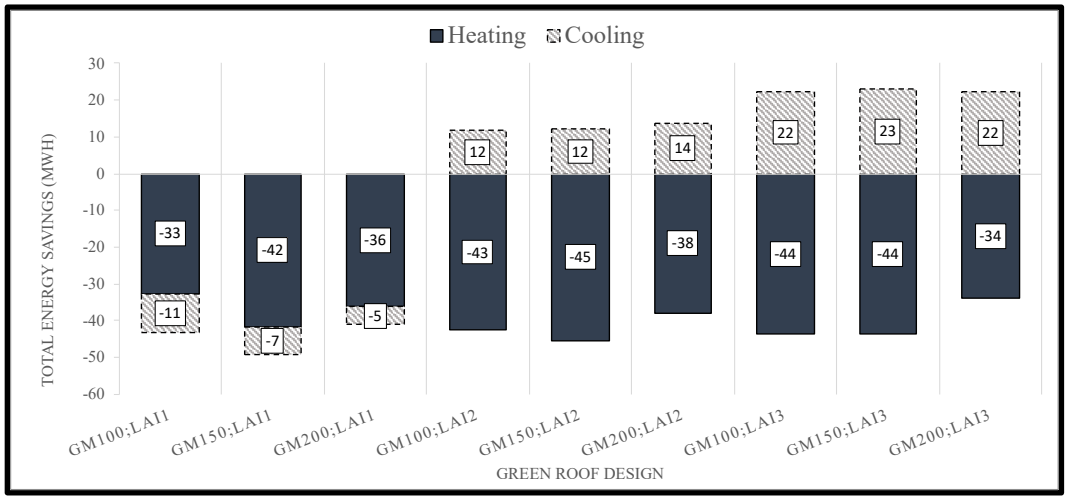

Figure 4-38: Total heating and cooling energy savings (MWh) of green roof compared to conventional roof for all growing media (GM) depths and LAIs; with 100 mm insulation layer – future climate (secondary school).

All green roof designs maintained DBGR value more than 1 for green roofs with insulation thicknesses of 50 mm under future conditions, shown in Figure 4-39. The growing media of 200 mm with an LAI of 3 achieved the highest DBGR value of 1.01 among all green roof designs with an insulation thickness of 80 mm. However, for designs with insulation thicknesses more than 80 mm, all green roof designs had DBGR less than 1 and required higher energy than the conventional roof.

The secondary school optimal green roof design under future conditions was not the same as the current climate conditions due to the shift in building cooling and heating consumption. The

suggested design under future conditions is the growing media depth of 200 mm with LAI of 3 and insulation thickness of 80 mm. The suggested optimal design consumes lower total energy compared to the conventional roof and provides the highest energy savings among other green roof designs (Figure 4-33).

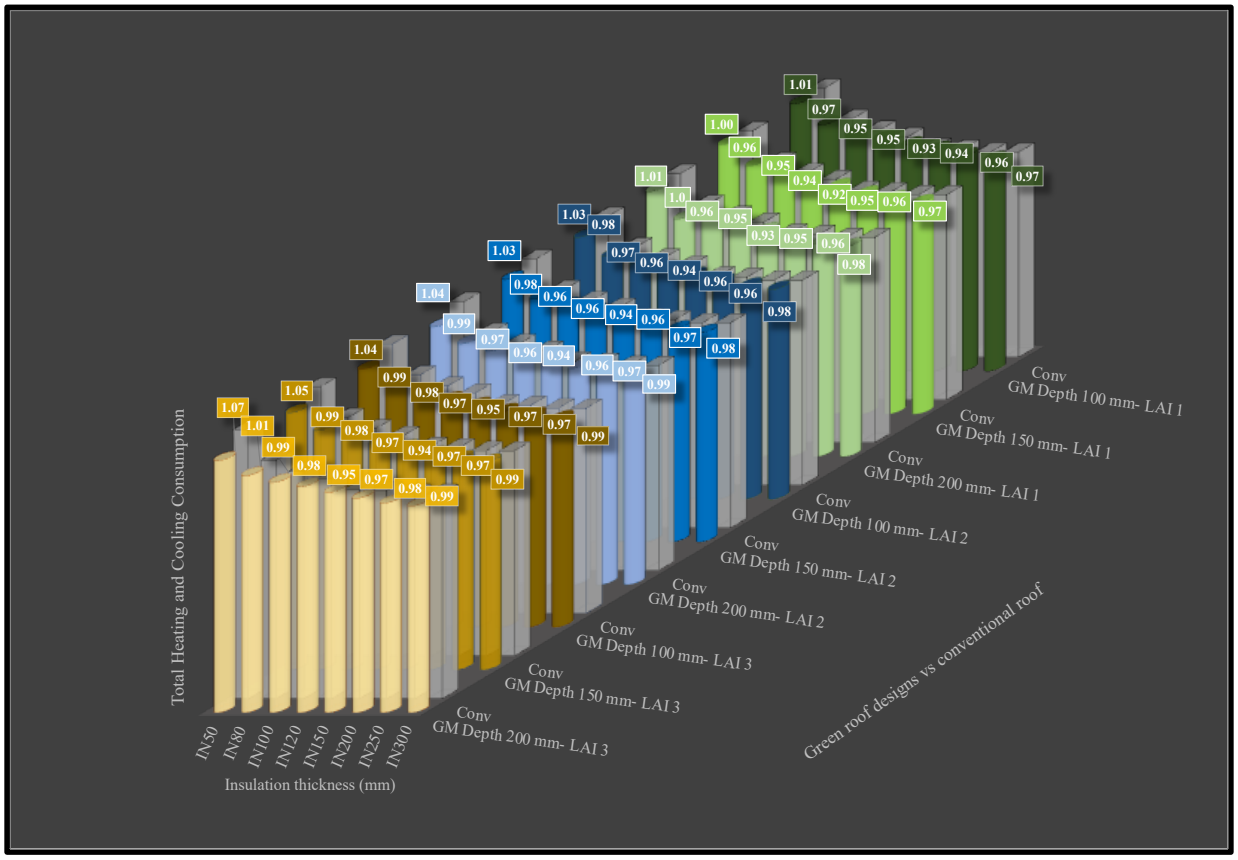

Figure 4-39: DBGR of all green roof designs under future climate conditions of 2080s (grey colour bars represent conventional roof) – secondary school.

All in all, under both current and future climate conditions, green roof design with a growing media depth of 200 mm and LAI of 3 performed best on lowering the total energy consumption of the secondary school compared to all other green roof designs. However, the added thermal insulation affected the green roof thermal performance. The use of green roofs with added insulation thickness did not enhance the green roof thermal performance but caused limitations. Under both current and future climate conditions, the uninsulated green roof designs had the highest total energy savings. As the insulation thickness increased, the thermal performance of the green roof on total energy consumption was impacted until, at a certain range, the added thermal insulation

thickness inhibited any thermal benefit provided by the green roof. Under the current climate conditions, the growing media depth 200 with an LAI of 3 had the highest energy savings among all green roof designs yet required more energy than the conventional roof when insulation thickness of 120 mm and higher were used. Under future climate conditions, growing media depth 200 mm with LAI of 3 caused the green roof to consume more energy than the conventional roof when insulation thickness of more than 80 mm were used.

Therefore, it is concluded for a secondary school building in the City of Toronto, use of green roofs compared to highly insulated conventional roof provides no benefit in terms of energy on lowering building energy consumption. However, green roofs would have strong potential to be used as retrofits on poorly insulated roofs. Uninsulated green roof (growing media depth 200 mm and LAI 3) showed up to 71.7% and 65% energy reduction compared to conventional uninsulated roofs under current and future conditions, respectively. Lastly, it is important to mention that this research's conclusions are specific to climate, building type, and green roof design parameters.

Chapter Five: Other Building Archetypes and Water Retention Performance of Green Roof

Chapter four concluded that the use of green roof on secondary school building type in the City of Toronto under current and future climate conditions with high thermal insulation thickness is not a suitable replacement for a conventional roof. Therefore, other building archetypes were selected to determine if the thermal performance of green roof would behave similarly. Green roof designs with a growing media depth of 100 mm, 150 mm and 200 mm and LAIs of 1, 2 and 3 were investigated on two building archetypes of office and hospital. Chapter four showed the green roof thermal performance changes by small magnitudes as the insulation thickness increases. Thus, the thermal insulation thicknesses considered for green roof designs in this section are low (50 mm), medium (120) mm and high (300 mm). Additionally, the green roof thermal performance without insulation on office and hospital archetypes is analysed. All in all, the objective of this chapter was to determine if the hospital and office building at insulation thicknesses of a low, medium, and high would have similar thermal performance as the secondary school.

In addition, the effect of the green roof on rainwater capture and runoff reduction for all three archetype buildings of secondary school, hospital and office, were measured and presented to showcase green roof stormwater retention benefits.

5.1 Office Building – Current and Future Climate

Current Climate

The green roof performance on building energy savings was lower than secondary school due to a smaller roof area. The uninsulated green roof design (growing media 200 and LAI 3) saved 31% of total energy by office building and 72% by the secondary school. The larger roof area and vegetation coverage of secondary school led to higher energy savings by the uninsulated green roof compared to the office building.

In Figure 5-1 the office building total energy consumption for all green roof designs and insulation thickness is provided. The uninsulated green roof with higher growing media depth and LAI of 3

resulted in the lowest building total energy consumption compared to other uninsulated green roof designs for the office building. The energy savings by the uninsulated green roof designs was more compared to insulated green roofs. This indicated that thermal insulation impacts the green roof performance and at high thicknesses the green roof designs behaved similarly in lowering the building energy consumption. Unlike the secondary school building, the green roof for all office designs maintained lower energy than the conventional roof at all insulation thicknesses. Although the energy consumed by the green roof designs and the conventional roof at insulation thickness of 300 mm were within the same range, the green roofs designs did not require higher energy than the conventional roof for office building (Figure 5-1). The building related characteristics, building system and services related to characteristics and occupant related characteristics that influence building energy consumption (Silva et al. 2012) caused different green roof thermal performance on office and secondary school buildings. The seasonal energy consumption for the office building is analysed to understand the difference in green roof thermal performance from secondary school.

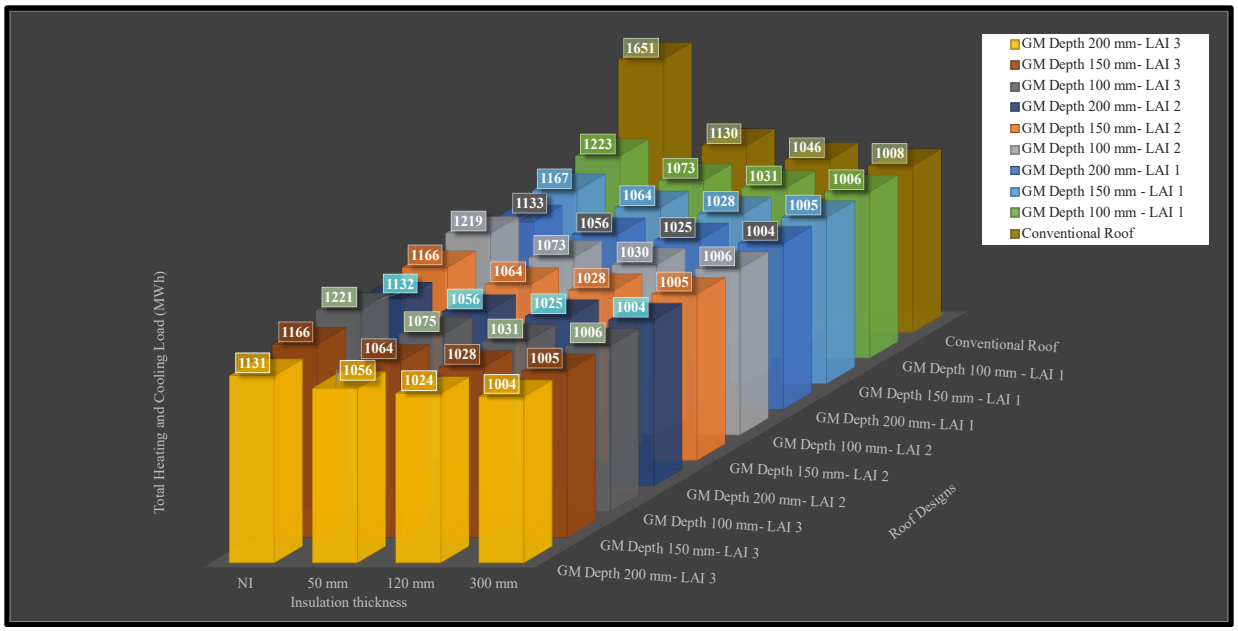

Figure 5-1: Total heating and cooling loads for all roof designs; all insulation thickness; LAIs; and growing media depths under current climate– Office building.

The seasonal cooling and heating consumption for office building were different compared to the secondary school due to the different building characteristics. Figure 5-2 and Figure 5-3 presents the seasonal heating and cooling loads for the conventional and green roof with the growing media

depth of 200 mm and LAI of 3 for different insulation thicknesses. The use of high growing media depth caused the green roof with all insulation thicknesses to require a lower heating load compared to the conventional roof during winter and fall (Figure 5-2). Additionally, the office building required no heating loads during the summer season; this was unlike the secondary school building, where heating loads were used throughout the year. Hence, no negative impact was caused by the green roof during the summer season compared to the conventional roof. The green roof on the office building at all insulation thicknesses maintained lower cooling loads compared to the conventional roof during summer due to the cooling effect provided (Figure 5-3). Therefore, the green roof's combined total heating and cooling loads were lower than the conventional roof in all seasons (Figure 5-4). Results on seasonal office analysis indicated that the building characteristics and system behaviour influence the green roof's thermal performance on building energy consumption.

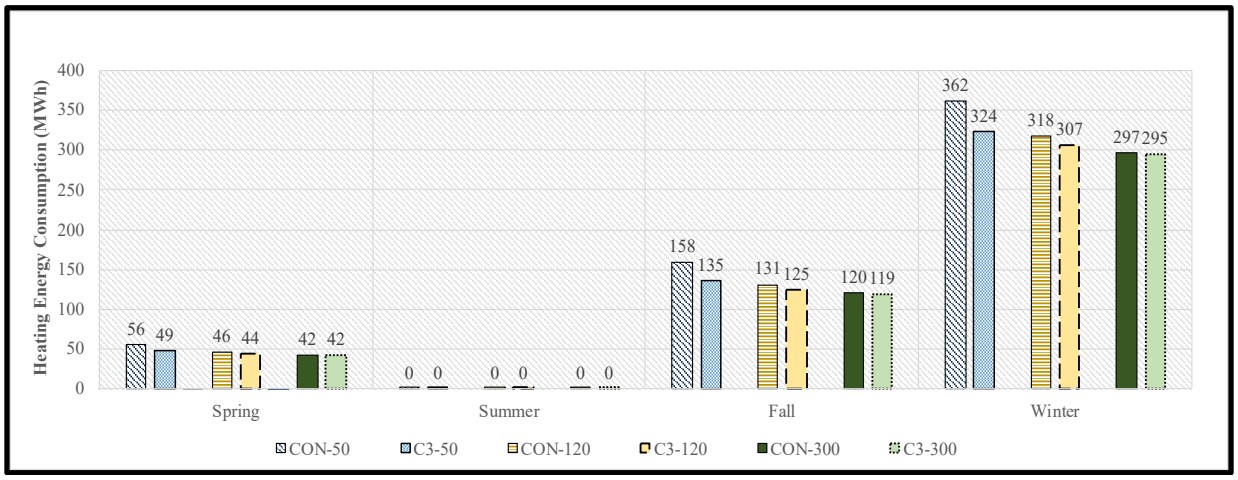

Figure 5-2: Seasonal heating loads for conventional and green roofs with growing media of 200 mm and LAI of 3 for insulation thicknesses 50 mm, 120 mm and 300 mm – current climate (office building).

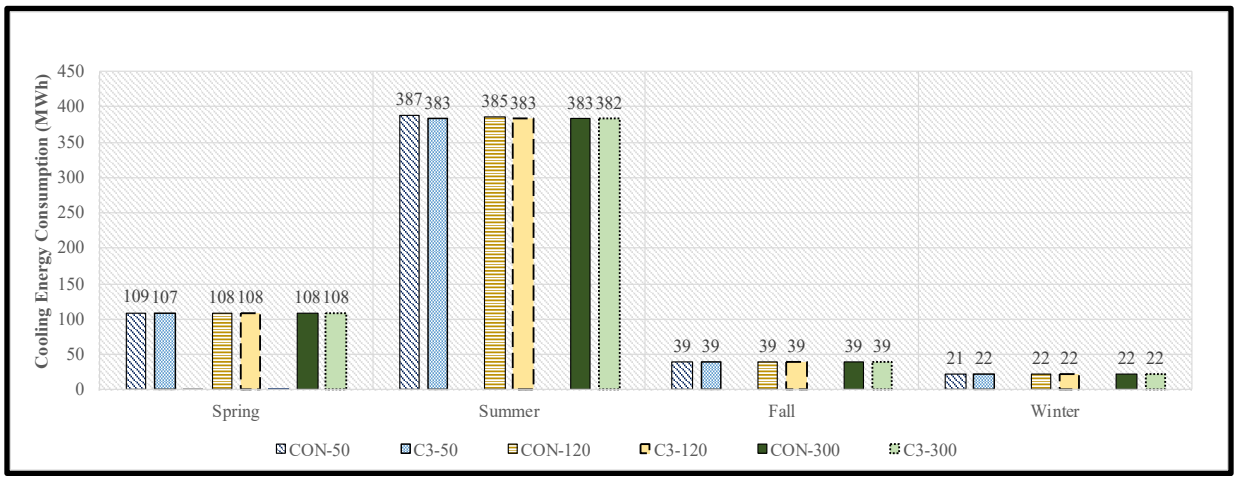

Figure 5-3: Seasonal cooling loads for conventional and green roofs with growing media of 200 mm and LAI of 3 for insulation thicknesses 50 mm, 120 mm and 300 mm – current climate (office building).

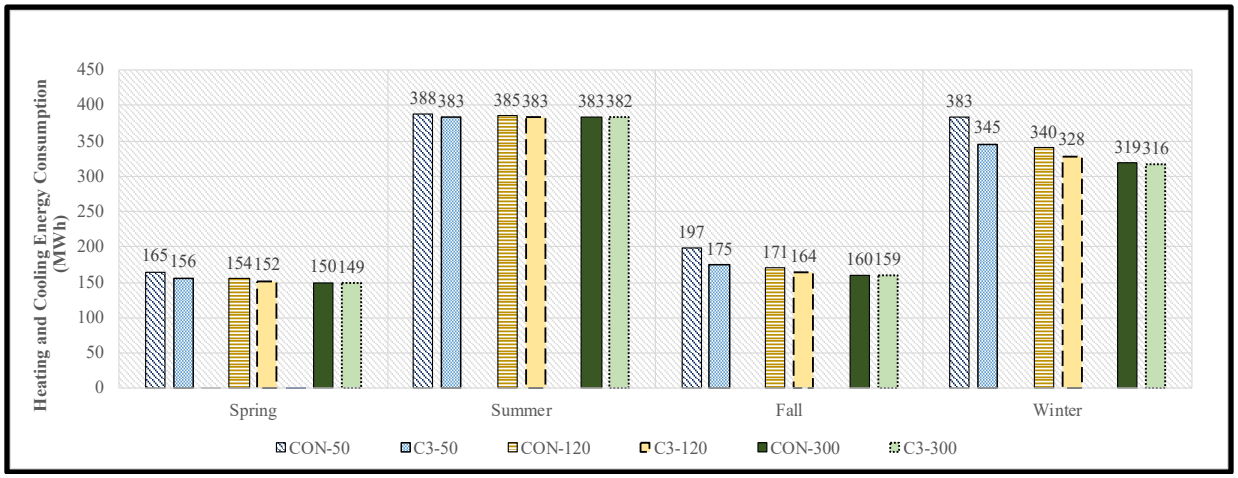

Figure 5-4: Seasonal total heating and cooling loads for conventional and green roofs with growing media of 200 mm and LAI of 3 for insulation thicknesses 50 mm, 120 mm and 300 mm – current climate (office building).

Figure 5-5 and Figure 5-6 present the energy savings by the office building for all green roof designs with insulation thicknesses of 50 mm and 300 mm. The total energy savings of heating and cooling loads combined remained positive for all green roof designs for all insulation thicknesses. This indicated that the conventional office roof with various insulation thicknesses of low to high consumed higher energy than the green roof. As observed in Figure 5-5, all green roof designs with insulation thickness of 50 mm had positive heating and cooling loads. The higher insulation provided by the green roof caused the green roof to lower the building heating loads more than the conventional roof. Additionally, the cooling provided by the green roof caused more cooling energy savings compared to the conventional roof. However, at high insulation thickness,

the green roof thermal performance was impacted, and the heating and cooling savings were lowered compared to green roofs with low insulation, shown in Figure 5-6. The plots for annual total heating and cooling consumption and savings for the office building under the current climate conditions for all green roofs are presented in Appendix C.

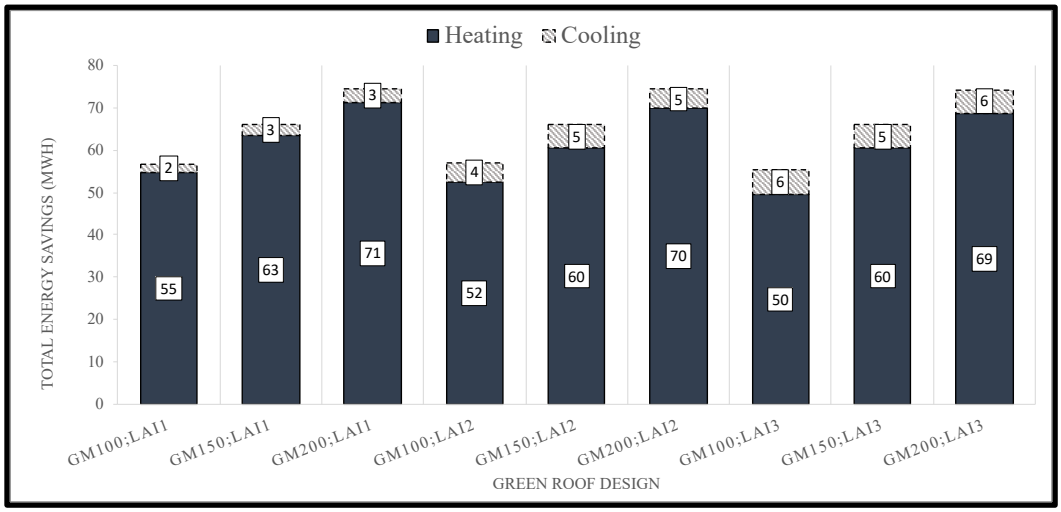

Figure 5-5: Total heating and cooling energy savings (MWh) of a green roof compared to a conventional roof for all growing media (GM) depths and LAIs; with 50 mm insulation layer – current climate (office building).

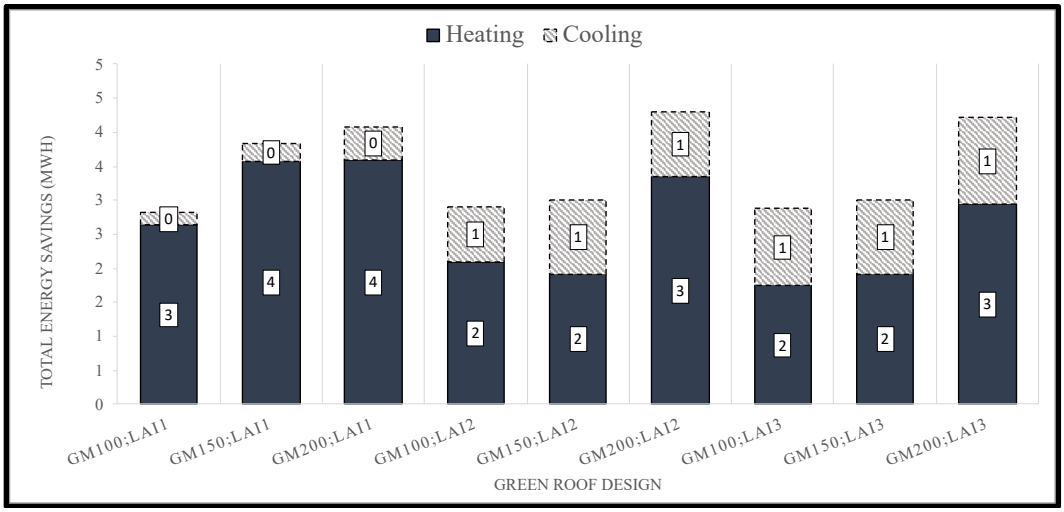

Figure 5-6: Total heating and cooling energy savings (MWh) of green roof compared to conventional roof for all growing media (GM) depths and LAIs; with 300 mm insulation layer – current climate (office building).

Figure 5-7 presents the DBGR of the office archetype for all green roof designs. Results showed that under the current climate conditions, green roofs with growing media of 200 mm and LAI of 1, 2 and 3 for insulation thicknesses of 50 mm all had a DBGR of 1.07. This indicated use of 50 mm insulation lowered the green roof efficacy and caused green roofs with a growing media depth

of 200 mm, and different LAIs to have similar DBGR values. As the insulation thickness increased, the DBGR value decreased for all green roof designs, and at insulation thickness of 300 mm, the value of DBGR for all green roofs reached a value of 1. Thus, the green roof thermal performance for the office building under current climate conditions indicated at high insulation thickness of 300 mm; both conventional and green roofs behaved similarly in building energy consumption.

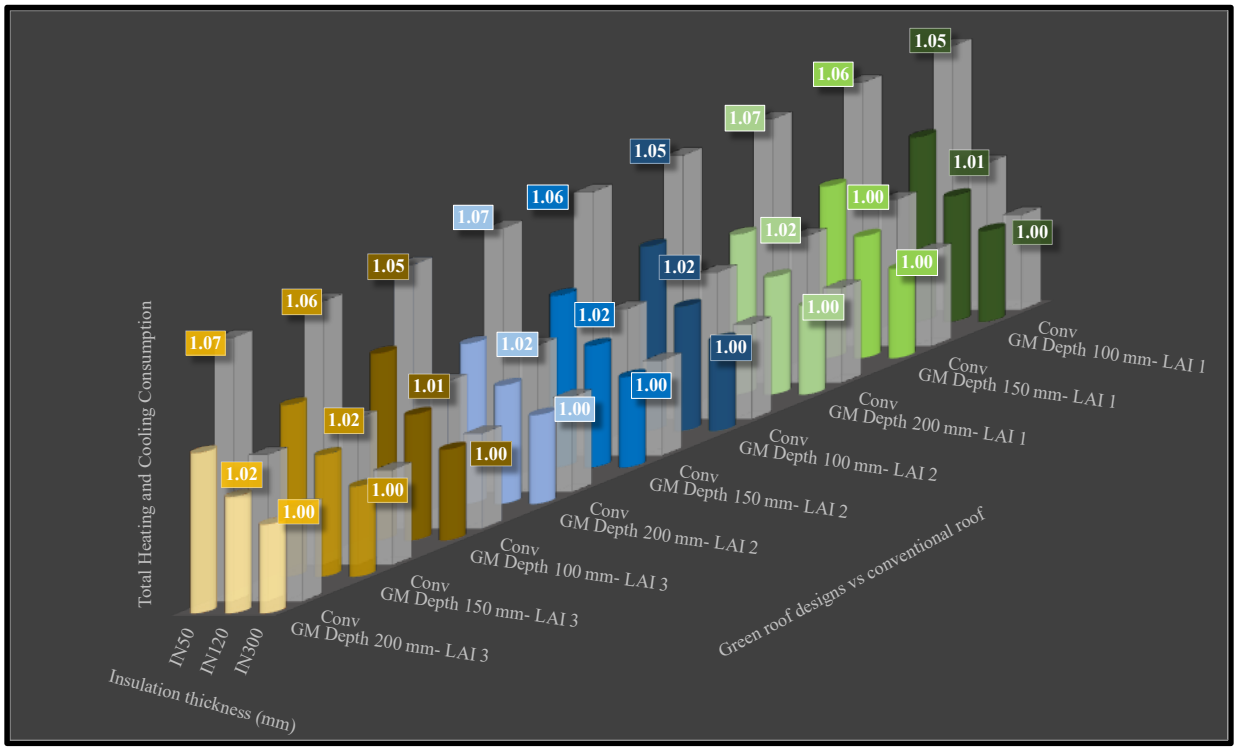

Figure 5-7: DBGR of all green roof designs under current climate conditions (grey colour bars represent conventional roof) – office building.

The optimal suggested design under current climate conditions for the office building is green roof with growing media depth of 200 mm and LAI of 3 for insulation thickness of 120 mm. The suggested design requires lower energy than the conventional roof and saves the highest cooling and heating loads among other green roof designs with insulation thickness of 120 mm. Annual total heating and cooling consumption and savings for the office building under current climate conditions for all green roofs are presented in Appendix C.

Future Climate

The heating and cooling consumption under future climate conditions shifted for the office building. Due to higher temperatures, building heating loads were decreased while the cooling loads increased. Therefore, the use of thermal insulation impacted the green roof thermal performance more compared to current climate conditions. The insulation layer is most effective in reducing the heating loads of buildings; hence the use of insulation in future climate conditions provides less benefit in reducing the total building energy consumption. Figure 5-8, presents the DBGR for the green roof designs under future climate for the office building. The DBGR value at insulation thickness of 50 mm was lower for the future than current climate conditions, indicating that the green roof provides less benefit in reducing the total building energy consumption compared to the conventional roof with the same insulation thickness. The green roof with a growing media depth of 200 mm, LAI of 3 and insulation thickness of 50 mm had a DBGR of 1.04 under future climate conditions, while the same green roof design under had a DBGR of 1.07 current climate conditions. At insulation thicknesses of 120 mm and lower the green roof designs decreased the building energy consumption compared to the conventional roof under future conditions. However, at a high insulation thickness (300 mm), the green roof's energy benefit was minimal compared to the conventional roof (Figure 5-8).

The optimal green roof design in the future remained the same as the current climate conditions for the office building. The suggested optimal design under future conditions is growing media depth of 200 mm and LAI of 3 with insulation thickness of 120 mm. This design consumes lower total energy compared to the conventional roof and provides the highest energy savings among other green roof designs with insulation thickness of 120 mm. Annual total heating and cooling consumption and savings for the office building under future climate conditions for all green roofs are presented in Appendix D.

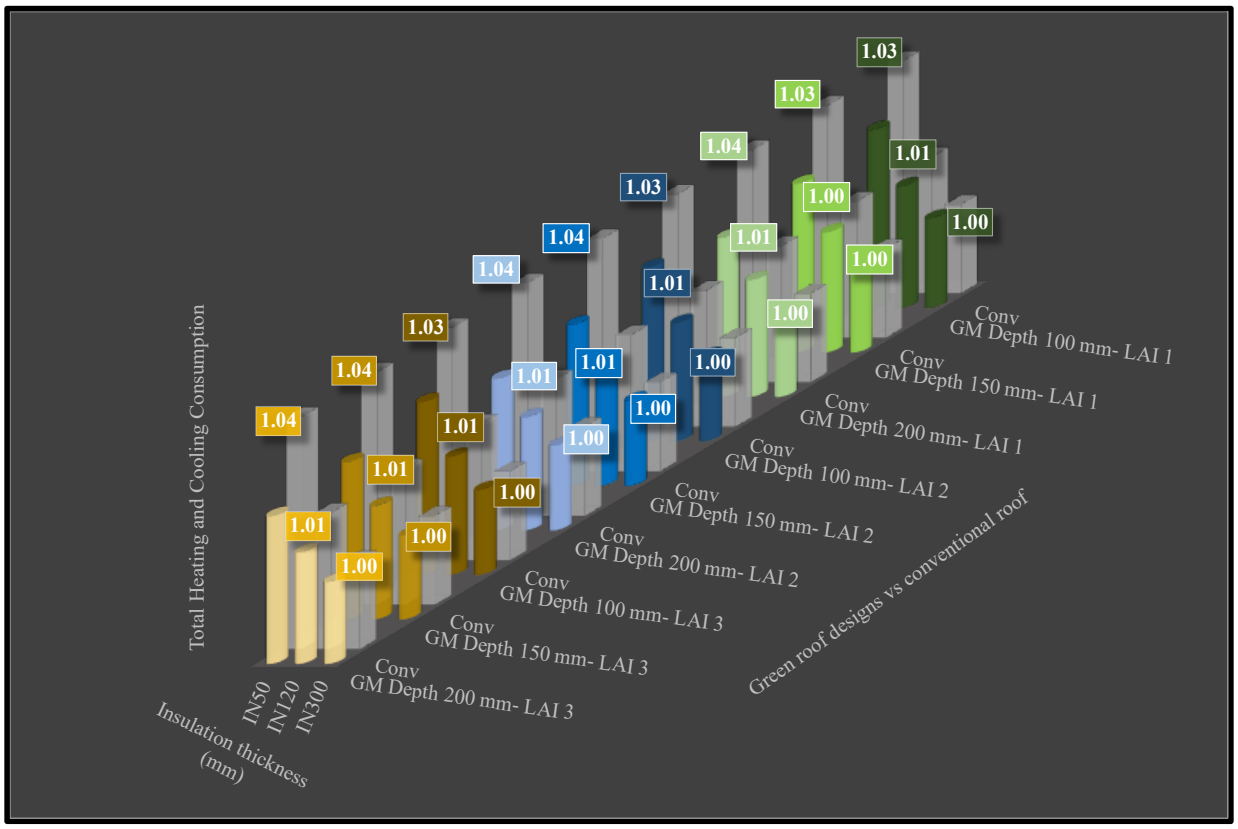

Figure 5-8: DBGR of all green roof designs under future climate conditions (grey colour bars represent conventional roof) – office building.

5.2 Hospital Building – Current and Future Climate

Current Climate

The green roof thermal performance on the hospital building was different compared to the office and secondary school. Figure 5-9, provides the annual total energy consumption for uninsulated and insulated conventional and green roof designs. Uninsulated green roof design with growing media of 200 mm and LAI of 3 performed the best in decreasing the building energy consumption compared to the conventional uninsulated roof. However, at medium insulation (120 mm thickness), the thermal performance for green roof designs changed; the green roof with the highest growing media depth and largest LAI was no longer the best-performed design in reducing the energy consumption of the building compared to other green roof designs. In Figure 5-9, at insulation thicknesses of 120 mm, the green roof with lower growing media required less energy than green roof designs with higher growing media depth. This difference was due to the different

characteristics of hospital buildings causing the green roof to use more heating loads compared to the conventional roof. The hospital building envelope is considered well insulated compared to office and school buildings. Therefore, using a green roof with higher insulation thickness caused the building to require more heating loads than a conventional roof. Figure 5-10 and Figure 5-11 presents the hospital seasonal heating loads for growing media of 150 mm and 200 mm with LAI of 3, respectively. The green roof with high insulation thickness required more heating loads during the winter season than the conventional roof. Results showed that as the growing media depth increased, the heating loads increased for insulation thickness of 120 mm and 300 mm than the conventional roof (Figure 5-10 and Figure 5-11). Due to the well-insulated envelope of the hospital building, the insulation provided by the green roof growing media with high insulation thickness led to more heating loads required than the conventional roof.

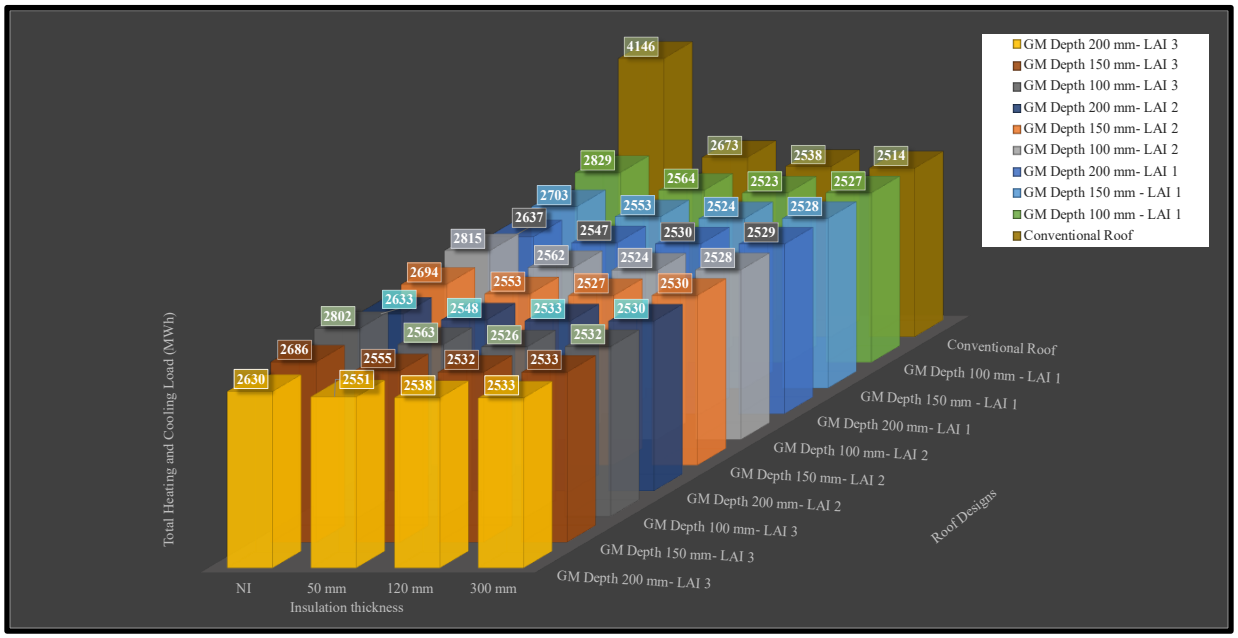

Figure 5-9: Total heating and cooling loads for all roof designs; all insulation thickness; LAIs; and growing media depths under current climate – hospital building.

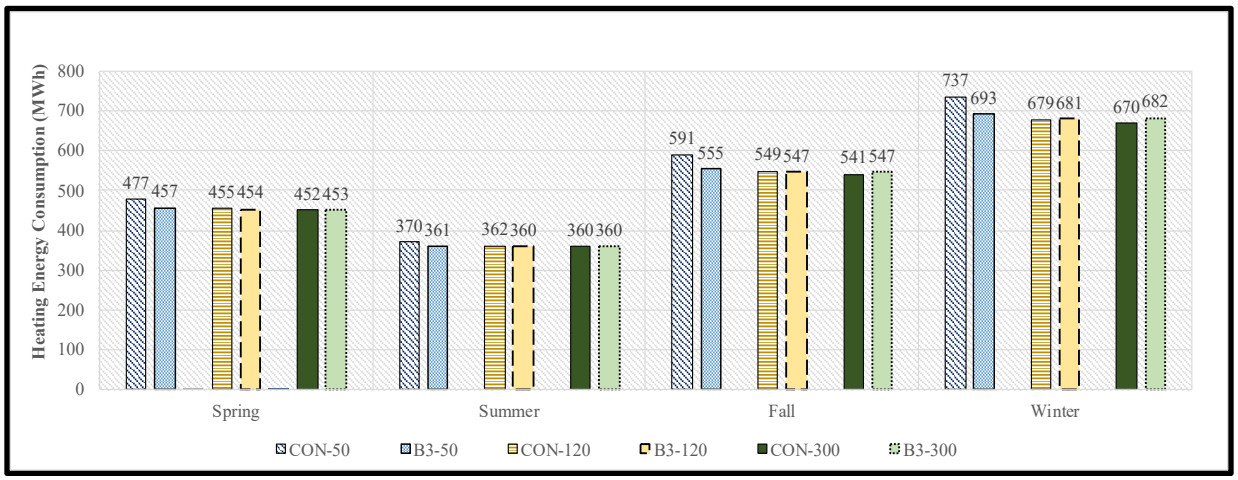

Figure 5-10: Seasonal heating loads for conventional and green roofs with growing media of 150 mm and LAI of 3 for insulation thicknesses 50 mm, 120 mm and 300 mm – current climate (hospital building).

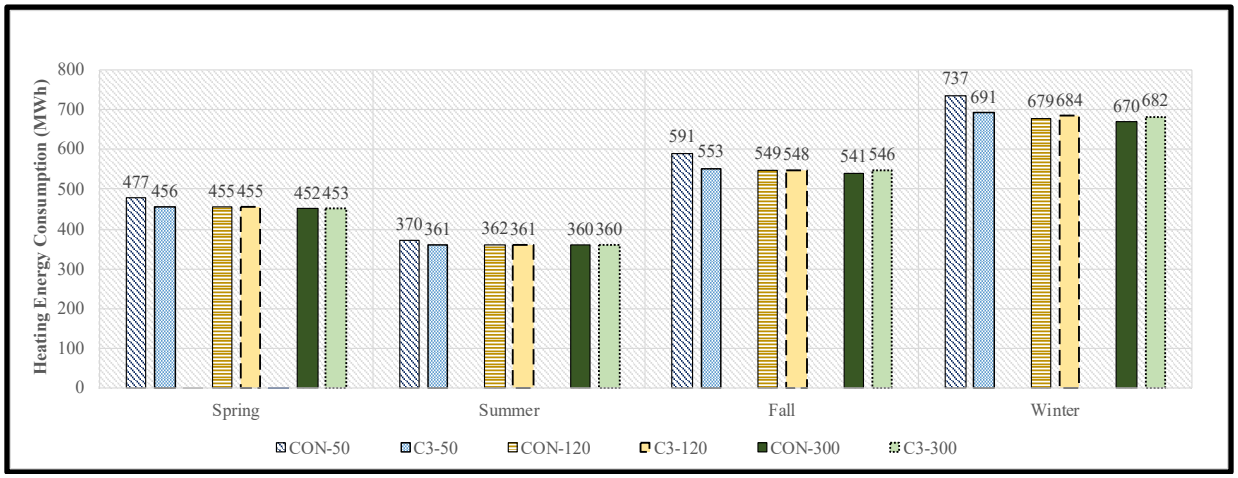

Figure 5-11: Seasonal heating loads for conventional and green roofs with growing media of 200 mm and LAI of 3 for insulation thicknesses 50 mm, 120 mm and 300 mm – current climate (hospital building).

During spring, fall and winter the green roof cooling loads remained unchanged with only small savings in summer cooling loads. Thus, higher green roof heating requirements led to higher total seasonal heating and cooling loads during winter than the conventional roof (Figure 5-12 and Figure 5-13). Generally, the thicker growing media depth with 120 mm and 300 mm insulation layers required higher heating loads. Therefore, green roof designs with a growing media depth of 200 mm and thicker insulation required more energy than green roof designs with a lower growing media depth of 100 mm and insulation thicknesses.

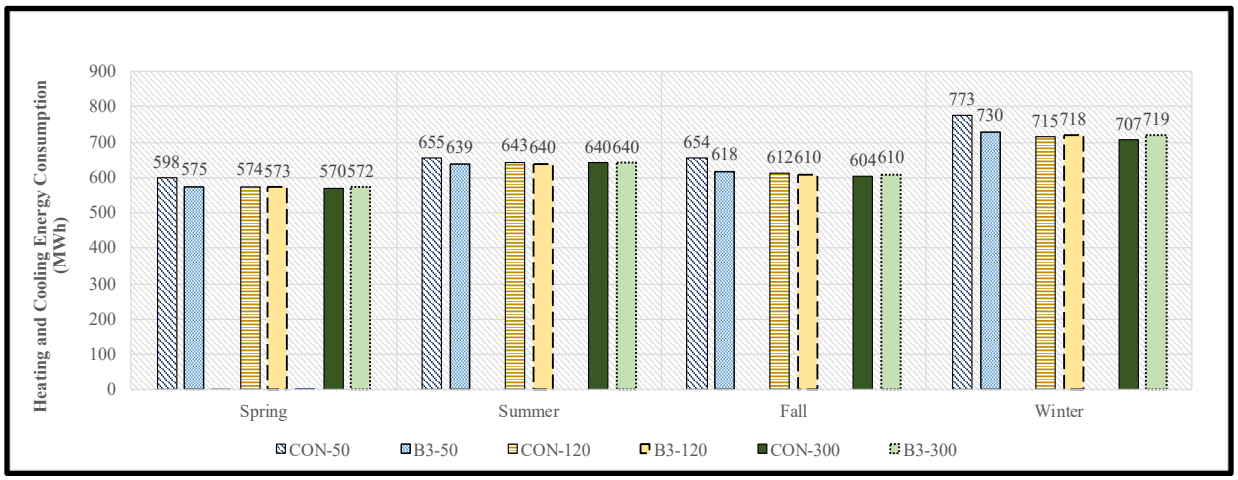

Figure 5-12: Seasonal total heating and cooling loads for conventional and green roofs with growing media of 150 mm and LAI of 3 for insulation thicknesses 50 mm, 120 mm and 300 mm – current climate (hospital building).

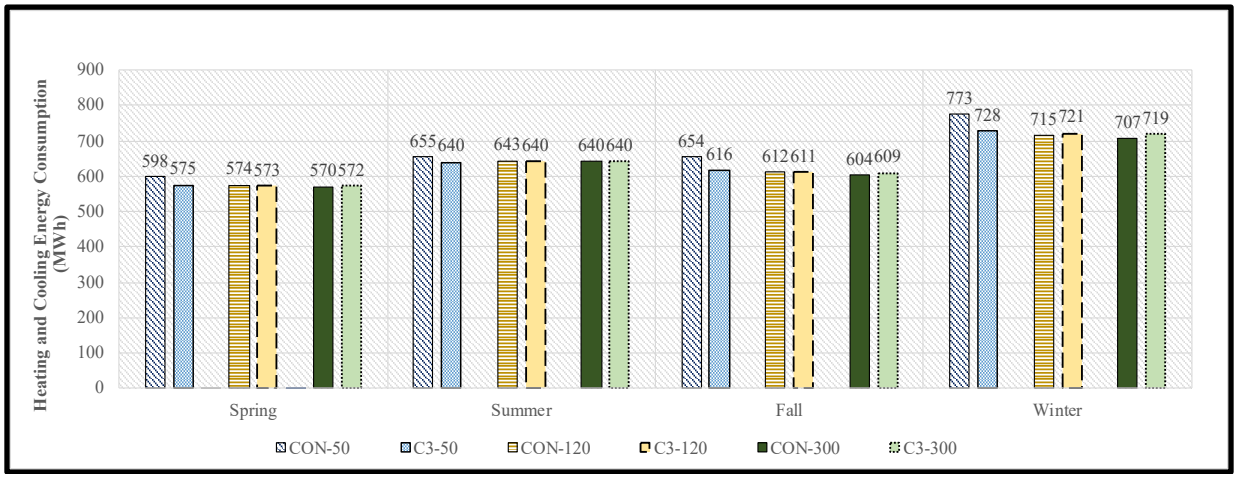

Figure 5-13: Seasonal total heating and cooling loads for conventional and green roofs with growing media of 200 mm and LAI of 3 for insulation thicknesses 50 mm, 120 mm and 300 mm – current climate (hospital building).

The annual total heating and cooling energy savings for all green roofs at a low insulation thickness of 50 mm were positive. However, higher heating loads required by the green roof compared to the conventional roof, at insulation thickness of 300 mm, caused negative heating energy savings (Figure 5-14). In addition, the insulation thickness also impacted the green roof cooling benefit and caused most green roof designs to have zero cooling savings. As a result, all green roof designs' total energy savings with insulation thickness of 300 mm were negative, and the benefit in terms of energy was minimal. Annual total heating and cooling consumption and savings for hospital building under current climate conditions for all green roofs are presented in Appendix E.

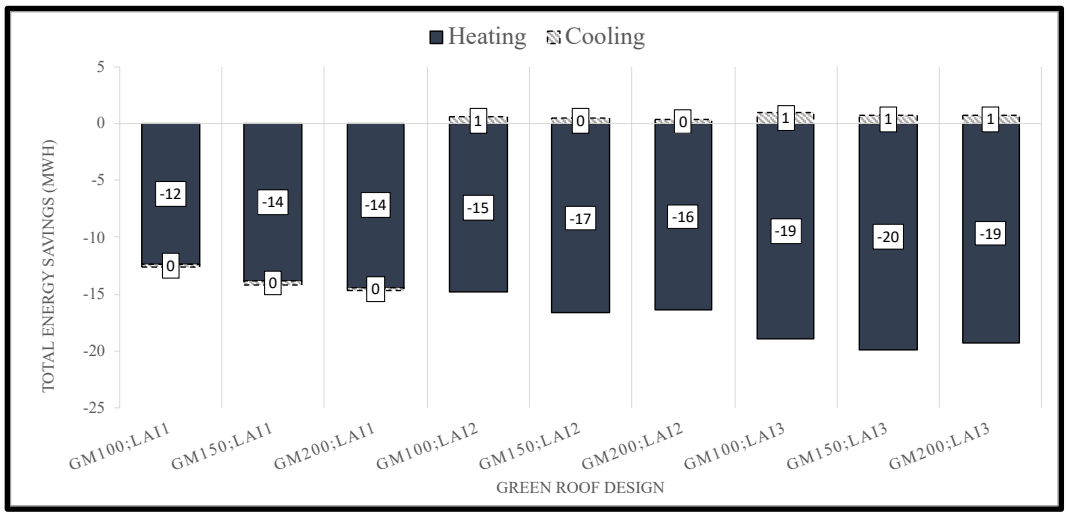

Figure 5-14: Total heating and cooling energy savings (MWh) of green roof compared to conventional roof for all growing media (GM) depths and LAIs; with 300 mm insulation layer – current climate (hospital building).

Figure 5-15 presents the hospital building DBGR values for all green roof designs under current climate conditions. At insulation thickness of 300 mm, all green roof designs performed poorly and had higher total energy consumption than conventional roofs. However, at lower insulation thickness of 50 mm and 120 mm, the DBGR for all green roof designs was higher than or equal to 1, indicating the green roof either required less energy or performed just as well as the conventional roof. Overall, the use of an insulation layer impacted the green roof thermal performance compared to the conventional roof, and even at low insulation thicknesses, most green roof designs behaved similarly and maintained the same DBGR values. The optimal green roof designs under current climate conditions for hospital building is growing media depth of 100 mm with LAI of 2 and insulation thickness of 120 mm. The suggested optimal design saves the highest cooling and heating loads among other green roof designs with same insulation thickness.

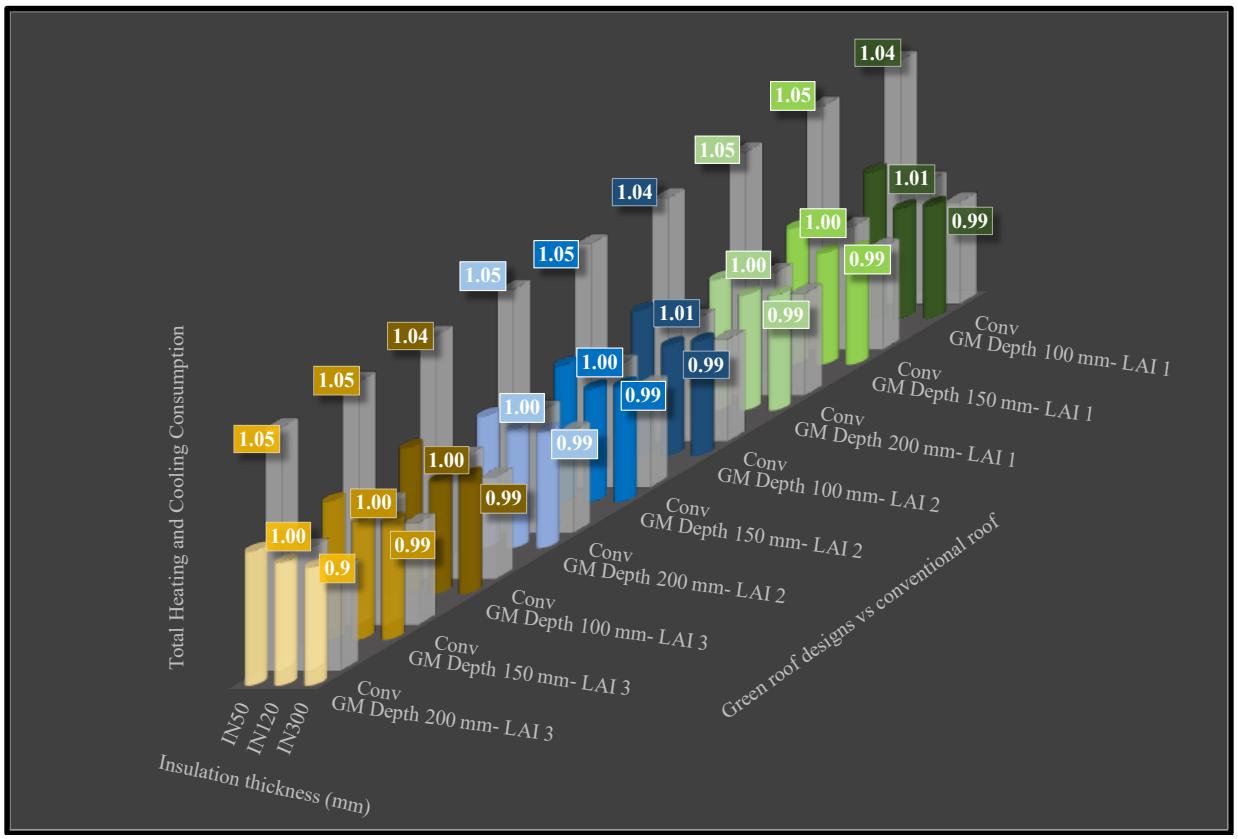

Figure 5-15: DBGR of all green roof designs under current climate (grey colour bars represent conventional roof) – hospital building.

Future climate

Due to the rise in temperatures under future climate conditions, the hospital building heating loads decreased, and the cooling loads increased. Both green roof and conventional roof heating loads compared to current climate conditions decreased; therefore, the impact of green roof on increasing the heating loads (compared to the conventional roof) during winter was lower under future climate conditions. Additionally, the green roof energy savings on cooling loads in summer was more compared to current climate conditions. This led the green roof at higher insulation thicknesses to have less negative heating energy saving and more positive cooling energy savings than current climate conditions. Figure 5-16 presents the annual energy savings at insulation thickness of 300 mm. Compared to Figure 5-14, the green roof under future climate conditions at insulation thickness of 300 mm has less negative energy savings. Under future climate conditions, the uninsulated green roof with growing media of 200 mm and LAI of 3 saved the highest energy compared to all other uninsulated green roof designs. However, as the insulation thickness

increased for insulated green roofs, the green roof thermal performance was impacted, and the green roof benefit on energy savings was limited.

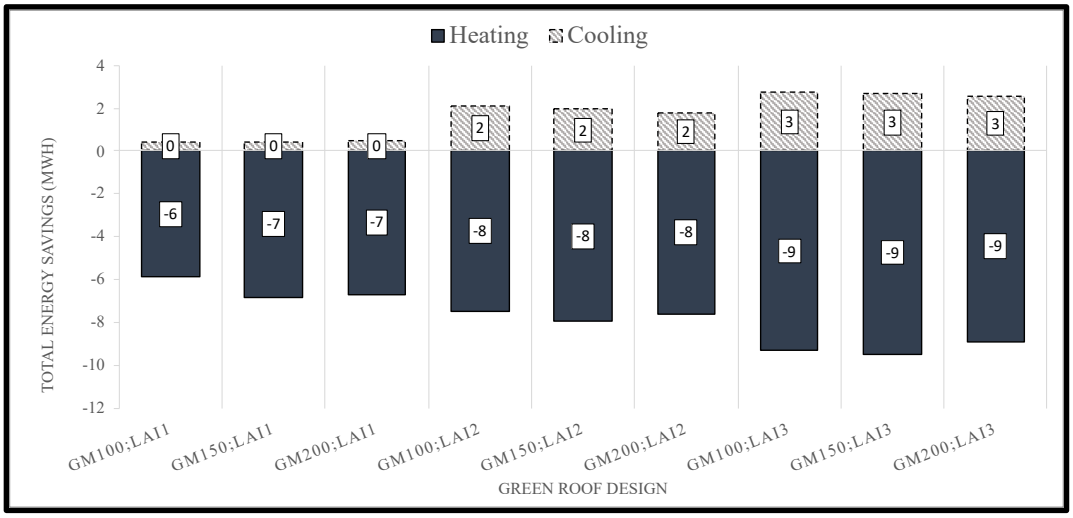

Figure 5-16: Total heating and cooling energy savings (MWh) of green roof compared to conventional roof for all growing media (GM) depths and LAIs; with 300 mm insulation layer – future climate (hospital building).

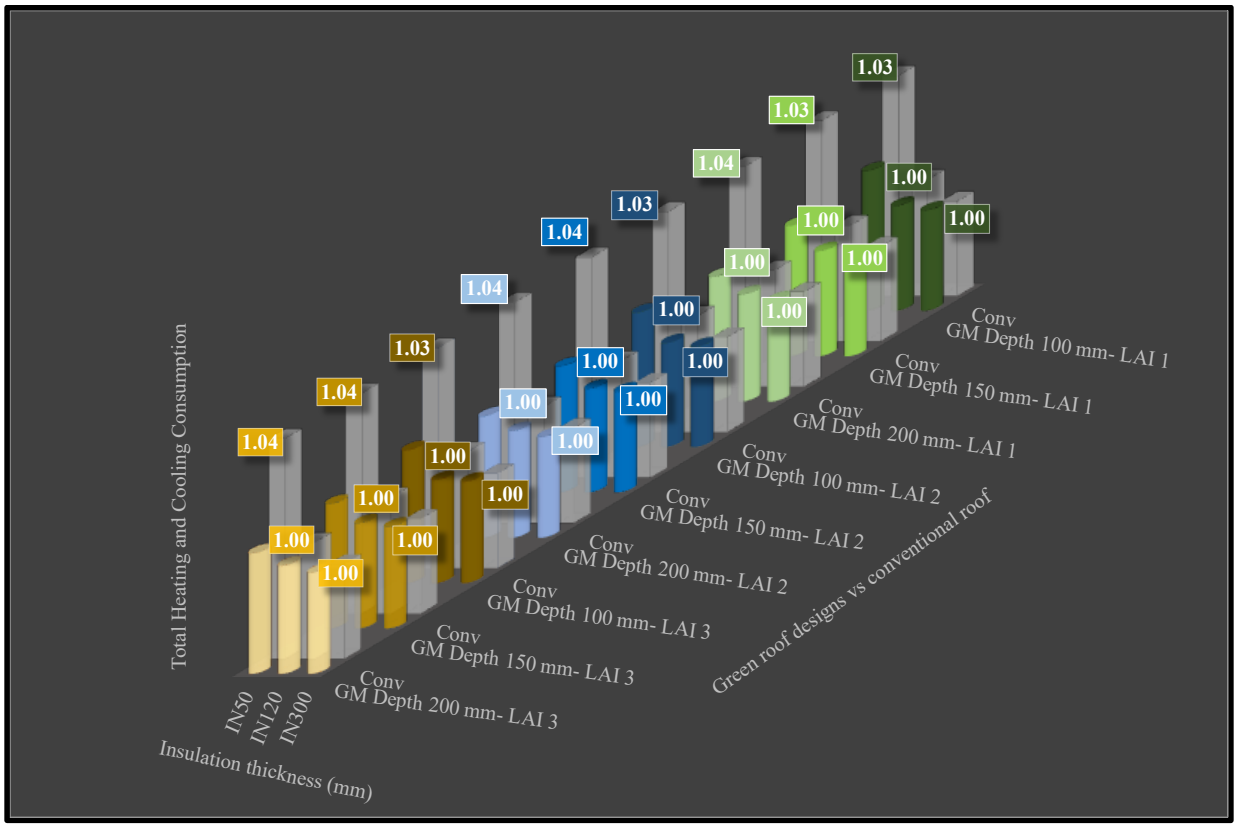

Figure 5-17: DBGR of all green roof designs under future climate (grey colour bars represent conventional roof) – hospital building.

Figure 5-17 provides the hospital building DBGR for all green roof designs under future climate conditions. The DBGR values show at insulation thicknesses of 120 mm and 300 mm, the green roof and conventional roof perform equally, and the green roof provides minimal benefit on decreasing building energy consumption. All green roof designs with insulation thicknesses of 50 mm showed DBGR values higher than 1, indicating that green roof designs with low insulation thicknesses provide energy benefit under future climate conditions. Green roofs with a growing media depth of 200 mm and LAI of 3 had the highest DBGR value of 1.4 under future climate conditions and provided the highest cooling and heating savings among all other green roof designs.

The hospital's optimal green roof design in the future was not the same as the current climate conditions. The design configuration suggested under future conditions for the hospital building is growing media depth of 100 mm and LAI of 3 with insulation thickness of 120 mm. The suggested optimal design has the lowest energy compared to the conventional roof and highest energy savings than all other green roof designs. All plots for annual total heating and cooling consumption and savings for hospital buildings under future climate for all green roofs are presented in Appendix F.

Overall, under both current and future climate conditions, results showed for all three archetypes of secondary school, office, and hospital building, the uninsulated green roof with growing media depth 200 mm and LAI of 3 achieved the highest energy savings among all other green roof designs, regardless of the difference in building characteristics. Although, once the insulation layer was added, the green roof thermal performance was affected. The added insulation thickness above 120 mm for the secondary school and hospital building caused higher green roof energy requirements than the conventional roof under current climate conditions. However, for the office building, the green roof maintained lower total energy compared to the conventional roof at all insulation thicknesses. The dissimilarity of the insulated green roof thermal performance on secondary school, office and hospital building were due to the different thermal behaviour and seasonal consumption of these buildings. Results indicated the thermal performance of insulated green roofs compared to conventional insulated roofs significantly depends on the building

characteristics under both current and future climate conditions. Therefore, optimal green roof designs may vary depending on the building type.

5.3 Green Roof Retention Performance

The runoff and rainwater captured by the green roof designs for all three archetypes were measured to showcase the green roofs water retention performance. EnergyPlus reports the green roof net annual runoff water. However, this feature is not explicitly validated, but it connects to the accuracy of the energy balance model. Green roof runoff is affected by the growing media composition characteristics and drainage layers, all of which are fixed in the Energyplus model.

$$\%\ Retained = \frac{Retained\ Water\ (Total\ Percipitation - Runoff)}{Total\ Percipitation} \qquad \text{Equation 15}$$

The water captured by the green roof was calculated using the runoff output from EnergyPlus. The amount of water retained is the total amount of precipitation subtracted by the water runoff. The percentage of water retained was calculated by Equation 15. Table 5-1 provides the stormwater runoff, water retained, and percentage of water retained by the green roof for all three building archetypes under current and future climate conditions. The green roof design chosen to calculate the water retained included growing media of 200 mm and LAI of 3 since this design was proven to be the best performed design (without insulation) in the previous sections for all archetypes. Results showed that the green roof captured 41% of stormwater for the secondary school under the current and 45% under the future climate conditions. The warmer climate conditions in the future lead to a higher vegetation transpiration and increase the rainwater captured (retained) by the green roof. Similar trends were observed for office and hospital buildings where a higher percentage of water was retained under future climate conditions. In addition, the increase of insulation thickness with green roof designs had a limited impact on water retention performance. Therefore, green roofs with and without insulation thickness could retain rainwater runoff unlike the conventional roof, where water is not captured. Overall, green roofs under both current and future climate conditions provided the benefit of reducing stormwater runoff, an advantage that the conventional roof did not provide.

Table 5-1: Runoff water and retained by green roof design, growing media 200 mm; LAI 3 no insulation, for secondary school, office, and hospital archetypes under current and future climates.

Archetype	Current Climate			Future Climate 2080s		
	Runoff (m)	**Retained (m)**	**%Retained**	**Runoff (m)**	**Retained (m)**	**%Retained**
Secondary School	0.464	0.322	41%	0.473	0.391	45%
Office	0.393	0.393	50%	0.411	0.453	52%
Hospital	0.4232	0.363	46%	0.4429	0.421	49%

Chapter Six: Conclusion and Recommendation for Future Research

In recent years, green roofs have shown potential in reducing building heating and cooling energy consumption. However, their thermal performance is highly climate-dependent. Thus, green roofs need to be designed specifically to the climate they are installed in. In 2012, the City of Toronto issued a by-law requiring buildings with an area greater than 2000 m^2 to have green roofs. Therefore, most new buildings in the City of Toronto have green roofs but with different green roof design parameters. Hence, investigating the impact of green roof design parameters on decreasing building energy consumption in the City of Toronto and optimizing green roof design is important. Additionally, the impact of climate change and shift in weather patterns in future conditions has made assessing green roof thermal performance under both current and future climate crucial. This research aimed to determine whether the use of extensive green roofs in Toronto would reduce building energy consumption under both current and future climate conditions.

Three design parameters that mostly impacted the thermal performance of green roofs were chosen to evaluate green roof thermal performance on buildings. The growing media layer of green roof has an insulating effect and impacts both the heating and cooling loads of the building. The green roof vegetated area impacts the building cooling loads through the process of evapotranspiration. The added thermal insulation layer was also considered in this research due to its insulation impact and reduction of heating loads. However, the added insulation layer is not a green roof design parameter, but in the City of Toronto, added insulation layer is a requirement in green roof structure due to Toronto being located in a heating-dominated region. Therefore, the impact of different green roof growing media depths, LAI values and added thermal insulation thicknesses were used to quantify the effect of these parameters on green roof thermal performance. The evaluation was performed through a sensitivity analysis to determine optimal green roof design. The green roof thermal performance was investigated through modelling, using EnergyPlus, on three different building archetypes: secondary school, office and hospital building. Three building types were chosen to evaluate the impact of building characteristics on green roof thermal performance and

determine if all building types have similar green roof optimal designs. The total heating and cooling loads for different green roof designs were compared to a conventional reference roof (building without a green roof). The thermal performance of green roof designs was quantified.

Results suggested uninsulated green roofs with a growing media depth of 200 mm and LAI of 3 would perform the best in reducing the total building heating and cooling loads compared to a conventional roof for all building archetypes. However, the addition of thermal insulation lowered the effectiveness of green roofs on decreasing the building energy consumption compared to conventional roofs. Furthermore, the insulated green roof thermal performance was different for each building archetype due to the different characteristics and seasonal heating and cooling energy consumption patterns.

For the secondary school building, both heating and cooling loads were consumed through all seasons. Results showed that insulation thickness caused the green roof to require more heating loads during spring and summer than the conventional roof with the same insulation thickness. At insulation thicknesses above 120 mm, any cooling benefit was negated by the increase of heating loads causing the net effect to be higher total energy consumption. This led to higher energy use by the green roof compared to the conventional roof at insulation thicknesses more than 120 mm. The suggested optimal design for the secondary school under the current climate was growing media depth of 200 mm with LAI of 3 and insulation thickness of 120 mm.

The office building throughout each season maintained lower cooling and heating loads compared to the conventional roof. Therefore, the insulation thickness did not negatively impact the green roof performance compared to a conventional roof for the office building. However, at high insulation thicknesses, the green roof thermal performance was limited, and the added thermal insulation had a dominant insulating effect. For the office building, the optimal green roof design under the current climate was growing media of 200 mm with LAI of 3 with insulation thickness of 120 mm.

Insulated green roofs caused the hospital to require more heating loads during the winter compared to the conventional roof with the same insulation thickness. The addition of insulation thicknesses

lowered the cooling benefit provided by the green roof. The small amount of cooling savings of the green roof was negated by higher heating loads. This led to green roofs providing no benefit in terms of energy compared to the conventional roof at insulation thicknesses higher than 120 mm under the current climate. The optimal green roof design under the current climate for the hospital building was growing media depth of 100 mm and LAI of 2 with insulation thickness of 120 mm.

Warmer temperatures in future conditions caused an increase in building cooling loads and a decrease in heating loads. Generally, insulated green roofs were no longer as effective in providing heating energy savings under future climate compared to current due to the decrease in heating loads in the future. Additionally, insulation inhibited the cooling savings provided by the green roof and led to lower green roof total energy savings at all insulation thicknesses. The optimal green roof designs for the secondary school building under future climate was a growing media of 200 mm and LAI of 3 with insulation thickness of 80 mm. The office building maintained the same optimal green roof design as the current climate with growing media depth of 200 mm, LAI of 3 and insulation thickness of 120 mm. For the hospital building, the suggested optimal green roof design was growing media depth of 100 mm and LAI of 3 with insulation thickness of 120 mm.

Under both current and future climate conditions, the uninsulated green roof with growing media depth of 200 mm and LAI of 3 achieved the highest energy savings among all other green roof designs for all three building archetypes. The thermal performance of the green roof was impacted as the insulation layer was increased, and at highly insulated roofs, the green roof provided minimal energy benefit compared to conventional roofs. Depending on the building characteristics, highly insulated green roofs could lead to higher energy usage compared to highly conventional insulated roofs. The added insulation thickness above 80 mm for the secondary school building caused higher green roof energy usage than the conventional roof under future climate conditions. However, the green roof maintained lower energy for the office building and hospital building compared to the conventional roof at insulation thicknesses of 120 mm and below. The dissimilarity of the insulated green roof thermal performance on secondary school, office and hospital building were due to different building characteristics. Therefore, the thermal performance of insulated green roofs compared to conventional insulated roofs significantly depends on the building type, and optimal green roof designs may vary.

Overall, findings in this research showed the added thermal insulation inhibits the green roof energy performance and lowers the green roof energy savings compared to conventional roofs for all building types. The use of insulated extensive green roofs in the City of Toronto would provide minimal benefit in terms of energy compared to the conventional insulated roofs. Hence, green roofs are most suitable for retrofits on poorly insulated buildings where the roof insulation is low. In addition, a green roof would be more effective in reducing the building energy consumption than a conventional uninsulated roof. In this research, under both current and future climate conditions, green roof also showed the benefit of reducing stormwater runoff, an advantage that the conventional roof did not provide.

In conclusion, even though green roofs provide minimal benefit in terms of energy compared to insulated conventional roofs, green roofs still offer other advantages that make them valuable features compared to the conventional roof, such as reducing stormwater runoff. Thus, the City of Toronto should continue to instal optimized green roof designs due to the multi-benefits they can provide.

Recommendation for Future Research

In this research, due to the constraining of the CCWorldWeatherGen tool in generating the current climate data, emission scenarios A2 was considered for predicting future climate conditions. In future research, more recent climate data under future climate scenarios such as RCP for various emission scenarios could be used. Additionally, the hourly precipitation data for the CWEC weather data was not available, and other climate sources were utilized in generating both current and future precipitation data. Thus, in future research, accessing current and future hourly precipitation data from the same climate source data station is recommended. This research also used statistical downscaling, morphing to generate future climate conditions due to the unavailability of all climate variables at an hourly duration of RCMs for Toronto climate. In future research, RCM data in generating future climate data is recommended since this method is physically consistent for different climate variables and isn't constrained by historical data.

The effect of other green roof characteristics such as plant height, leaf albedo, growing media thermal conductivity, density, and specific heat on thermal performance could be evaluated in

future research. In this research, the thermal performance of extensive green roofs was only assessed. In future research, the focus could be shifted to intensive green roofs on energy reduction in the City of Toronto under both current and future climate. Lastly, this research showed that green roof thermal behaviour is dependent on building type, precisely when the thermal insulation layer is used. Therefore, evaluating green roof performance under a variety of other building archetypes is essential. In addition, EnergyPlus ignores the heat released or gained due to phase changes of growing media water, precipitation heat flux and heat flux due to vertical transport of water in the growing media. Future work could focus on modelling refinements and incorporating capture of these phenomena.

Bibliography

Al-Ghussain, Loiy. 2019. “Global Warming: Review on Driving Forces and Mitigation.” Environmental Progress and Sustainable Energy. https://doi.org/10.1002/ep.13041.

Ascione, Fabrizio, Nicola Bianco, Filippo de’ Rossi, Gianluca Turni, and Giuseppe Peter Vanoli. 2013. “Green Roofs in European Climates. Are Effective Solutions for the Energy Savings in Air-Conditioning?” Applied Energy 104: 845–59. https://doi.org/10.1016/j.apenergy.2012.11.068.

Belcher, S. E., J. N. Hacker, and D. S. Powell. 2005. “Constructing Design Weather Data for Future Climates.” Building Services Engineering Research and Technology 26 (1): 49–61. https://doi.org/10.1191/0143624405bt112oa.

Berardi, Umberto. 2016. “The Outdoor Microclimate Benefits and Energy Saving Resulting from Green Roofs Retrofits.” Energy and Buildings 121: 217–29. https://doi.org/10.1016/j.enbuild.2016.03.021.

Berardi, Umberto, Amir Hosein GhaffarianHoseini, and Ali GhaffarianHoseini. 2014. “State-of-the-Art Analysis of the Environmental Benefits of Green Roofs.” Applied Energy 115: 411-428. https://doi.org/10.1016/j.apenergy.2013.10.047.

Berardi, Umberto, and Pouriya Jafarpur. 2020. “Assessing the Impact of Climate Change on Building Heating and Cooling Energy Demand in Canada.” Renewable and Sustainable Energy Reviews 121: 109681. https://doi.org/10.1016/j.rser.2019.109681.

Bevilacqua, Piero, Domenico Mazzeo, Roberto Bruno, and Natale Arcuri. 2016. “Experimental Investigation of the Thermal Performances of an Extensive Green Roof in the Mediterranean Area.” Energy and Buildings 122: 63–79. https://doi.org/10.1016/j.enbuild.2016.03.062.

Blanusa, Tijana, M. Madalena Vaz Monteiro, Federica Fantozzi, Eleni Vysini, Yu Li, and Ross W.F. Cameron. 2013. “Alternatives to Sedum on Green Roofs: Can Broad Leaf Perennial Plants Offer Better ‘Cooling Service’?” Building and Environment 59: 99–106. https://doi.org/10.1016/j.buildenv.2012.08.011.

Cascone, Stefano, Federico Catania, Antonio Gagliano, and Gaetano Sciuto. 2018. “A Comprehensive Study on Green Roof Performance for Retrofitting Existing Buildings.” Building and Environment 136: 227–39. https://doi.org/10.1016/j.buildenv.2018.03.052.

Castleton, H. F., V. Stovin, S. B.M. Beck, and J. B. Davison. 2010a. “Green Roofs; Building Energy Savings and the Potential for Retrofit.” Energy and Buildings 42: 1582-1591. https://doi.org/10.1016/j.enbuild.2010.05.004.

Chan, A. L.S., and T. T. Chow. 2013. “Energy and Economic Performance of Green Roof System under Future Climatic Conditions in Hong Kong.” Energy and Buildings 64: 182–198. https://doi.org/10.1016/j.enbuild.2013.05.015.

City of Toronto Green Roof Bylaw. City of Toronto. Accessed February 2, 2021. https://www.toronto.ca/city-government/planning-development/official-plan-guidelines/green-roofs/green-roof-bylaw/.

Crawley, D.B., 2003. Impact of climate change in buildings. Paper presented at the Proceedings of the 2003 CIBSE/ASHRAE Conference. University of Strathclyde, Scotland, UK, 2003. https://www.researchgate.net/profile/Drury-

Crawley/publication/228553732_Impact_of_Climate_Change_on_Buildings/links/0f317534de130d2454000000/Impact-of-Climate-Change-on-Buildings.pdf

Czemiel Berndtsson, Justyna. 2010. “Green Roof Performance towards Management of Runoff Water Quantity and Quality: A Review.” Ecological Engineering 36: 351-360. https://doi.org/10.1016/j.ecoleng.2009.12.014.

Dickinson, R. Brannon, B. “Generating Future Weather Files For Resilience.” Paper presented at PLEA 2016 Los Angeles - 36th International Conference on Passive and Low Energy Architecture. San Francisco, CA. 2016. https://www.weathershift.com/Generating%20Future%20Weather%20Files.pdf

D’Orazio, M., C. di Perna, and E. di Giuseppe. 2012. “Green Roof Yearly Performance: A Case Study in a Highly Insulated Building under Temperate Climate.” Energy and Buildings 55: 439–451. https://doi.org/10.1016/j.enbuild.2012.09.009.

Division, Energy and City of Toronto. 2017. “TransformTO: Climate Action for a Healthy, Equitable & Prosperous Toronto.” City of Toronto. 63. Accessed January 10, 2021. https://www.toronto.ca/wp-content/uploads/2020/02/92f8-TransformTO-Climate-Action-for-a-Healthy-Equitable-Prosperous-Toronto-Implementation-Update-2017-and-2018.pdf

Eksi, Mert, D. Bradley Rowe, Indrek S. Wichman, and Jeff A. Andresen. 2017. “Effect of Substrate Depth, Vegetation Type, and Season on Green Roof Thermal Properties.” Energy and Buildings 145: 174–187. https://doi.org/10.1016/j.enbuild.2017.04.017.

Environment Canada. 2013. Canadian Climate Normals 1998-2010 Station Data. Government of Canada. Accessed December 18, 2020. https://climate.weather.gc.ca/climate_normals/.

Francis, Robert A., and Jamie Lorimer. 2011. “Urban Reconciliation Ecology: The Potential of Living Roofs and Walls.” Journal of Environmental Management 92(6): 1429-1437. https://doi.org/10.1016/j.jenvman.2011.01.012.

Frankenstein, S. Koenig, G. 2004. “FASST Vegetation Models.” Hanover, New Hampshire, US Army Corps of Engineers. 39. Accessed May 20, 2020. https://apps.dtic.mil/sti/pdfs/ADA428989.pdf

Getter, Kristin L., D. Bradley Rowe, and Jeffrey A. Andresen. 2007a. “Quantifying the Effect of Slope on Extensive Green Roof Stormwater Retention.” Ecological Engineering 31 (4): 225–31. https://doi.org/10.1016/j.ecoleng.2007.06.004.

Getter, Kristin L., D. Bradley Rowe, Jeff A. Andresen, and Indrek S. Wichman. 2011b. “Seasonal Heat Flux Properties of an Extensive Green Roof in a Midwestern U.S. Climate.” Energy and Buildings 43 (12): 3548–3557. https://doi.org/10.1016/j.enbuild.2011.09.018.

Ghaffarianhoseini, Amirhosein, Nur Dalilah Dahlan, Umberto Berardi, Ali Ghaffarianhoseini, Nastaran Makaremi, and Mahdiar Ghaffarianhoseini. 2013. “Sustainable Energy Performances of Green Buildings: A Review of Current Theories, Implementations and Challenges.” Renewable and Sustainable Energy Reviews 25: 1–17. https://doi.org/10.1016/j.rser.2013.01.010.

Gomes, M. Glória, C. M. Silva, Ana Sofia Valadas, and Marcelo Silva. 2019a. “Impact of Vegetation, Substrate, and Irrigation on the Energy Performance of Green Roofs in a Mediterranean Climate.” Water 11 (10). https://doi.org/10.3390/w11102016.

Guan, Lisa. 2009. “Preparation of Future Weather Data to Study the Impact of Climate Change on Buildings.” Building and Environment 44 (4): 793–800. https://doi.org/10.1016/j.buildenv.2008.05.021.

He Yang, Hang Yu, Akihito Ozaki, and Nannan Dong. 2020. “Thermal and Energy Performance of Green Roof and Cool Roof: A Comparison Study in Shanghai Area.” Journal of Cleaner Production 267. https://doi.org/10.1016/j.jclepro.2020.122205.

Herrera, Manuel, Sukumar Natarajan, David A. Coley, Tristan Kershaw, Alfonso P. Ramallo-González, Matthew Eames, Daniel Fosas, and Michael Wood. 2017. “A Review of Current and Future Weather Data for Building Simulation.” Building Services Engineering Research and Technology 38 (5): 602-627. https://doi.org/10.1177/0143624417705937.

International Energy Agency (IEA). 2020. “Global Energy Reviews 2019: The latest trends in energy emissions in 2019.” OECD Publishing, Paris. 50. Accessed July 19, 2020. https://doi.org/10.1787/90c8c125-en.

International Energy Agency (IEA). 2018. “Global Energy & CO_2 Status Report 2017.” IEA, Paris. 14. Accessed June 19, 2020. https://www.iea.org/reports/global-energy-co2-status-report-2017

IPCC. 2000a. “Report on Emissions Scenarios: A Special Report of Intergovernmental Panel on Climate Change Working Group III.” Cambridge University Press. 599. Accessed November 1, 2020. https://www.ipcc.ch/site/assets/uploads/2018/03/emissions_scenarios-1.pdf

IPCC. 2014b. “Climate Change 2014: Synthesis Report: A Report of the Intergovernmental Plane on Climate Change.” Geneva, Switzerland. 151. Accessed November 1, 2020. https://www.ipcc.ch/site/assets/uploads/2018/05/SYR_AR5_FINAL_full_wcover.pdf

Jaffal, Issa, Salah Eddine Ouldboukhitine, and Rafik Belarbi. 2012. “A Comprehensive Study of the Impact of Green Roofs on Building Energy Performance.” Renewable Energy 43 (July): 157–164. https://doi.org/10.1016/j.renene.2011.12.004

Ka’bi, A.H. 2020. “Comparison of Energy Simulation Applications Used in Green Building.” Ann. Telecommun. 75, 271-290. https://doi.org/10.1007/s12243-020-00771-6.

Karachaliou, P., Mat Santamouris, and Helli Pangalou. 2016. “Experimental and Numerical Analysis of the Energy Performance of a Large Scale Intensive Green Roof System Installed on an Office Building in Athens.” Energy and Buildings 114: 256–64. https://doi.org/ 10.1016/j.enbuild.2015.04.055.

Kumar, Rakesh, and S. C. Kaushik. 2005. “Performance Evaluation of Green Roof and Shading for Thermal Protection of Buildings.” Building and Environment 40 (11): 1505–1511. https://doi.org/ 10.1016/j.buildenv.2004.11.015.

Liu, K and Minor, J. 2005. “Performance Evaluation of an Extensive Green Roof.” National Research Council of Canada. City of Toronto. 1-11. http://nparc.cisti-icist.nrc-cnrc.gc.ca/npsi/ctrl?lang=en

Lundholm, Jeremy T., Brett M. Weddle, and J. Scott Macivor. 2014. “Snow Depth and Vegetation Type Affect Green Roof Thermal Performance in Winter.” Energy and Buildings 84: 299–307. https://doi.org/10.1016/j.enbuild.2014.07.093

MacIvor, J. Scott, Liat Margolis, Matthew Perotto, and Jennifer A.P. Drake. 2016. “Air Temperature Cooling by Extensive Green Roofs in Toronto Canada.” Ecological Engineering 95: 36–42. https://doi.org/10.1016/j.ecoleng.2016.06.050.

Mahmoodzadeh, Milad, Phalguni Mukhopadhyaya, and Caterina Valeo. 2020. “Effects of Extensive Green Roofs on Energy Performance of School Buildings in Four North American Climates.” Water (Switzerland) 12 (1). https://doi.org/10.3390/w12010006.

Maiolo, Mario, Behrouz Pirouz, Roberto Bruno, Stefania Anna Palermo, Natale Arcuri, and Patrizia Piro. 2020. “The Role of the Extensive Green Roofs on Decreasing Building Energy Consumption in the Mediterranean Climate.” Sustainability (Switzerland) 12 (1). https://doi.org/10.3390/su12010359.

Mentens, Jeroen, Dirk Raes, and Martin Hermy. 2006. “Green Roofs as a Tool for Solving the Rainwater Runoff Problem in the Urbanized 21st Century?” Landscape and Urban Planning 77 (3): 217–226. https://doi.org/10.1016/j.landurbplan.2005.02.010.

Meteorological Service of Canada (MSC). 2008. Updated user’s manual: Canadian weather energy and engineering data sets (CWEEDS files) and Canadian weather for energy calculation (CWEC files). Accessed September 27, 2020. http://climate.weather.gc.ca/prods_servs/engineering_e.html

Moazami, Amin, Vahid M. Nik, Salvatore Carlucci, and Stig Geving. 2019. “Impacts of Future Weather Data Typology on Building Energy Performance – Investigating Long-Term Patterns of Climate Change and Extreme Weather Conditions.” Applied Energy 238 (March): 696–720. https://doi.org/10.1016/j.apenergy.2019.01.085

Monterusso, Michael A, D Bradley Rowe, and Clayton L Rugh. 2005. “Establishment and Persistence of Sedum Spp. and Native Taxa for Green Roof Applications.” American Society or Horticultural Science 40 (2): 391-396. https://doi.org/10.21273/HORTSCI.40.2.391.

Moody, Seth S., and David J. Sailor. 2013. “Development and Application of a Building Energy Performance Metric for Green Roof Systems.” Energy and Buildings 60: 262–69. https://doi.org/10.1016/j.enbuild.2013.02.002.

Natural Resources Canada (NRCan). 2013. “Survey of Commercial and Institutional Energy Use: Buildings 2009”. Natural Resource Canada. Ottawa. 52 Accessed January 19, 2021. https://oee.nrcan.gc.ca/publications/statistics/scieu/2009/pdf/scieu2009buildings.pdf

Olivieri, F., C. di Perna, M. D’Orazio, L. Olivieri, and J. Neila. 2013. “Experimental Measurements and Numerical Model for the Summer Performance Assessment of Extensive Green Roofs in a Mediterranean Coastal Climate.” Energy and Buildings 63: 1–14. https://doi.org/10.1016/j.enbuild.2013.03.054.

Ouldboukhitine, Salah Eddine, Rafik Belarbi, and Rabah Djedjig. 2012. “Characterization of Green Roof Components: Measurements of Thermal and Hydrological Properties.” Building and Environment 56: 78–85. https://doi.org/10.1016/j.buildenv.2012.02.024.

Pianella, Andrea, Robin E. Clarke, Nicholas S.G. Williams, Zhengdong Chen, and Lu Aye. 2016. “Steady-State and Transient Thermal Measurements of Green Roof Substrates.” Energy and Buildings 131: 123–31. https://doi.org/10.1016/j.enbuild.2016.09.024.

Rincon, Daniela. 2020. “Probabilistic flood risk assessment under climate change scenarios in the Humber river watershed.” Master’s thesis., York University.

Robert, Amélie, and Michaël Kummert. 2012. “Designing Net-Zero Energy Buildings for the Future Climate, Not for the Past.” Building and Environment 55: 150–58. https://doi.org/10.1016/j.buildenv.2011.12.014.

Roche, Pablo la, and Umberto Berardi. 2014. “Comfort and Energy Savings with Active Green Roofs.” Energy and Buildings 82: 492–504. https://doi.org/10.1016/j.enbuild.2014.07.055.

Roetzel, Astrid, and Aris Tsangrassoulis. 2012. “Impact of Climate Change on Comfort and Energy Performance in Offices.” Building and Environment 57: 349–61. https://doi.org/10.1016/j.buildenv.2012.06.002.

Saadatian, Omidreza, K. Sopian, E. Salleh, C. H. Lim, Safa Riffat, Elham Saadatian, Arash Toudeshki, and M. Y. Sulaiman. 2013. “A Review of Energy Aspects of Green Roofs.” Renewable and Sustainable Energy Reviews 23: 155-168. https://doi.org/10.1016/j.rser.2013.02.022.

Sailor, D. J. 2008. “A Green Roof Model for Building Energy Simulation Programs.” Energy and Buildings 40 (8): 1466–78. https://doi.org/10.1016/j.enbuild.2008.02.001

Sailor, D J, and B Bass. 2014. “Development and Features of the Green Roof Energy Calculator.” SailorBass Journal of Living Architecture. 1(3): 36-58 http://greenroofs.org/resources/JOLA2014Volume1(Issue3)SailorBass.

Sailor, D. J., and M. Hagos. 2011. “An Updated and Expanded Set of Thermal Property Data for Green Roof Growing Media.” Energy and Buildings 43 (9): 2298–2303. https://doi.org/10.1016/j.enbuild.2011.05.014.

Sailor, David J., Timothy B. Elley, and Max Gibson. 2012. “Exploring the Building Energy Impacts of Green Roof Design Decisions-a Modeling Study of Buildings in Four Distinct Climates.” Journal of Building Physics 35 (4): 372–91. https://doi.org/10.1177/1744259111420076.

Santamouris, M. 2014. “Cooling the Cities - A Review of Reflective and Green Roof Mitigation Technologies to Fight Heat Island and Improve Comfort in Urban Environments.” Solar Energy 103: 682–703. https://doi.org/10.1016/j.solener.2012.07.003.

Scherba, Adam, David J. Sailor, Todd N. Rosenstiel, and Carl C. Wamser. 2011. “Modeling Impacts of Roof Reflectivity, Integrated Photovoltaic Panels and Green Roof Systems on Sensible Heat Flux into the Urban Environment.” Building and Environment 46 (12): 2542–2551. https://doi.org/10.1016/j.buildenv.2011.06.012.

Shafique, Muhammad, Reeho Kim, and Muhammad Rafiq. 2018. “Green Roof Benefits, Opportunities and Challenges – A Review.” Renewable and Sustainable Energy Reviews 60: 757-773. https://doi.org/10.1016/j.rser.2018.04.006.

Simmons, Mark T., Brian Gardiner, Steve Windhager, and Jeannine Tinsley. 2008. “Green Roofs Are Not Created Equal: The Hydrologic and Thermal Performance of Six Different Extensive Green Roofs and Reflective and Non-Reflective Roofs in a Sub-Tropical Climate.” Urban Ecosystems 11 (4): 339–348. https://doi.org/ 10.1007/s11252-008-0069-4.

Sims, Andrew W., Clare E. Robinson, Charles C. Smart, James A. Voogt, Geoffrey J. Hay, Jeremey T. Lundholm, Brandon Powers, and Denis M. O’Carroll. 2016. “Retention Performance of Green Roofs in Three Different Climate Regions.” Journal of Hydrology 542: 115–24. https://doi.org/10.1016/j.jhydrol.2016.08.055.

Silva, M N K de, and Y G Sandanayake. 2012. “Building Energy Consumption Factors: a literature review and future research.” Paper presented at the World Construction Conference 2012-Global Challenges in Construction Industry, Colombo, Sir Lanka, June 28-30. http://dl.lib.uom.lk/handle/123/12050

Squier, Mallory, and Cliff I. Davidson. 2016. “Heat Flux and Seasonal Thermal Performance of an Extensive Green Roof.” Building and Environment 107: 235–244. https://doi.org/10.1016/j.buildenv.2016.07.025

Takakura, T, S Kitade, and E Goto. 2001. “Cooling Effect of Greenery Cover over a Building.” Energy and Buildings. 31: 1-6. https://doi.org/10.1016/S0378-7788(98)00063-2

Talebi, Ashkan, Scott Bagg, Brent E. Sleep, and Denis M. O’Carroll. 2019. “Water Retention Performance of Green Roof Technology: A Comparison of Canadian Climates.” Ecological Engineering 126: 1–15. https://doi.org/10.1016/j.ecoleng.2018.10.006.

Tang, Xin, and Ming Qu. 2016. “Phase Change and Thermal Performance Analysis for Green Roofs in Cold Climates.” Energy and Buildings 121: 165–175. https://doi.org/10.1016/j.enbuild.2016.03.069.

United Nations Environment Programme. 2019. “Towards a zero-emissions, efficient and resilient buildings and construction sector 2019 Global Status report”. 39. https://iea.blob.core.windows.net/assets/3da9daf9-ef75-4a37-b3da-a09224e299dc/2019_Global_Status_Report_for_Buildings_and_Construction.pdf

University of Southampton. 2009. CCWorldWeatherGen tool. Accessed October 19, 2020. http://www.energy.soton.ac.uk/ccworldweathergen/

U.S. Deparment of Energy (DOE). 2010. “EnergyPlus engineering reference”. The Reference to EnergyPlus Calculations; U.S. DOE: Washington, DC, USA. 1741. https://energyplus.net/sites/all/modules/custom/nrel_custom/pdfs/pdfs_v9.2.0/EngineeringReference.pdf

U.S. Department of Energy (DOE). 2018. Commercial building prototype models. Accessed November 14, 2020. https://www.energycodes.gov/development/commercial/prototype_models

VanWoert, Nicholaus D., D. Bradley Rowe, Jeffrey A. Andresen, Clayton L. Rugh, R. Thomas Fernandez, and Lan Xiao. 2005. “Green Roof Stormwater Retention.” Journal of Environmental Quality 34 (3): 1036–1044. https://doi.org/10.2134/jeq2004.0364.

Vera, Sergio, Camilo Pinto, Felipe Victorero, Waldo Bustamante, Carlos Bonilla, Jorge Gironás, and Victoria Rojas. 2015. “Influence of Plant and Substrate Characteristics of Vegetated Roofs on a Supermarket Energy Performance Located in a Semiarid Climate.” In Energy Procedia 78:1171–1176. https://doi.org/10.1016/j.egypro.2015.11.089.

Virk, Gurdane, Antonia Jansz, Anna Mavrogianni, Anastasia Mylona, Jenny Stocker, and Michael Davies. 2015. “Microclimatic Effects of Green and Cool Roofs in London and Their Impacts on Energy Use for a Typical Office Building.” Energy and Buildings 88: 214–228. https://doi.org/10.1016/j.enbuild.2014.11.039.

Wilde, Pieter de, and David Coley. 2012. “The Implications of a Changing Climate for Buildings.” Building and Environment 55: 1-7. https://doi.org/10.1016/j.buildenv.2012.03.014

Yang, Junjing, Devi llamathy Mohan Kumar, Andri Pyrgou, Adrian Chong, Mat Santamouris, Denia Kolokotsa, and Siew Eang Lee. 2018. “Green and Cool Roofs’ Urban Heat Island Mitigation Potential in Tropical Climate.” Solar Energy 173: 597–609. https://doi.org/10.1016/j.solener.2018.08.006

Zeng, Chao, Xuelian Bai, Lexiang Sun, Yunzhou Zhang, and Yanping Yuan. 2017. “Optimal Parameters of Green Roofs in Representative Cities of Four Climate Zones in China: A Simulation Study.” Energy and Buildings 150 (1): 118–131. https://doi.org/10.1016/j.enbuild.2017.05.079.

Zhang, Zheng, Christopher Szota, Tim D. Fletcher, Nicholas S.G. Williams, and Claire Farrell. 2019. “Green Roof Storage Capacity Can Be More Important than Evapotranspiration for Retention

Performance." Journal of Environmental Management 232: 404–412. 10.1016/j.jenvman.2018.11.070.

Zhang, X., Flato, G., Kirchmeier-Young, M., Vincent, L., Wan, H., Wang, X., Rong, R., Fyfe, J., Li, G., Kharin, V.V. 2019. "Temperature and Precipitation Across Canada. Canada's Changing Climate Report." Government of Canada, Ottawa, ON. 112-193. Accessed January 27, 2021. https://www.nrcan.gc.ca/sites/www.nrcan.gc.ca/files/energy/Climate-change/pdf/CCCR_FULLREPORT-EN-FINAL.pdf

Appendices

Appendix A: Energy Savings and Seasonal Cooling/Heating Loads – Current Climate Condition Secondary School

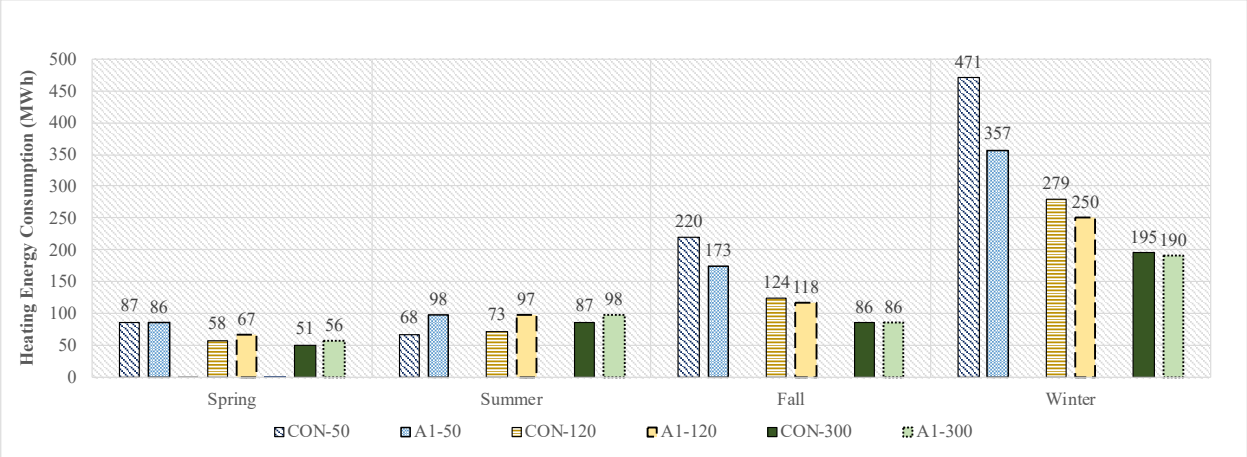

Figure A - 1: Seasonal cooling loads for conventional roof and green roof with design of growing media of 100 mm and LAI of 1 for insulation thicknesses 50 mm, 120 mm and 300 mm – current climate (secondary school building).

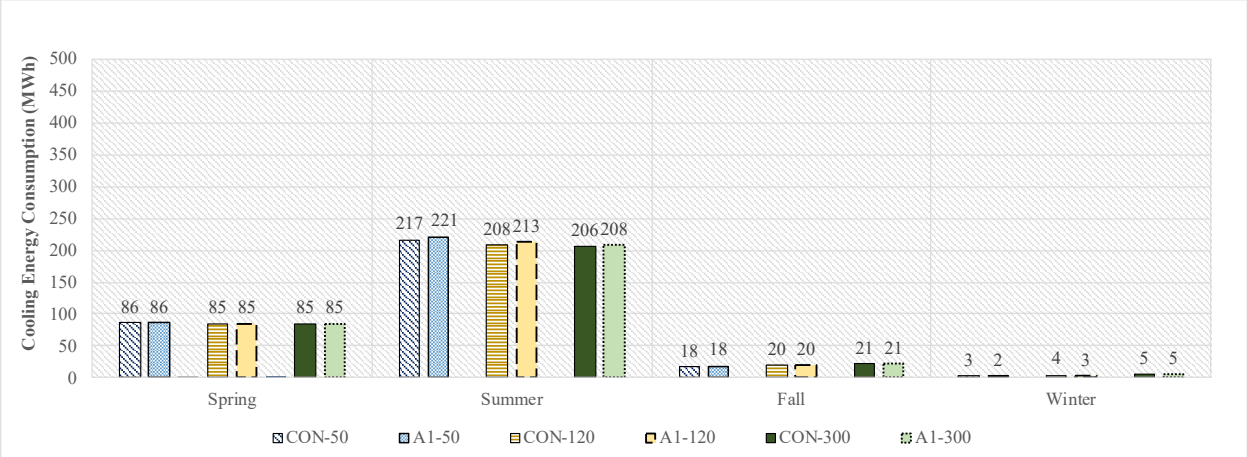

Figure A - 2: Seasonal cooling loads for conventional roof and green roof with design of growing media of 100 mm and LAI of 1 for insulation thicknesses 50 mm, 120 mm and 300 mm – current climate (secondary school building).

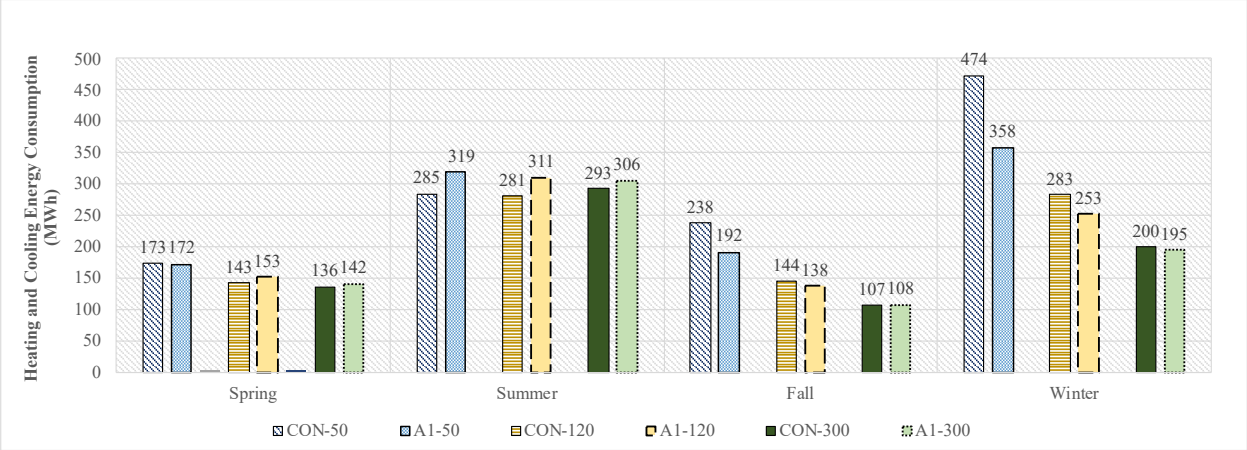

Figure A - 3: Seasonal total heating and cooling loads for conventional roof and green roof with design of growing media of 100 mm and LAI of 1 for insulation thicknesses 50 mm, 120 mm and 300 mm – current climate (secondary school building).

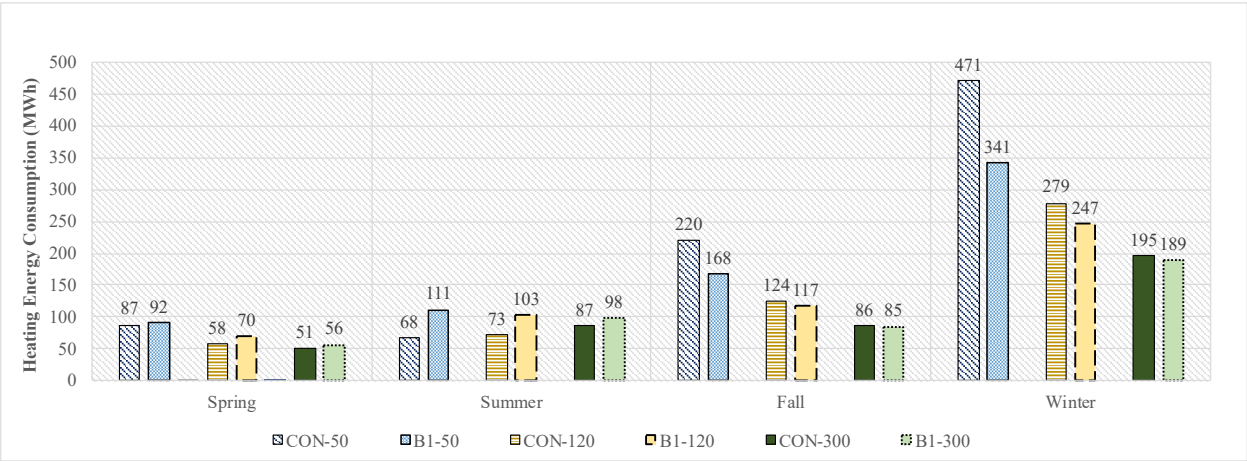

Figure A - 4: Seasonal heating loads for conventional roof and green roof with design of growing media of 150 mm and LAI of 1 for insulation thicknesses 50 mm, 120 mm and 300 mm – current climate (secondary school building).

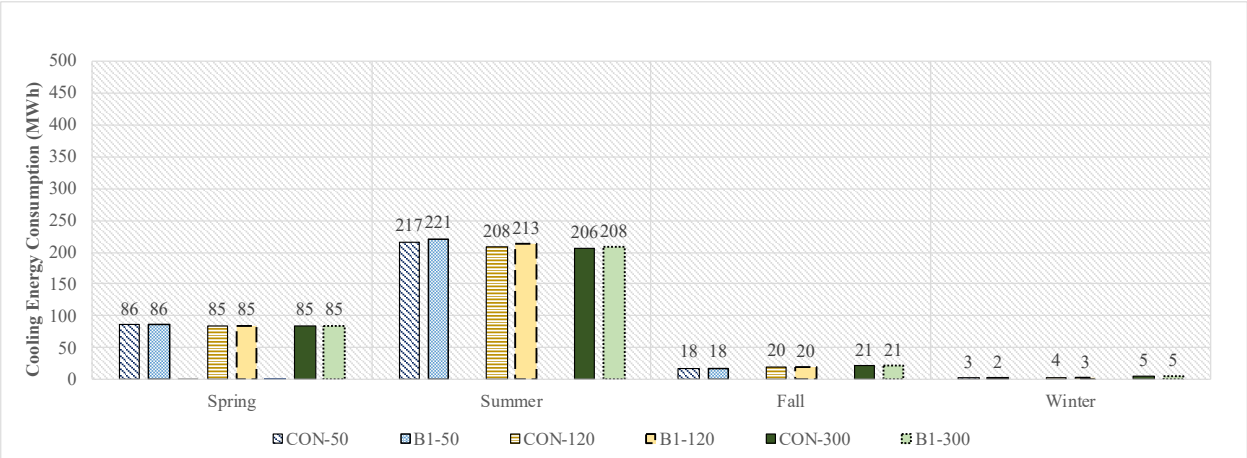

Figure A - 5: Seasonal cooling loads for conventional roof and green roof with design of growing media of 150 mm and LAI of 1 for insulation thicknesses 50 mm, 120 mm and 300 mm – current climate (secondary school building).

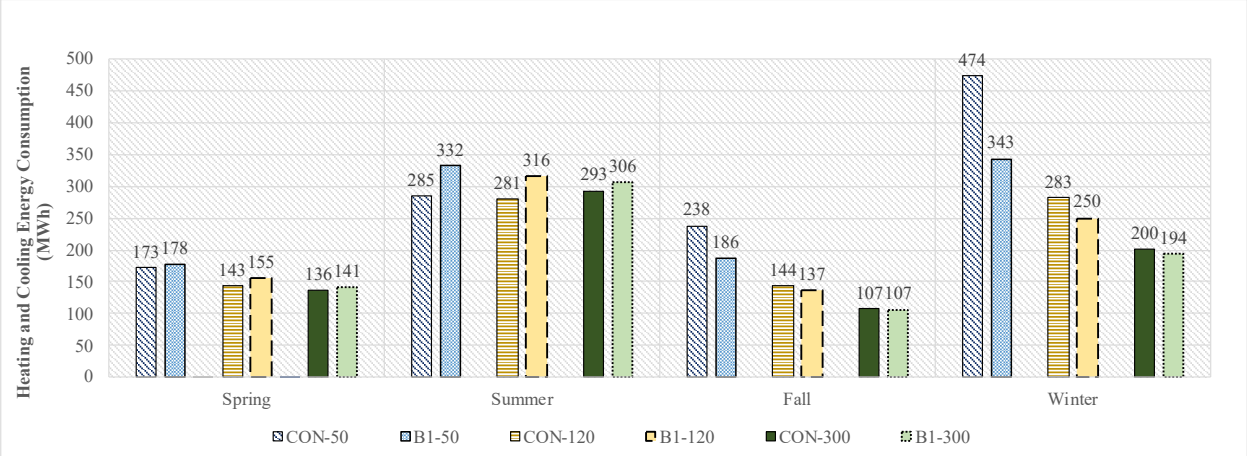

Figure A - 6: Seasonal total heating and cooling loads for conventional roof and green roof with design of growing media of 150 mm and LAI of 1 for insulation thicknesses 50 mm, 120 mm and 300 mm – current climate (secondary school building).

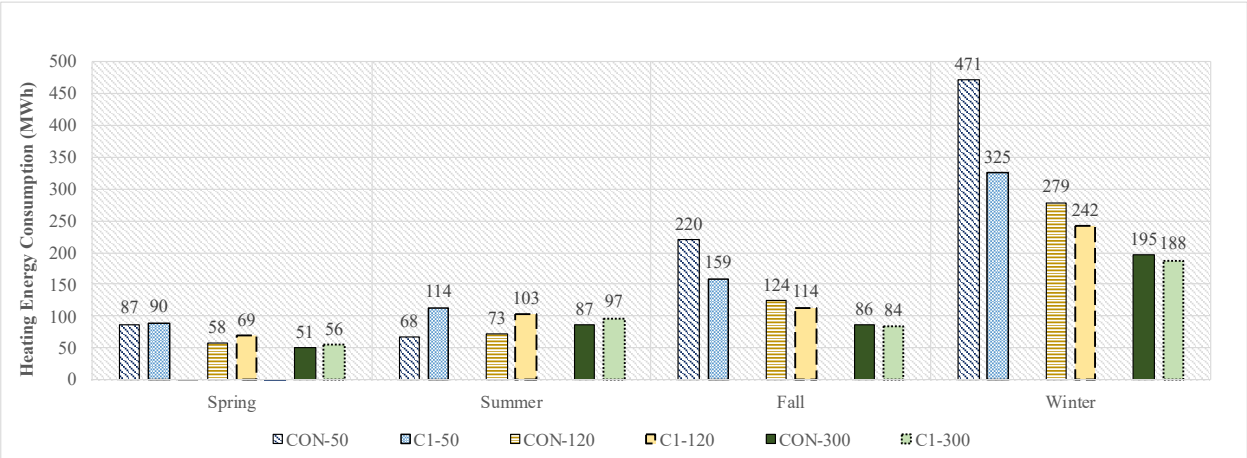

Figure A - 7: Seasonal heating loads for conventional roof and green roof with design of growing media of 200 mm and LAI of 1 for insulation thicknesses 50 mm, 120 mm and 300 mm – current climate (secondary school building).

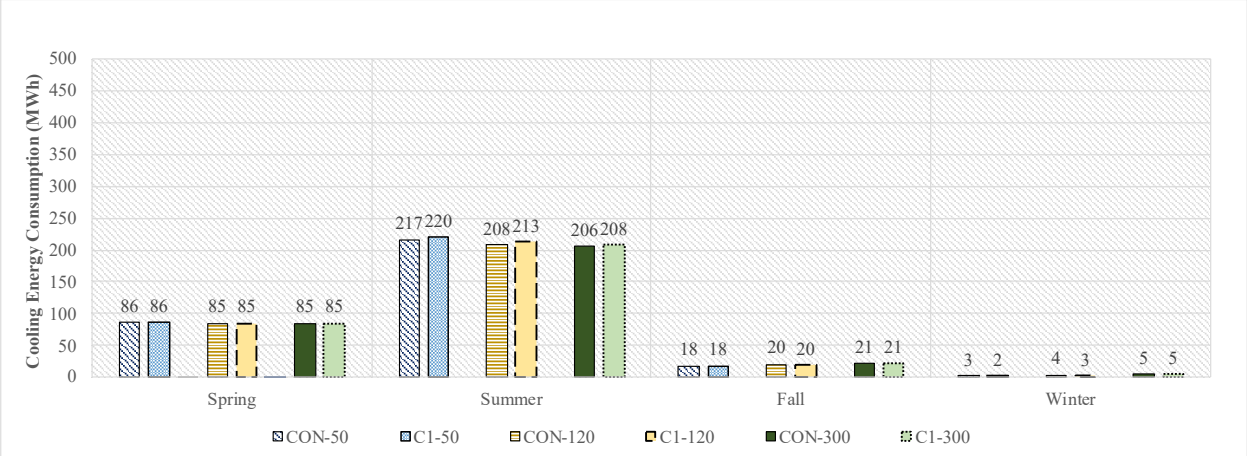

Figure A - 8: Seasonal cooling loads for conventional roof and green roof with design of growing media of 200 mm and LAI of 1 for insulation thicknesses 50 mm, 120 mm and 300 mm – current climate (secondary school building).

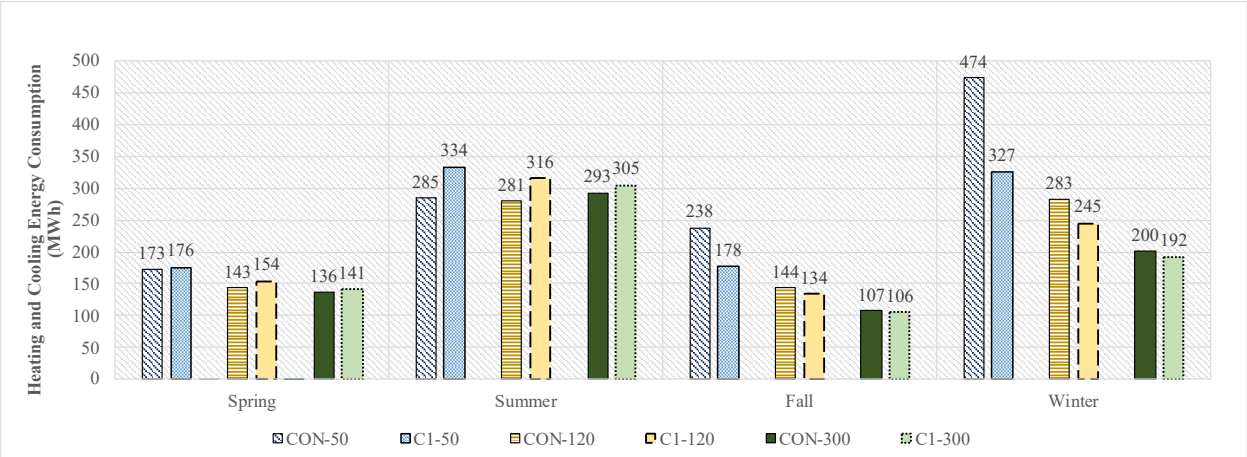

Figure A - 9: Seasonal total heating and cooling loads for conventional roof and green roof with design of growing media of 200 mm and LAI of 1 for insulation thicknesses 50 mm, 120 mm and 300 mm – current climate (secondary school building).

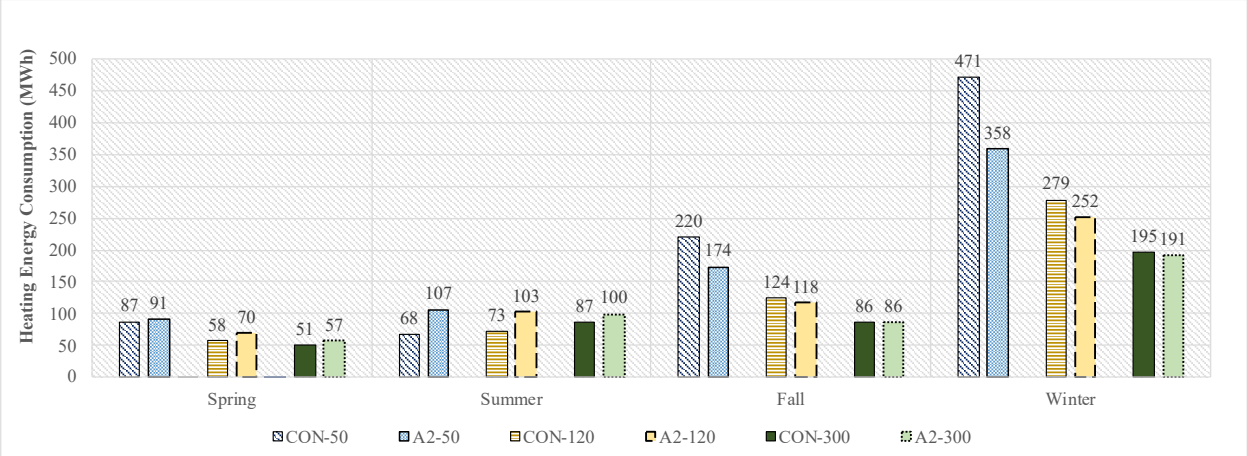

Figure A - 10: Seasonal heating loads for conventional roof and green roof with design of growing media of 100 mm and LAI of 2 for insulation thicknesses 50 mm, 120 mm and 300 mm – current climate (secondary school building).

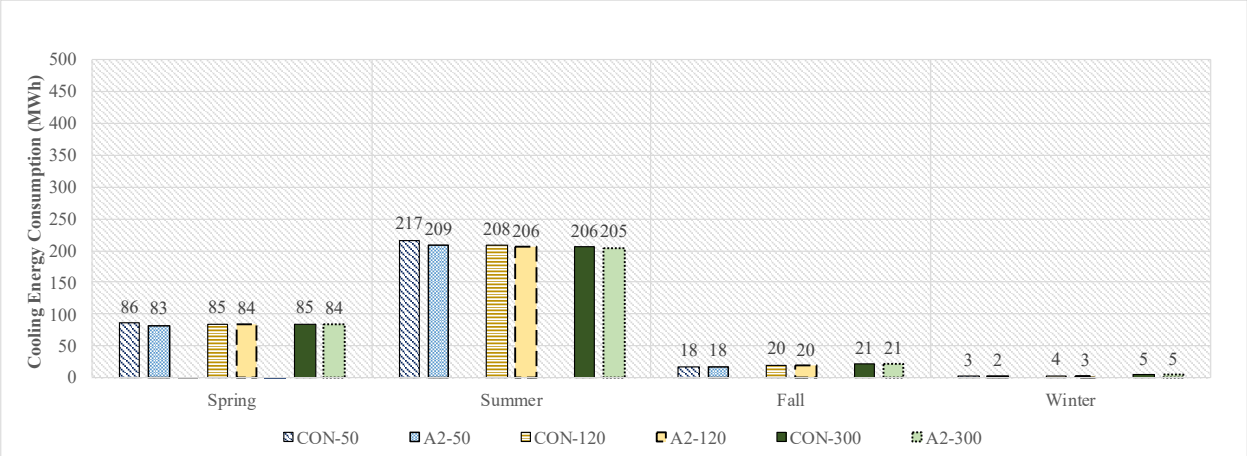

Figure A - 11: Seasonal cooling loads for conventional roof and green roof with design of growing media of 100 mm and LAI of 2 for insulation thicknesses 50 mm, 120 mm and 300 mm – current climate (secondary school building).

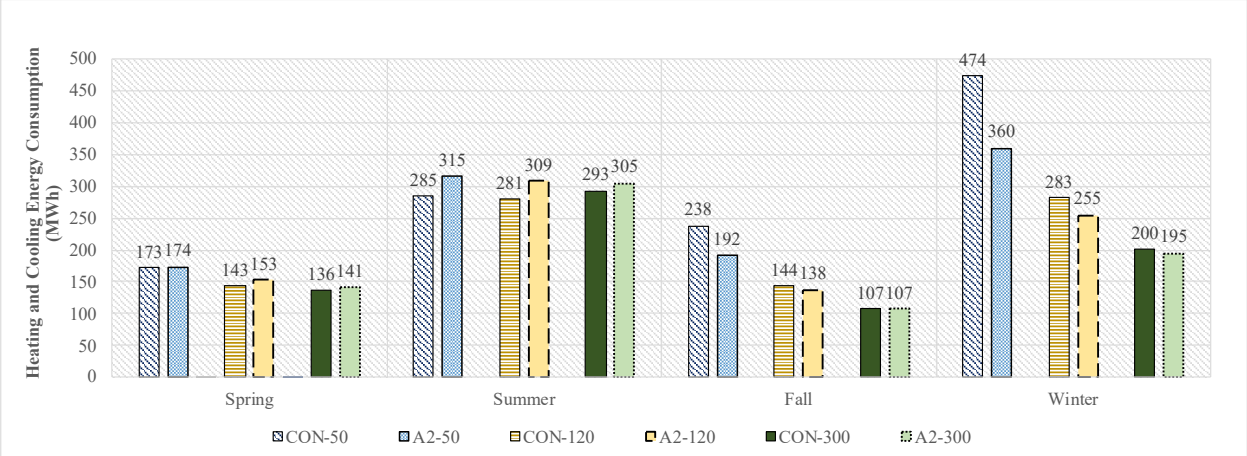

Figure A - 12: Seasonal total heating and cooling loads for conventional roof and green roof with design of growing media of 100 mm and LAI of 2 for insulation thicknesses 50 mm, 120 mm and 300 mm – current climate (secondary school building).

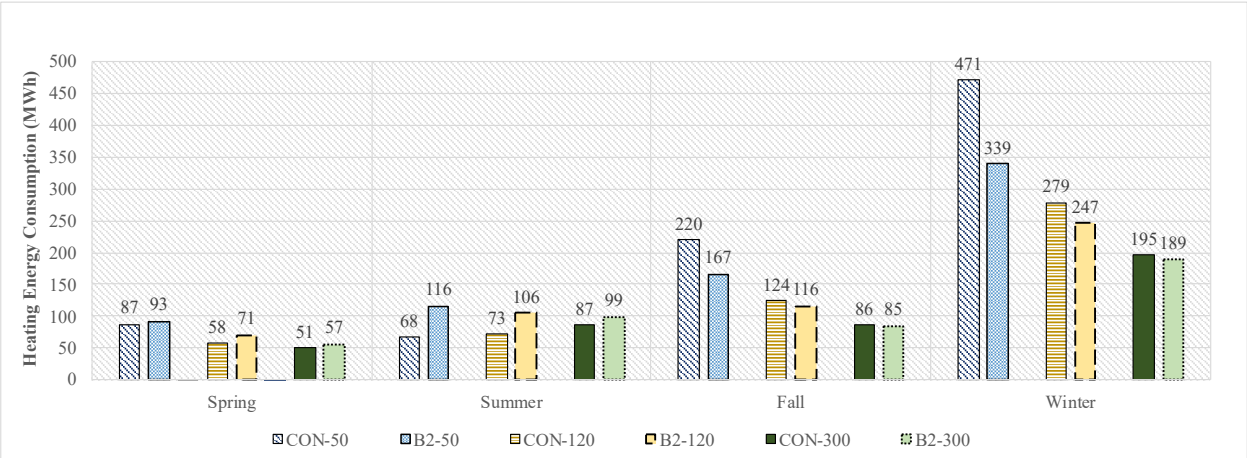

Figure A - 13: Seasonal heating loads for conventional roof and green roof with design of growing media of 150 mm and LAI of 2 for insulation thicknesses 50 mm, 120 mm and 300 mm – current climate (secondary school building).

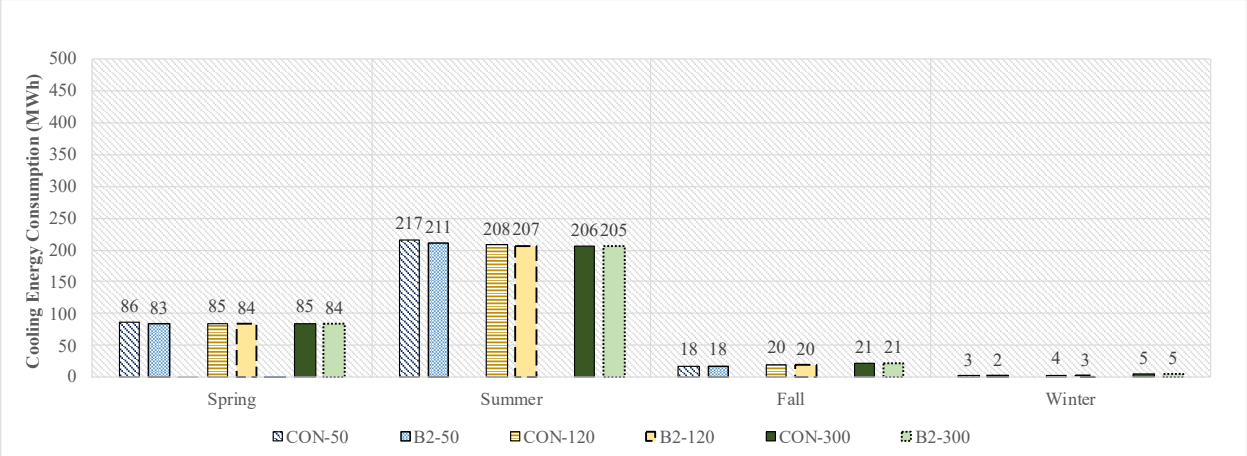

Figure A - 14: Seasonal cooling loads for conventional roof and green roof with design of growing media of 150 mm and LAI of 2 for insulation thicknesses 50 mm, 120 mm and 300 mm – current climate (secondary school building).

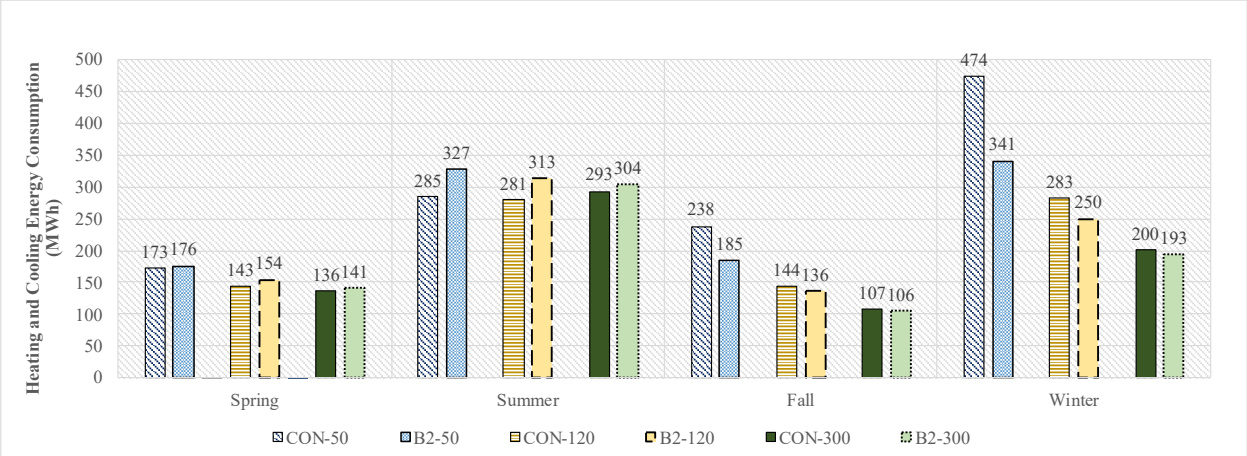

Figure A - 15: Seasonal total heating and cooling loads for conventional roof and green roof with design of growing media of 150 mm and LAI of 2 for insulation thicknesses 50 mm, 120 mm and 300 mm – current climate (secondary school building).

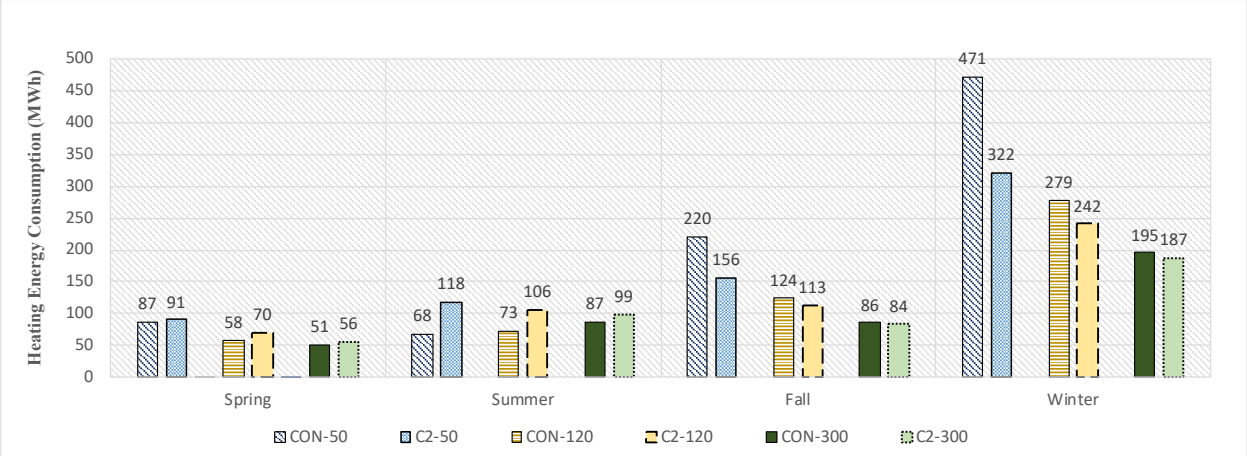

Figure A - 16: Seasonal heating loads for conventional roof and green roof with design of growing media of 200 mm and LAI of 2 for insulation thicknesses 50 mm, 120 mm and 300 mm – current climate (secondary school building).

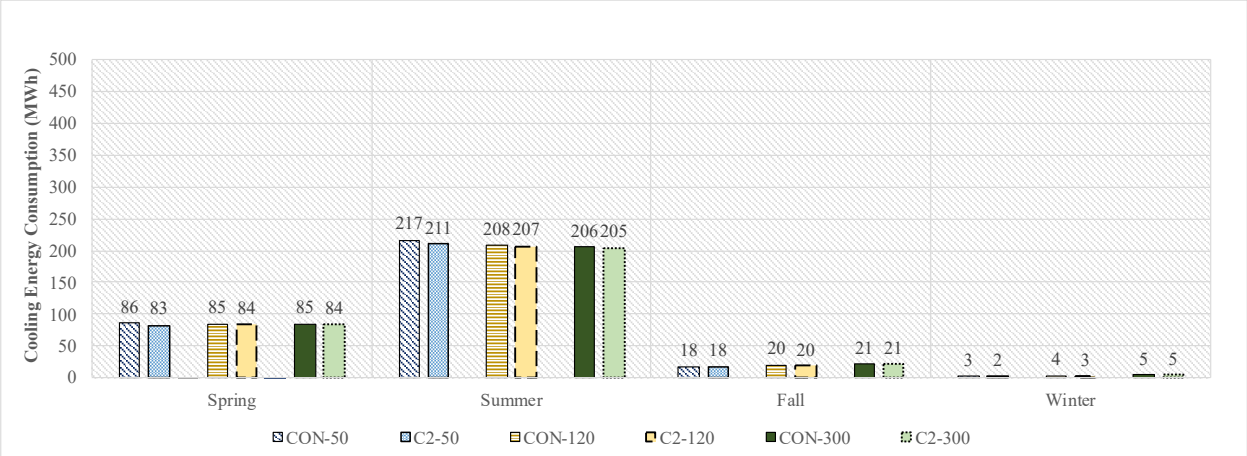

Figure A - 17: Seasonal cooling loads for conventional roof and green roof with design of growing media of 200 mm and LAI of 2 for insulation thicknesses 50 mm, 120 mm and 300 mm – current climate (secondary school building).

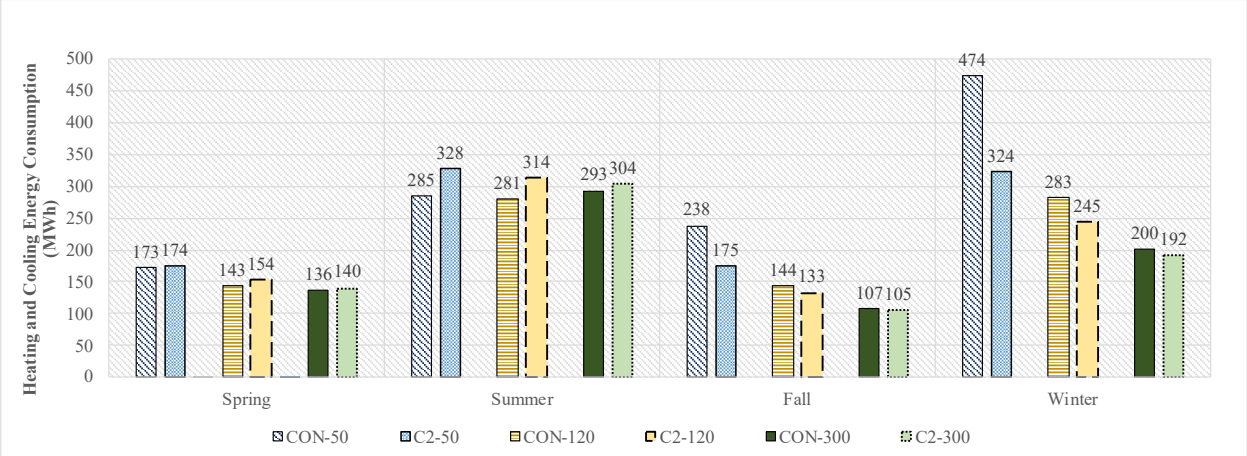

Figure A - 18: Seasonal total heating and cooling loads for conventional roof and green roof with design of growing media of 200 mm and LAI of 2 for insulation thicknesses 50 mm, 120 mm and 300 mm – current climate (secondary school building).

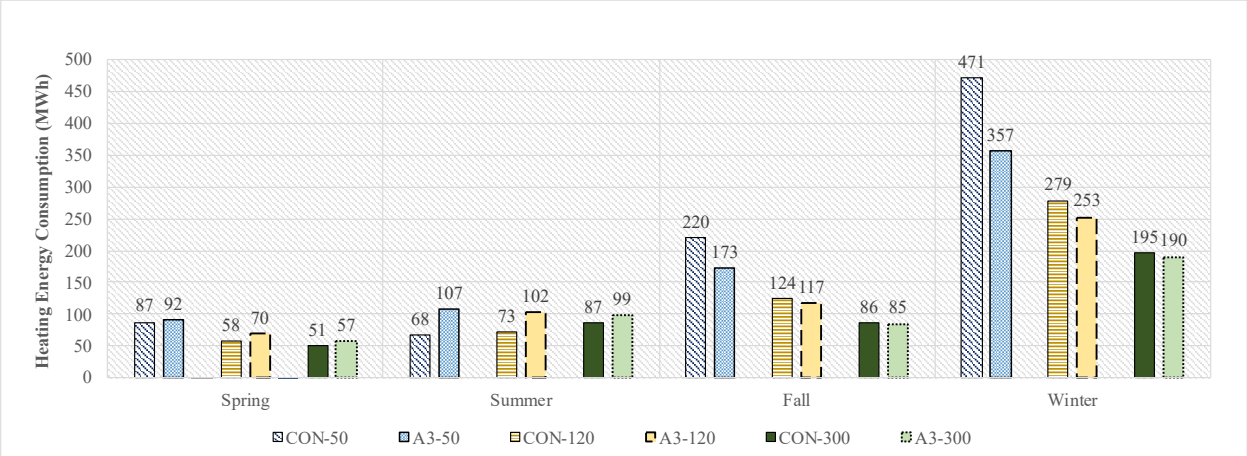

Figure A - 19: Seasonal heating loads for conventional roof and green roof with design of growing media of 100 mm and LAI of 3 for insulation thicknesses 50 mm, 120 mm and 300 mm – current climate (secondary school building).

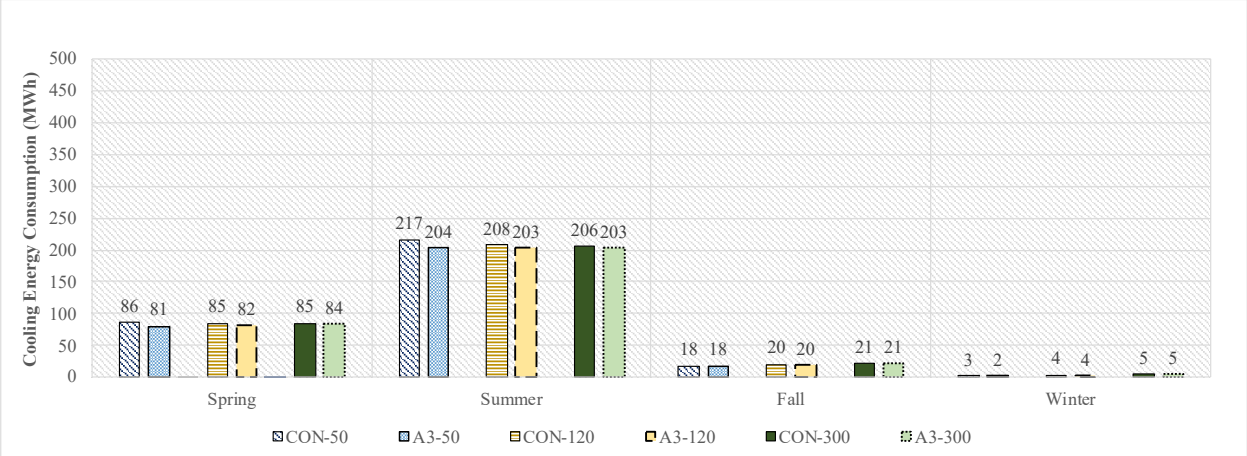

Figure A - 20: Seasonal cooling loads for conventional roof and green roof with design of growing media of 100 mm and LAI of 3 for insulation thicknesses 50 mm, 120 mm and 300 mm – current climate (secondary school building).

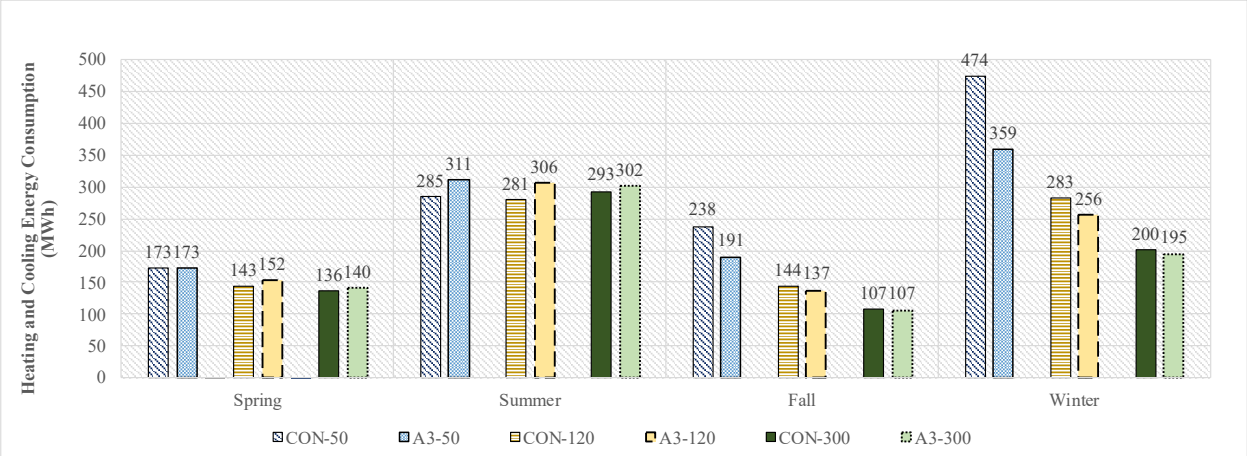

Figure A - 21: Seasonal total heating and cooling loads for conventional roof and green roof with design of growing media of 100 mm and LAI of 3 for insulation thicknesses 50 mm, 120 mm and 300 mm – current climate (secondary school building).

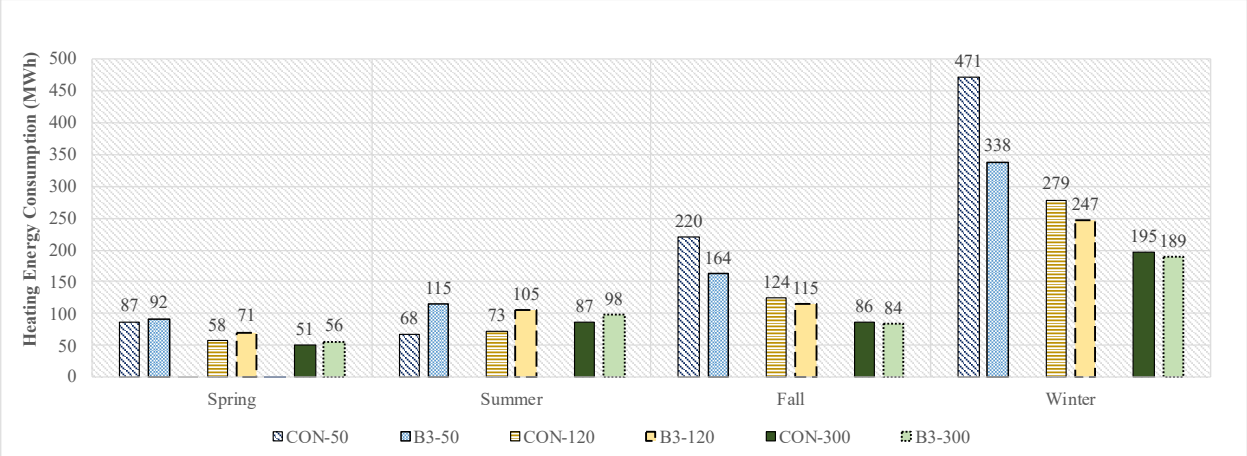

Figure A - 22: Seasonal heating loads for conventional roof and green roof with design of growing media of 150 mm and LAI of 3 for insulation thicknesses 50 mm, 120 mm and 300 mm – current climate (secondary school building).

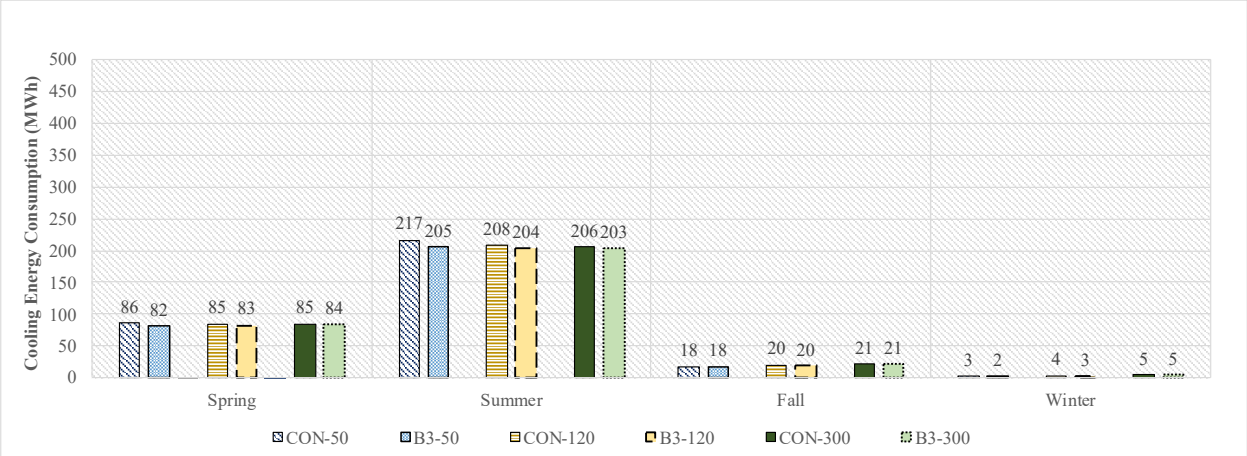

Figure A - 23: Seasonal cooling loads for conventional roof and green roof with design of growing media of 150 mm and LAI of 3 for insulation thicknesses 50 mm, 120 mm and 300 mm – current climate (secondary school building).

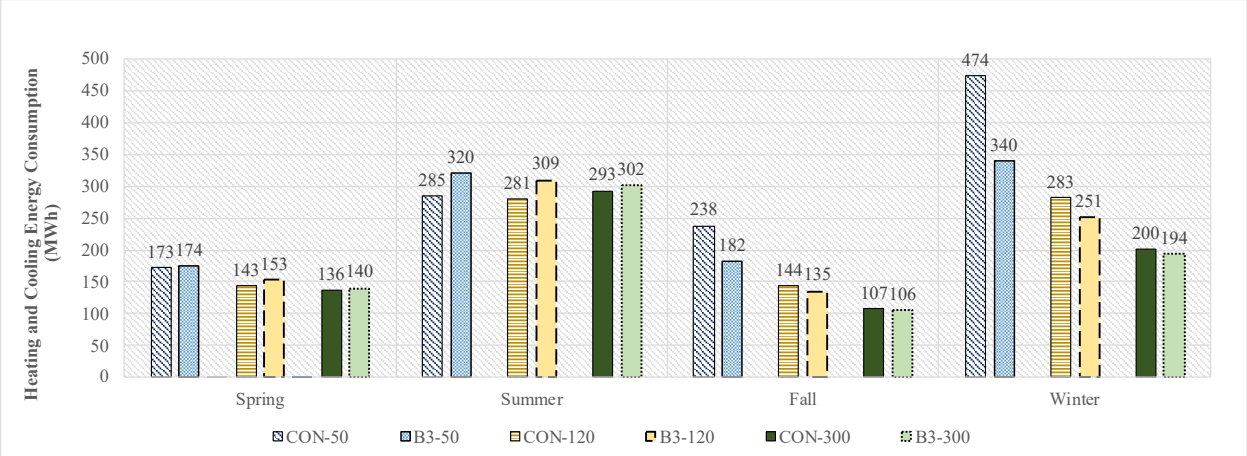

Figure A - 24: Seasonal total heating and cooling loads for conventional roof and green roof with design of growing media of 150 mm and LAI of 3 for insulation thicknesses 50 mm, 120 mm and 300 mm – current climate (secondary school building).

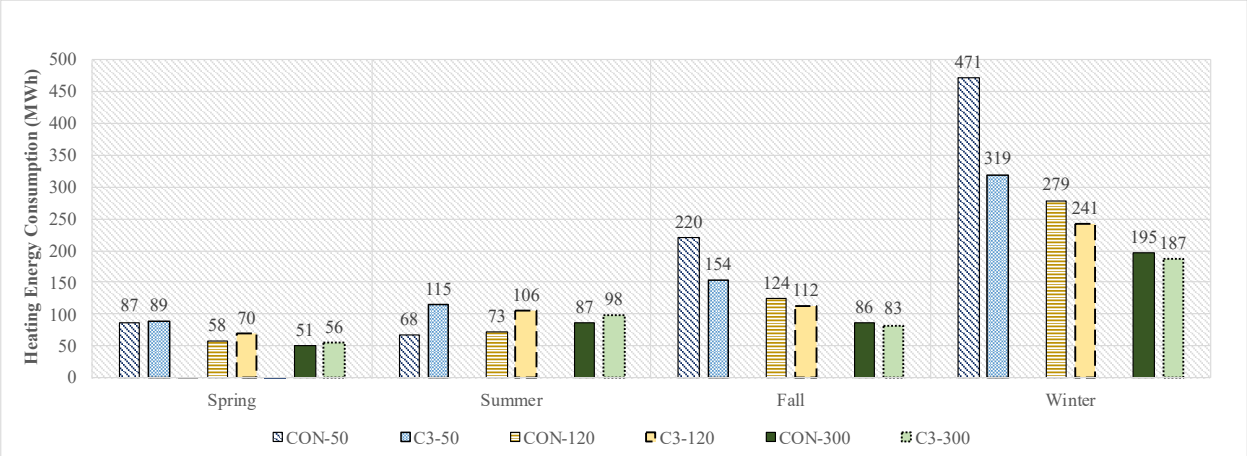

Figure A - 25: Seasonal heating loads for conventional roof and green roof with design of growing media of 200 mm and LAI of 3 for insulation thicknesses 50 mm, 120 mm and 300 mm – current climate (secondary school building).

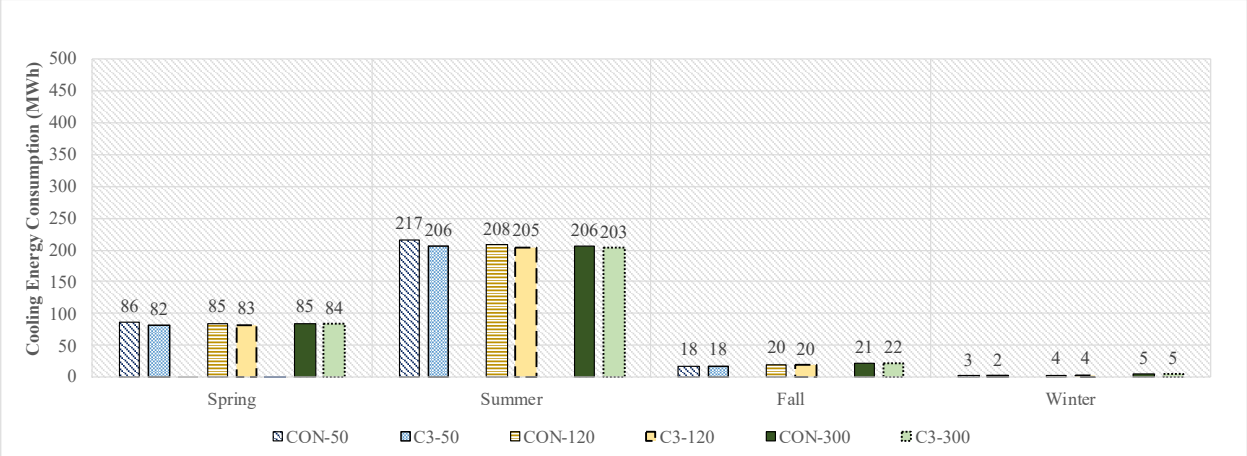

Figure A - 26: Seasonal cooling loads for conventional roof and green roof with design of growing media of 200 mm and LAI of 3 for insulation thicknesses 50 mm, 120 mm and 300 mm – current climate (secondary school building).

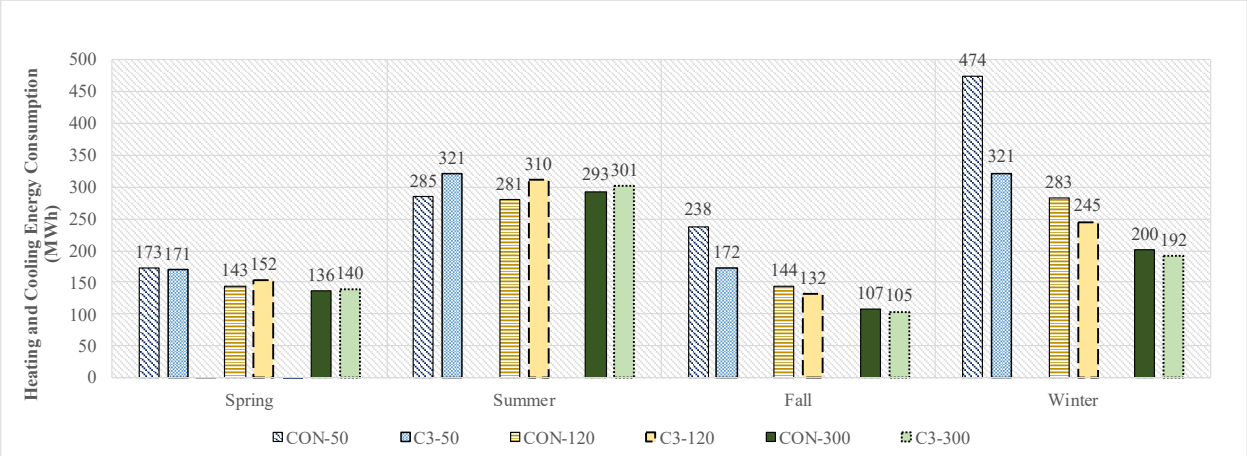

Figure A - 27: Seasonal total heating and cooling loads for conventional roof and green roof with design of growing media of 200 mm and LAI of 3 for insulation thicknesses 50 mm, 120 mm and 300 mm – current climate (secondary school building).

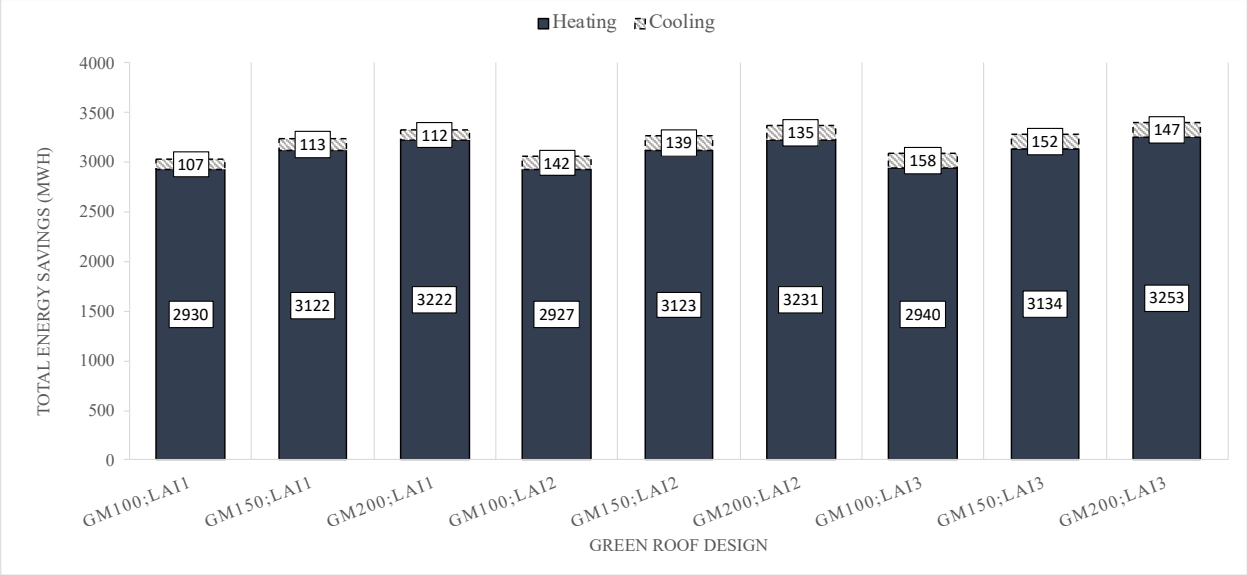

Figure A - 28: Total heating and cooling energy savings (MWh) of green roof compared to conventional roof for all growing media (GM) depths and LAIs; without insulation layer – current climate (secondary school building).

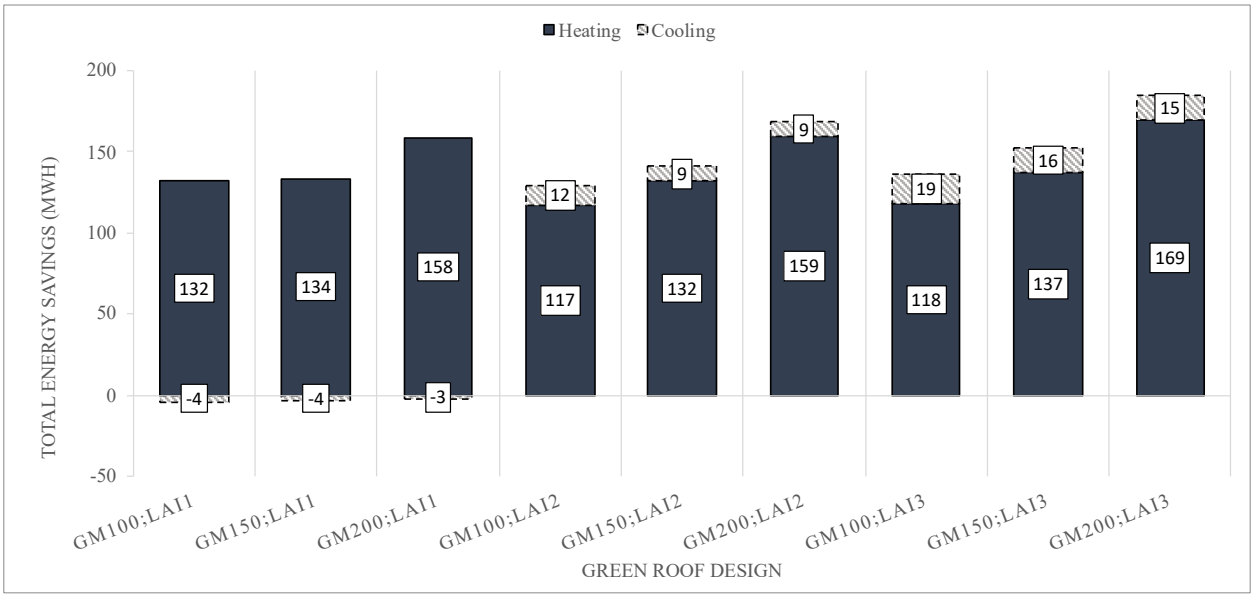

Figure A - 29: Total heating and cooling energy savings (MWh) of green roof compared to conventional roof for all growing media (GM) depths and LAIs; with 50 mm insulation layer – current climate (secondary school building).

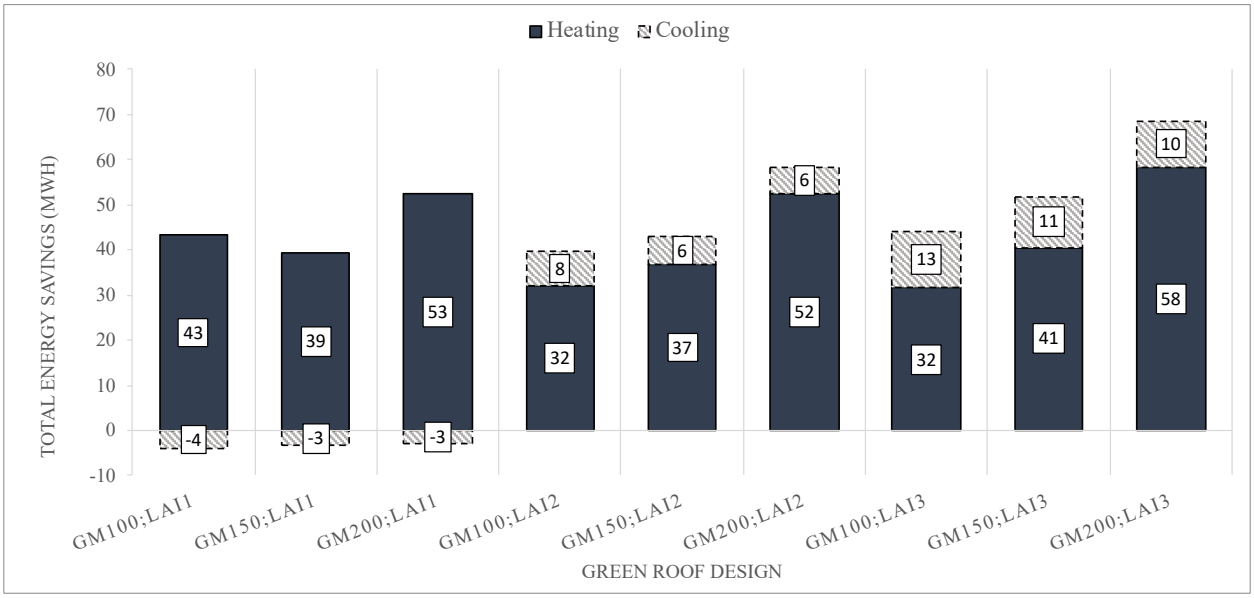

Figure A - 30: Total heating and cooling energy savings (MWh) of green roof compared to conventional roof for all growing media (GM) depths and LAIs; with 80 mm insulation layer – current climate (secondary school building).

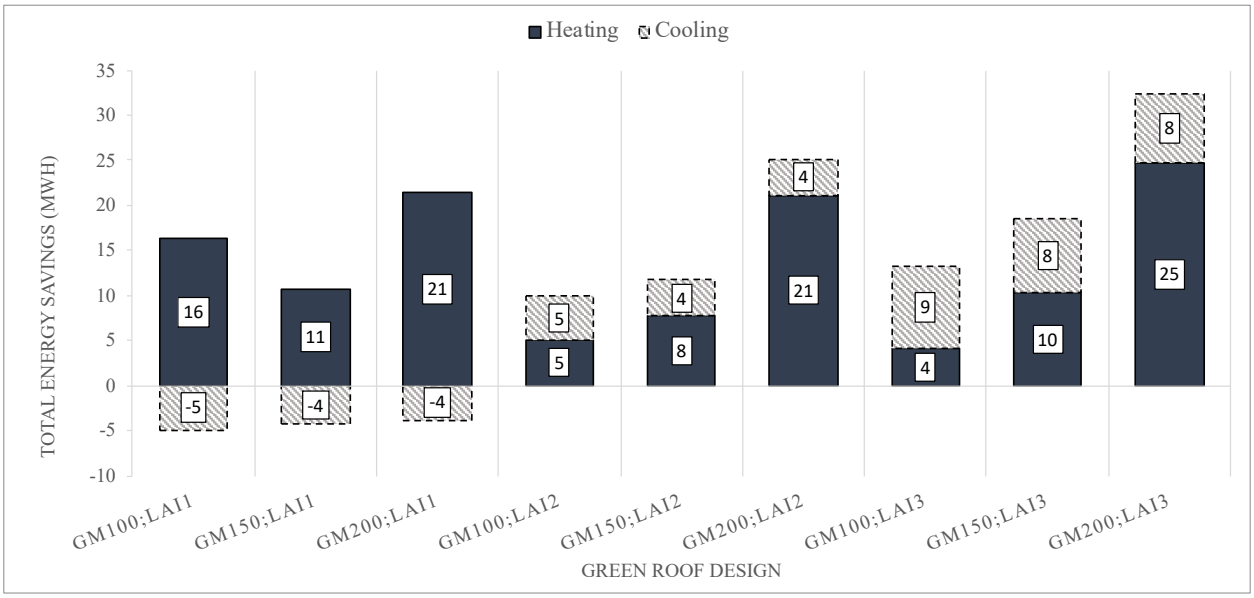

Figure A - 31: Total heating and cooling energy savings (MWh) of green roof compared to conventional roof for all growing media (GM) depths and LAIs; with 100 mm insulation layer – current climate (secondary school building).

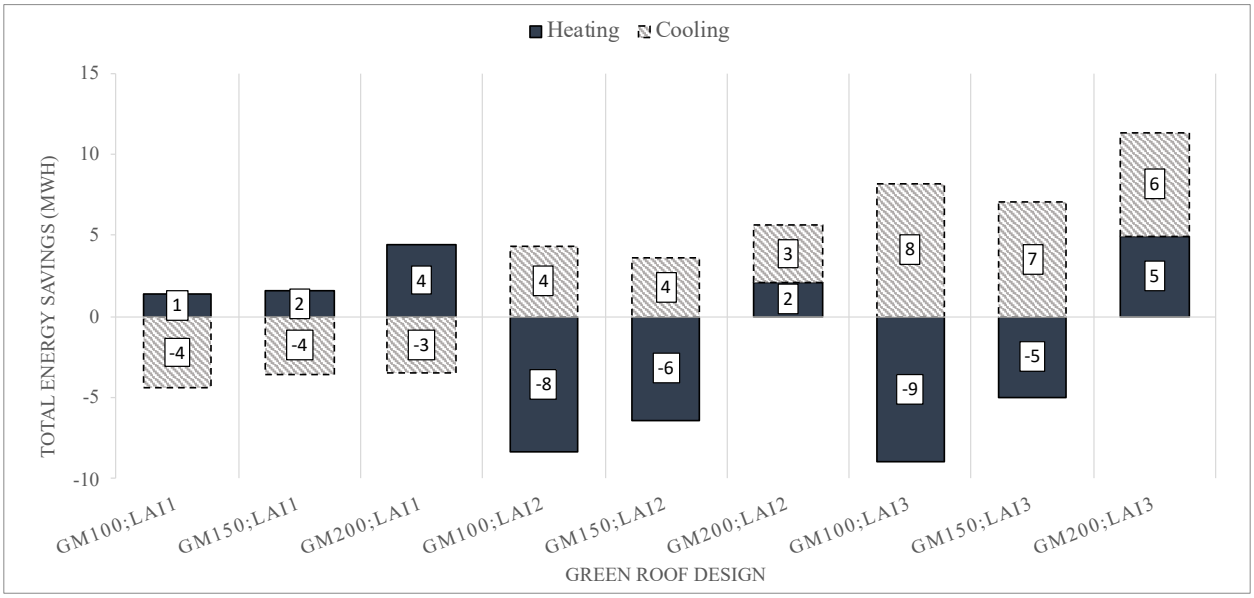

Figure A - 32: Total heating and cooling energy savings (MWh) of green roof compared to conventional roof for all growing media (GM) depths and LAIs; with 120 mm insulation layer – current climate (secondary school building).

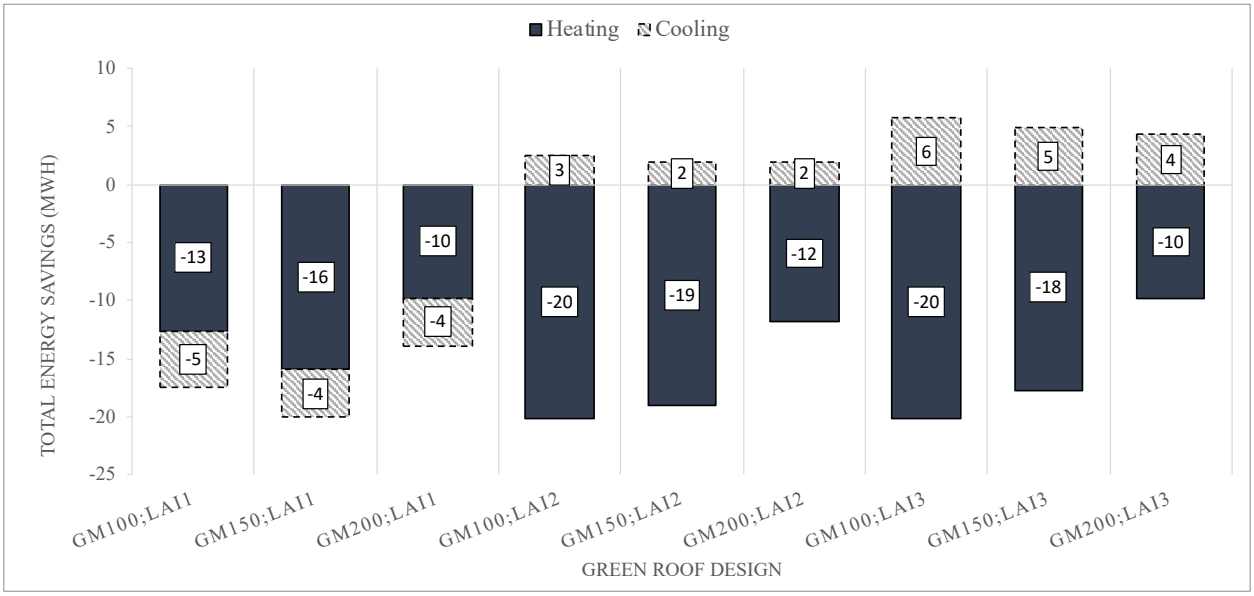

Figure A - 33: Total heating and cooling energy savings (MWh) of green roof compared to conventional roof for all growing media (GM) depths and LAIs; with 150 mm insulation layer – current climate (secondary school building).

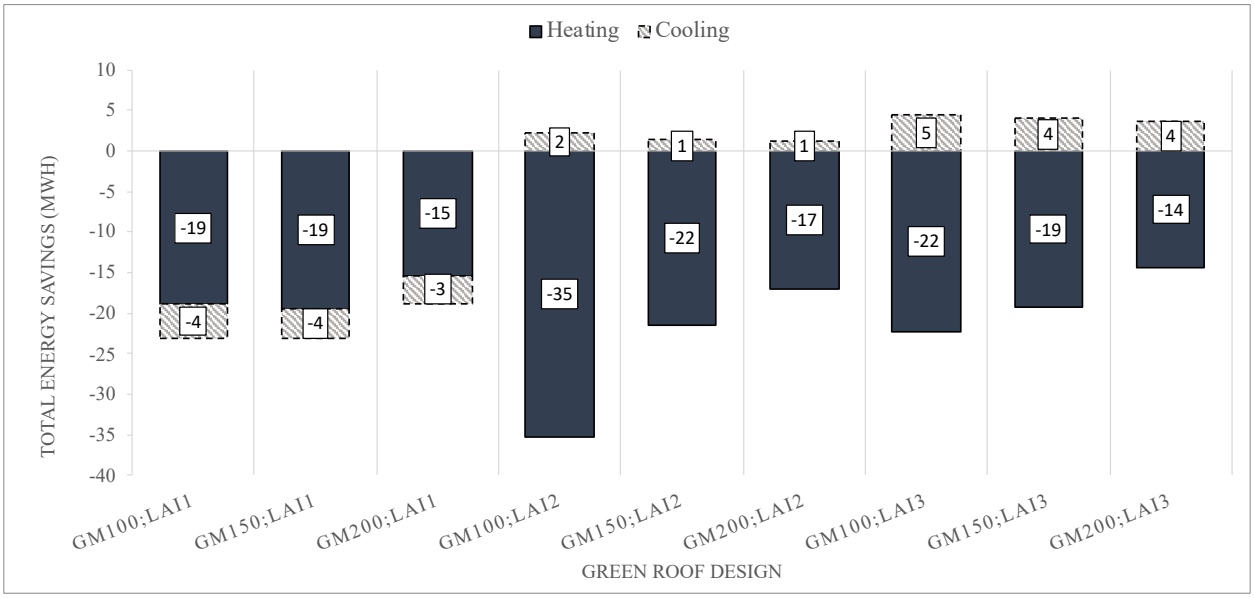

Figure A - 34: Total heating and cooling energy savings (MWh) of green roof compared to conventional roof for all growing media (GM) depths and LAIs; with 200 mm insulation layer – current climate (secondary school building).

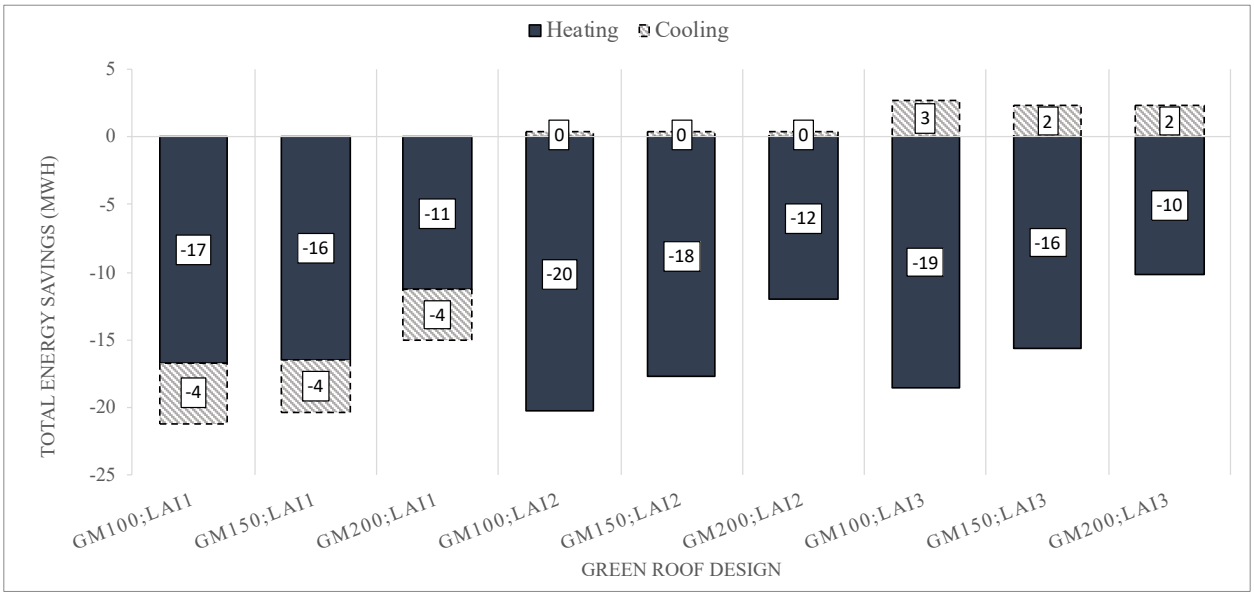

Figure A - 35: Total heating and cooling energy savings (MWh) of green roof compared to conventional roof for all growing media (GM) depths and LAIs; with 250 mm insulation layer – current climate (secondary school building).

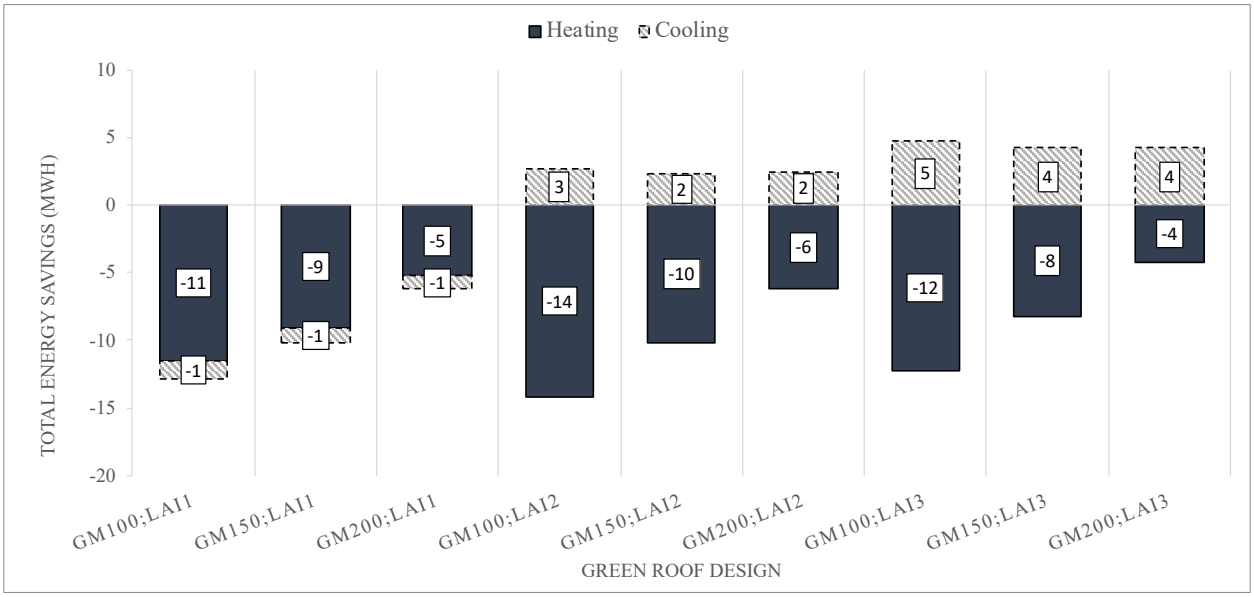

Figure A - 36: Total heating and cooling energy savings (MWh) of green roof compared to conventional roof for all growing media (GM) depths and LAIs; with 300 mm insulation layer – current climate (secondary school building).

Appendix B: Energy Savings and Seasonal Cooling/Heating Loads – Future Climate Condition Secondary School

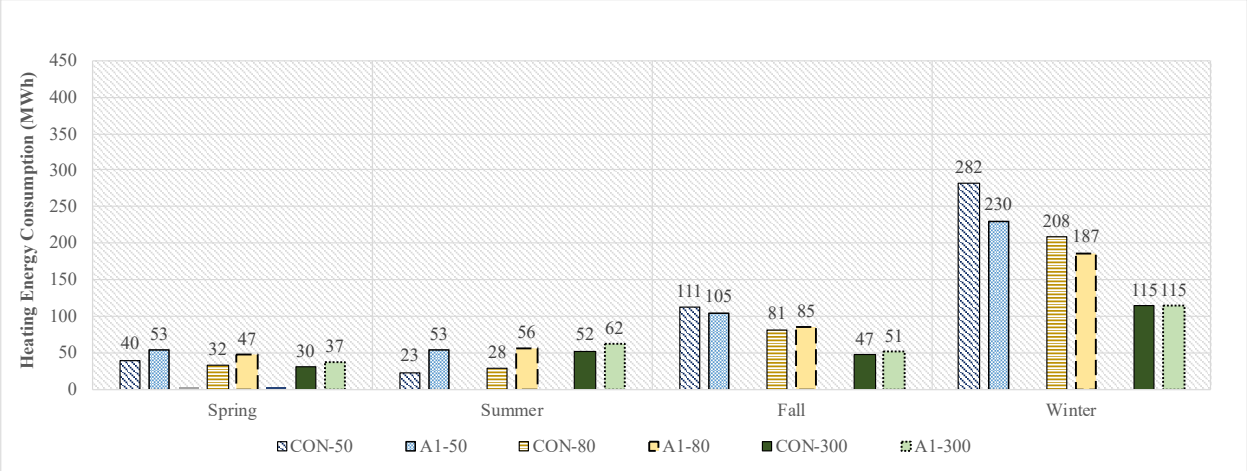

Figure B - 1: Seasonal heating loads for conventional roof and green roof with design of growing media of 100 mm and LAI of 1 for insulation thicknesses 50 mm, 80 mm and 300 mm – future climate (secondary school building).

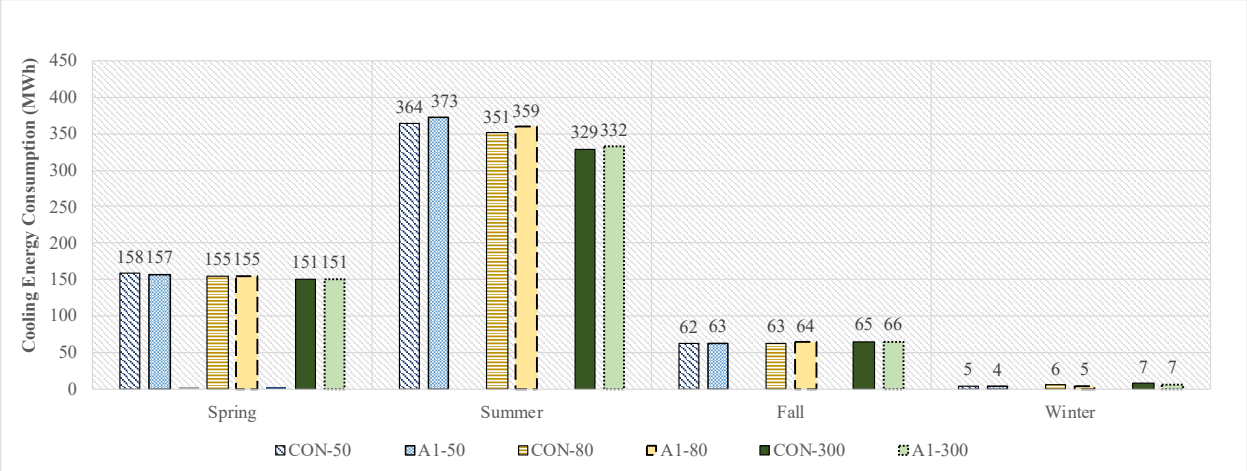

Figure B - 2: Seasonal cooling loads for conventional roof and green roof with design of growing media of 100 mm and LAI of 1 for insulation thicknesses 50 mm, 80 mm and 300 mm – future climate (secondary school building).

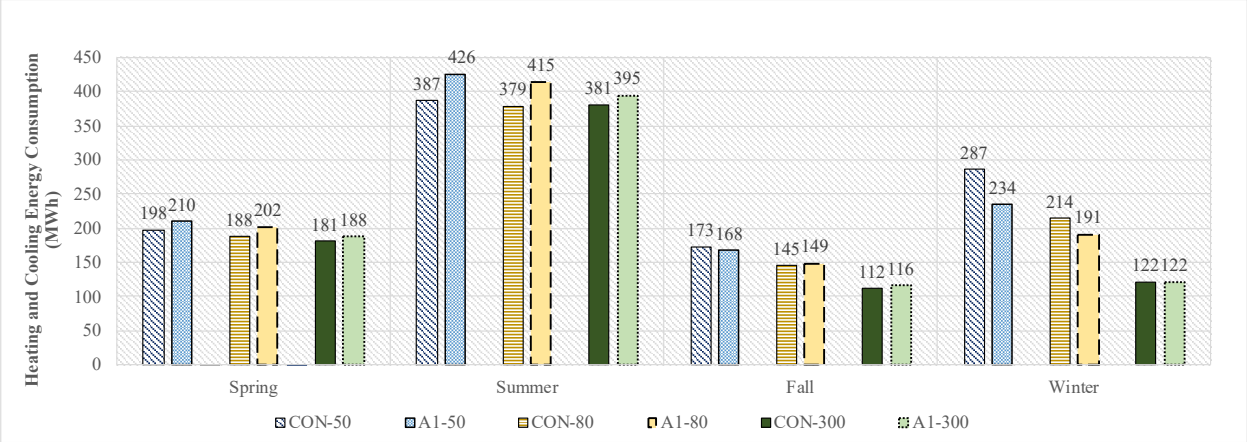

Figure B - 3: Seasonal total heating and cooling loads for conventional roof and green roof with design of growing media of 100 mm and LAI of 1 for insulation thicknesses 50 mm, 80 mm and 300 mm – future climate (secondary school building).

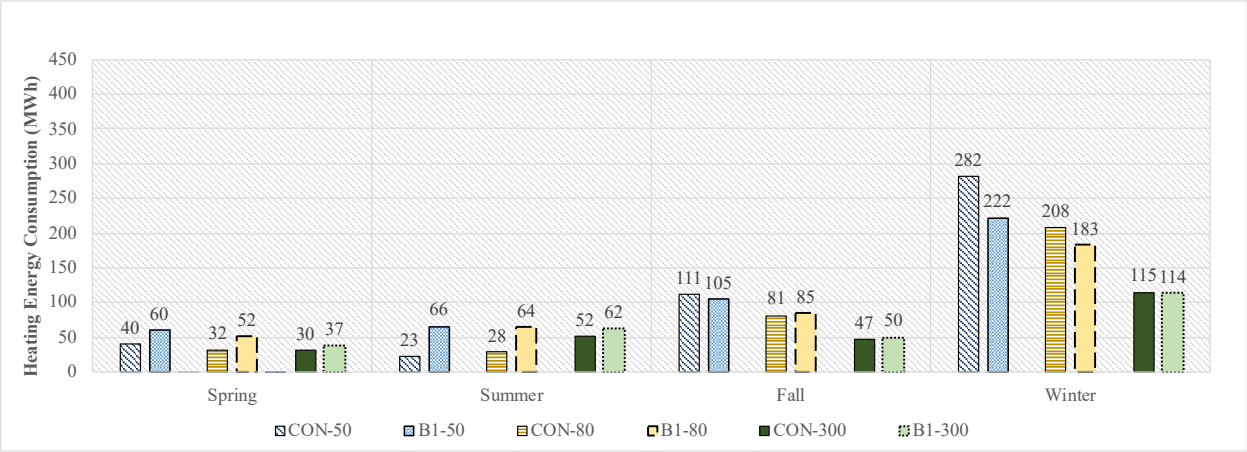

Figure B - 4: Seasonal heating loads for conventional roof and green roof with design of growing media of 150 mm and LAI of 1 for insulation thicknesses 50 mm, 80 mm and 300 mm – future climate (secondary school building).

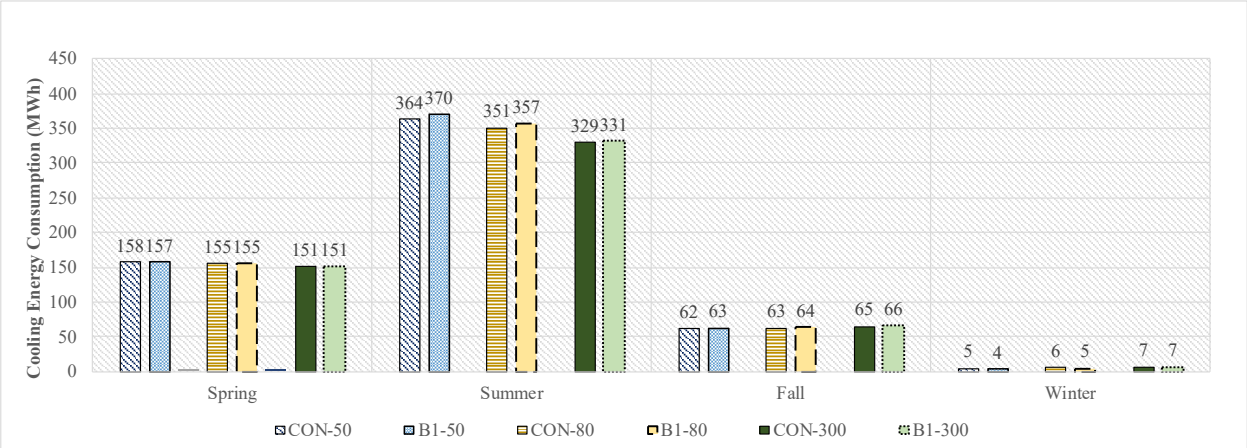

Figure B - 5: Seasonal cooling loads for conventional roof and green roof with design of growing media of 150 mm and LAI of 1 for insulation thicknesses 50 mm, 80 mm and 300 mm – future climate (secondary school building).

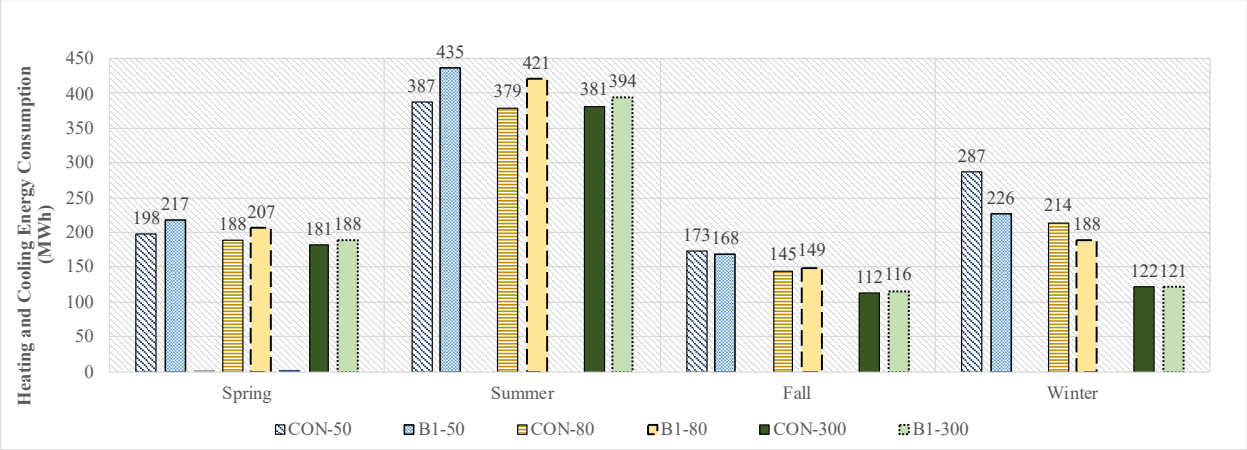

Figure B - 6: Seasonal total heating and cooling loads for conventional roof and green roof with design of growing media of 150 mm and LAI of 1 for insulation thicknesses 50 mm, 80 mm and 300 mm – future climate (secondary school building).

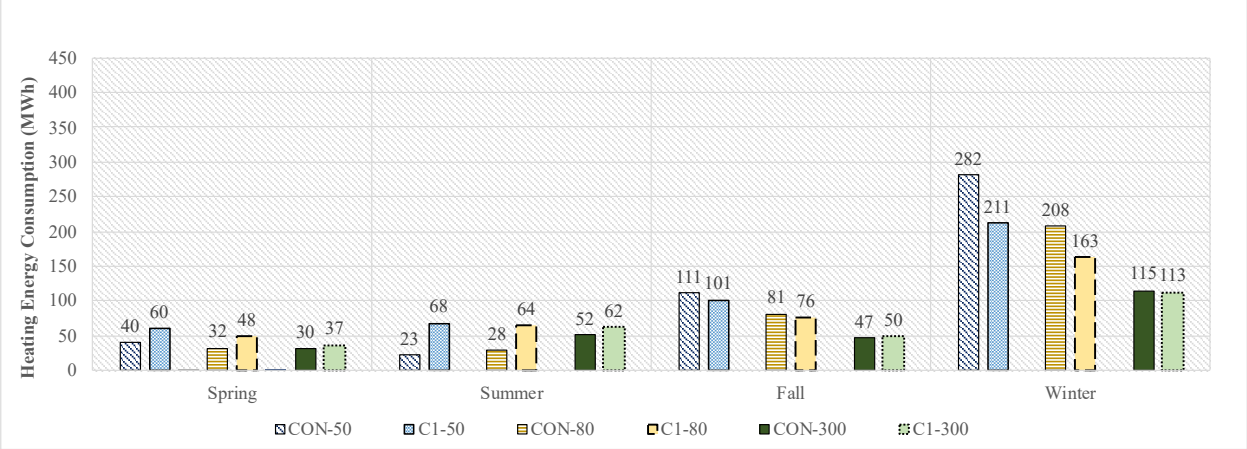

Figure B - 7: Seasonal heating loads for conventional roof and green roof with design of growing media of 200 mm and LAI of 1 for insulation thicknesses 50 mm, 80 mm and 300 mm – future climate (secondary school building).

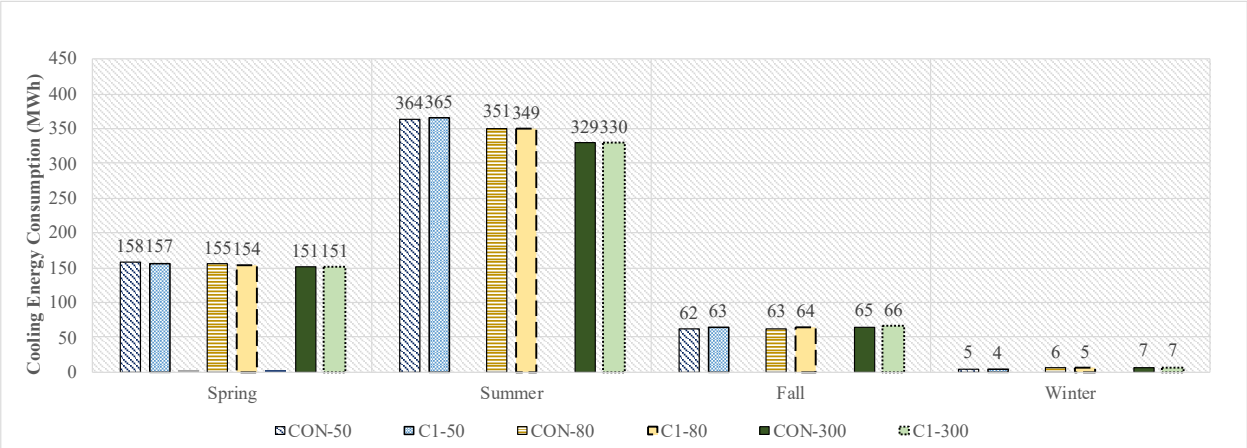

Figure B - 8: Seasonal cooling loads for conventional roof and green roof with design of growing media of 200 mm and LAI of 1 for insulation thicknesses 50 mm, 80 mm and 300 mm – future climate (secondary school building).

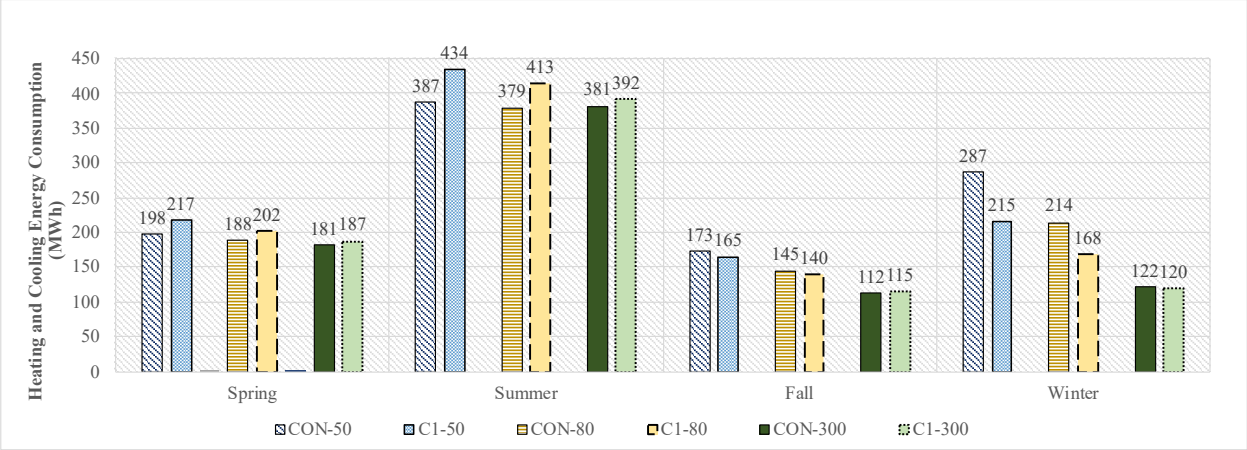

Figure B - 9: Seasonal total heating and cooling loads for conventional roof and green roof with design of growing media of 200 mm and LAI of 1 for insulation thicknesses 50 mm, 80 mm and 300 mm – future climate (secondary school building).

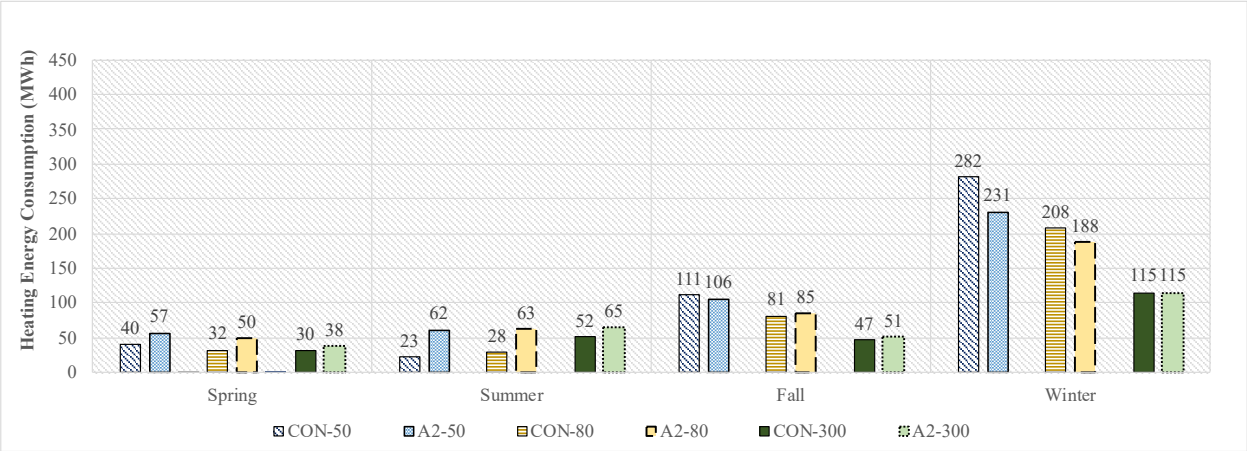

Figure B - 10: Seasonal heating loads for conventional roof and green roof with design of growing media of 100 mm and LAI of 2 for insulation thicknesses 50 mm, 80 mm and 300 mm – future climate (secondary school building).

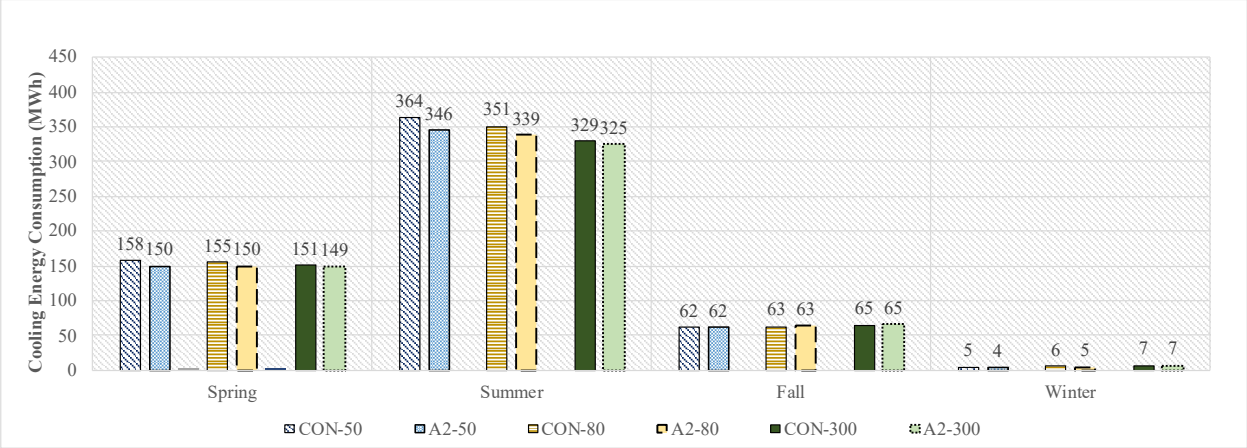

Figure B - 11: Seasonal cooling loads for conventional roof and green roof with design of growing media of 100 mm and LAI of 2 for insulation thicknesses 50 mm, 80 mm and 300 mm – future climate (secondary school building).

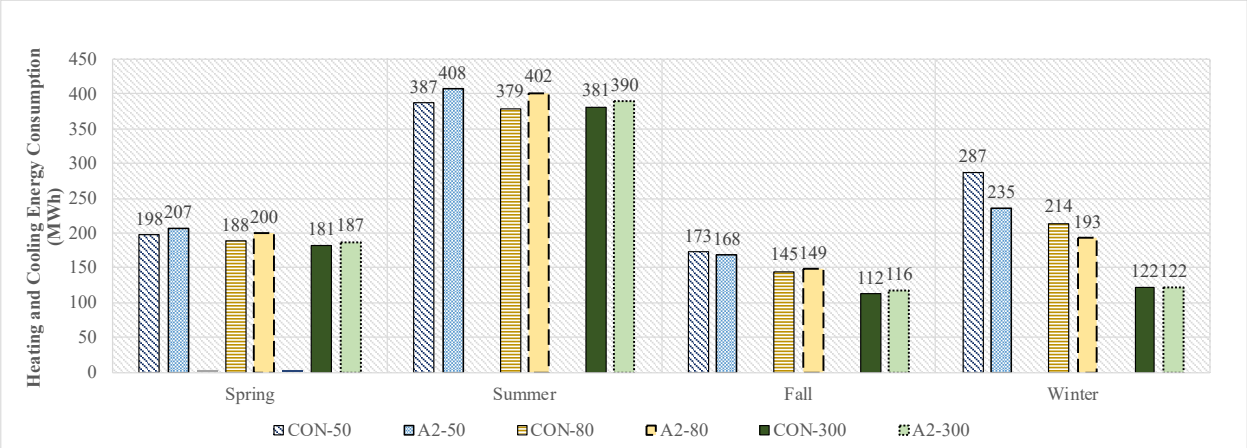

Figure B - 12: Seasonal total heating and cooling loads for conventional roof and green roof with design of growing media of 100 mm and LAI of 2 for insulation thicknesses 50 mm, 80 mm and 300 mm – future climate (secondary school building).

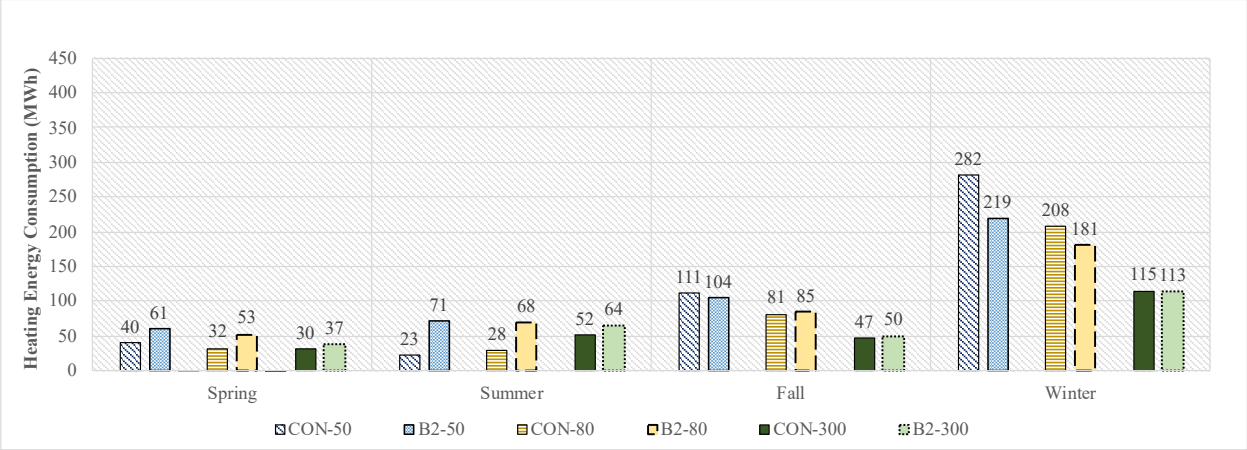

Figure B - 13: Seasonal heating loads for conventional roof and green roof with design of growing media of 150 mm and LAI of 2 for insulation thicknesses 50 mm, 80 mm and 300 mm – future climate (secondary school building).

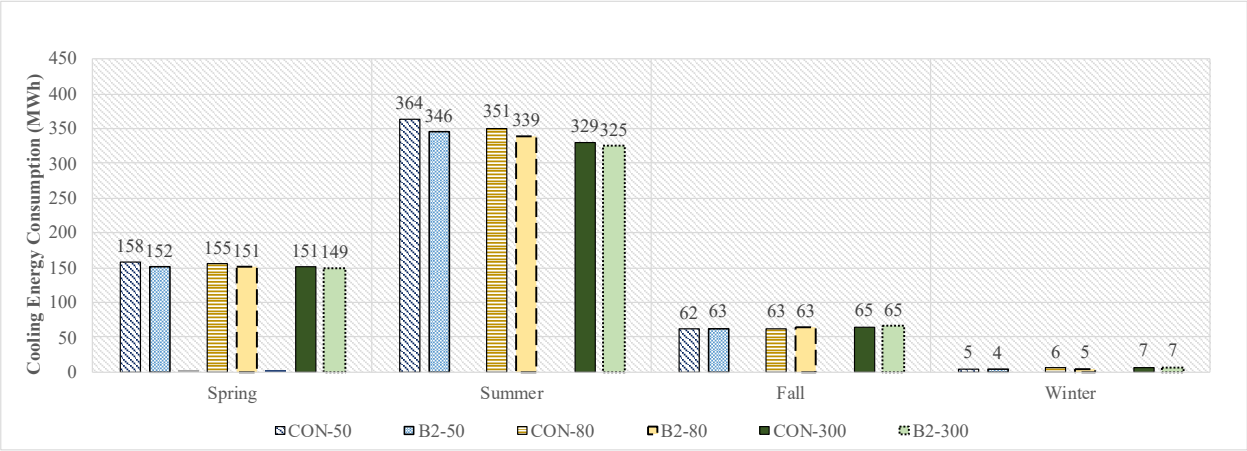

Figure B - 14: Seasonal cooling loads for conventional roof and green roof with design of growing media of 150 mm and LAI of 2 for insulation thicknesses 50 mm, 80 mm and 300 mm – future climate (secondary school building).

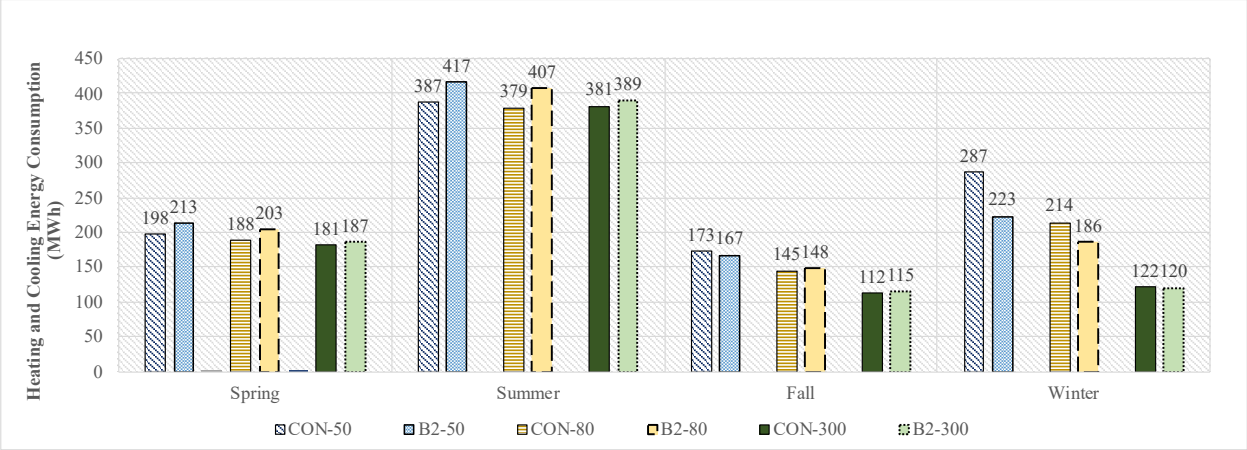

Figure B - 15: Seasonal total heating and cooling loads for conventional roof and green roof with design of growing media of 150 mm and LAI of 2 for insulation thicknesses 50 mm, 80 mm and 300 mm – future climate (secondary school building).

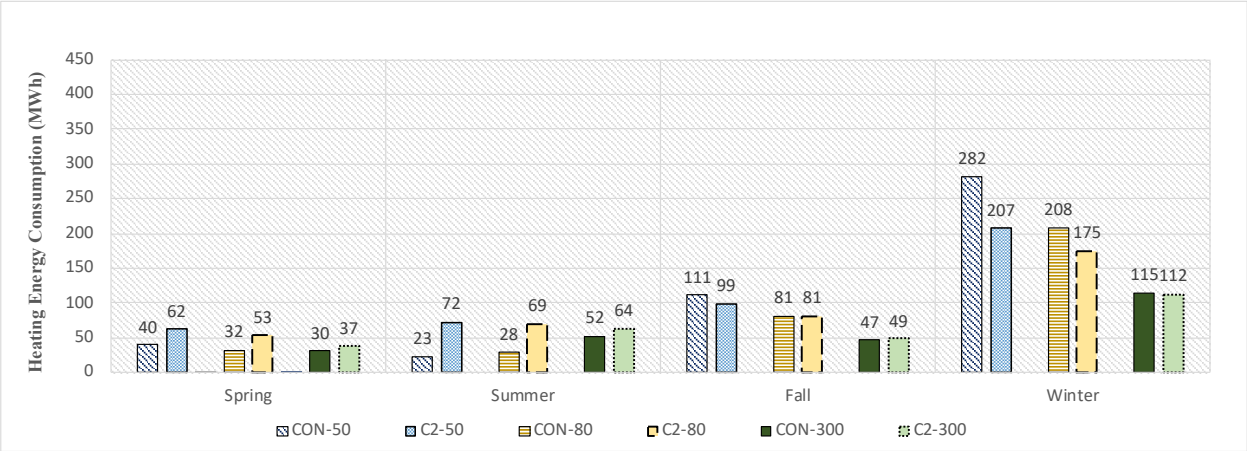

Figure B - 16: Seasonal heating loads for conventional roof and green roof with design of growing media of 200 mm and LAI of 2 for insulation thicknesses 50 mm, 120 mm and 300 mm – future climate (secondary school building).

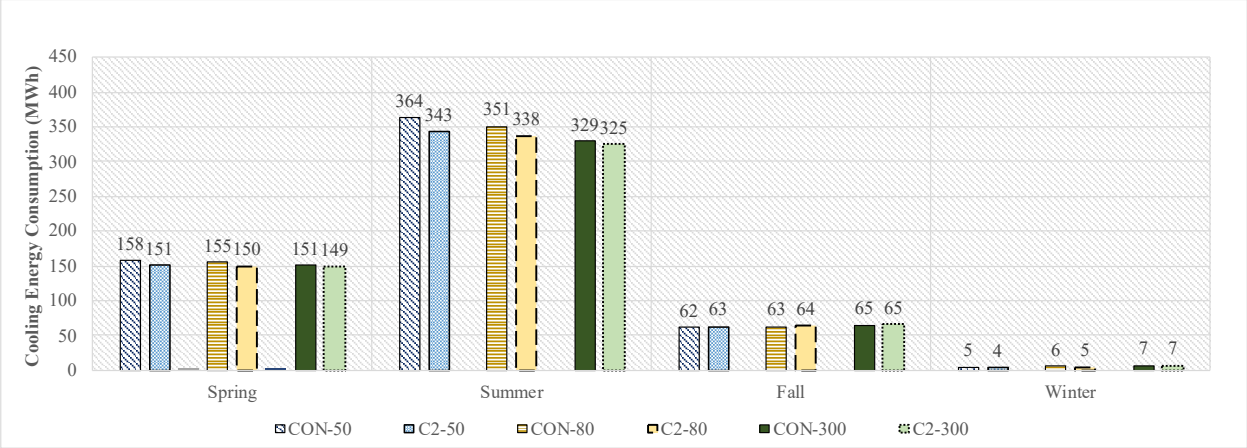

Figure B - 17: Seasonal cooling loads for conventional roof and green roof with design of growing media of 200 mm and LAI of 2 for insulation thicknesses 50 mm, 80 mm and 300 mm – future climate (secondary school building).

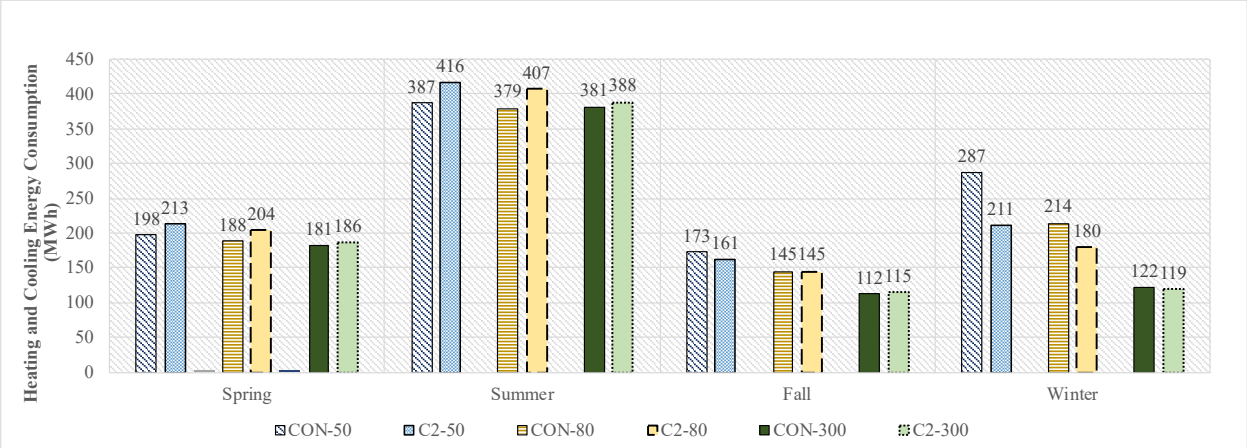

Figure B - 18: Seasonal total heating and cooling loads for conventional roof and green roof with design of growing media of 200 mm and LAI of 2 for insulation thicknesses 50 mm, 80 mm and 300 mm – future climate (secondary school building).

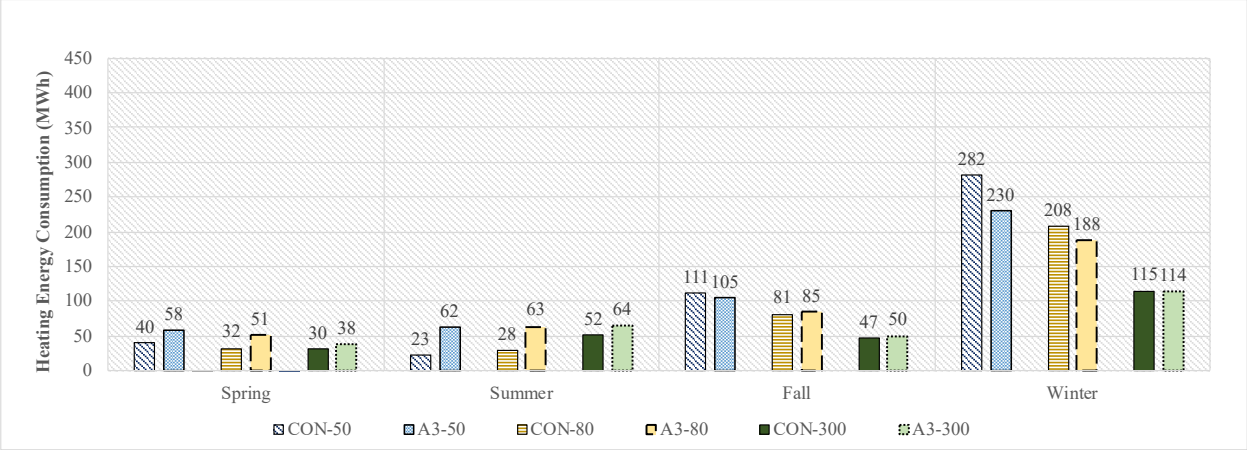

Figure B - 19: Seasonal heating loads for conventional roof and green roof with design of growing media of 100 mm and LAI of 3 for insulation thicknesses 50 mm, 80 mm and 300 mm – future climate (secondary school building).

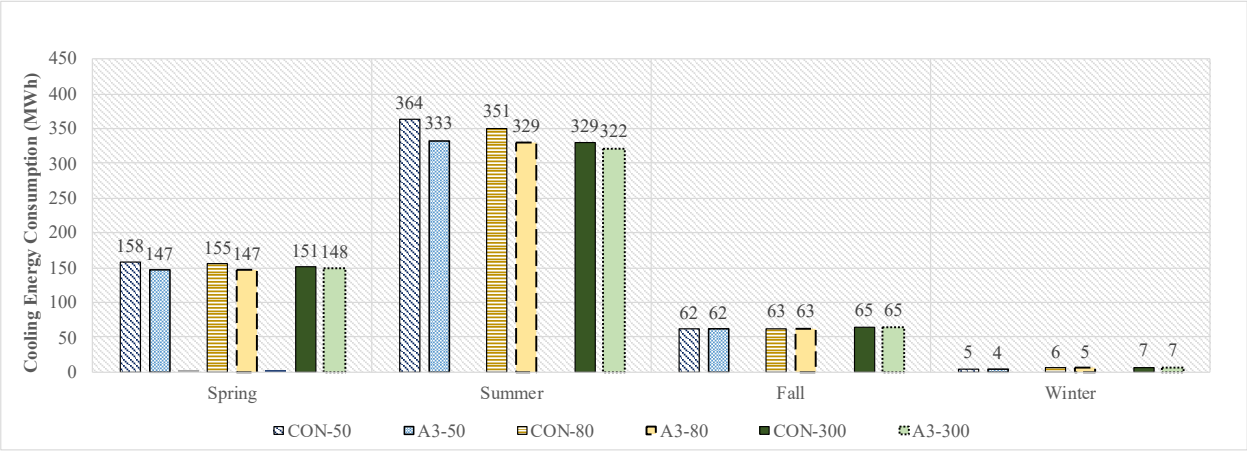

Figure B - 20: Seasonal cooling loads for conventional roof and green roof with design of growing media of 100 mm and LAI of 3 for insulation thicknesses 50 mm, 80 mm and 300 mm – future climate (secondary school building).

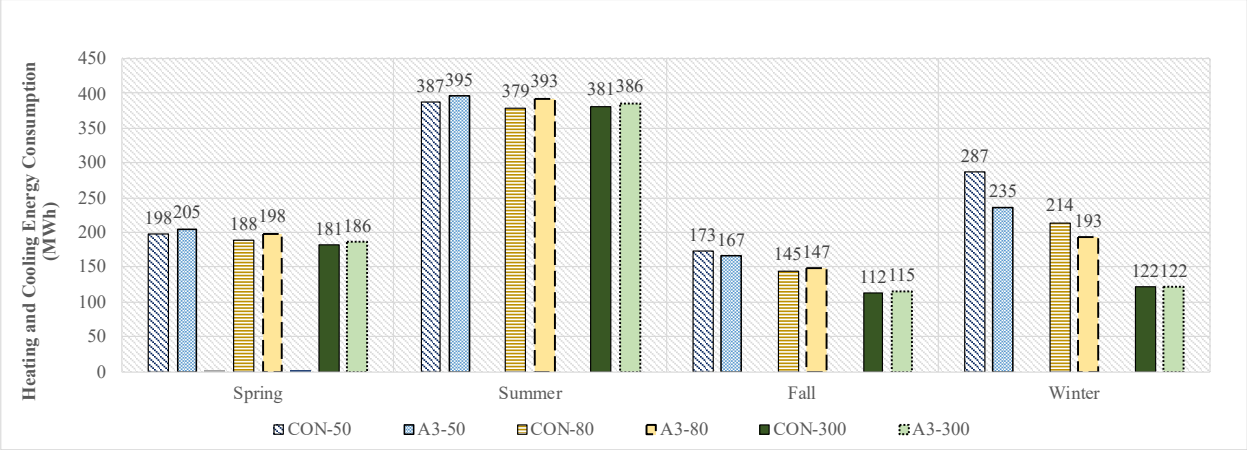

Figure B - 21: Seasonal total heating and cooling loads for conventional roof and green roof with design of growing media of 100 mm and LAI of 3 for insulation thicknesses 50 mm, 80 mm and 300 mm – future climate (secondary school building).

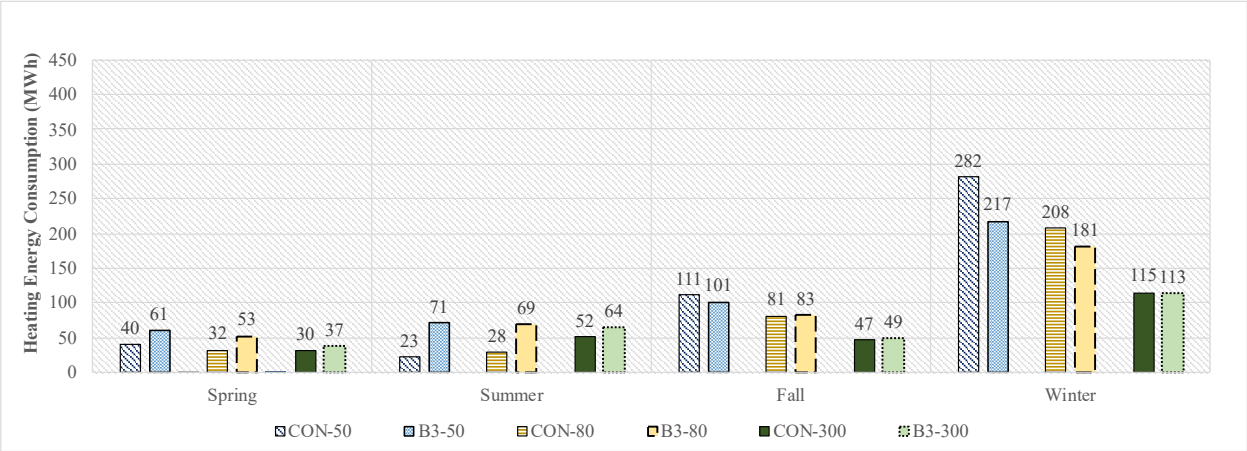

Figure B - 22: Seasonal heating loads for conventional roof and green roof with design of growing media of 150 mm and LAI of 3 for insulation thicknesses 50 mm, 80 mm and 300 mm – future climate (secondary school building).

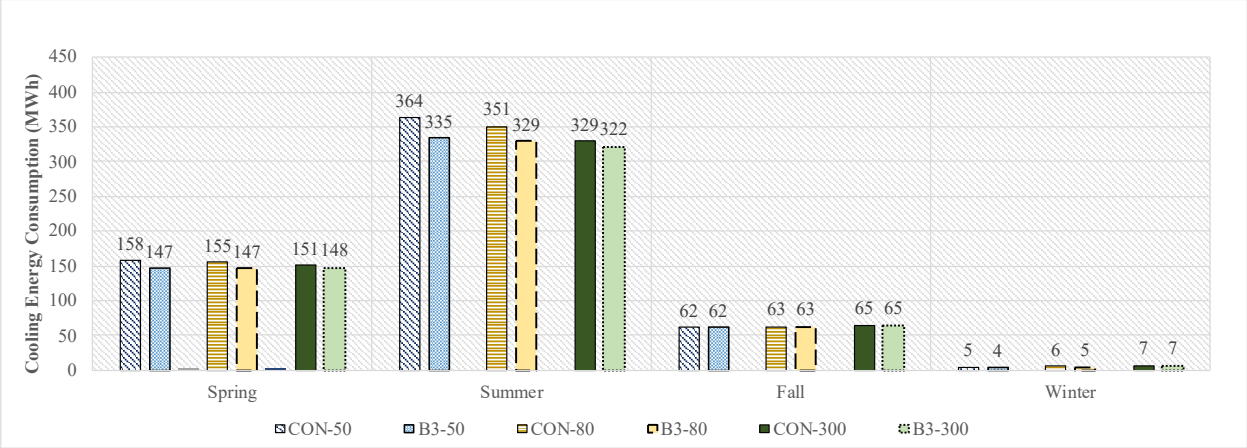

Figure B - 23: Seasonal cooling loads for conventional roof and green roof with design of growing media of 150 mm and LAI of 3 for insulation thicknesses 50 mm, 80 mm and 300 mm – future climate (secondary school building).

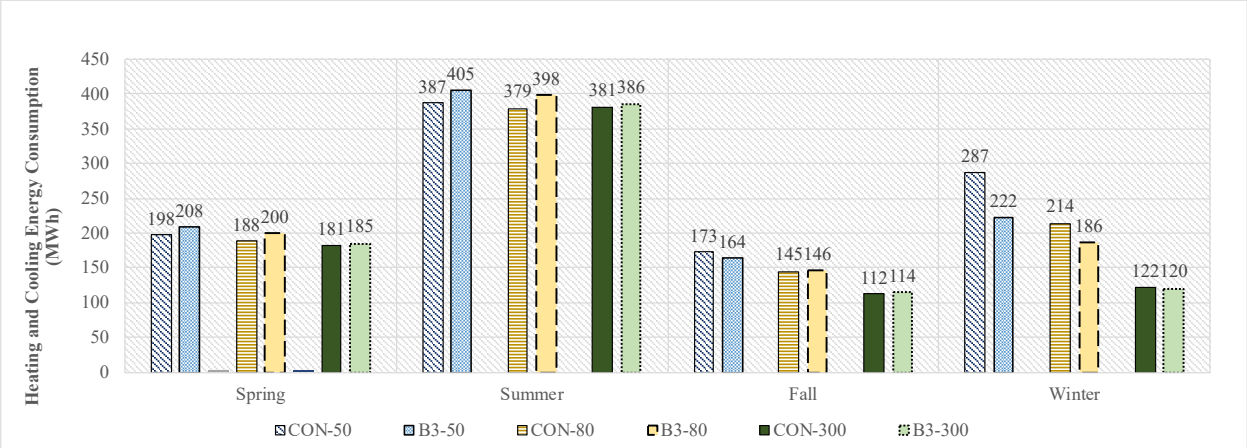

Figure B - 24: Seasonal total heating and cooling loads for conventional roof and green roof with design of growing media of 150 mm and LAI of 3 for insulation thicknesses 50 mm, 80 mm and 300 mm – future climate (secondary school building).

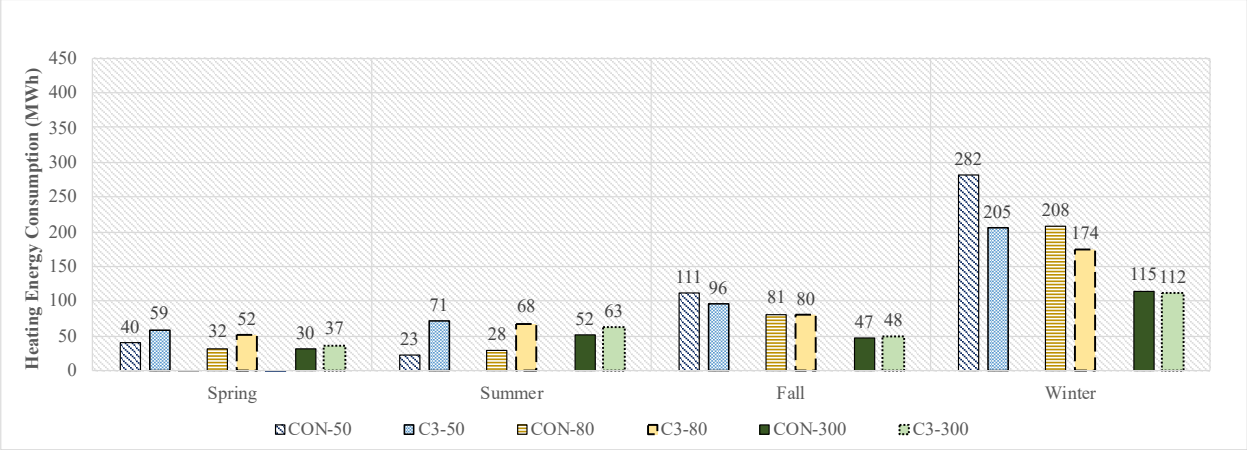

Figure B - 25: Seasonal heating loads for conventional roof and green roof with design of growing media of 200 mm and LAI of 3 for insulation thicknesses 50 mm, 80 mm and 300 mm – future climate (secondary school building).

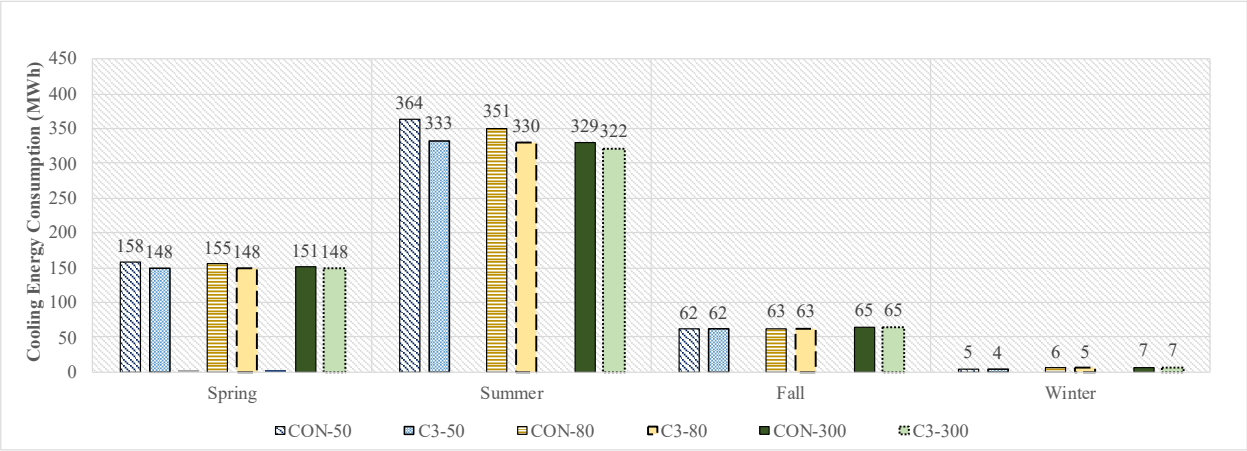

Figure B - 26: Seasonal cooling loads for conventional roof and green roof with design of growing media of 200 mm and LAI of 3 for insulation thicknesses 50 mm, 80 mm and 300 mm – future climate (secondary school building).

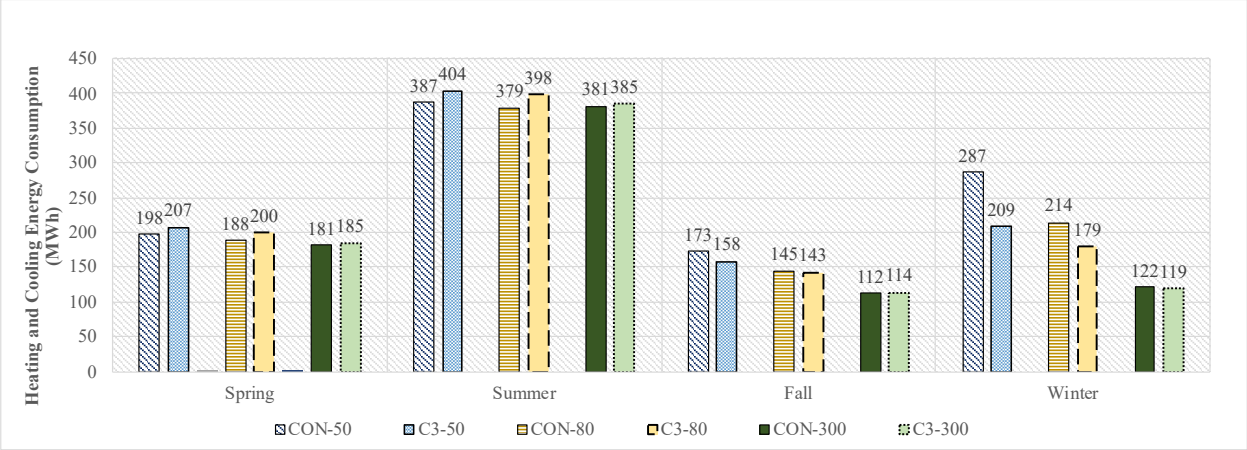

Figure B - 27: Seasonal total heating and cooling loads for conventional roof and green roof with design of growing media of 200 mm and LAI of 3 for insulation thicknesses 50 mm, 80 mm and 300 mm – future climate (secondary school building).

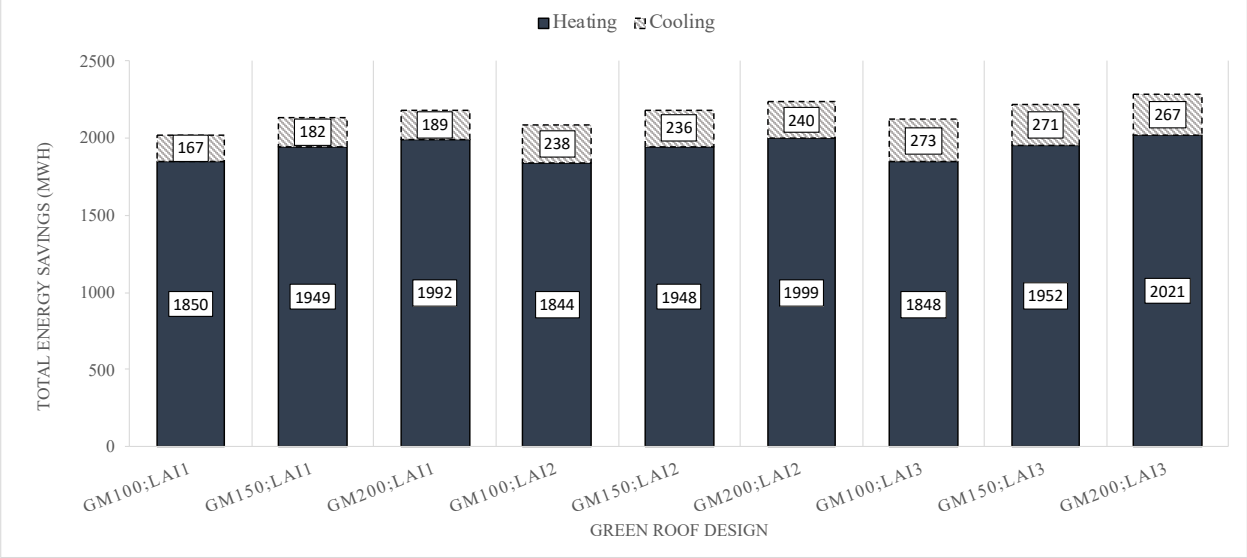

Figure B - 28: Total heating and cooling energy savings (MWh) of green roof compared to conventional roof for all growing media (GM) depths and LAIs; without insulation layer – future climate (secondary school building).

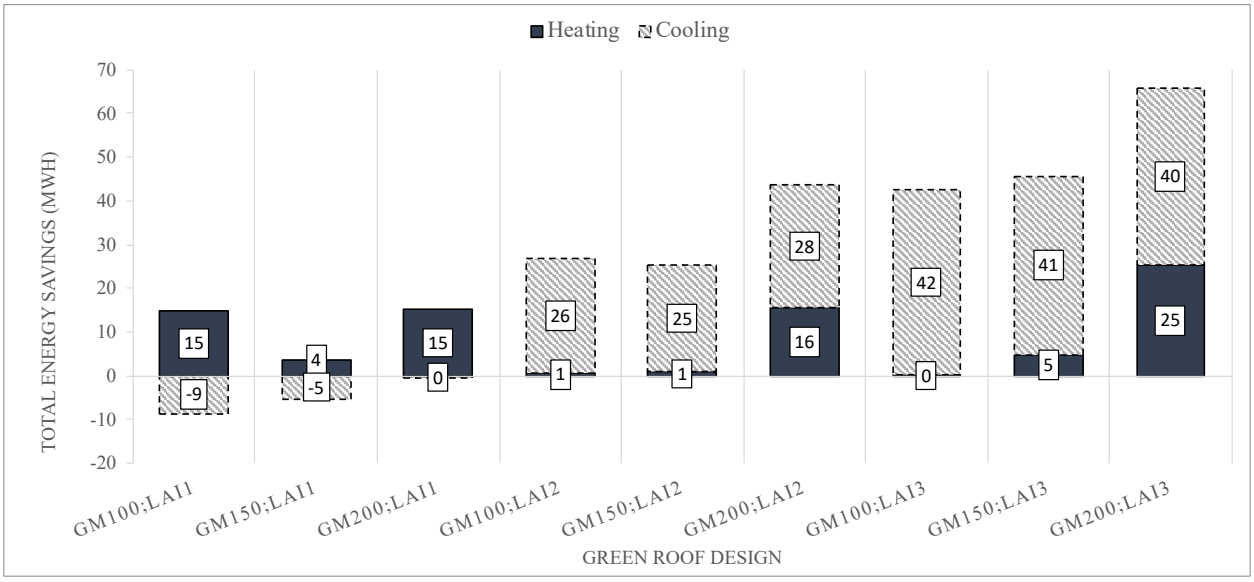

Figure B - 29: Total heating and cooling energy savings (MWh) of green roof compared to conventional roof for all growing media (GM) depths and LAIs; with 50 mm insulation layer – future climate (secondary school building).

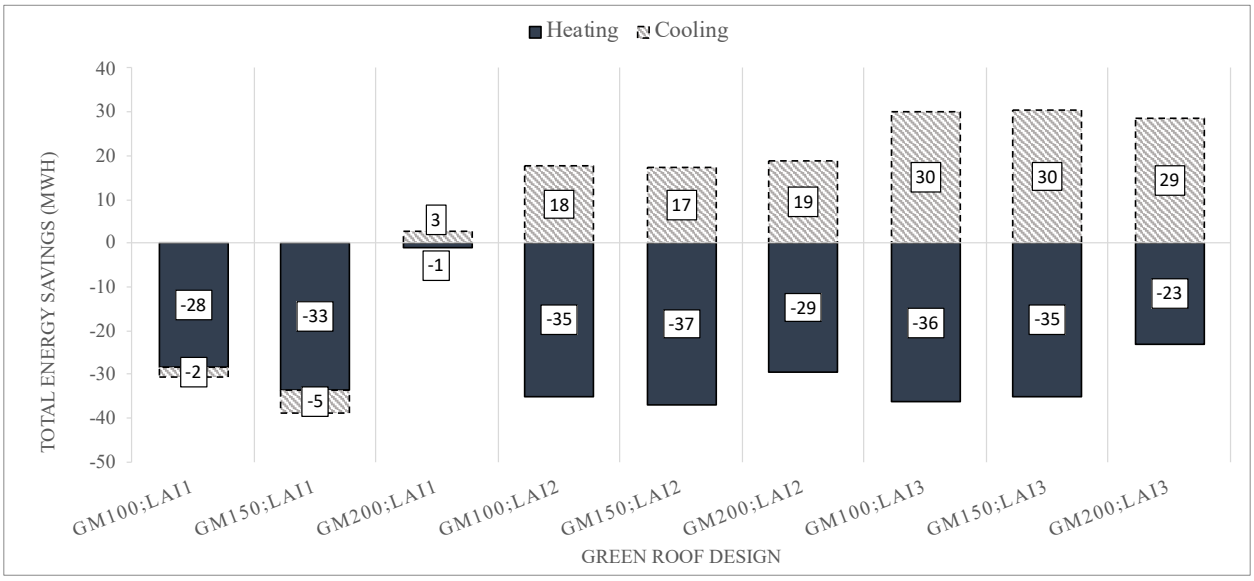

Figure B - 30: Total heating and cooling energy savings (MWh) of green roof compared to conventional roof for all growing media (GM) depths and LAIs; with 80 mm insulation layer – future climate (secondary school building).

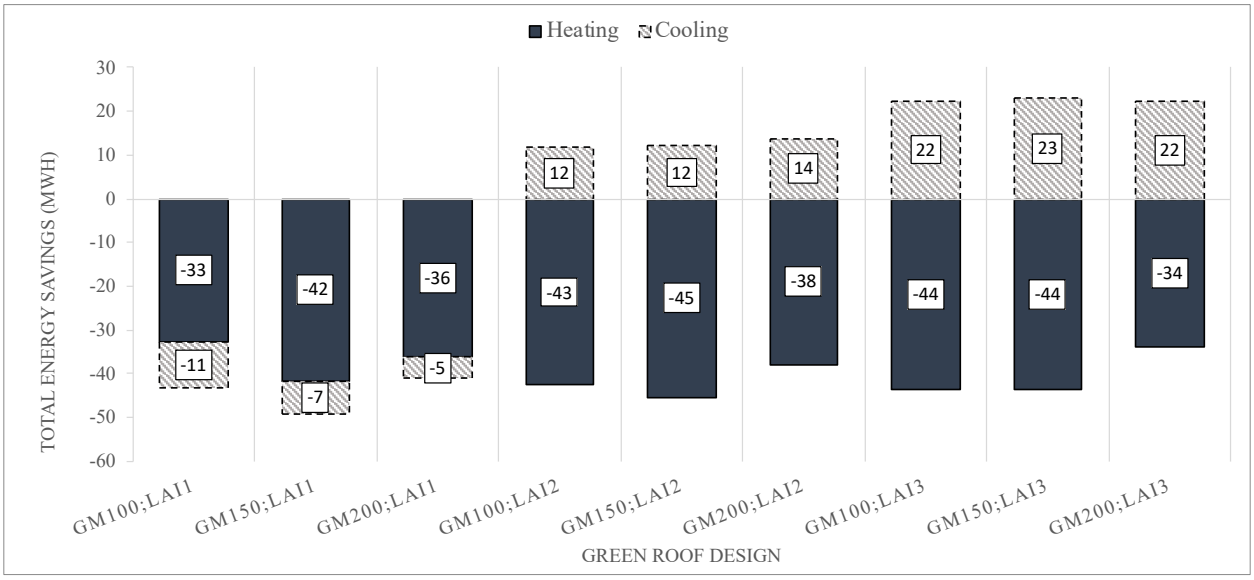

Figure B - 31: Total heating and cooling energy savings (MWh) of green roof compared to conventional roof for all growing media (GM) depths and LAIs; with 100 mm insulation layer – future climate (secondary school building).

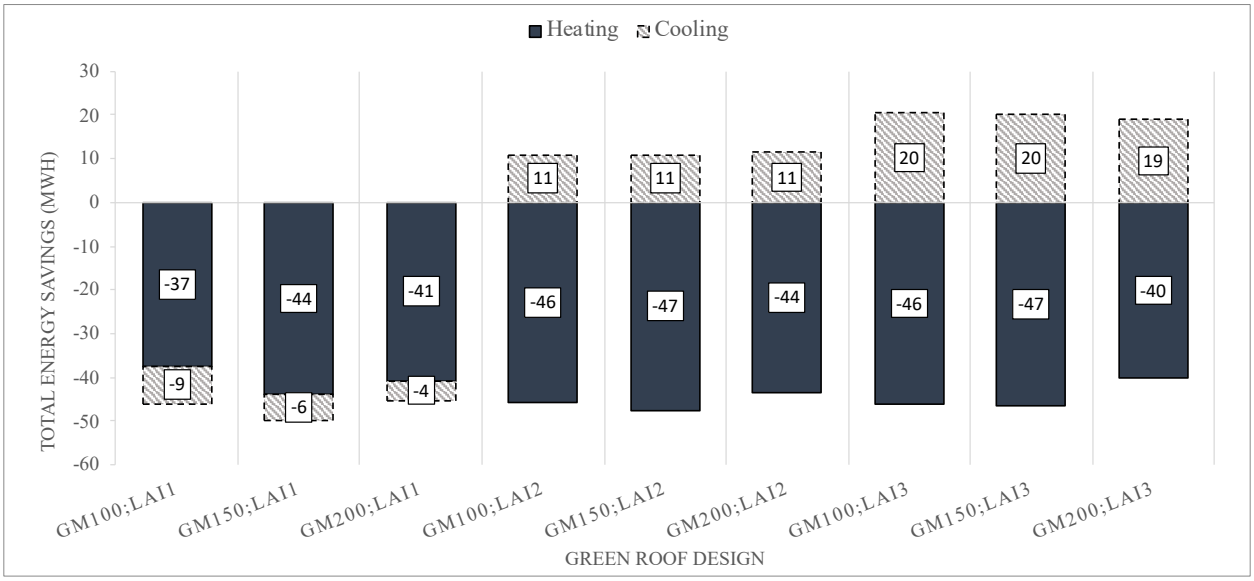

Figure B - 32: Total heating and cooling energy savings (MWh) of green roof compared to conventional roof for all growing media (GM) depths and LAIs; with 120 mm insulation layer – future climate (secondary school building).

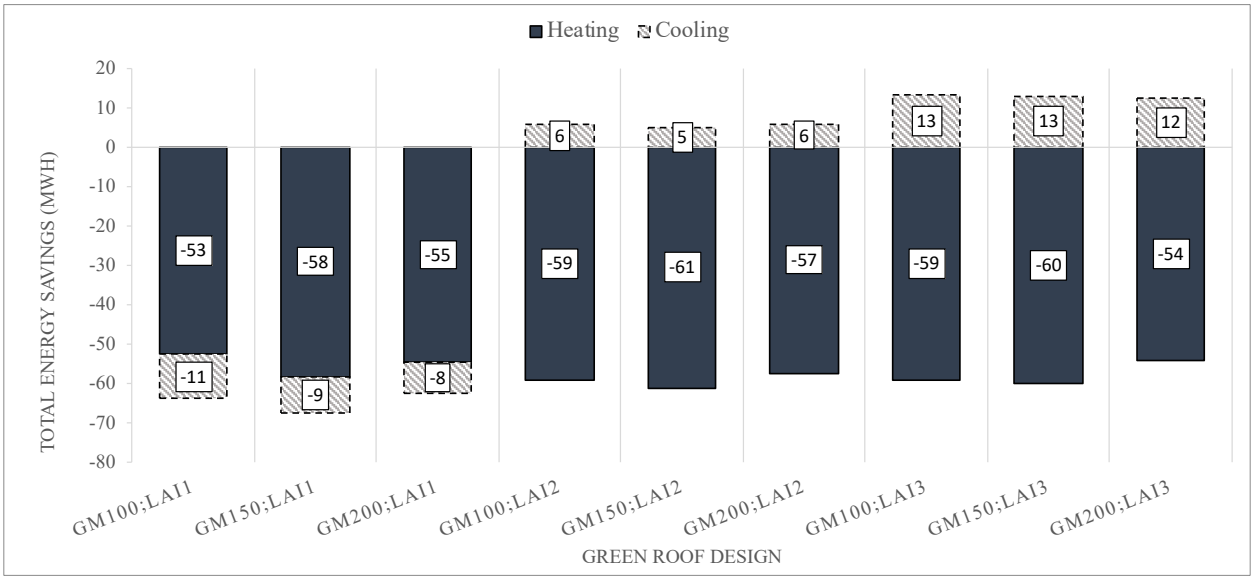

Figure B - 33: Total heating and cooling energy savings (MWh) of green roof compared to conventional roof for all growing media (GM) depths and LAIs; with 150 mm insulation layer – future climate (secondary school building).

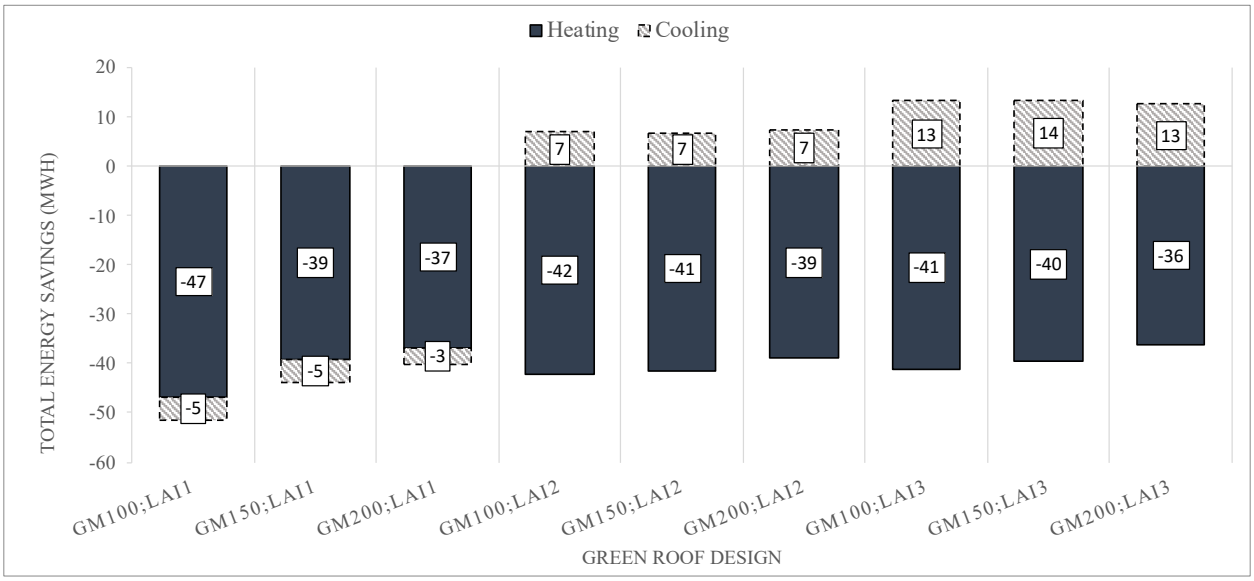

Figure B - 34: Total heating and cooling energy savings (MWh) of green roof compared to conventional roof for all growing media (GM) depths and LAIs; with 200 mm insulation layer – future climate (secondary school building).

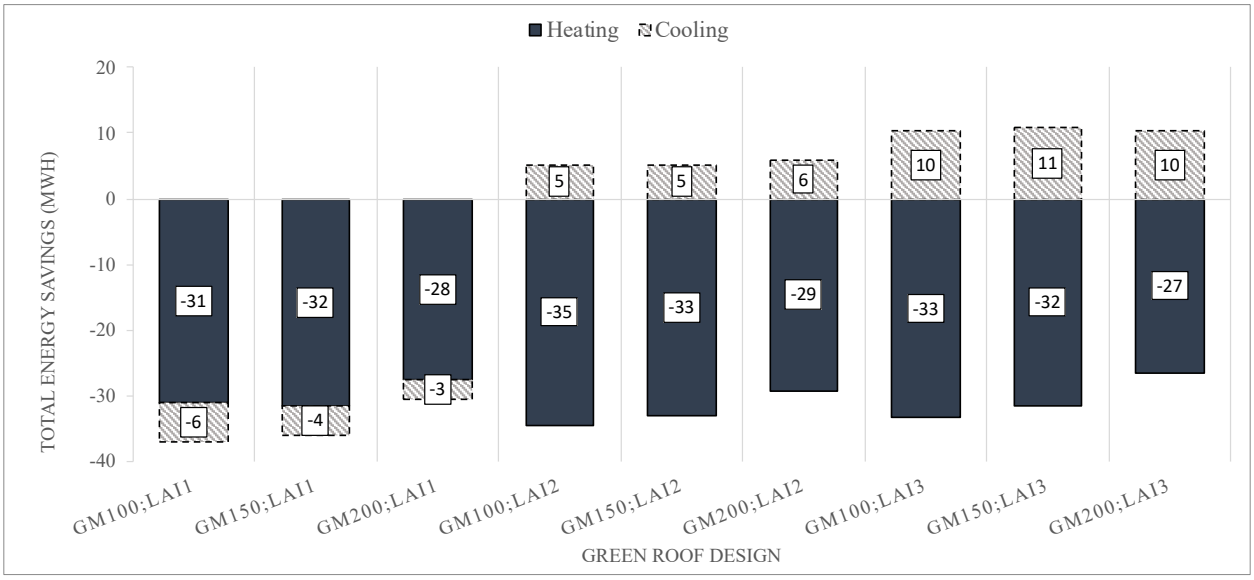

Figure B - 35: Total heating and cooling energy savings (MWh) of green roof compared to conventional roof for all growing media (GM) depths and LAIs; with 250 mm insulation layer – future climate (secondary school building).

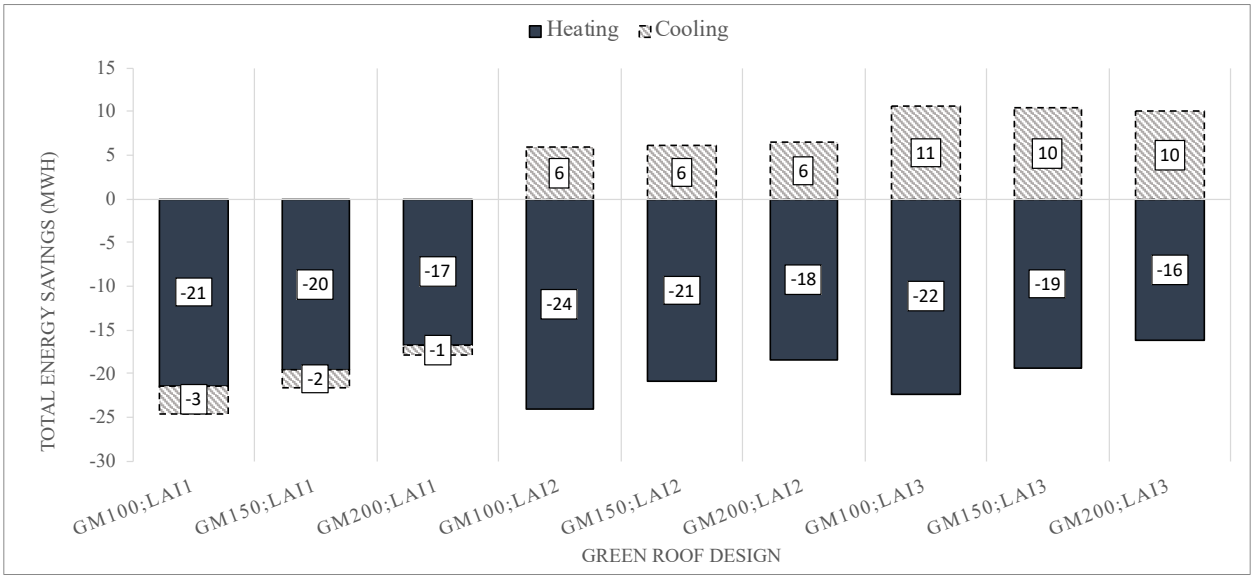

Figure B - 36: Total heating and cooling energy savings (MWh) of green roof compared to conventional roof for all growing media (GM) depths and LAIs; with 300 mm insulation layer – future climate (secondary school building).

Appendix C: Annual Energy Consumption and Savings for Cooling/Heating Loads – Current Climate Condition Office

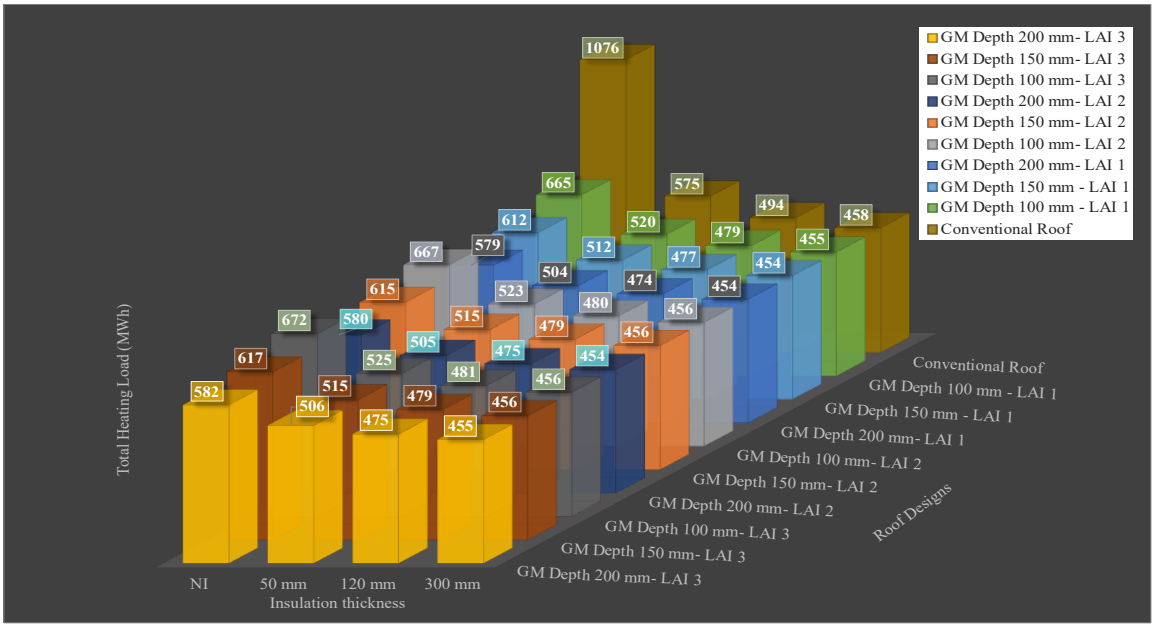

Figure C - 1: Total heating loads for all roof designs; all insulation thickness; LAIs; and growing media depths under current climate – Office building.

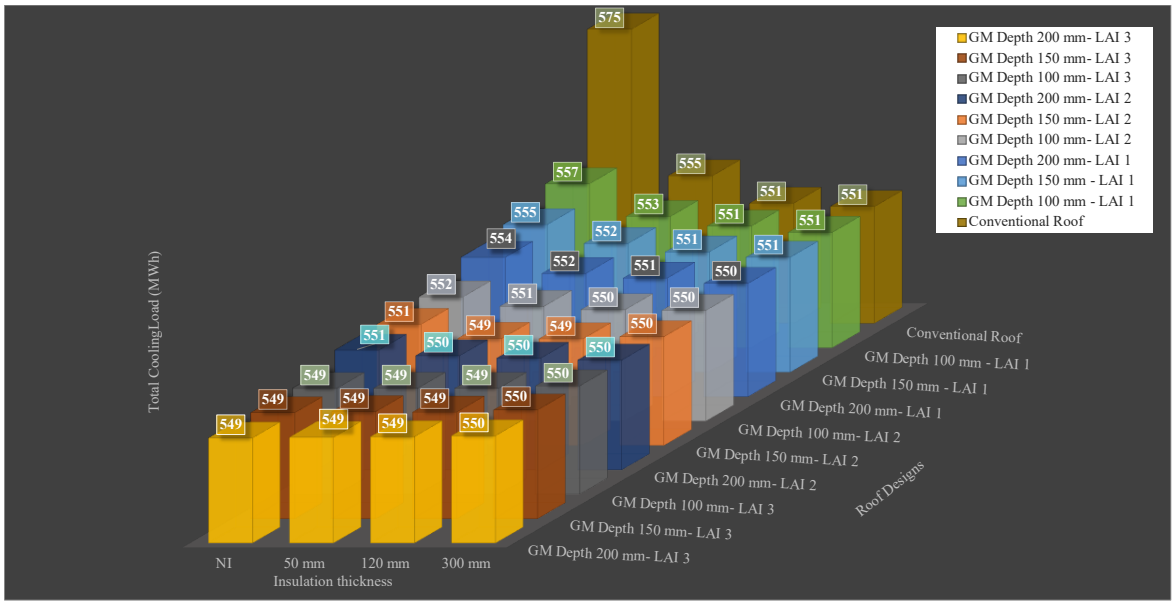

Figure C - 2: Total cooling loads for all roof designs; all insulation thickness; LAIs; and growing media depths under current climate – Office building.

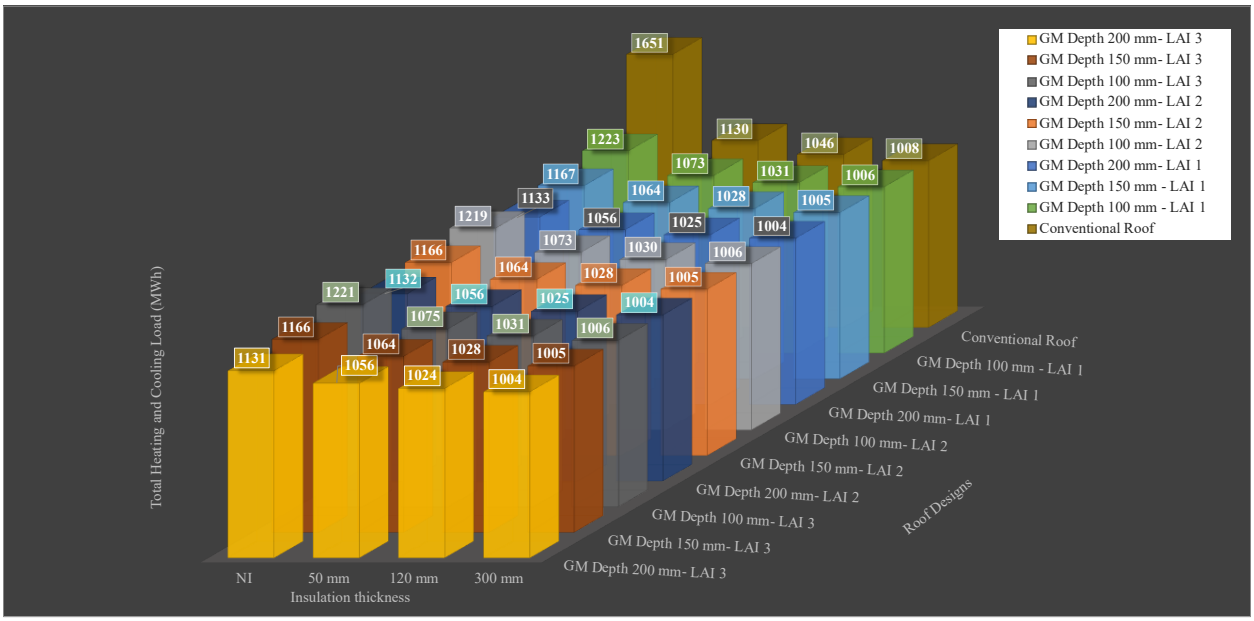

Figure C - 3: Total heating and cooling loads for all roof designs; all insulation thickness; LAIs; and growing media depths under current climate – Office building.

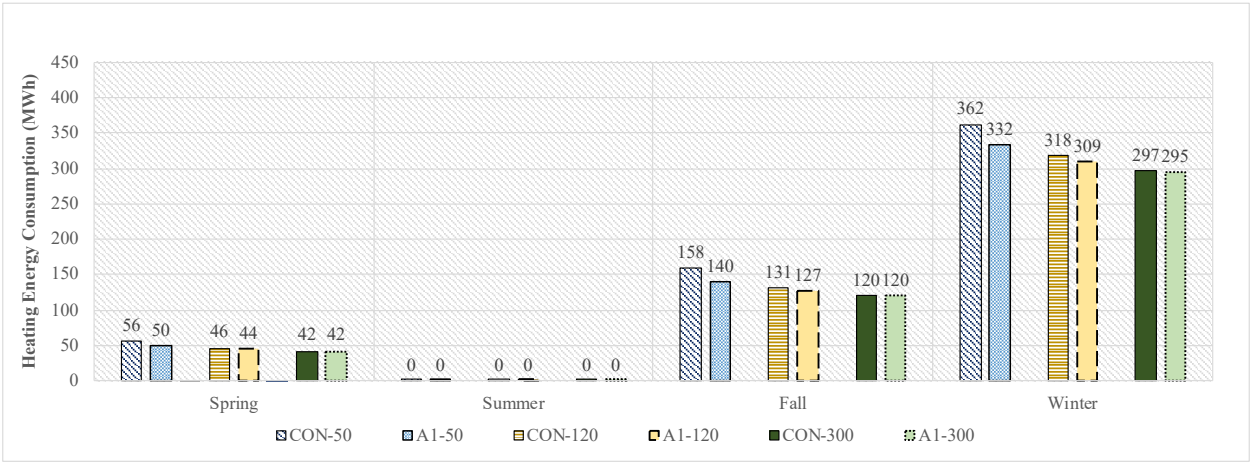

Figure C - 4: Seasonal heating loads for conventional roof and green roof with design of growing media of 100 mm and LAI of 1 for insulation thicknesses 50 mm, 120 mm and 300 mm – current climate (office building).

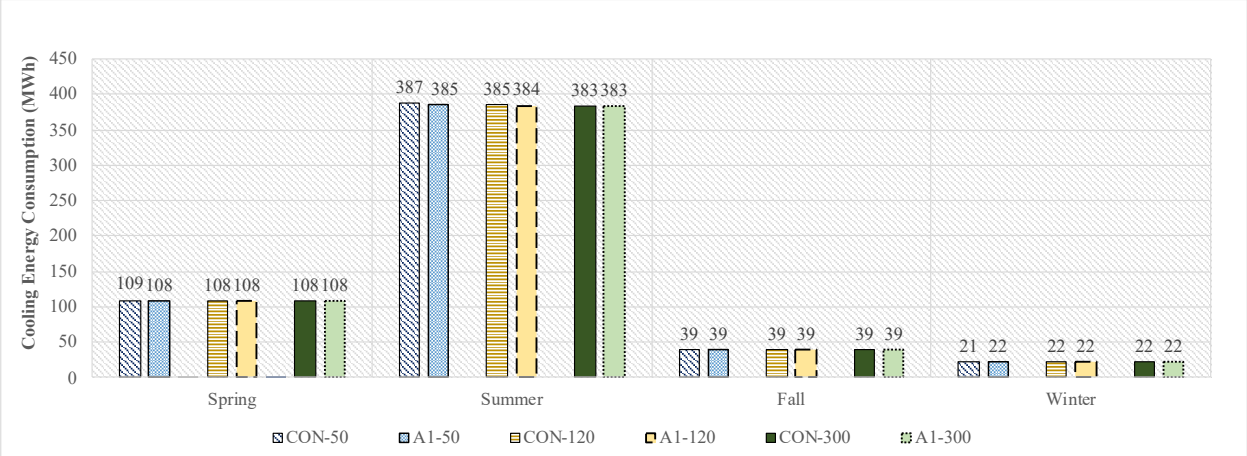

Figure C - 5: Seasonal cooling loads for conventional roof and green roof with design of growing media of 100 mm and LAI of 1 for insulation thicknesses 50 mm, 120 mm and 300 mm – current climate (office building).

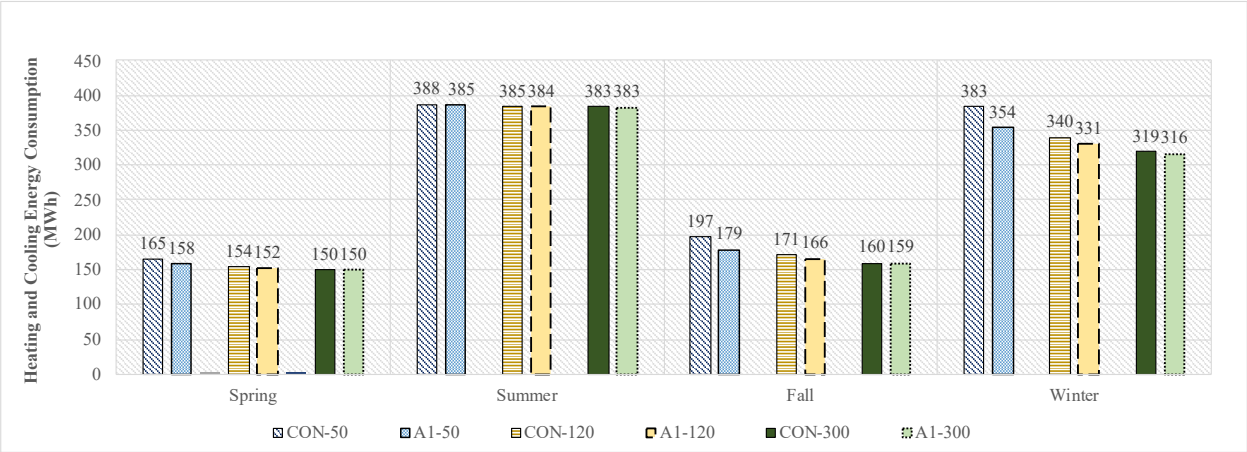

Figure C - 6: Seasonal total heating and cooling loads for conventional roof and green roof with design of growing media of 100 mm and LAI of 1 for insulation thicknesses 50 mm, 120 mm and 300 mm – current climate (office building).

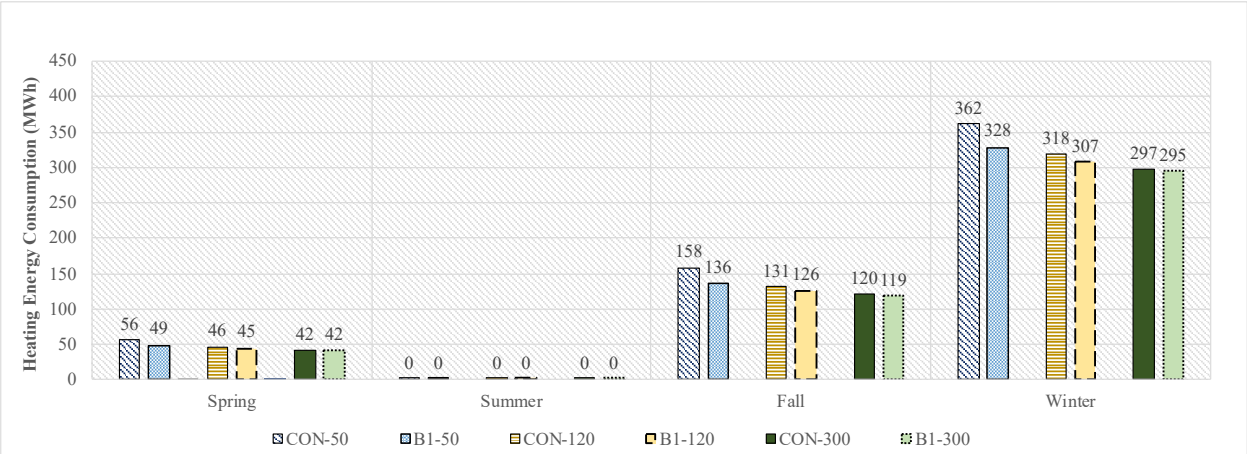

Figure C - 7: Seasonal heating loads for conventional roof and green roof with design of growing media of 150 mm and LAI of 1 for insulation thicknesses 50 mm, 120 mm and 300 mm – current climate (office building).

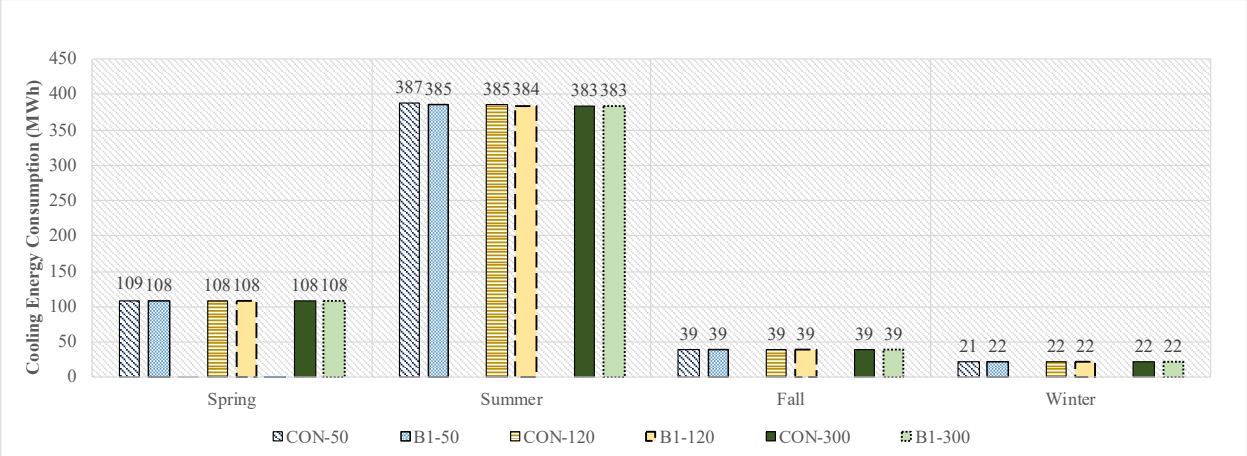

Figure C - 8: Seasonal cooling loads for conventional roof and green roof with design of growing media of 150 mm and LAI of 1 for insulation thicknesses 50 mm, 120 mm and 300 mm – current climate (office building).

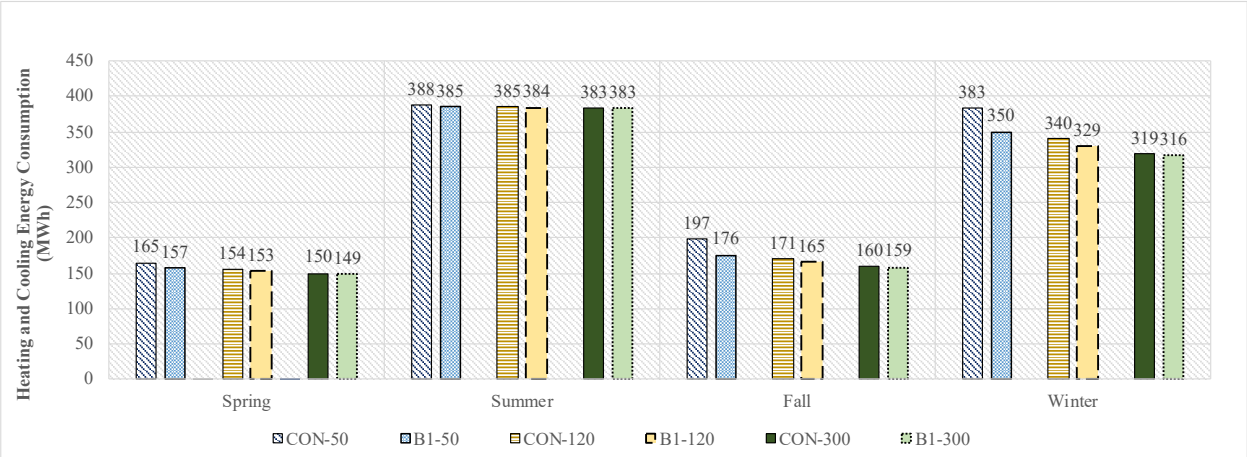

Figure C - 9: Seasonal total heating and cooling loads for conventional roof and green roof with design of growing media of 150 mm and LAI of 1 for insulation thicknesses 50 mm, 120 mm and 300 mm – current climate (office building).

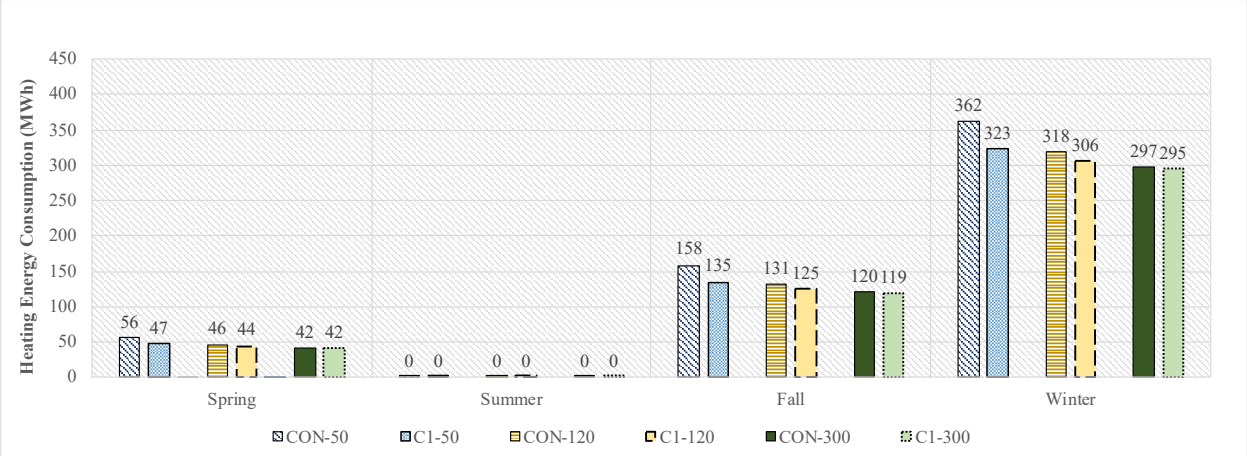

Figure C - 10: Seasonal heating loads for conventional roof and green roof with design of growing media of 200 mm and LAI of 1 for insulation thicknesses 50 mm, 120 mm and 300 mm – current climate (office building).

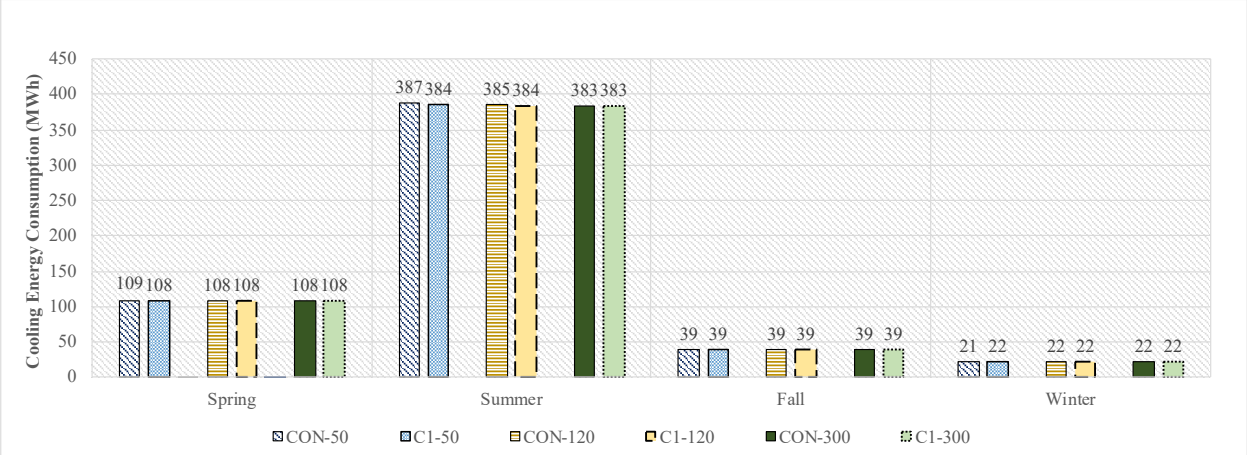

Figure C - 11: Seasonal cooling loads for conventional roof and green roof with design of growing media of 200 mm and LAI of 1 for insulation thicknesses 50 mm, 120 mm and 300 mm – current climate (office building).

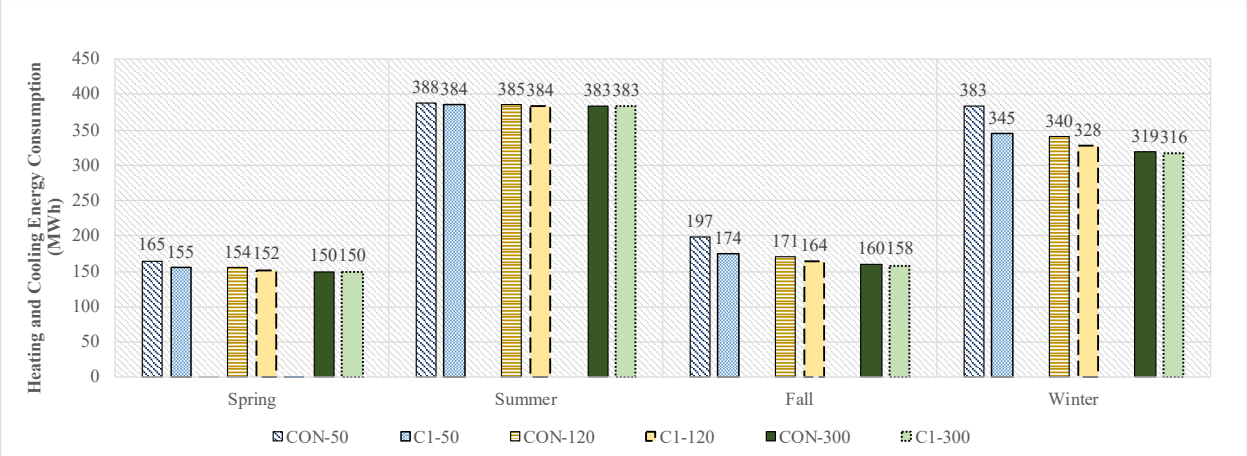

Figure C - 12: Seasonal total heating and cooling loads for conventional roof and green roof with design of growing media of 200 mm and LAI of 1 for insulation thicknesses 50 mm, 120 mm and 300 mm – current climate (office building).

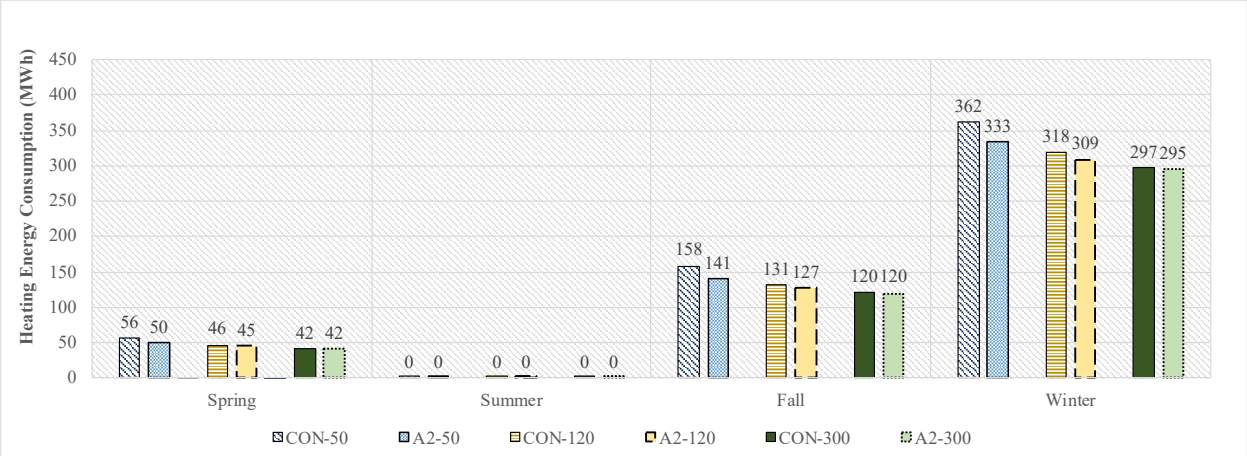

Figure C - 13: Seasonal heating loads for conventional roof and green roof with design of growing media of 100 mm and LAI of 2 for insulation thicknesses 50 mm, 120 mm and 300 mm – current climate (office building).

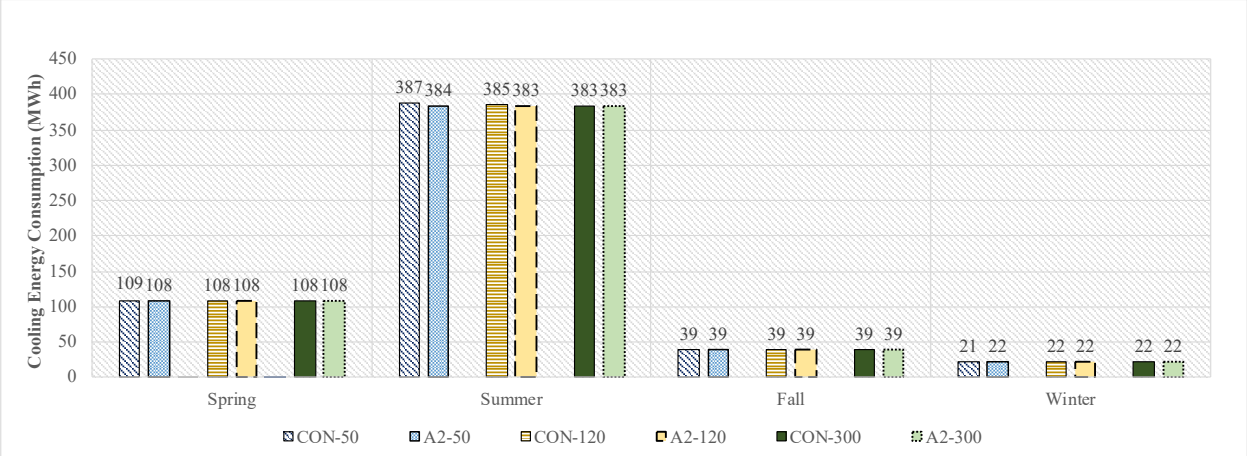

Figure C - 14: Seasonal cooling loads for conventional roof and green roof with design of growing media of 100 mm and LAI of 2 for insulation thicknesses 50 mm, 120 mm and 300 mm – current climate (office building).

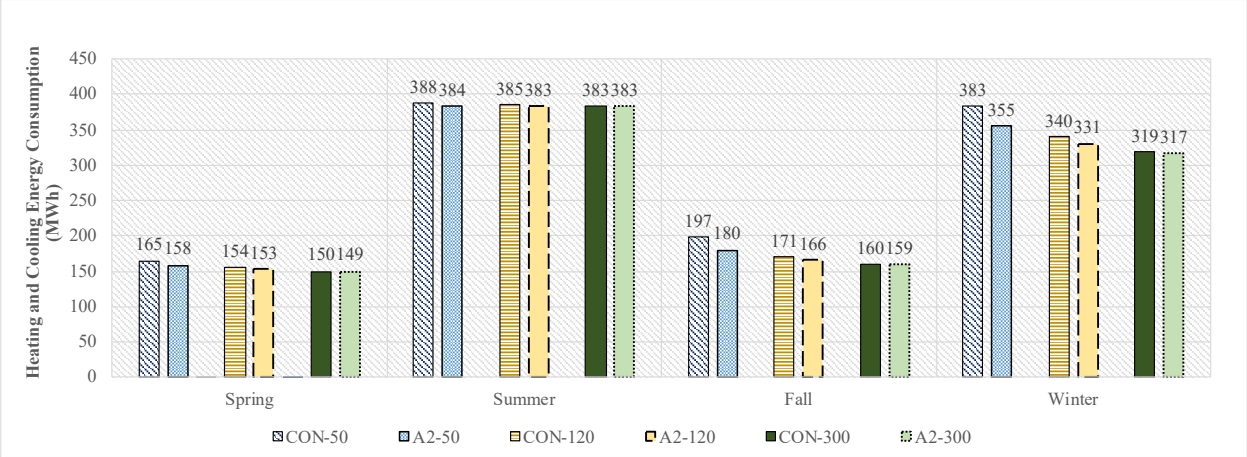

Figure C - 15: Seasonal total heating and cooling loads for conventional roof and green roof with design of growing media of 100 mm and LAI of 2 for insulation thicknesses 50 mm, 120 mm and 300 mm – current climate (office building).

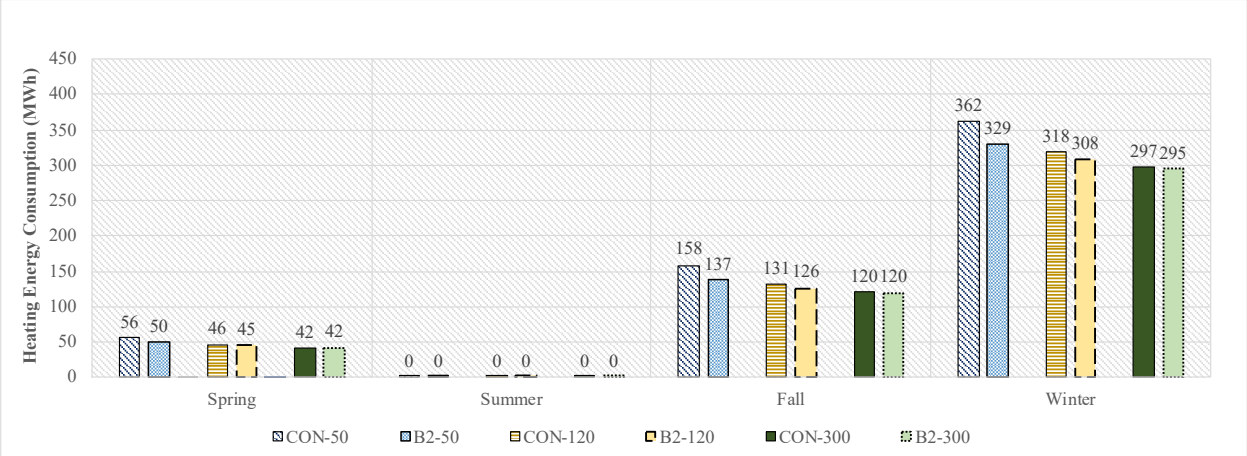

Figure C - 16: Seasonal heating loads for conventional roof and green roof with design of growing media of 150 mm and LAI of 2 for insulation thicknesses 50 mm, 120 mm and 300 mm – current climate (office building).

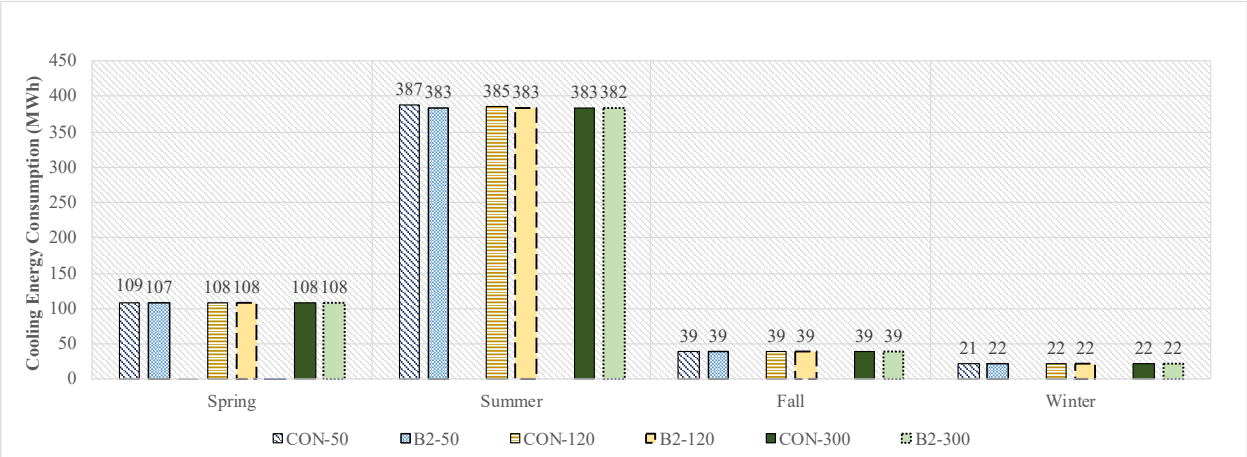

Figure C - 17: Seasonal cooling loads for conventional roof and green roof with design of growing media of 150 mm and LAI of 2 for insulation thicknesses 50 mm, 120 mm and 300 mm – current climate (office building).

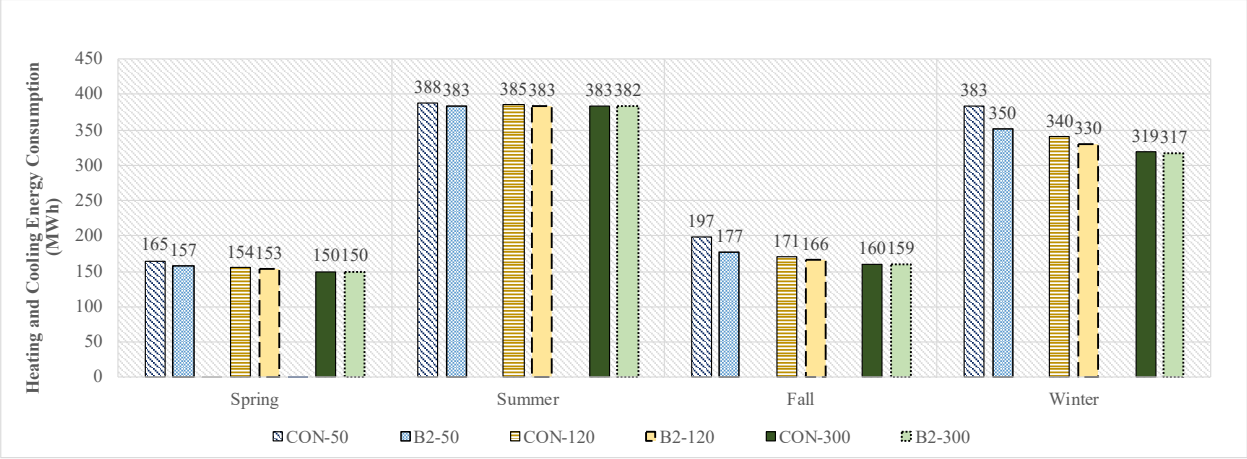

Figure C - 18: Seasonal total heating and cooling loads for conventional roof and green roof with design of growing media of 150 mm and LAI of 2 for insulation thicknesses 50 mm, 120 mm and 300 mm – current climate (office building).

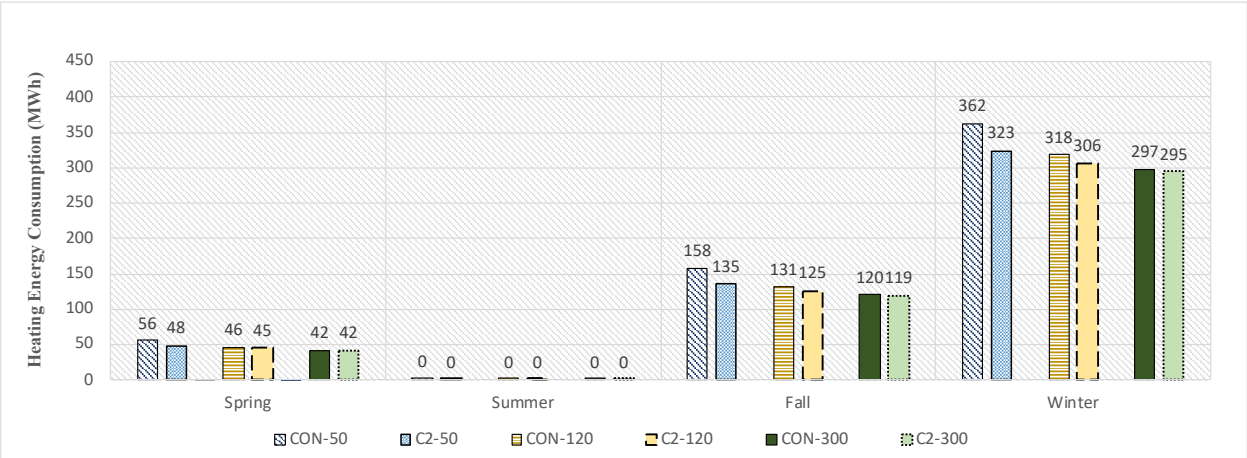

Figure C - 19: Seasonal heating loads for conventional roof and green roof with design of growing media of 200 mm and LAI of 2 for insulation thicknesses 50 mm, 120 mm and 300 mm – current climate (office building).

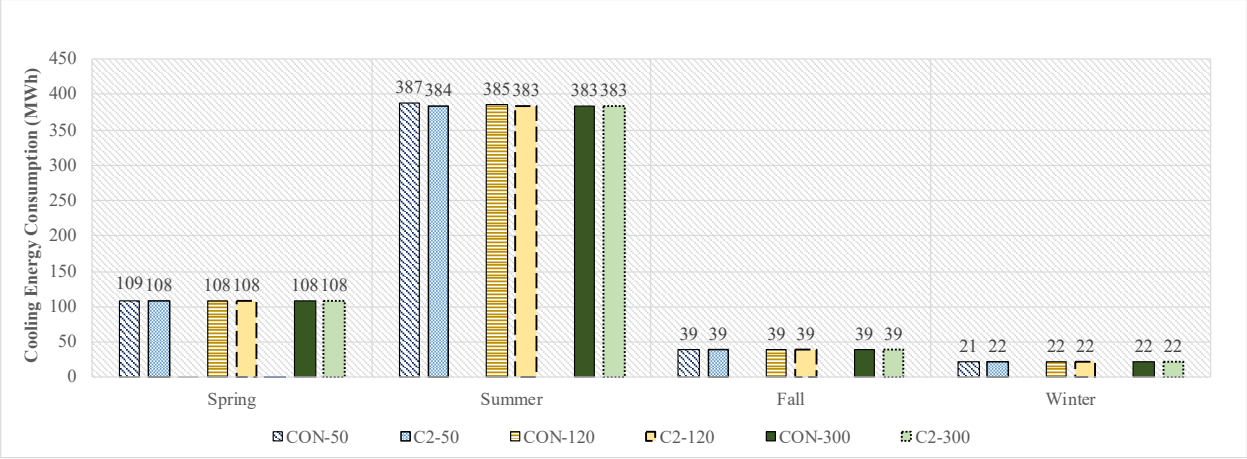

Figure C - 20: Seasonal cooling loads for conventional roof and green roof with design of growing media of 200 mm and LAI of 2 for insulation thicknesses 50 mm, 120 mm and 300 mm – current climate (office building).

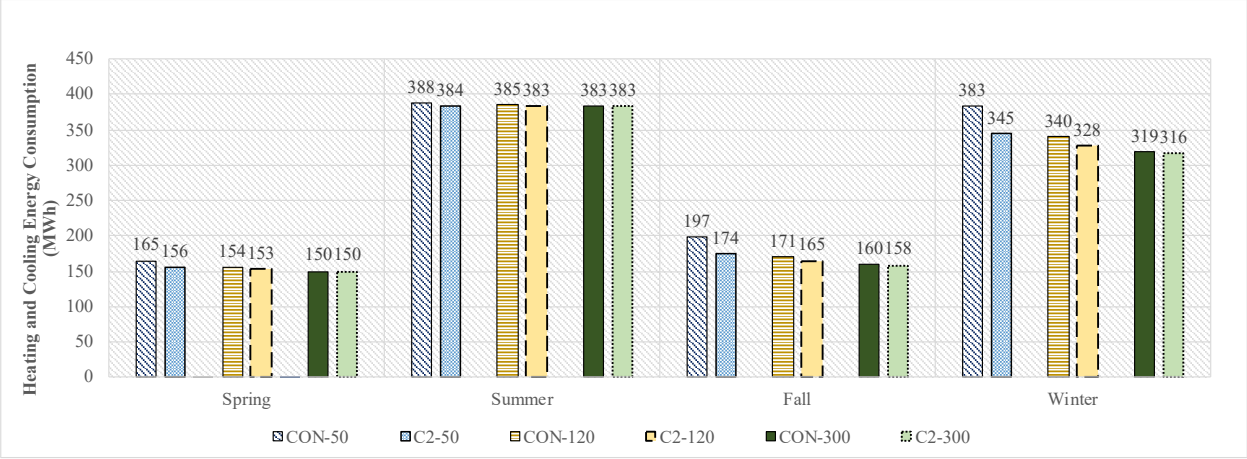

Figure C - 21: Seasonal total heating and cooling loads for conventional roof and green roof with design of growing media of 200 mm and LAI of 2 for insulation thicknesses 50 mm, 120 mm and 300 mm – current climate (office building).

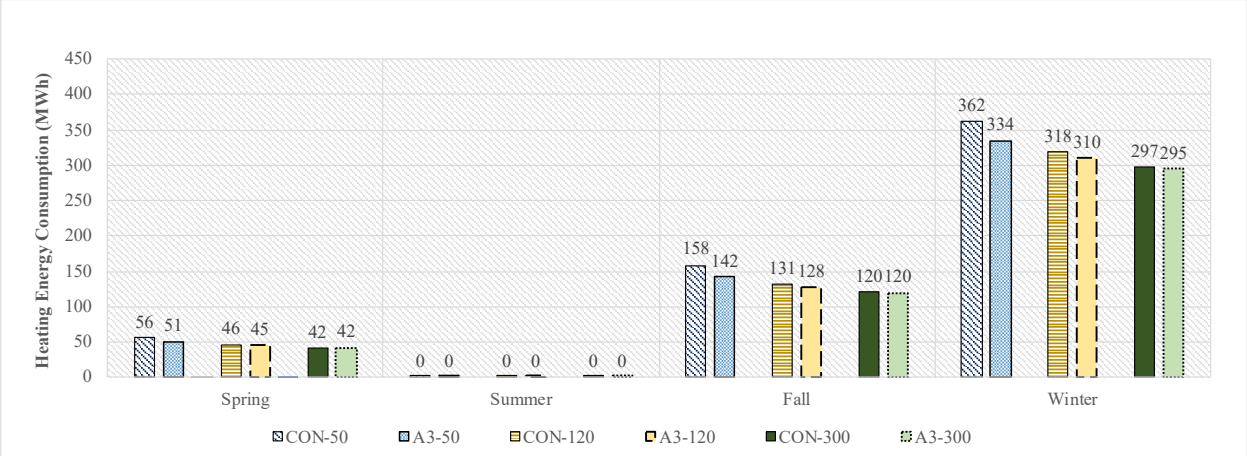

Figure C - 22: Seasonal heating loads for conventional roof and green roof with design of growing media of 100 mm and LAI of 3 for insulation thicknesses 50 mm, 120 mm and 300 mm – current climate (office building).

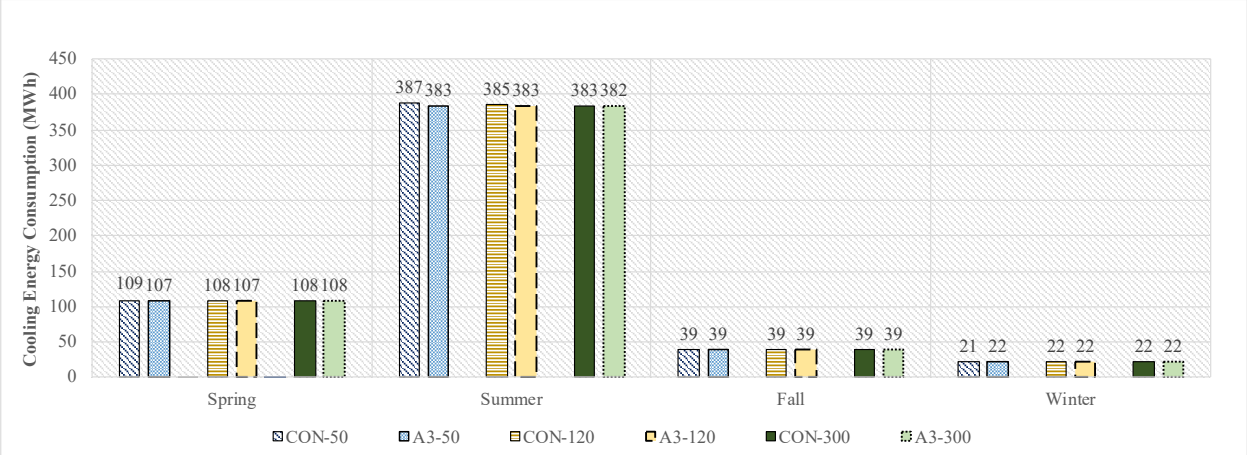

Figure C - 23: Seasonal cooling loads for conventional roof and green roof with design of growing media of 100 mm and LAI of 3 for insulation thicknesses 50 mm, 120 mm and 300 mm – current climate (office building).

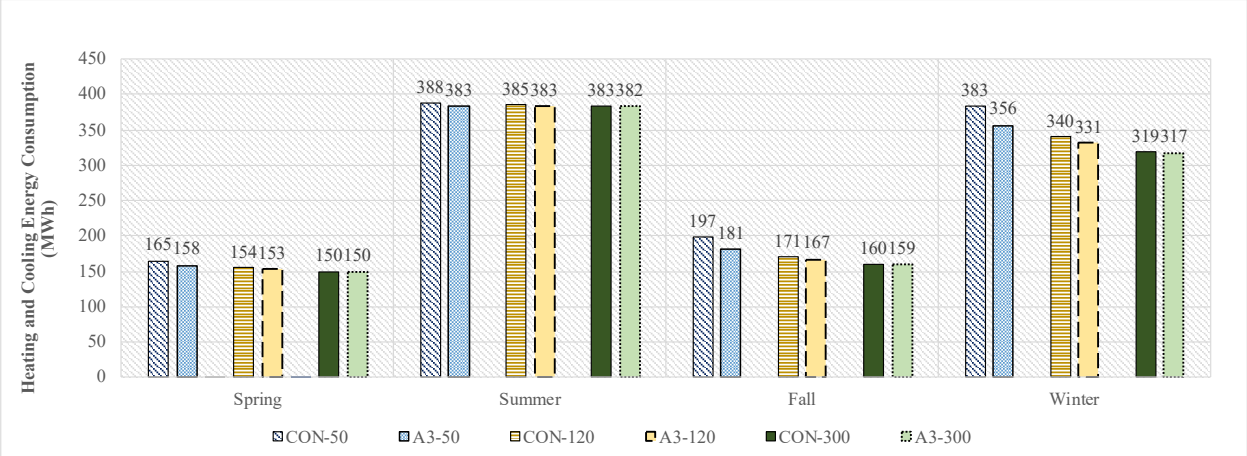

Figure C - 24: Seasonal total heating and cooling loads for conventional roof and green roof with design of growing media of 100 mm and LAI of 3 for insulation thicknesses 50 mm, 120 mm and 300 mm – current climate (office building).

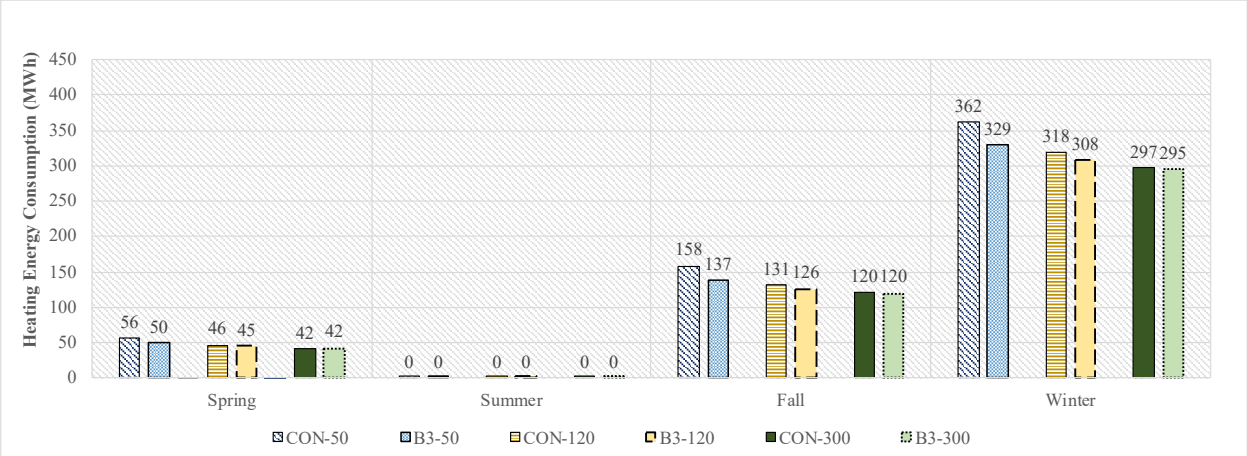

Figure C - 25: Seasonal heating loads for conventional roof and green roof with design of growing media of 150 mm and LAI of 3 for insulation thicknesses 50 mm, 120 mm and 300 mm – current climate (office building).

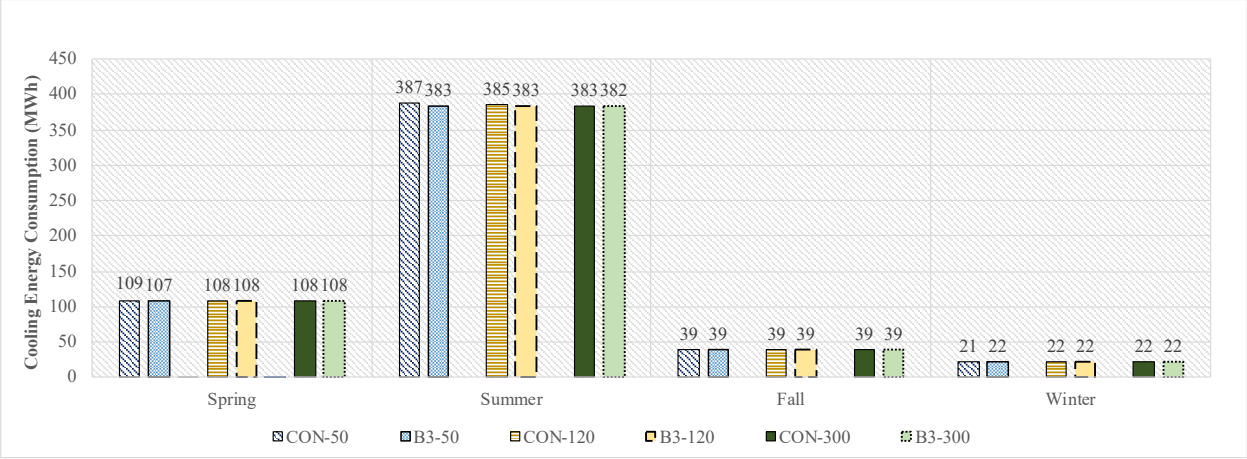

Figure C - 26: Seasonal cooling loads for conventional roof and green roof with design of growing media of 150 mm and LAI of 3 for insulation thicknesses 50 mm, 120 mm and 300 mm – current climate (office building).

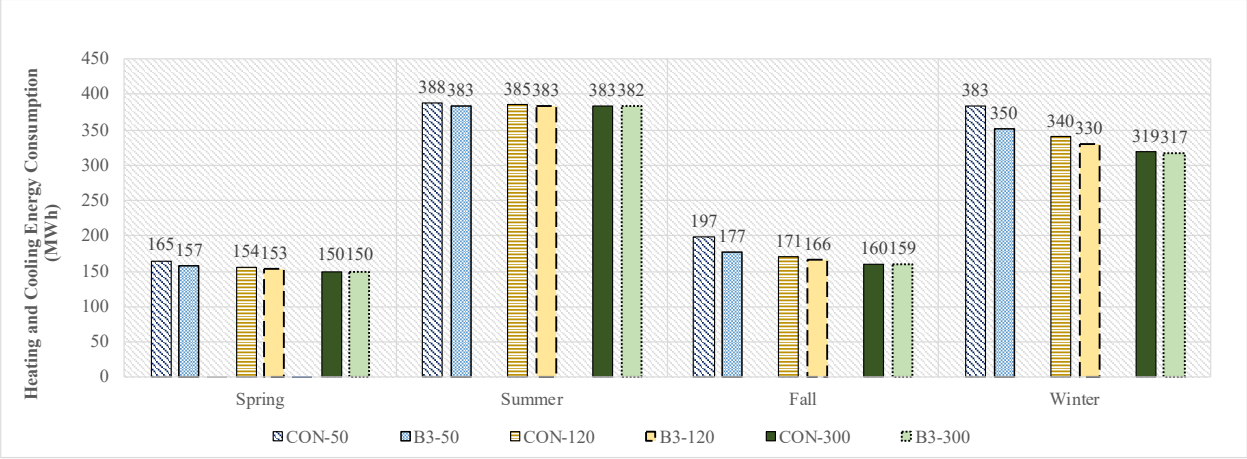

Figure C - 27: Seasonal total heating and cooling loads for conventional roof and green roof with design of growing media of 150 mm and LAI of 3 for insulation thicknesses 50 mm, 120 mm and 300 mm – current climate (office building).

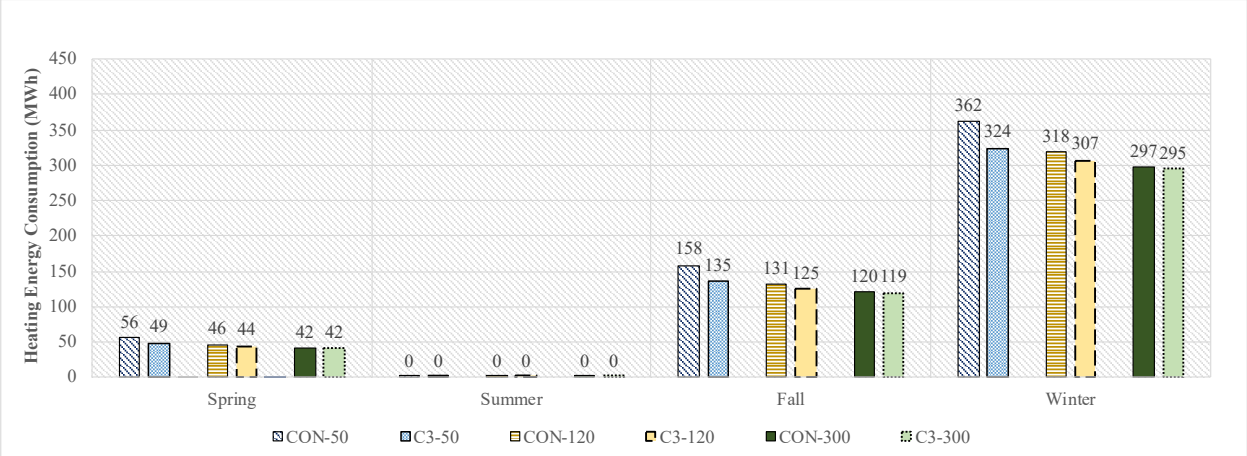

Figure C - 28: Seasonal heating loads for conventional roof and green roof with design of growing media of 200 mm and LAI of 3 for insulation thicknesses 50 mm, 120 mm and 300 mm – current climate (office building).

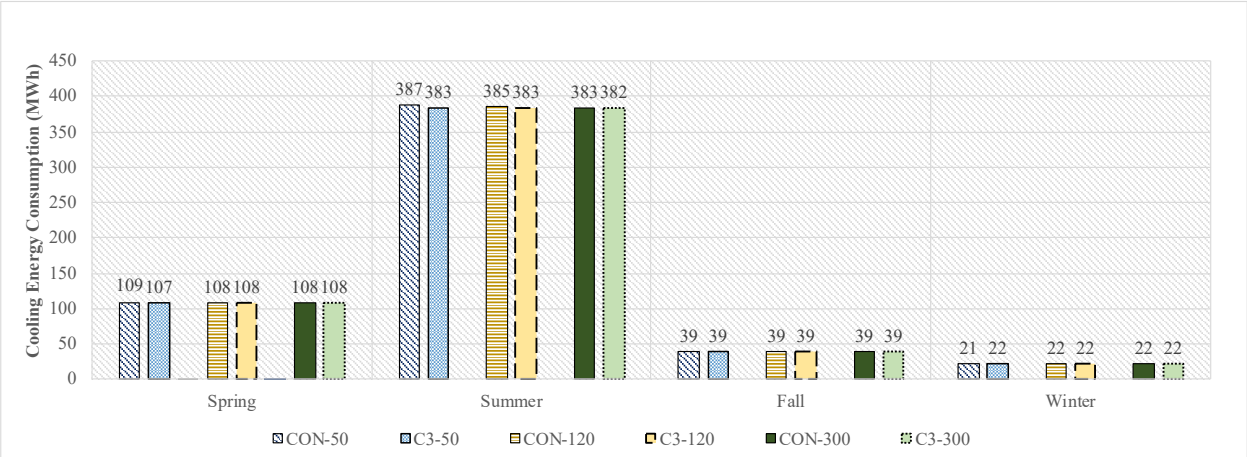

Figure C - 29: Seasonal cooling loads for conventional roof and green roof with design of growing media of 200 mm and LAI of 3 for insulation thicknesses 50 mm, 120 mm and 300 mm – current climate (office building).

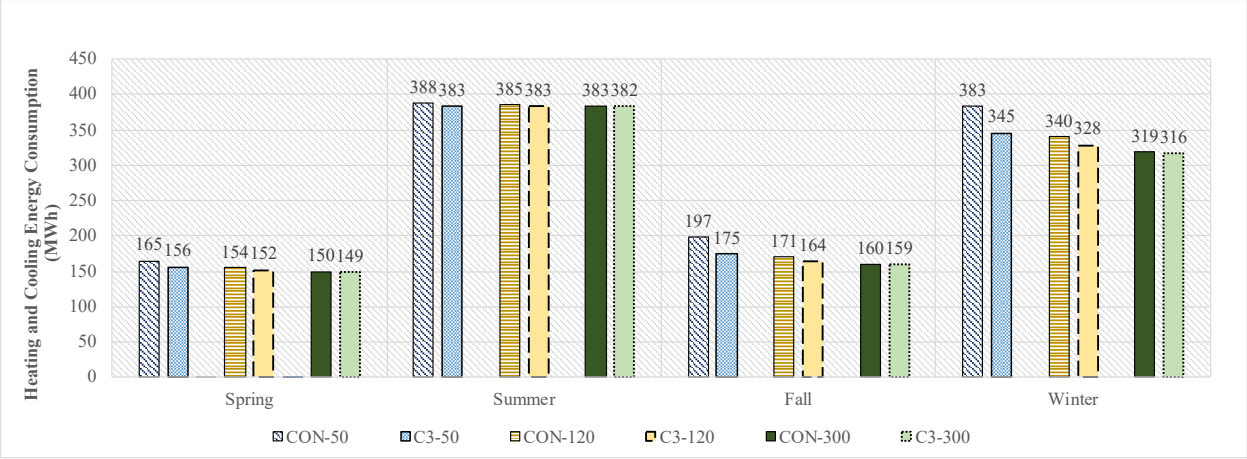

Figure C - 30: Seasonal total heating and cooling loads for conventional roof and green roof with design of growing media of 200 mm and LAI of 3 for insulation thicknesses 50 mm, 120 mm and 300 mm – current climate (office building).

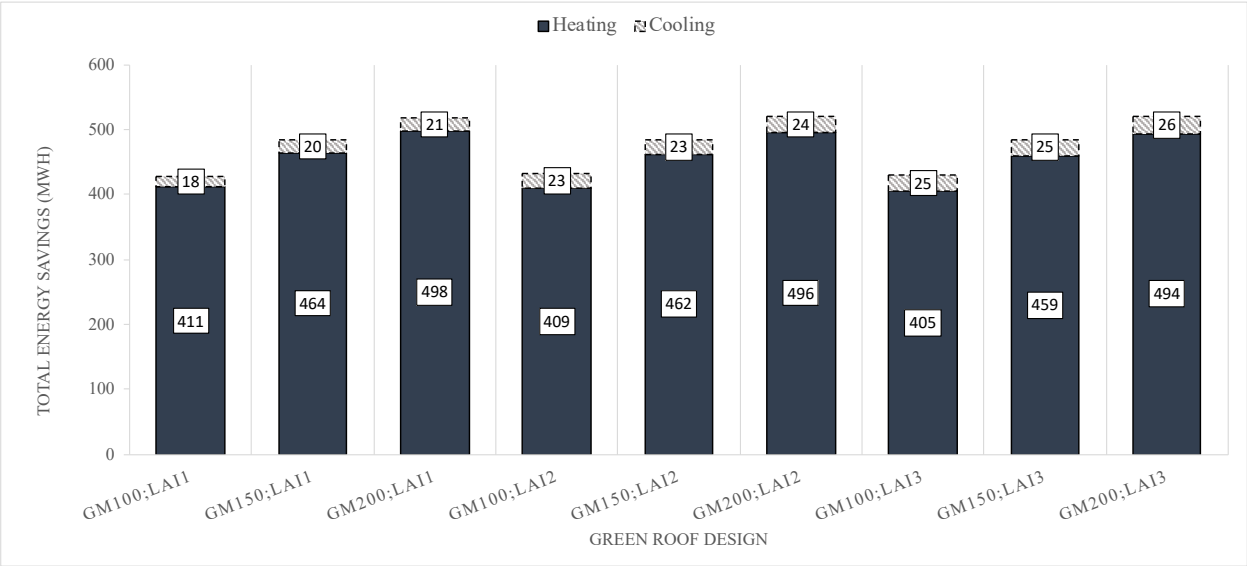

Figure C - 31: Total heating and cooling energy savings (MWh) of green roof compared to conventional roof for all growing media (GM) depths and LAIs; without insulation layer – current climate (office building).

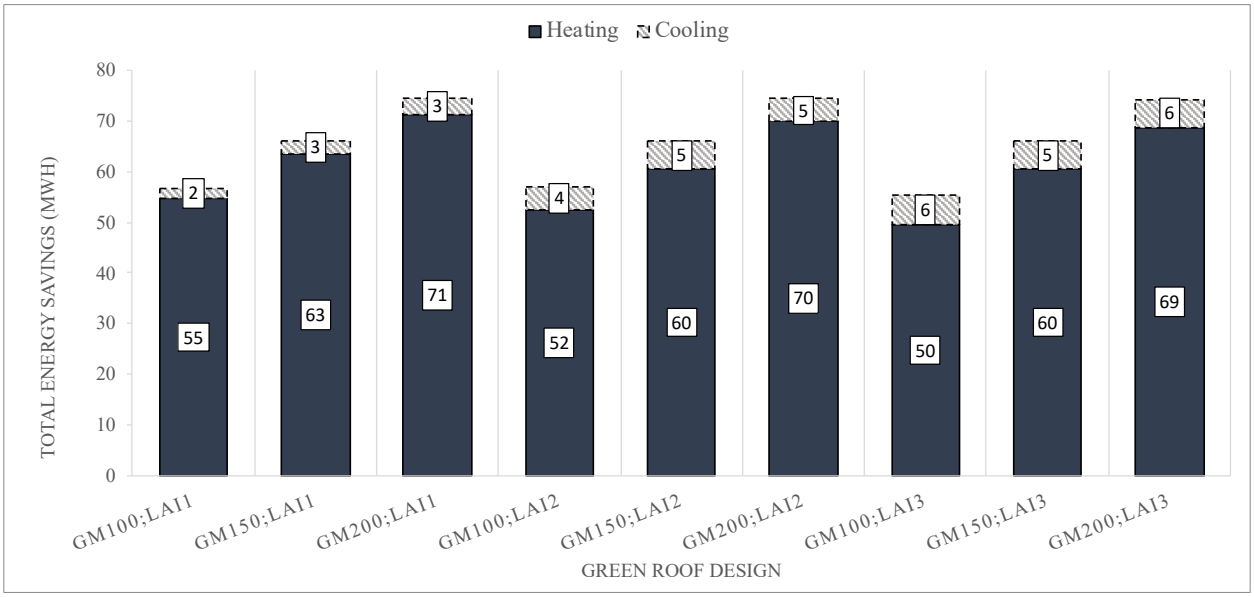

Figure C - 32: Total heating and cooling energy savings (MWh) of green roof compared to conventional roof for all growing media (GM) depths and LAIs; with 50 mm insulation layer – current climate (office building).

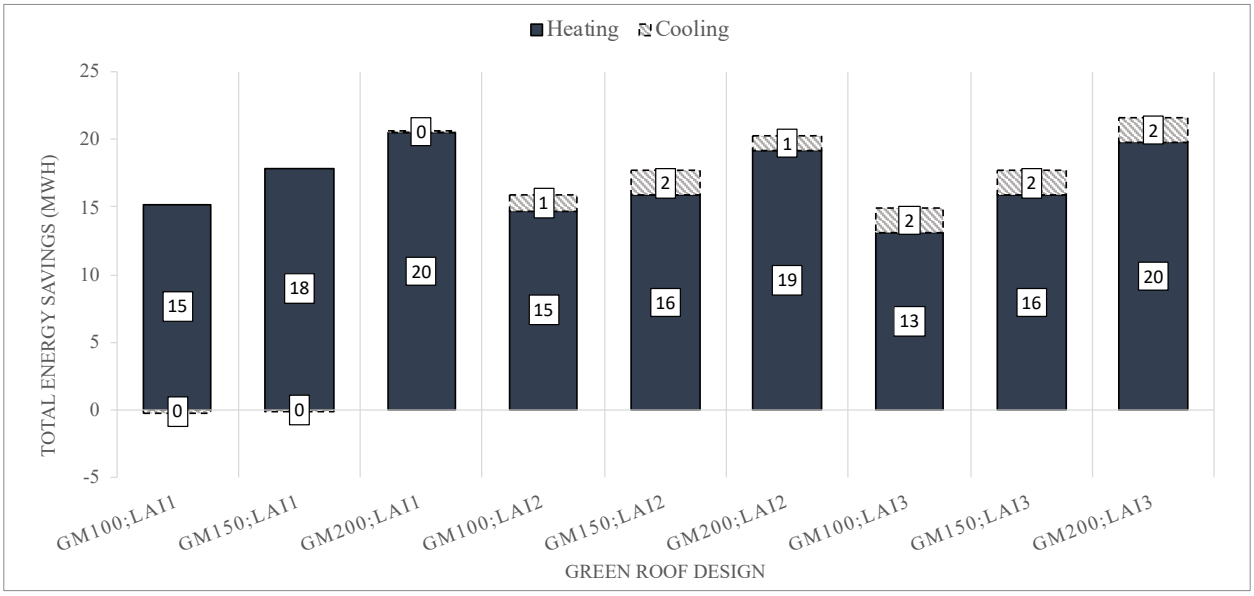

Figure C - 33: Total heating and cooling energy savings (MWh) of green roof compared to conventional roof for all growing media (GM) depths and LAIs; with 120 mm insulation layer – current climate (office building).

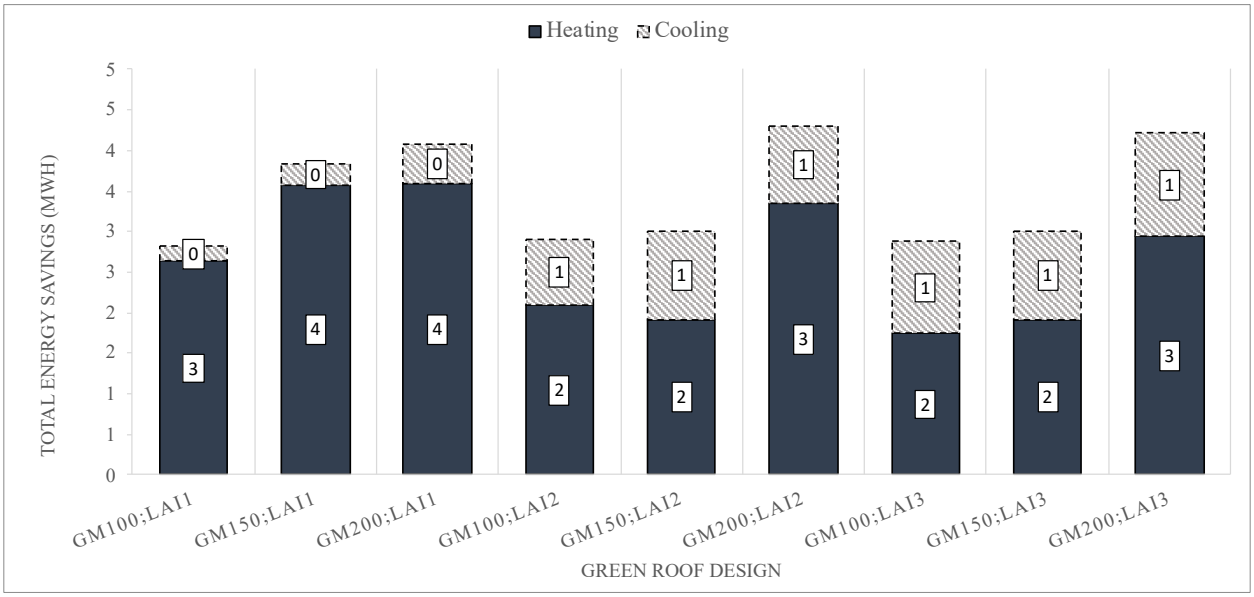

Figure C - 34: Total heating and cooling energy savings (MWh) of green roof compared to conventional roof for all growing media (GM) depths and LAIs; with 300 mm insulation layer – current climate (office building).

Appendix D: Annual Energy Consumption and Savings for Cooling/Heating Loads – Future Climate Condition Office Building

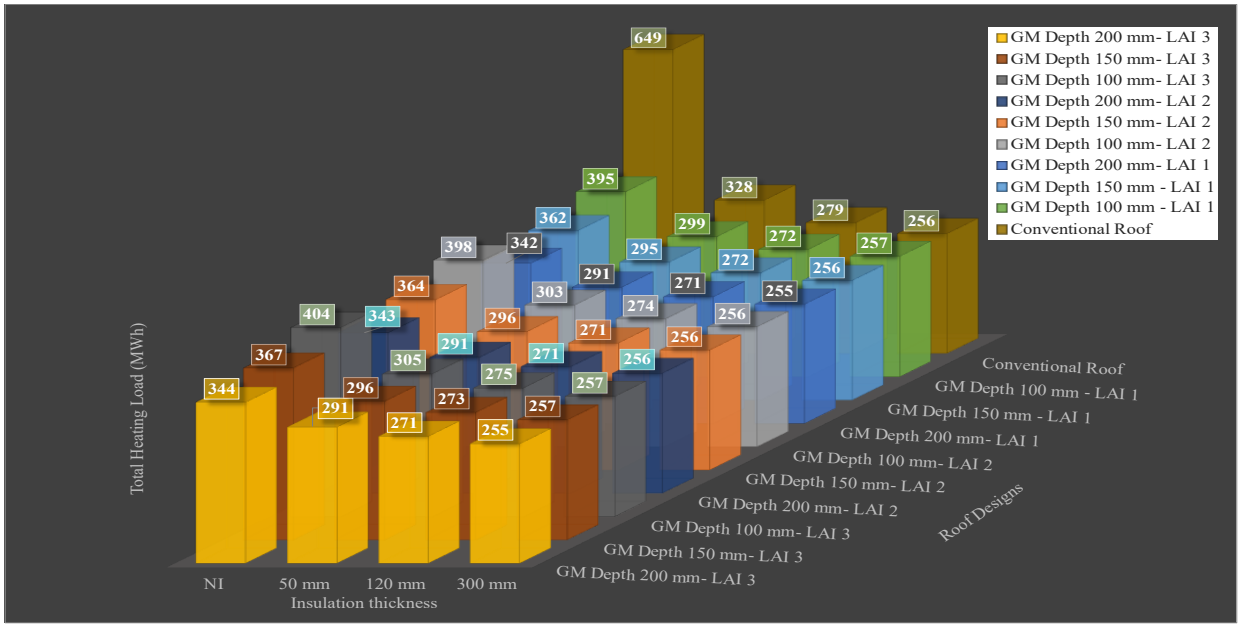

Figure D - 1: Total heating loads for all roof designs; all insulation thickness; LAIs; and growing media depths under future climate – office building.

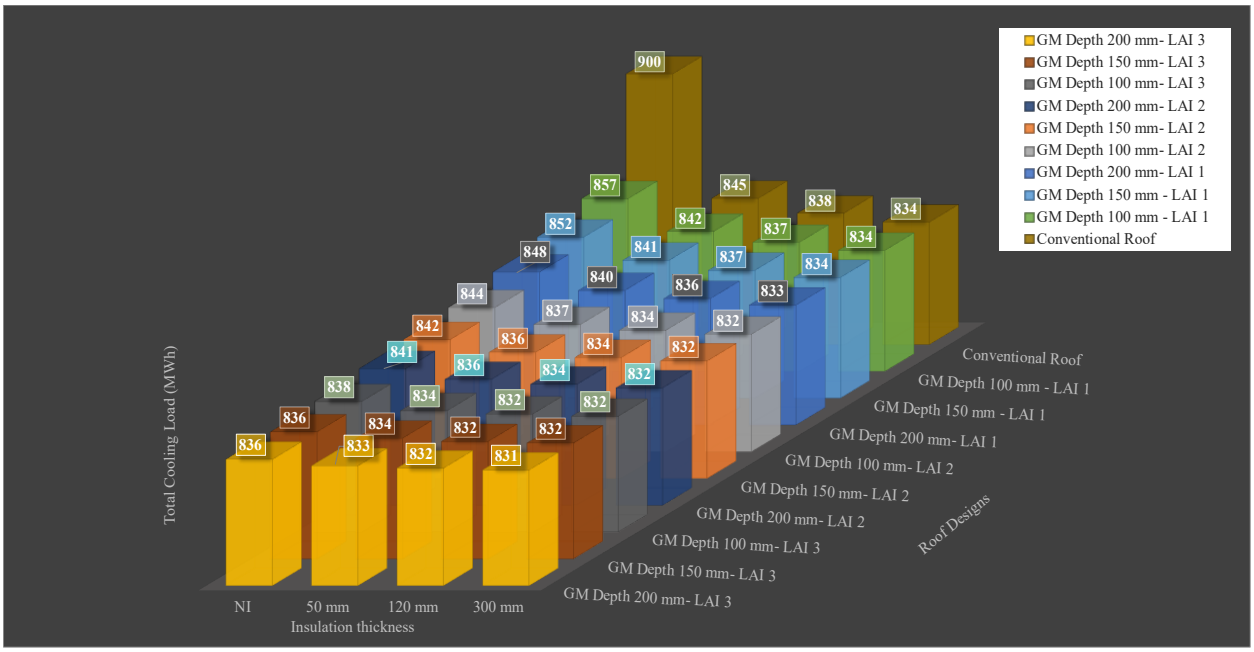

Figure D - 2: Total cooling loads for all roof designs; all insulation thickness; LAIs; and growing media depths under future climate – office building.

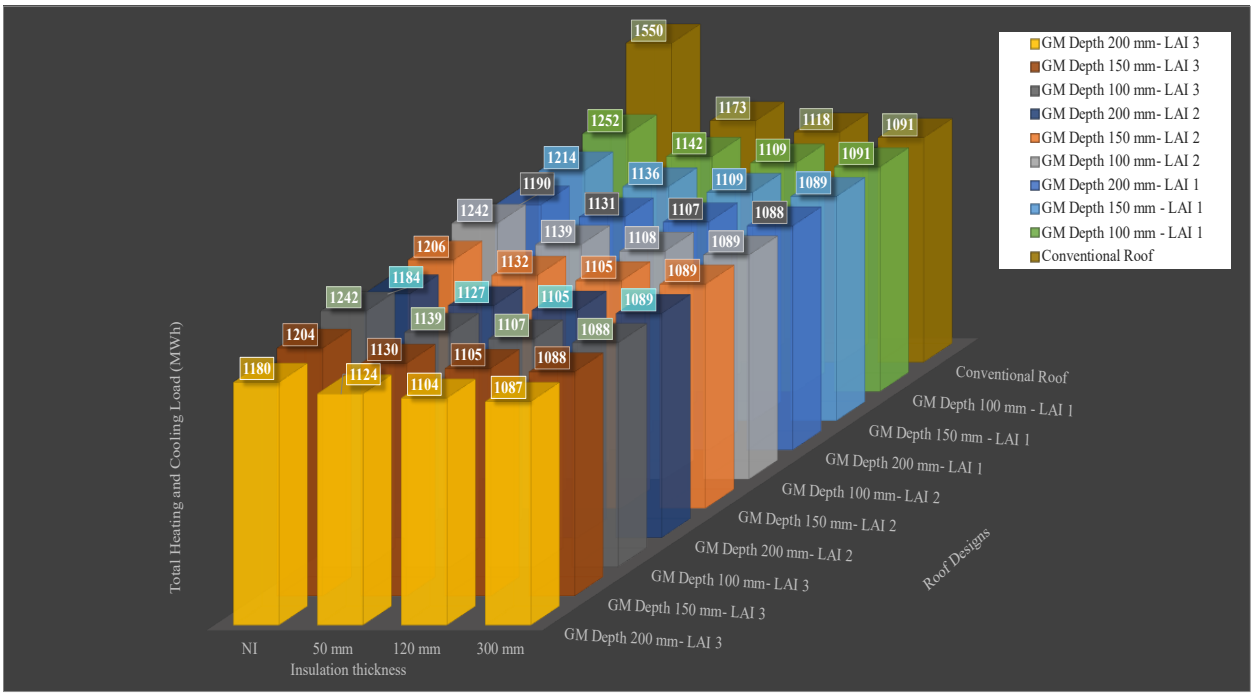

Figure D - 3: Total heating and cooling loads for all roof designs; all insulation thickness; LAIs; and growing media depths under future climate – office building.

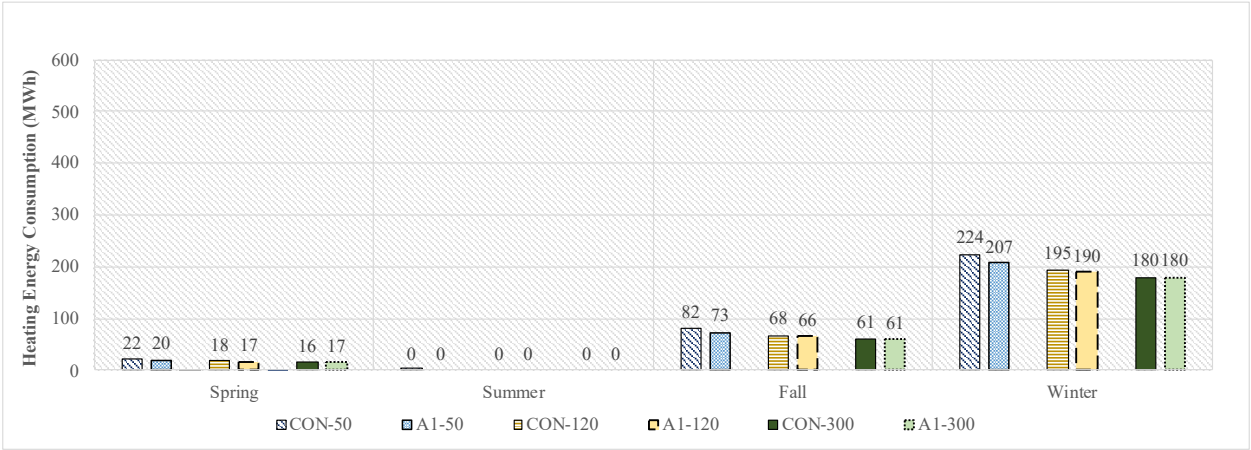

Figure D - 4: Seasonal heating loads for conventional roof and green roof with design of growing media of 100 mm and LAI of 1 for insulation thicknesses 50 mm, 120 mm and 300 mm – future climate (office building).

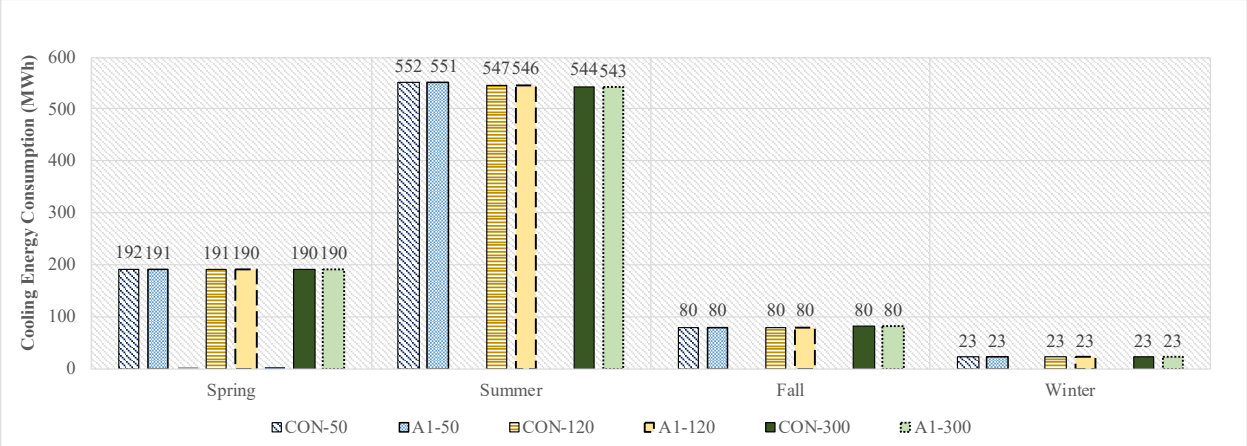

Figure D - 5: Seasonal cooling loads for conventional roof and green roof with design of growing media of 100 mm and LAI of 1 for insulation thicknesses 50 mm, 120 mm and 300 mm – future climate (office building).

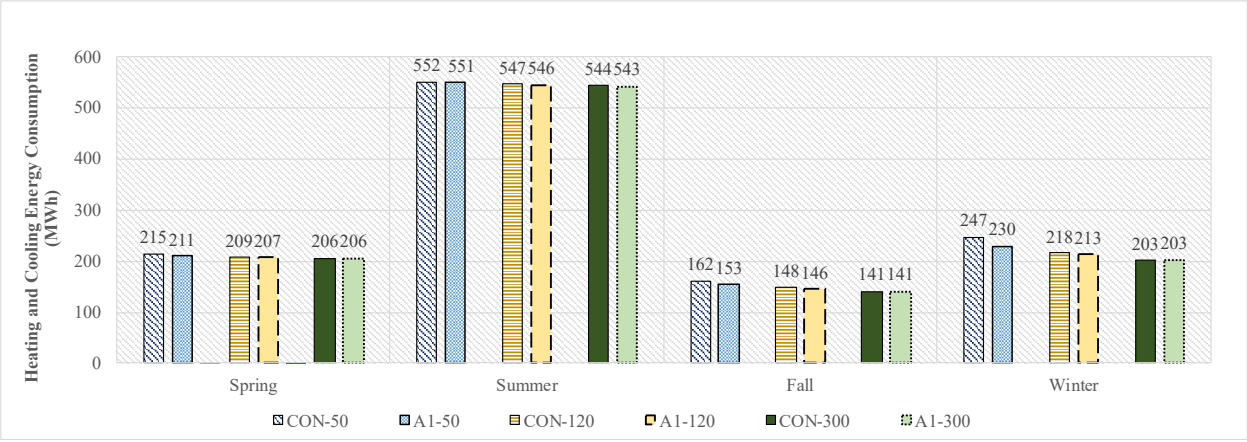

Figure D - 6: Seasonal total heating and cooling loads for conventional roof and green roof with design of growing media of 100 mm and LAI of 1 for insulation thicknesses 50 mm, 120 mm and 300 mm – future climate (office building).

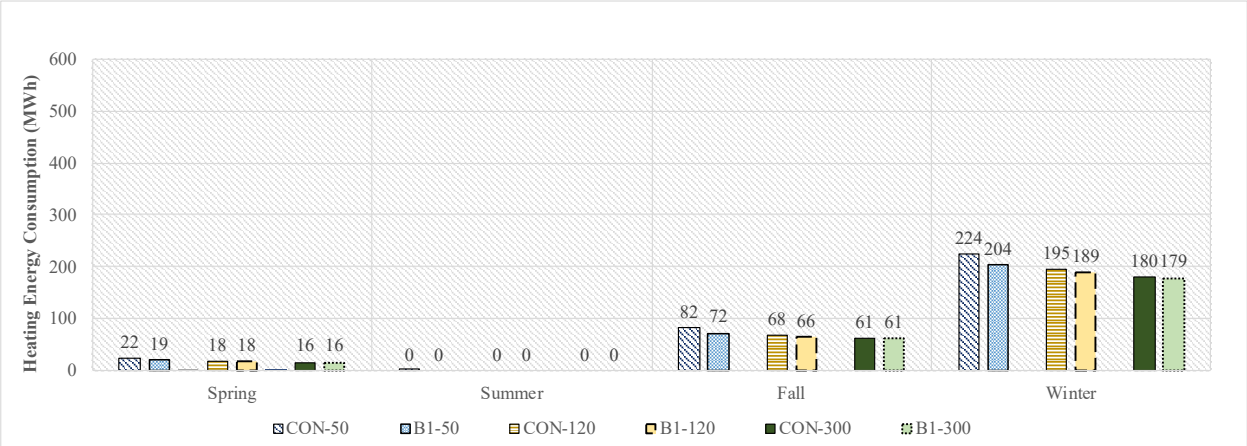

Figure D - 7: Seasonal heating loads for conventional roof and green roof with design of growing media of 150 mm and LAI of 1 for insulation thicknesses 50 mm, 120 mm and 300 mm – future climate (office building).

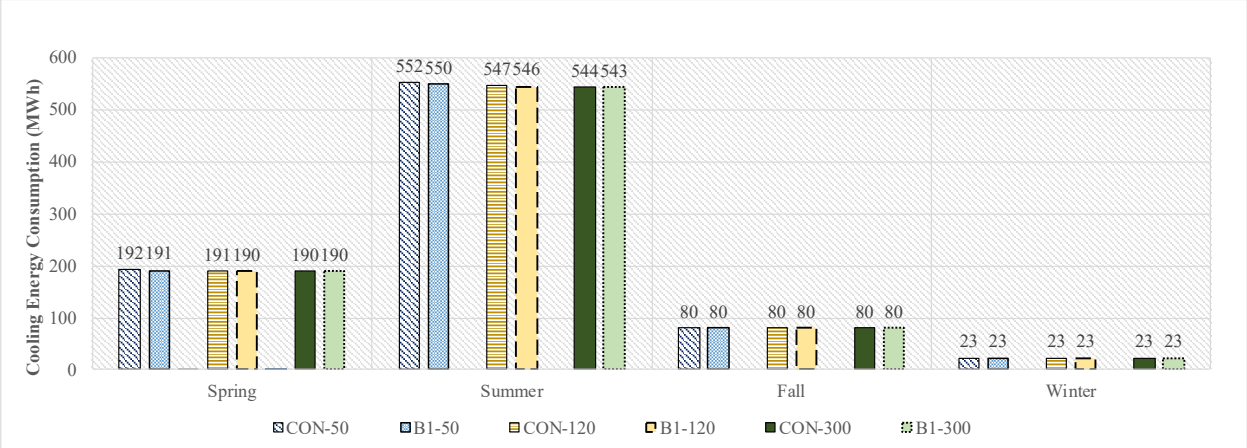

Figure D - 8: Seasonal cooling loads for conventional roof and green roof with design of growing media of 100 mm and LAI of 1 for insulation thicknesses 50 mm, 120 mm and 300 mm – future climate (office building).

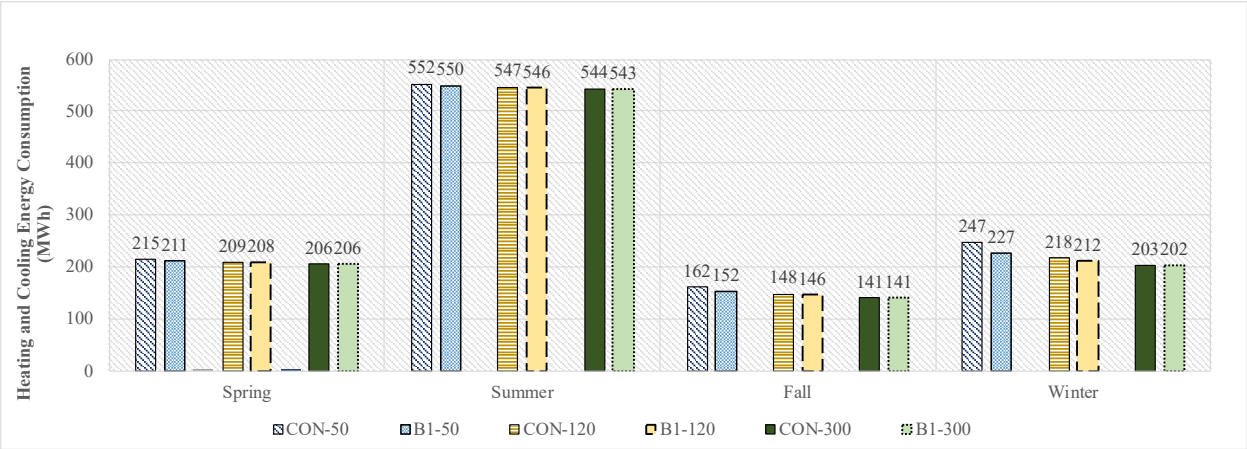

Figure D - 9: Seasonal total heating and cooling loads for conventional roof and green roof with design of growing media of 150 mm and LAI of 1 for insulation thicknesses 50 mm, 120 mm and 300 mm – future climate (office building).

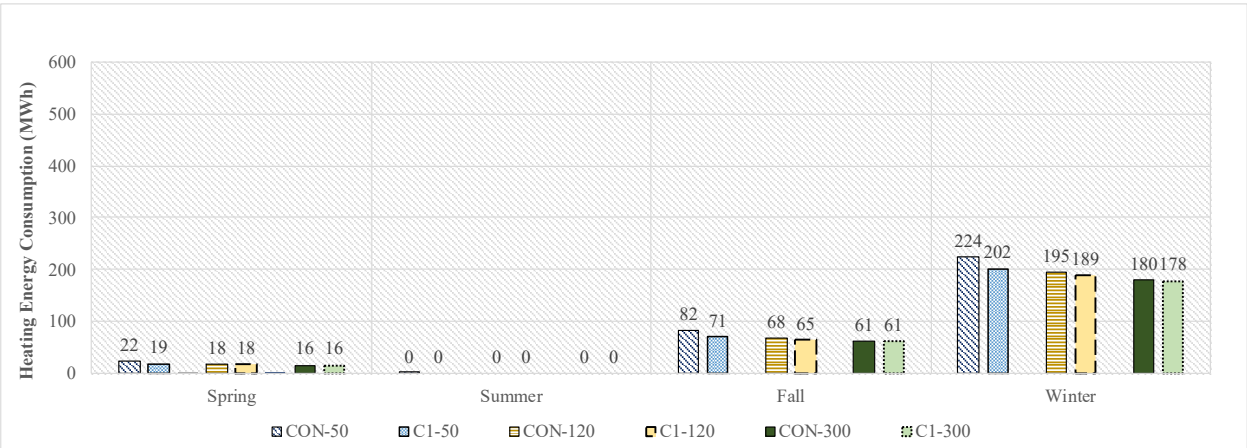

Figure D - 10: Seasonal heating loads for conventional roof and green roof with design of growing media of 200 mm and LAI of 1 for insulation thicknesses 50 mm, 120 mm and 300 mm – future climate (office building).

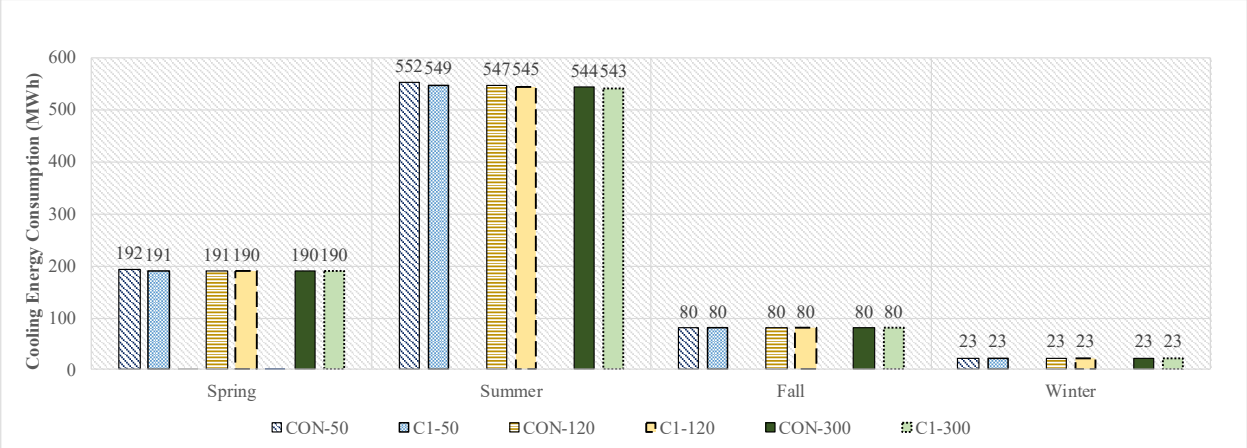

Figure D - 11: Seasonal cooling loads for conventional roof and green roof with design of growing media of 200 mm and LAI of 1 for insulation thicknesses 50 mm, 120 mm and 300 mm – future climate (office building).

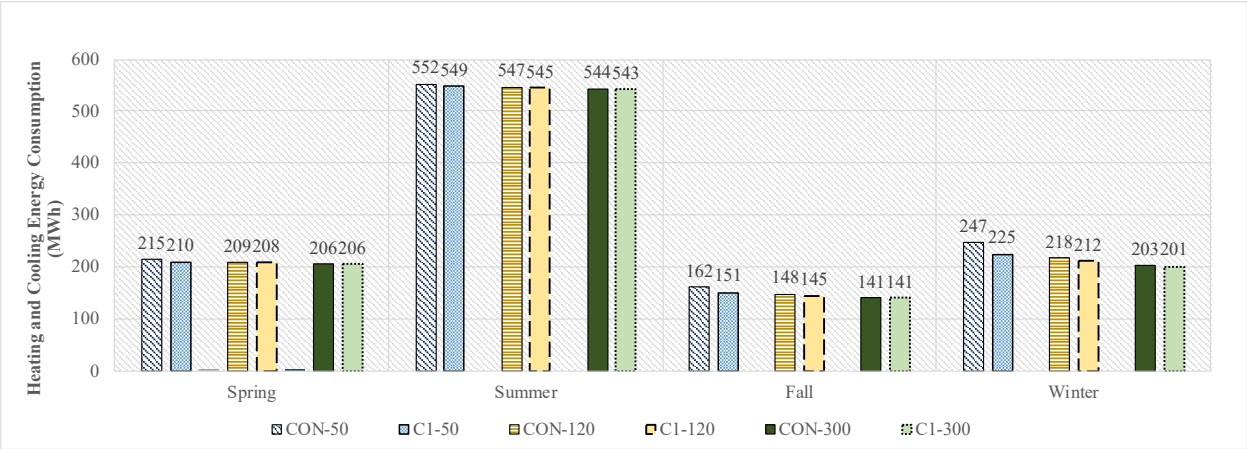

Figure D - 12: Seasonal total heating and cooling loads for conventional roof and green roof with design of growing media of 200 mm and LAI of 1 for insulation thicknesses 50 mm, 120 mm and 300 mm – future climate (office building).

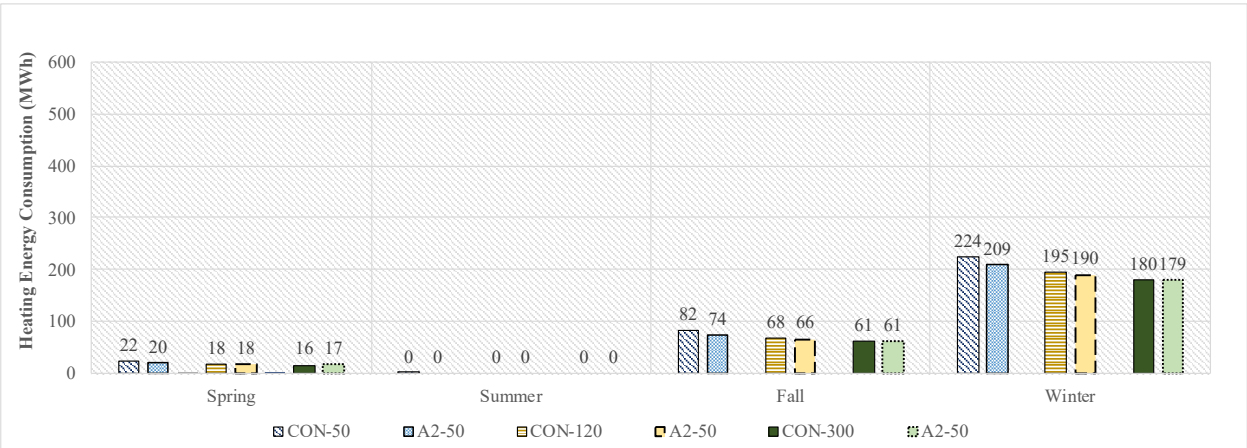

Figure D - 13: Seasonal heating loads for conventional roof and green roof with design of growing media of 100 mm and LAI of 2 for insulation thicknesses 50 mm, 120 mm and 300 mm – future climate (office building).

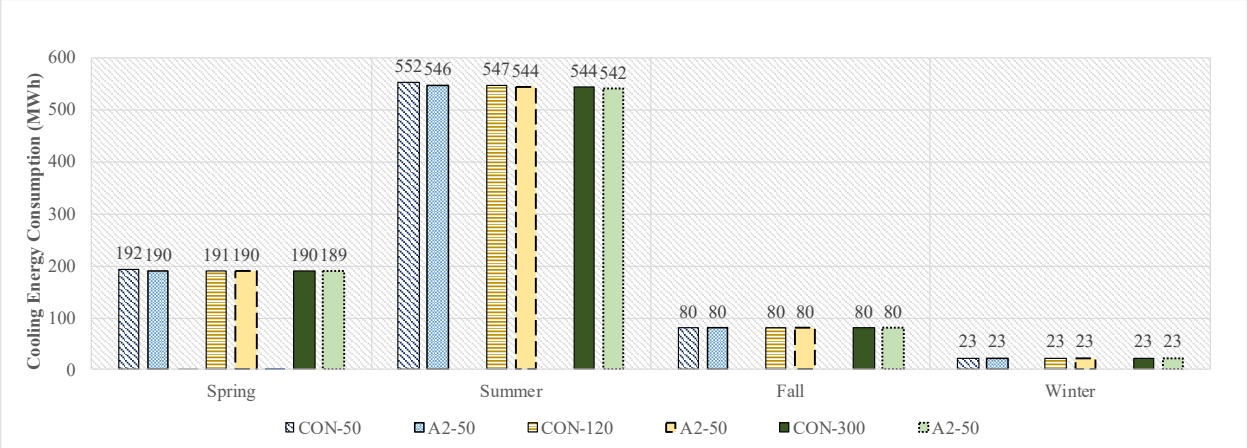

Figure D - 14: Seasonal cooling loads for conventional roof and green roof with design of growing media of 100 mm and LAI of 2 for insulation thicknesses 50 mm, 120 mm and 300 mm – future climate (office building).

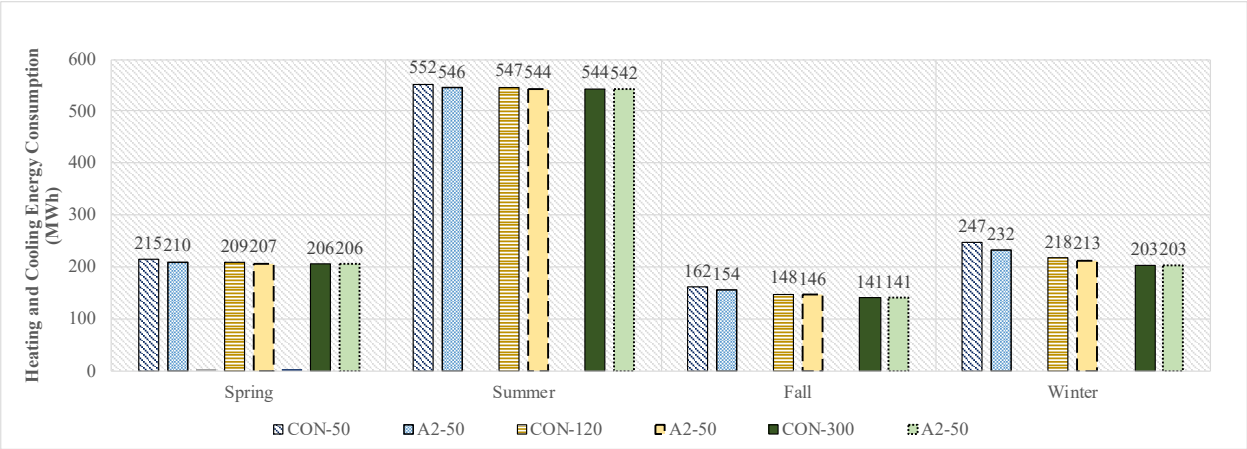

Figure D - 15: Seasonal total heating and cooling loads for conventional roof and green roof with design of growing media of 100 mm and LAI of 2 for insulation thicknesses 50 mm, 120 mm and 300 mm – future climate (office building).

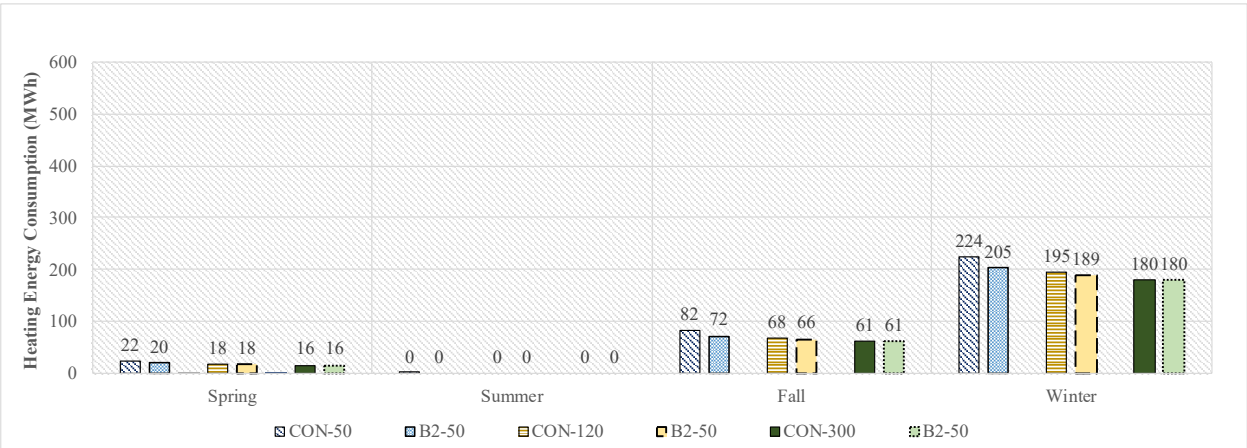

Figure D - 16: Seasonal heating loads for conventional roof and green roof with design of growing media of 150 mm and LAI of 2 for insulation thicknesses 50 mm, 120 mm and 300 mm – future climate (office building).

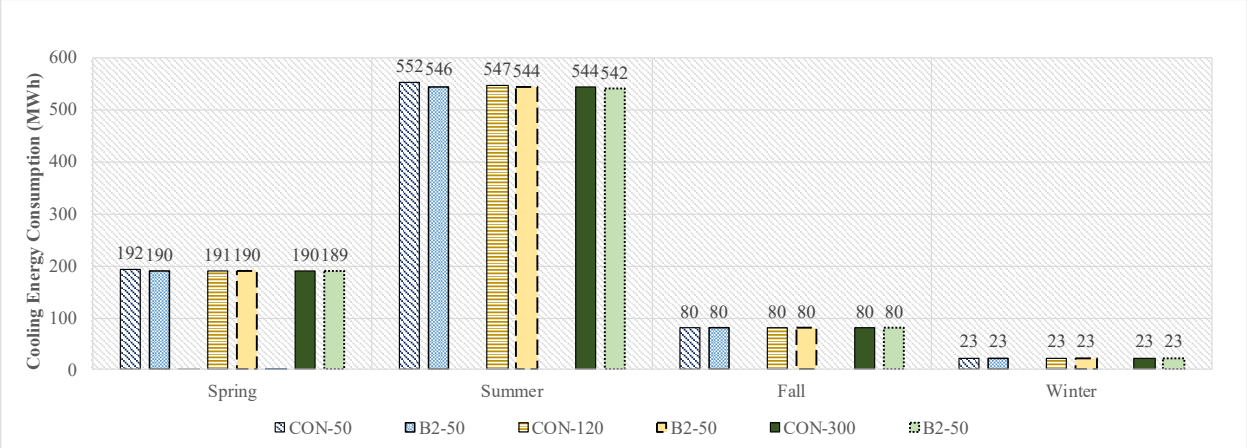

Figure D - 17: Seasonal cooling loads for conventional roof and green roof with design of growing media of 150 mm and LAI of 2 for insulation thicknesses 50 mm, 120 mm and 300 mm – future climate (office building).

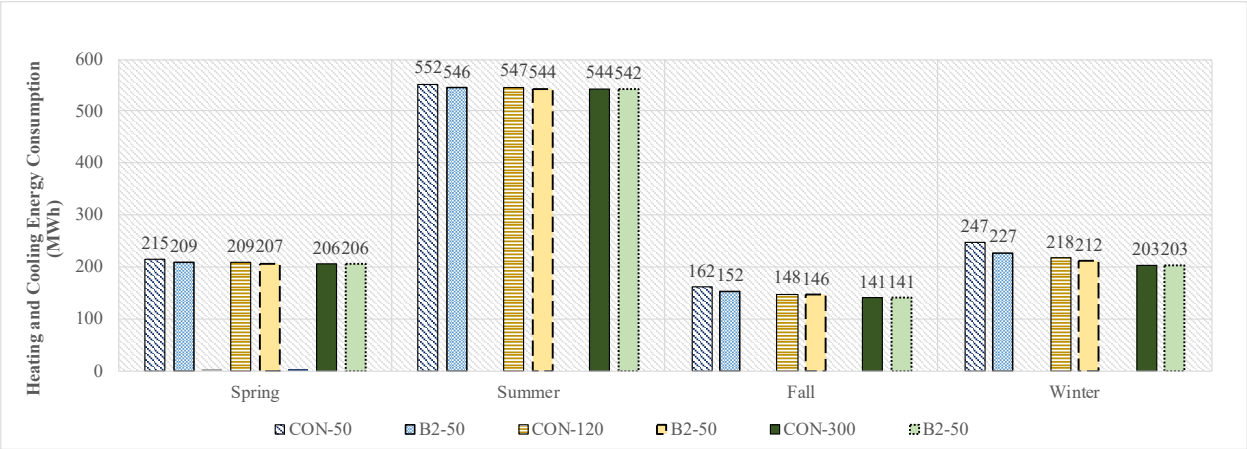

Figure D - 18: Seasonal total heating and cooling loads for conventional roof and green roof with design of growing media of 150 mm and LAI of 2 for insulation thicknesses 50 mm, 120 mm and 300 mm – future climate (office building).

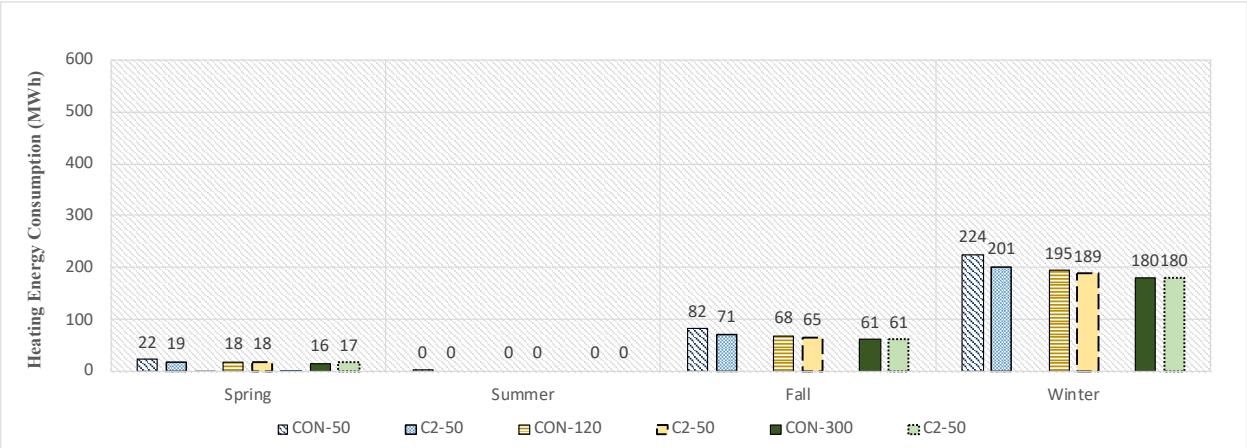

Figure D - 19: Seasonal heating loads for conventional roof and green roof with design of growing media of 200 mm and LAI of 2 for insulation thicknesses 50 mm, 120 mm and 300 mm – future climate (office building).

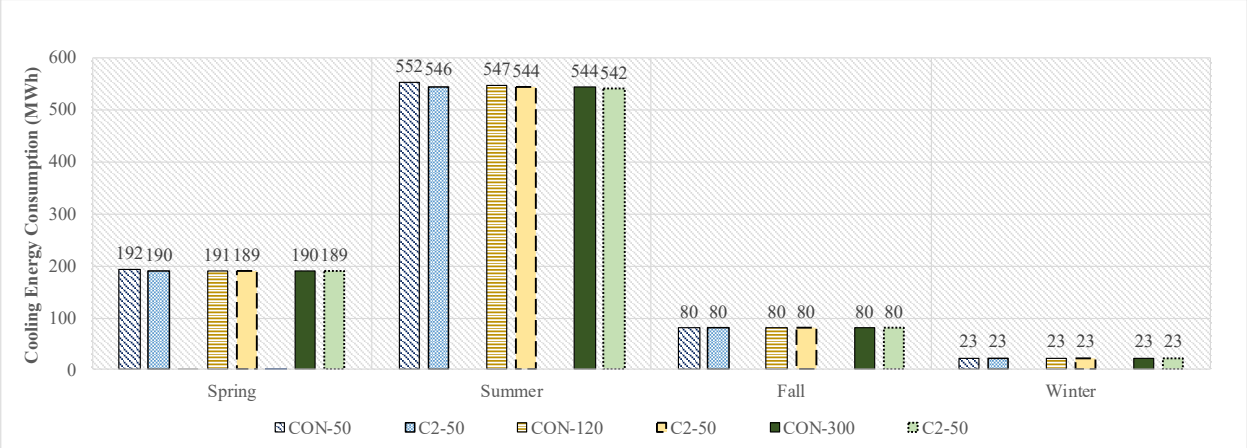

Figure D - 20: Seasonal cooling loads for conventional roof and green roof with design of growing media of 200 mm and LAI of 2 for insulation thicknesses 50 mm, 120 mm and 300 mm – future climate (office building).

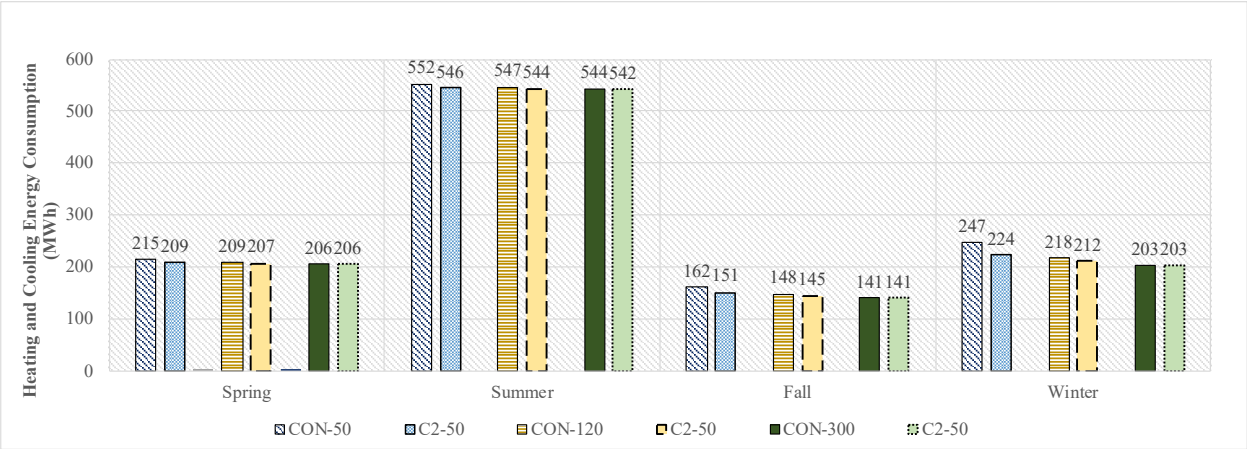

Figure D - 21: Seasonal total heating and cooling loads for conventional roof and green roof with design of growing media of 200 mm and LAI of 2 for insulation thicknesses 50 mm, 120 mm and 300 mm – future climate (office building).

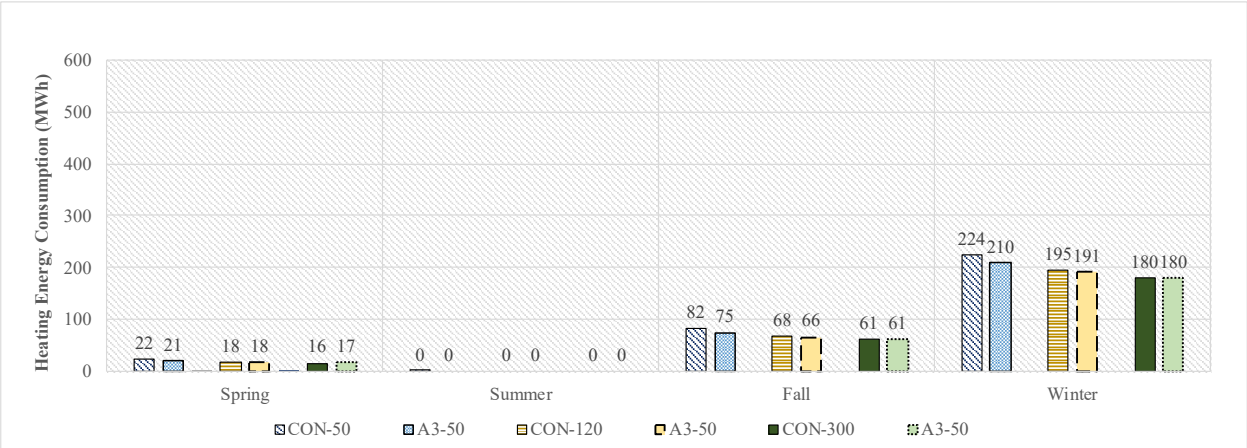

Figure D - 22: Seasonal heating loads for conventional roof and green roof with design of growing media of 100 mm and LAI of 3 for insulation thicknesses 50 mm, 120 mm and 300 mm – future climate (office building).

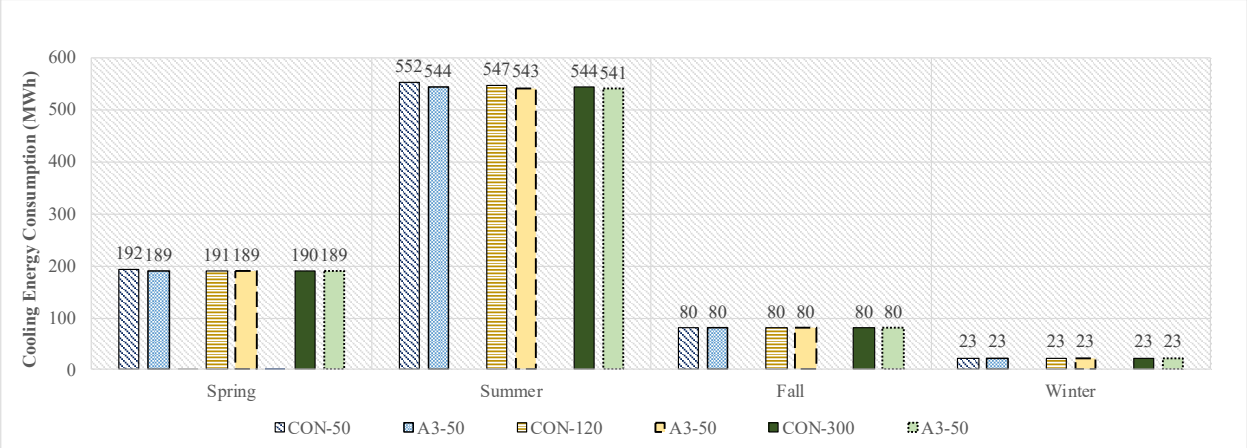

Figure D - 23: Seasonal cooling loads for conventional roof and green roof with design of growing media of 100 mm and LAI of 3 for insulation thicknesses 50 mm, 120 mm and 300 mm – future climate (office building).

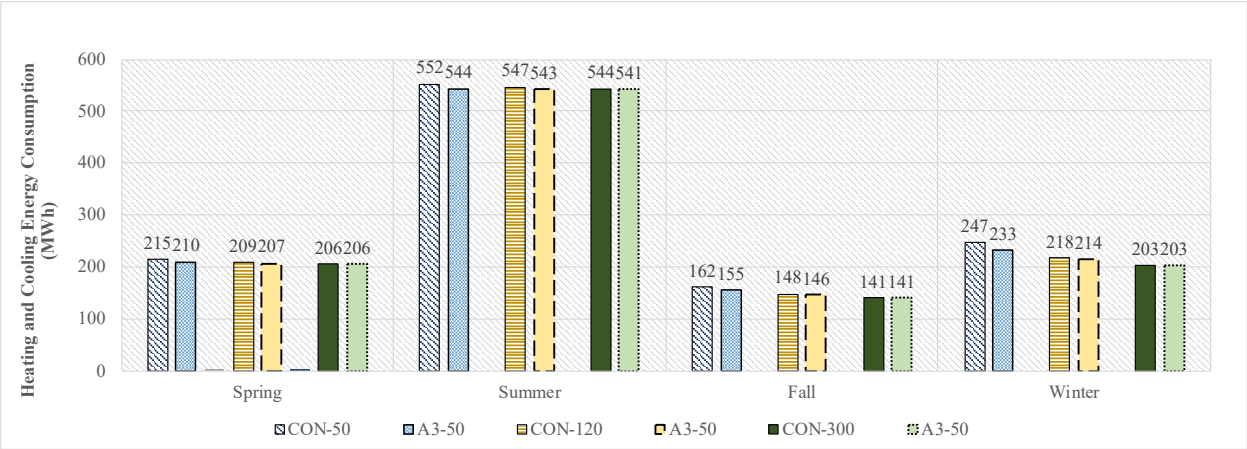

Figure D - 24: Seasonal total heating and cooling loads for conventional roof and green roof with design of growing media of 100 mm and LAI of 3 for insulation thicknesses 50 mm, 120 mm and 300 mm – future climate (office building).

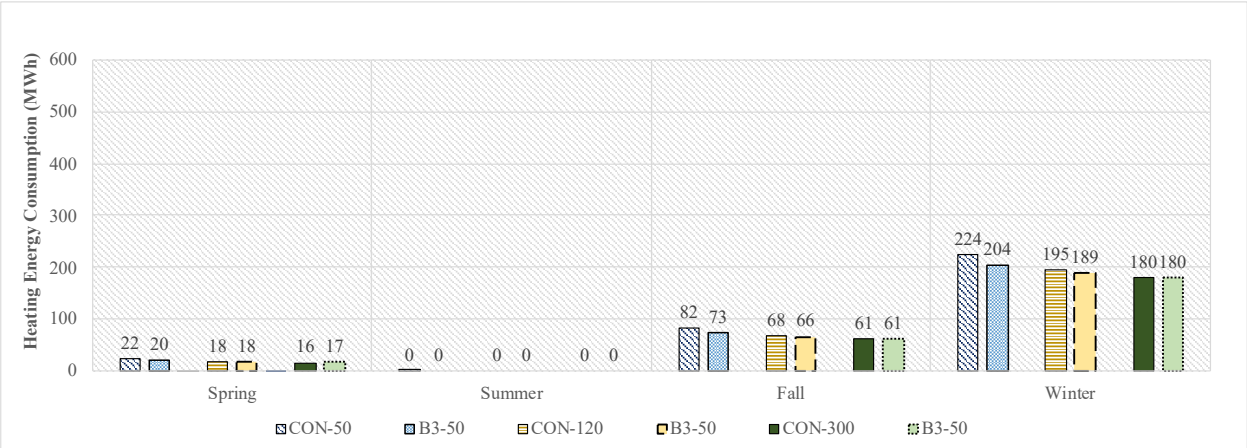

Figure D - 25: Seasonal heating loads for conventional roof and green roof with design of growing media of 150 mm and LAI of 3 for insulation thicknesses 50 mm, 120 mm and 300 mm – future climate (office building).

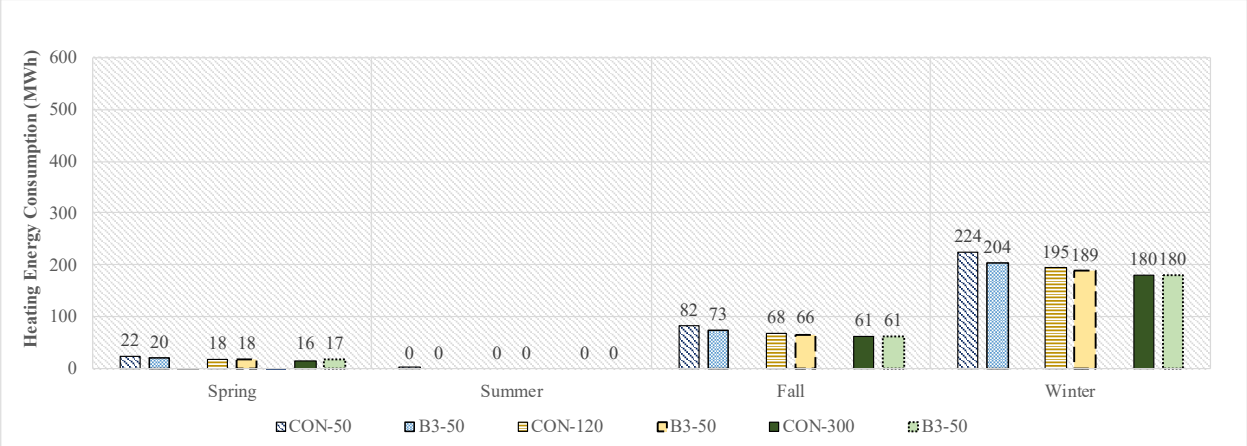

Figure D - 26: Seasonal cooling loads for conventional roof and green roof with design of growing media of 150 mm and LAI of 3 for insulation thicknesses 50 mm, 120 mm and 300 mm – future climate (office building).

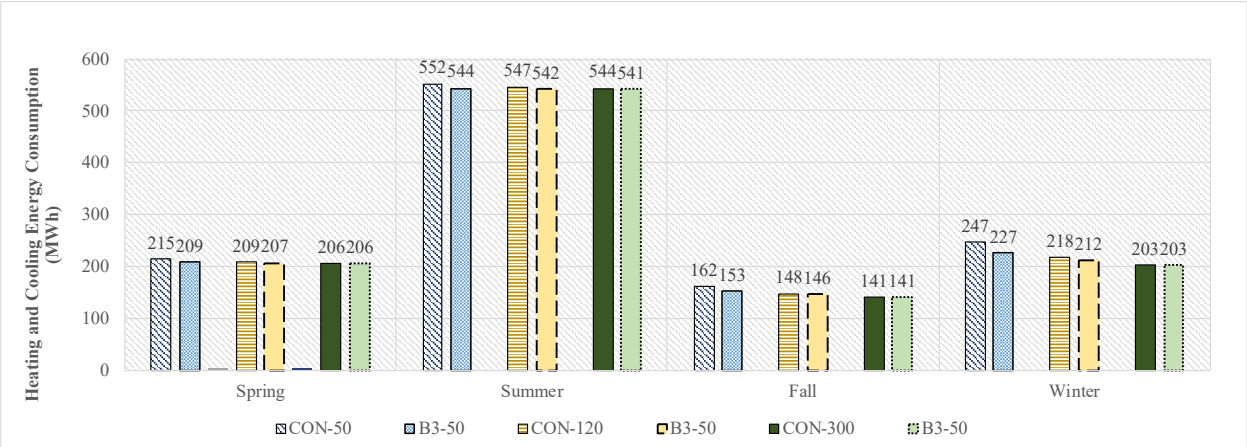

Figure D - 27: Seasonal total heating and cooling loads for conventional roof and green roof with design of growing media of 150 mm and LAI of 3 for insulation thicknesses 50 mm, 120 mm and 300 mm – future climate (office building).

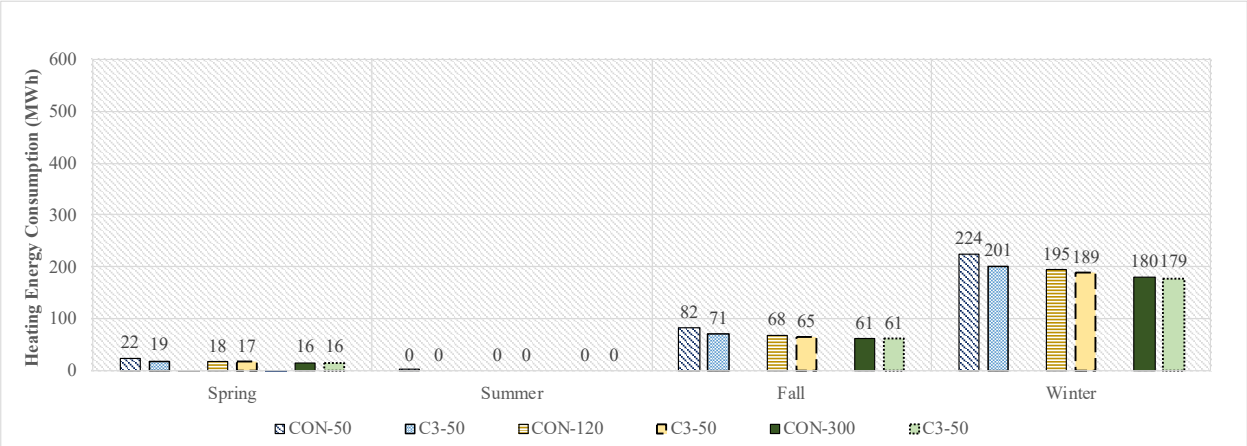

Figure D - 28: Seasonal heating loads for conventional roof and green roof with design of growing media of 200 mm and LAI of 3 for insulation thicknesses 50 mm, 120 mm and 300 mm – future climate (office building).

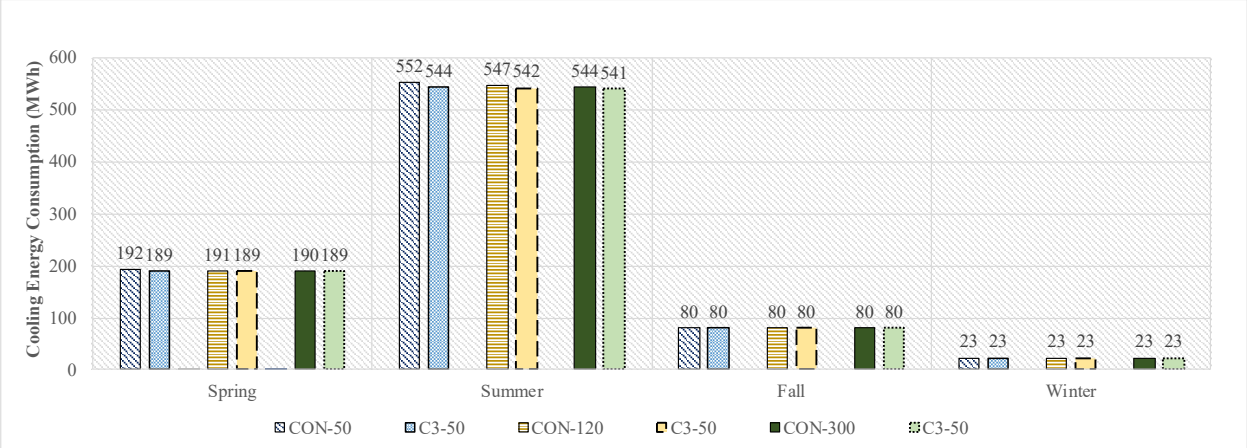

Figure D - 29: Seasonal cooling loads for conventional roof and green roof with design of growing media of 200 mm and LAI of 3 for insulation thicknesses 50 mm, 120 mm and 300 mm – future climate (office building).

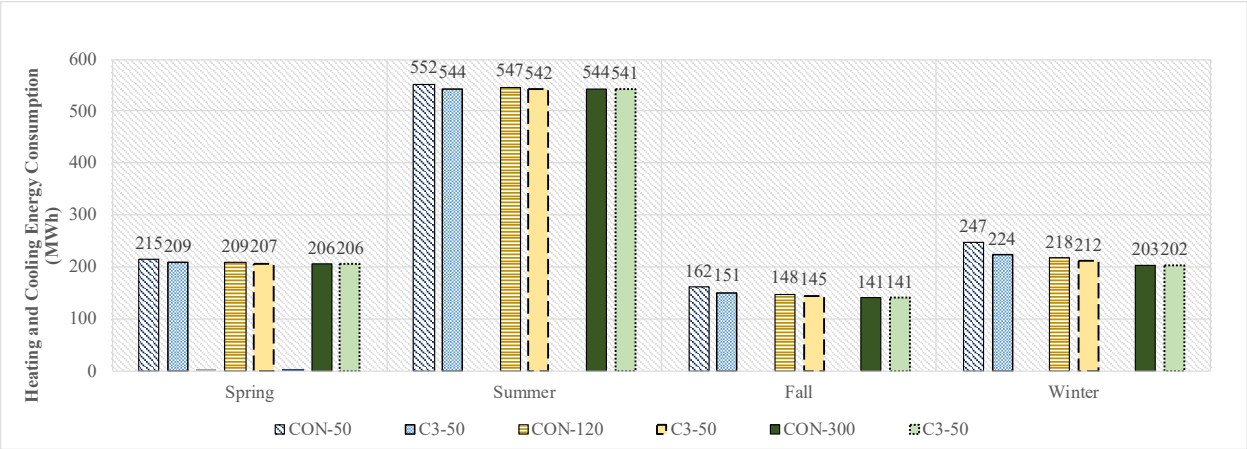

Figure D - 30: Seasonal total heating and cooling loads for conventional roof and green roof with design of growing media of 200 mm and LAI of 3 for insulation thicknesses 50 mm, 120 mm and 300 mm – future climate (office building).

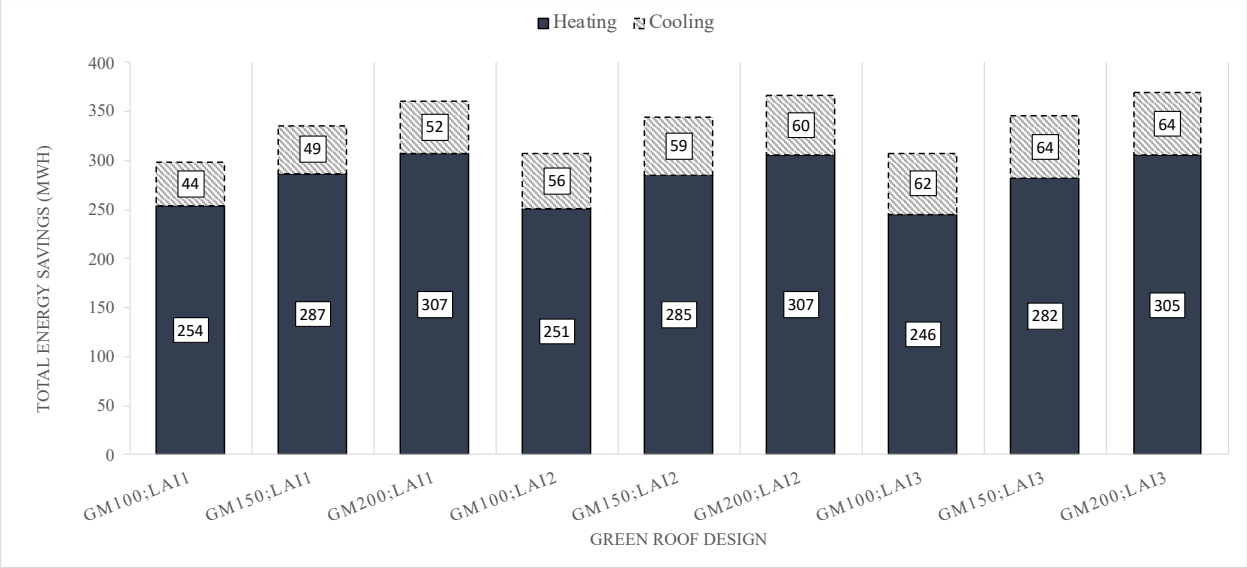

Figure D - 31: Total heating and cooling energy savings (MWh) of green roof compared to conventional roof for all growing media (GM) depths and LAIs; without insulation layer – future climate (office building).

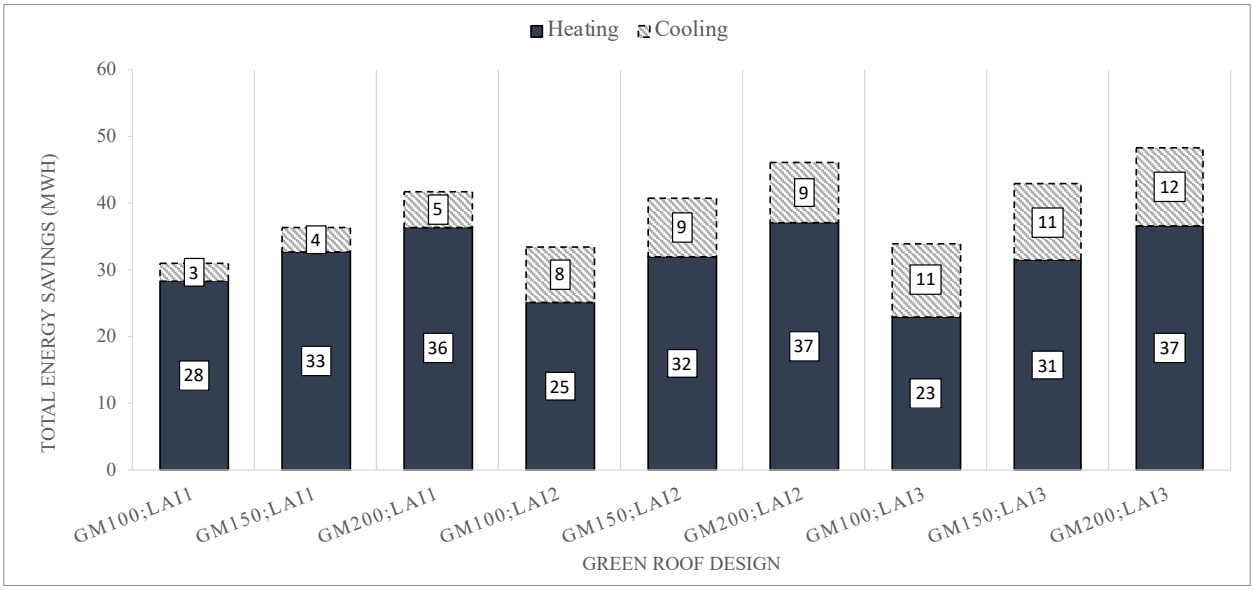

Figure D - 32: Total heating and cooling energy savings (MWh) of green roof compared to conventional roof for all growing media (GM) depths and LAIs; with 50 mm insulation layer – future climate (office building).

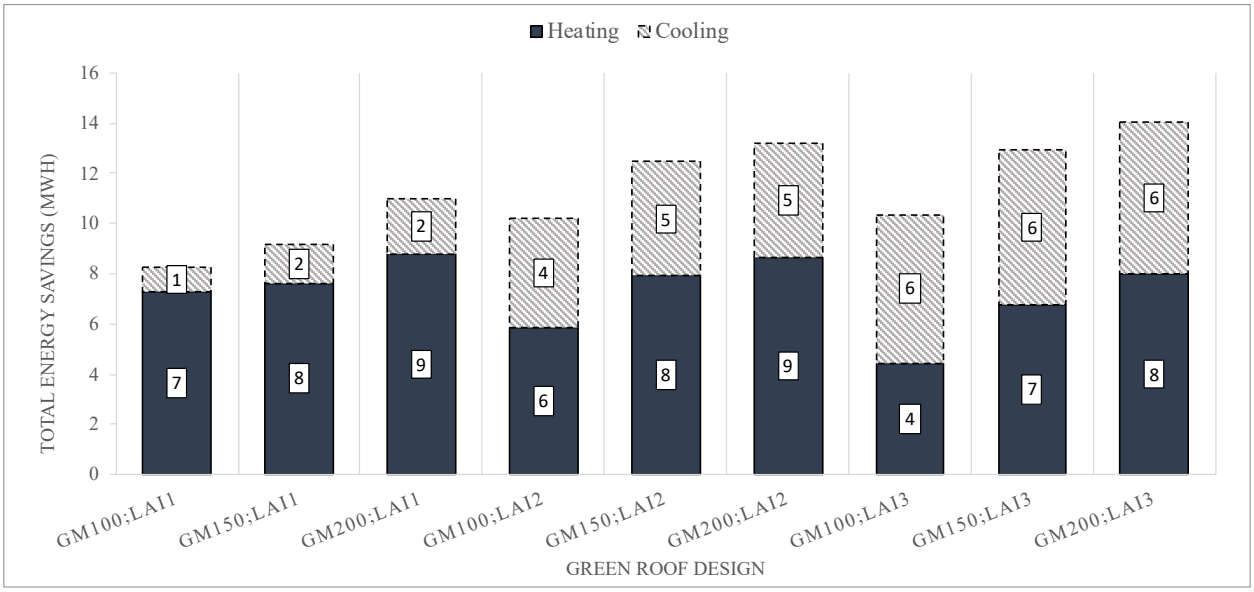

Figure D - 33: Total heating and cooling energy savings (MWh) of green roof compared to conventional roof for all growing media (GM) depths and LAIs; with 120 mm insulation layer – future climate (office building).

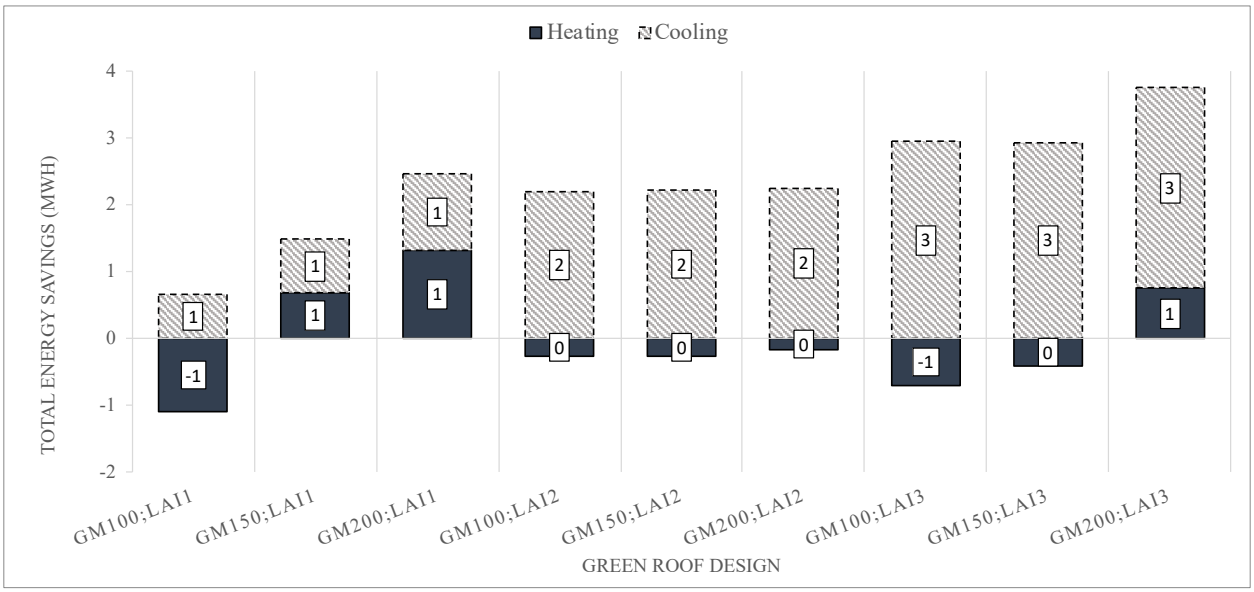

Figure D - 34: Total heating and cooling energy savings (MWh) of green roof compared to conventional roof for all growing media (GM) depths and LAIs; with 300 mm insulation layer – future climate (office building).

Appendix E: Annual Energy Consumption and Savings for Cooling/Heating Loads – Current Climate Condition Hospital Building

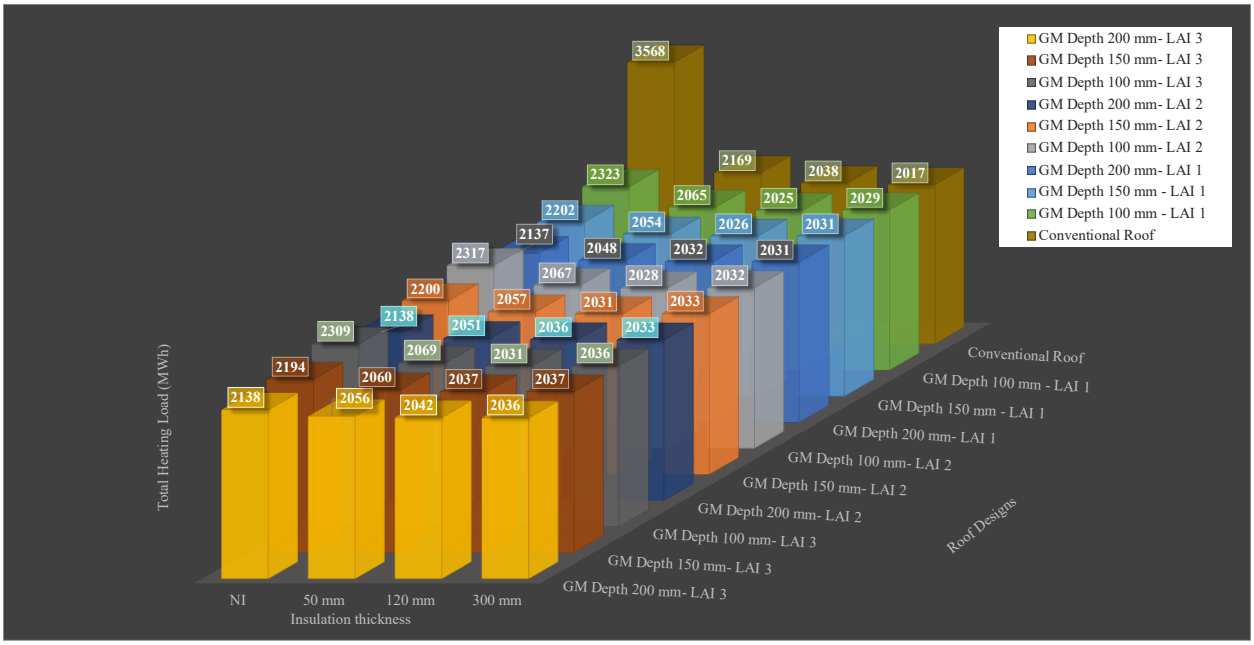

Figure E - 1: Total heating loads for all roof designs; all insulation thickness; LAIs; and growing media depths under current climate – hospital building.

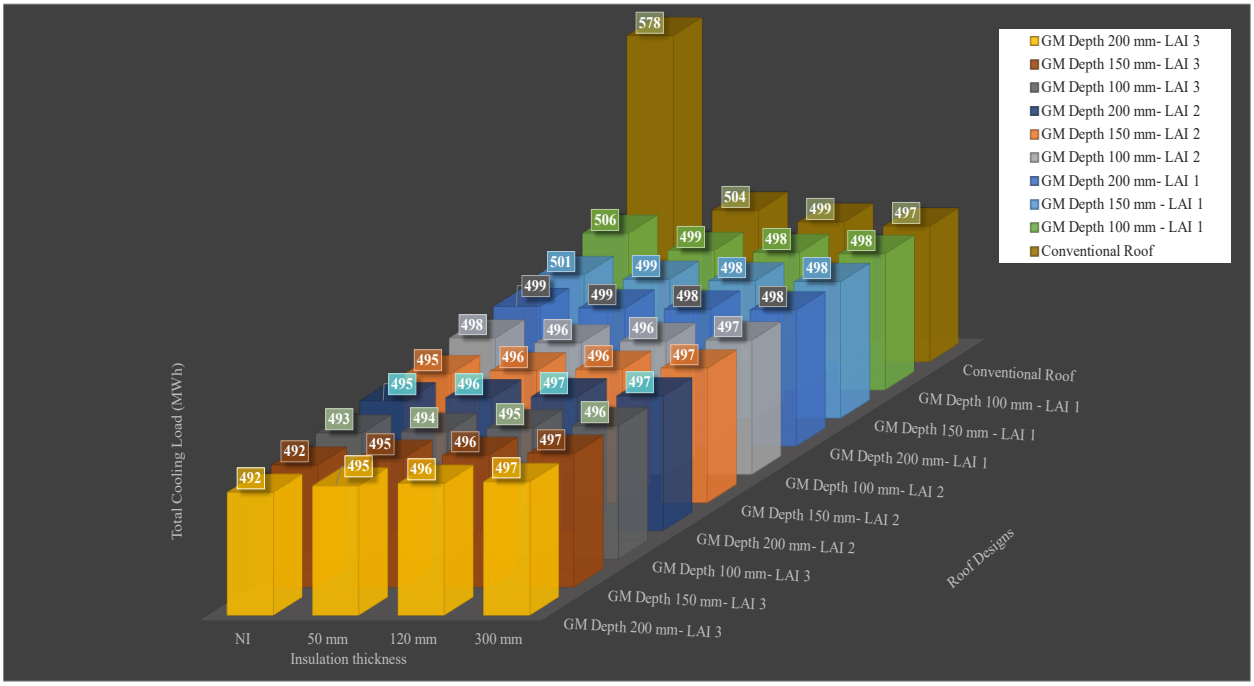

Figure E - 2: Total cooling loads for all roof designs; all insulation thickness; LAIs; and growing media depths under current climate – hospital building.

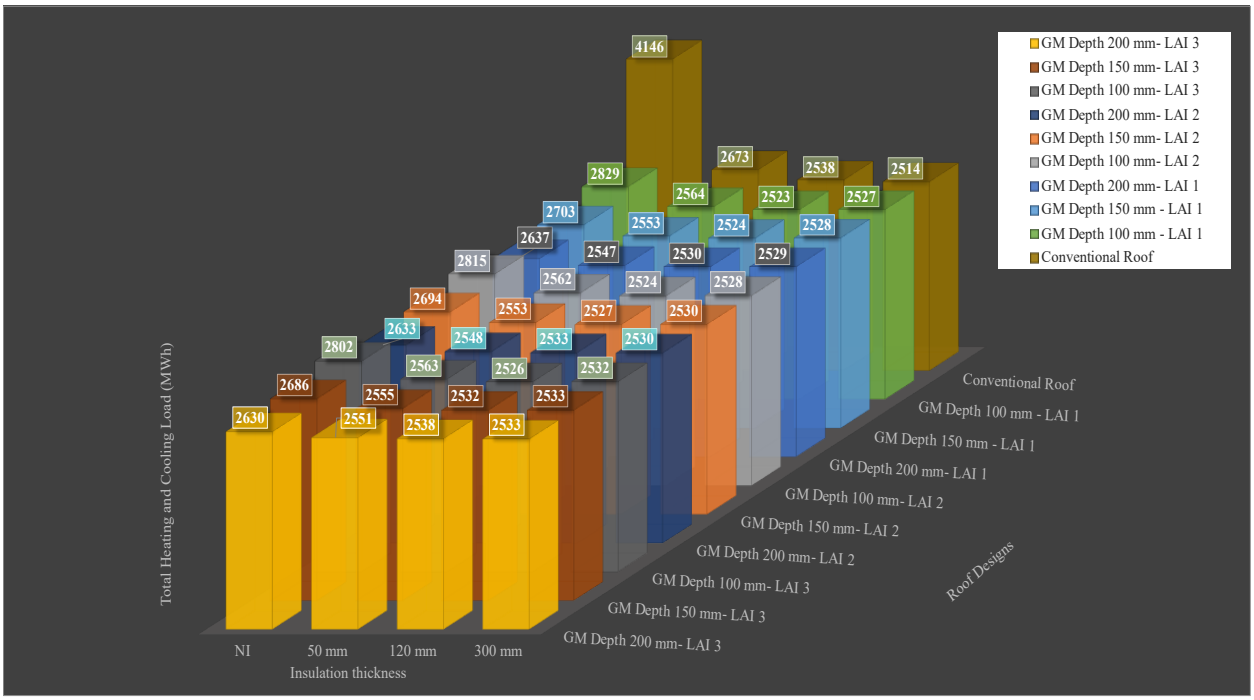

Figure E - 3: Total heating and cooling loads for all roof designs; all insulation thickness; LAIs; and growing media depths under current climate – hospital building.

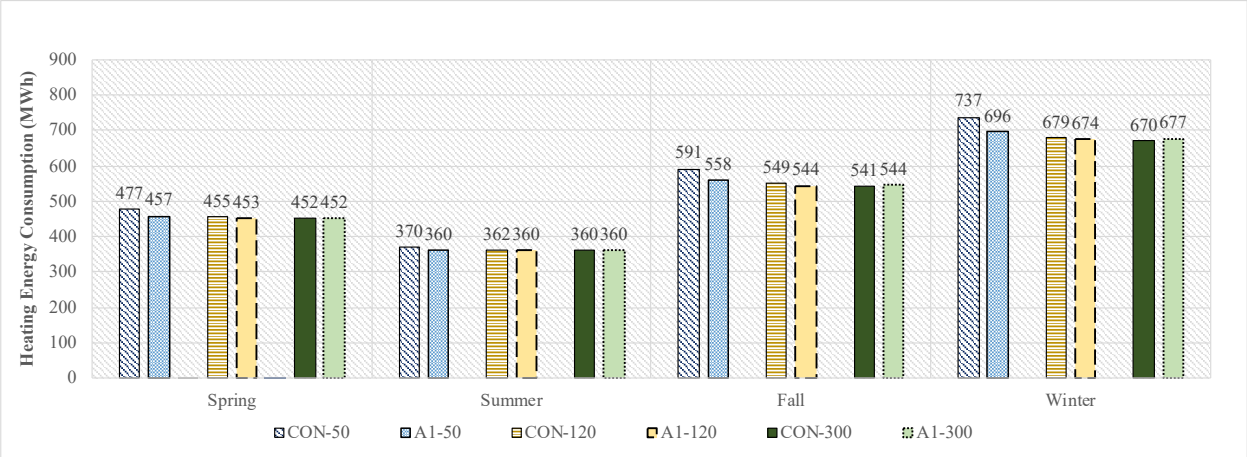

Figure E - 4: Seasonal heating loads for conventional roof and green roof with design of growing media of 100 mm and LAI of 1 for insulation thicknesses 50 mm, 120 mm and 300 mm – current climate (hospital building).

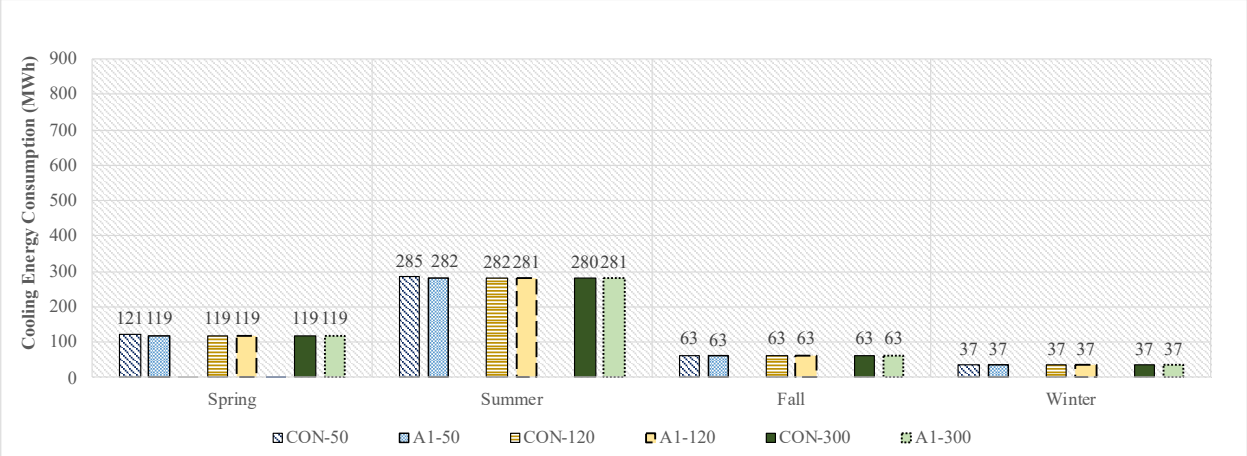

Figure E - 5: Seasonal cooling loads for conventional roof and green roof with design of growing media of 100 mm and LAI of 1 for insulation thicknesses 50 mm, 120 mm and 300 mm – current climate (hospital building).

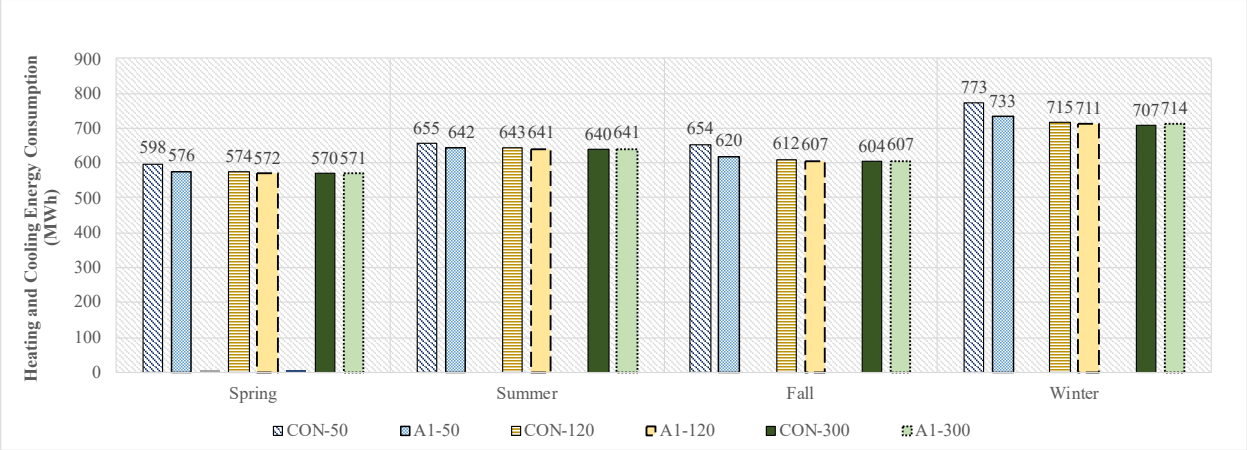

Figure E - 6: Seasonal total heating and cooling loads for conventional roof and green roof with design of growing media of 100 mm and LAI of 1 for insulation thicknesses 50 mm, 120 mm and 300 mm – current climate (hospital building).

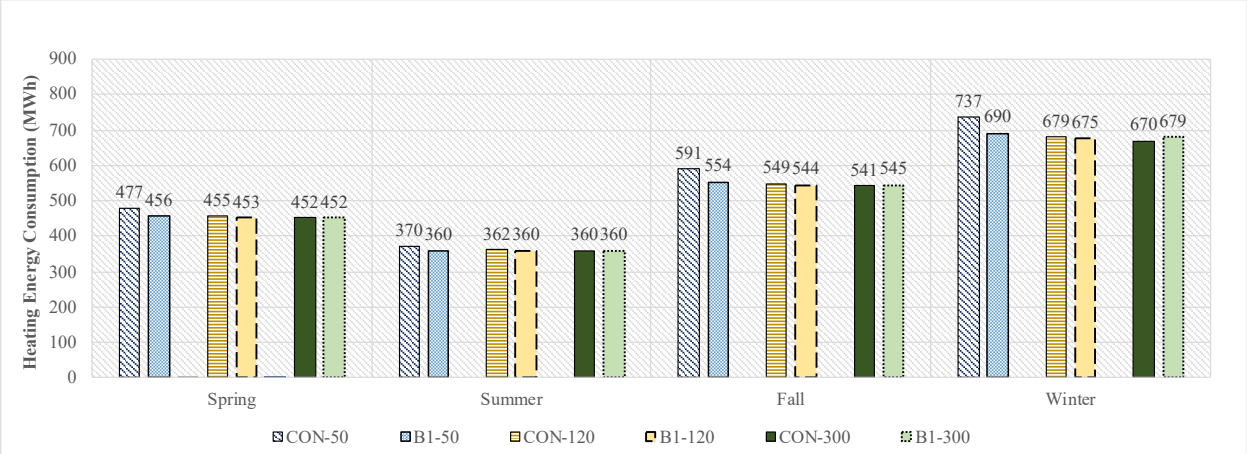

Figure E - 7: Seasonal heating loads for conventional roof and green roof with design of growing media of 150 mm and LAI of 1 for insulation thicknesses 50 mm, 120 mm and 300 mm – current climate (hospital building).

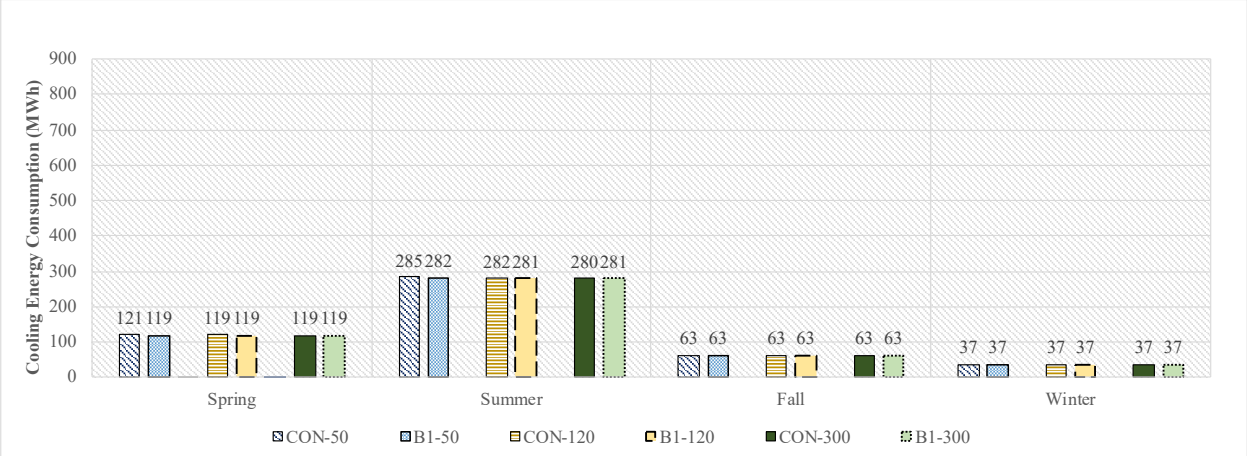

Figure E - 8: Seasonal cooling loads for conventional roof and green roof with design of growing media of 150 mm and LAI of 1 for insulation thicknesses 50 mm, 120 mm and 300 mm – current climate (hospital building).

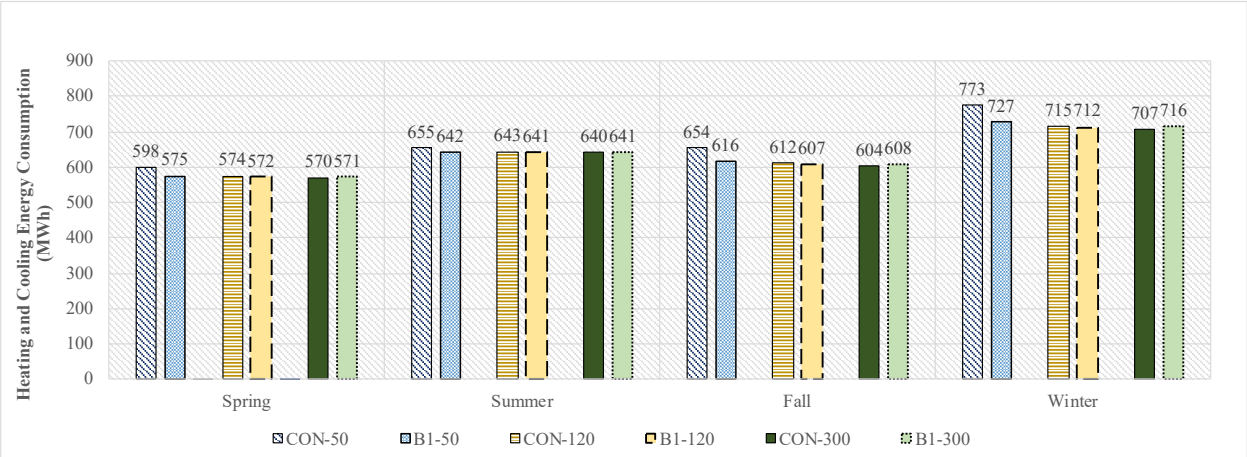

Figure E - 9: Seasonal total heating and cooling loads for conventional roof and green roof with design of growing media of 150 mm and LAI of 1 for insulation thicknesses 50 mm, 120 mm and 300 mm – current climate (hospital building).

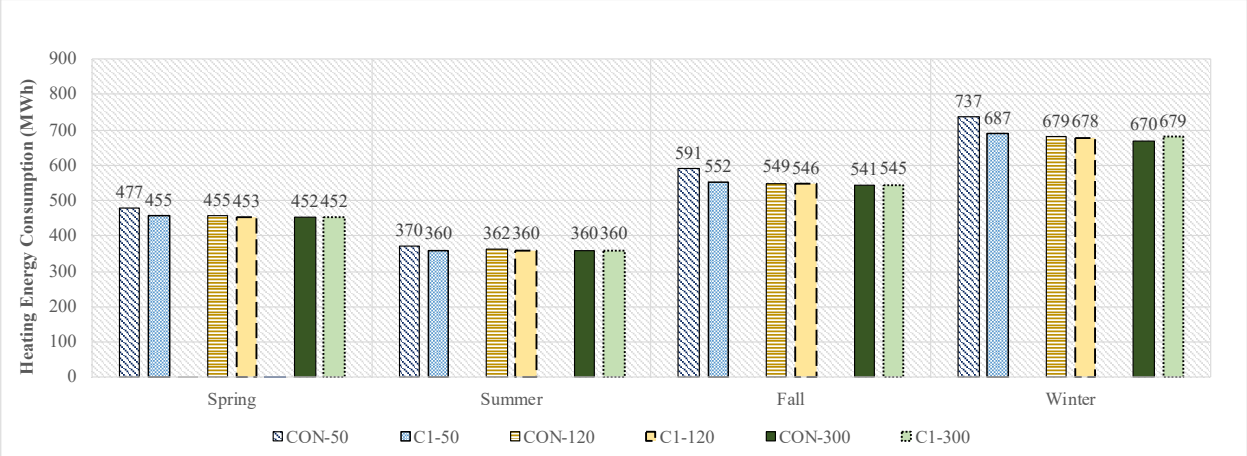

Figure E - 10: Seasonal heating loads for conventional roof and green roof with design of growing media of 200 mm and LAI of 1 for insulation thicknesses 50 mm, 120 mm and 300 mm – current climate (hospital building).

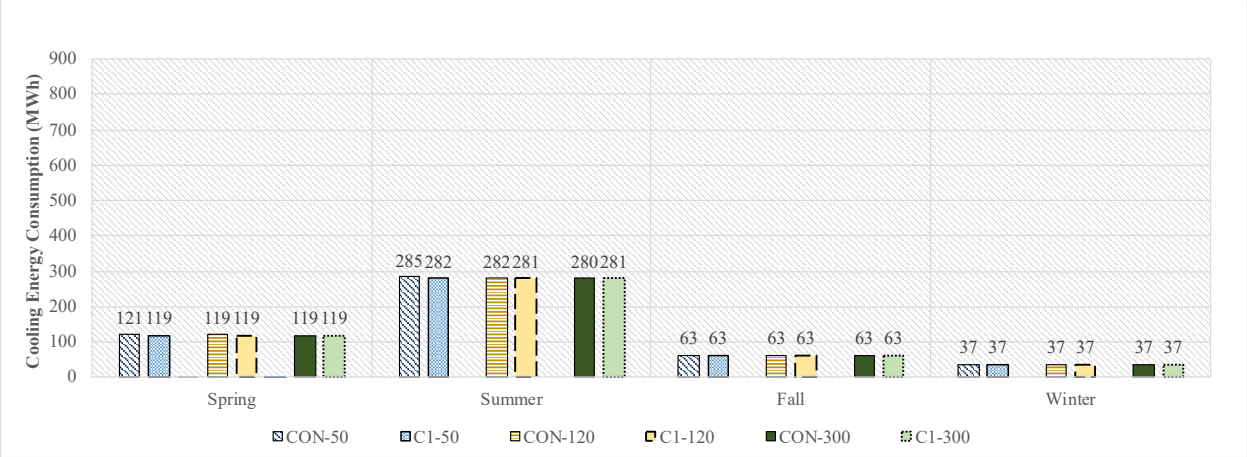

Figure E - 11: Seasonal cooling loads for conventional roof and green roof with design of growing media of 200 mm and LAI of 1 for insulation thicknesses 50 mm, 120 mm and 300 mm – current climate (hospital building).

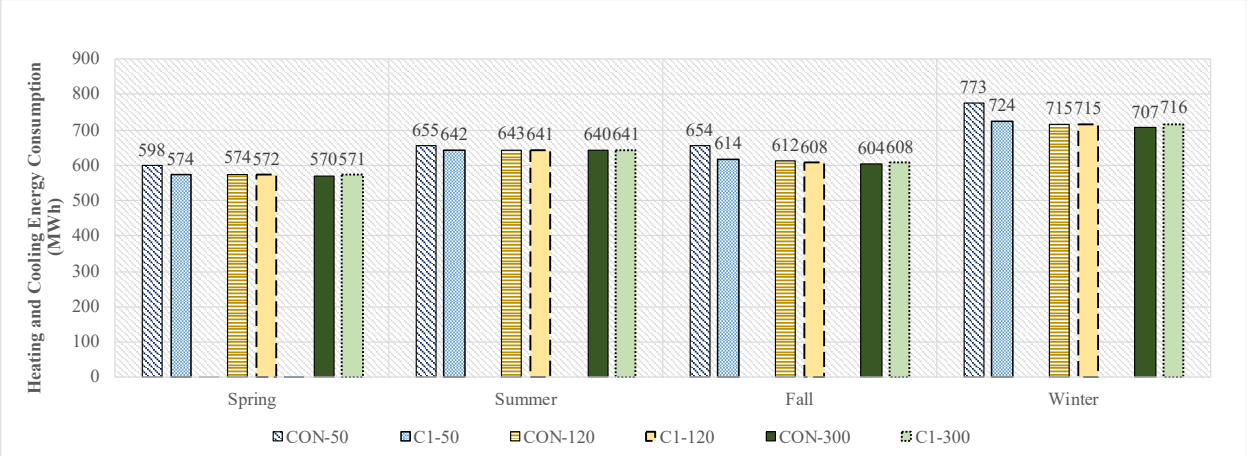

Figure E - 12: Seasonal total heating and cooling loads for conventional roof and green roof with design of growing media of 200 mm and LAI of 1 for insulation thicknesses 50 mm, 120 mm and 300 mm – current climate (hospital building).

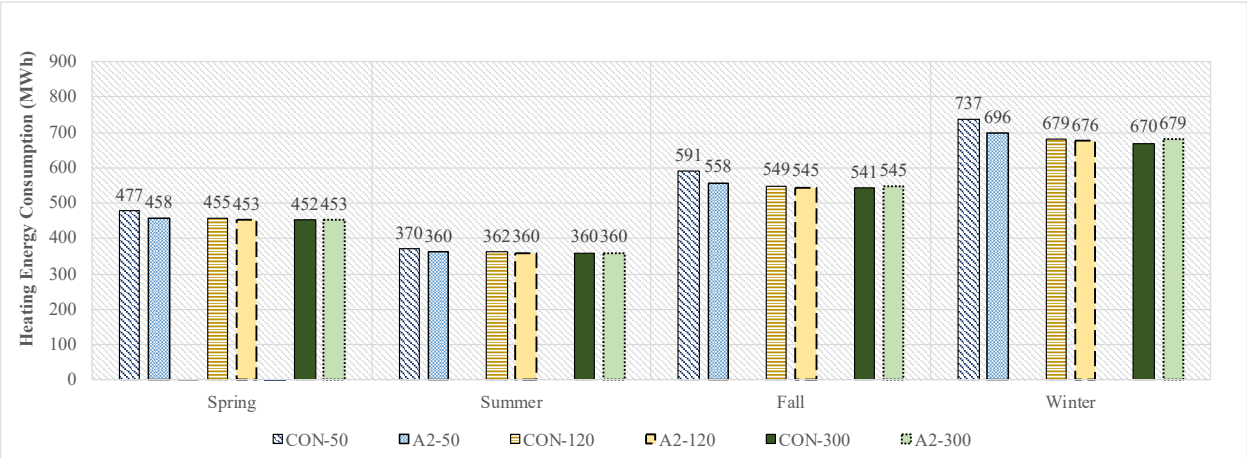

Figure E - 13: Seasonal heating loads for conventional roof and green roof with design of growing media of 100 mm and LAI of 2 for insulation thicknesses 50 mm, 120 mm and 300 mm – current climate (hospital building).

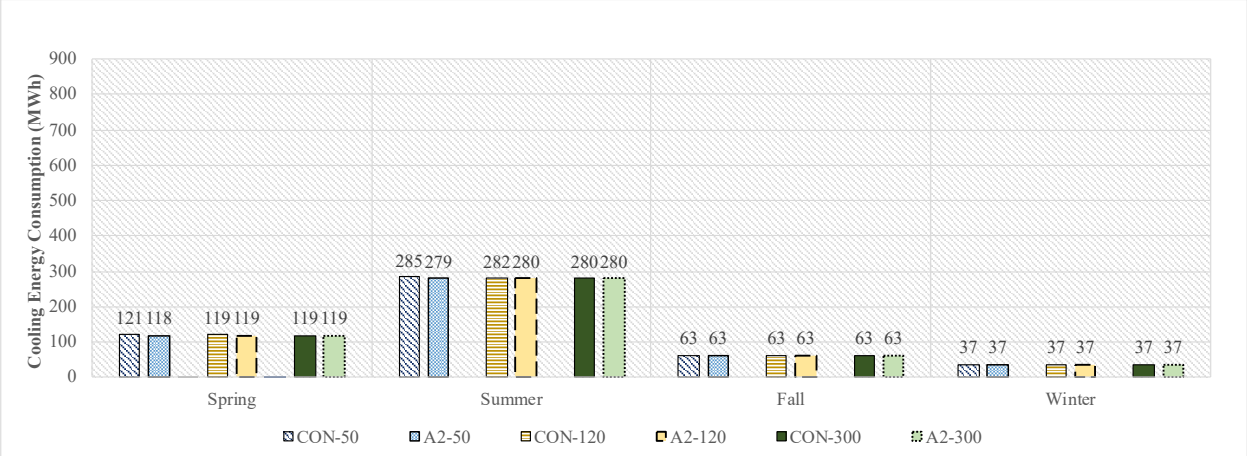

Figure E - 14: Seasonal cooling loads for conventional roof and green roof with design of growing media of 100 mm and LAI of 2 for insulation thicknesses 50 mm, 120 mm and 300 mm – current climate (hospital building).

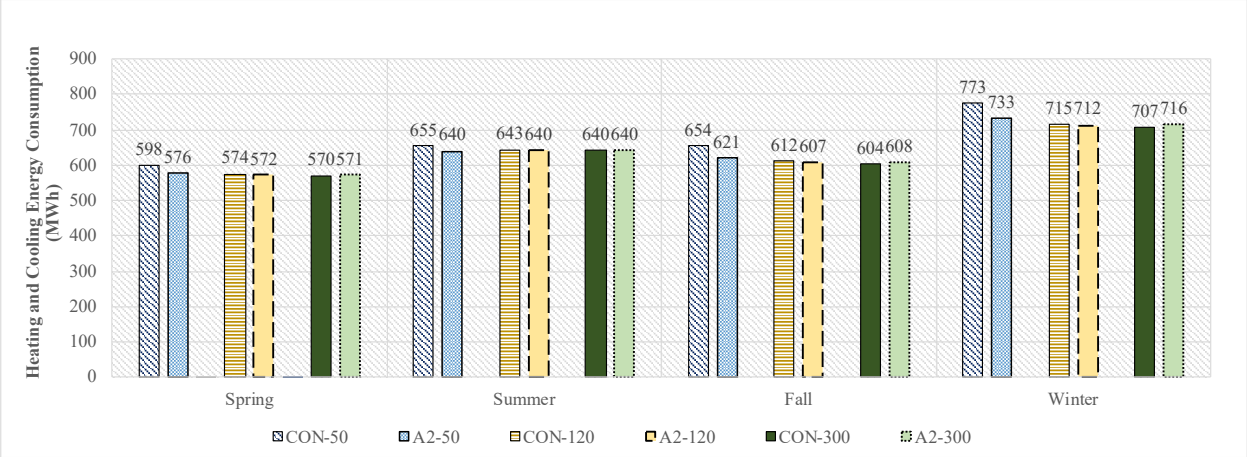

Figure E - 15: Seasonal total heating and cooling loads for conventional roof and green roof with design of growing media of 100 mm and LAI of 2 for insulation thicknesses 50 mm, 120 mm and 300 mm – current climate (hospital building).

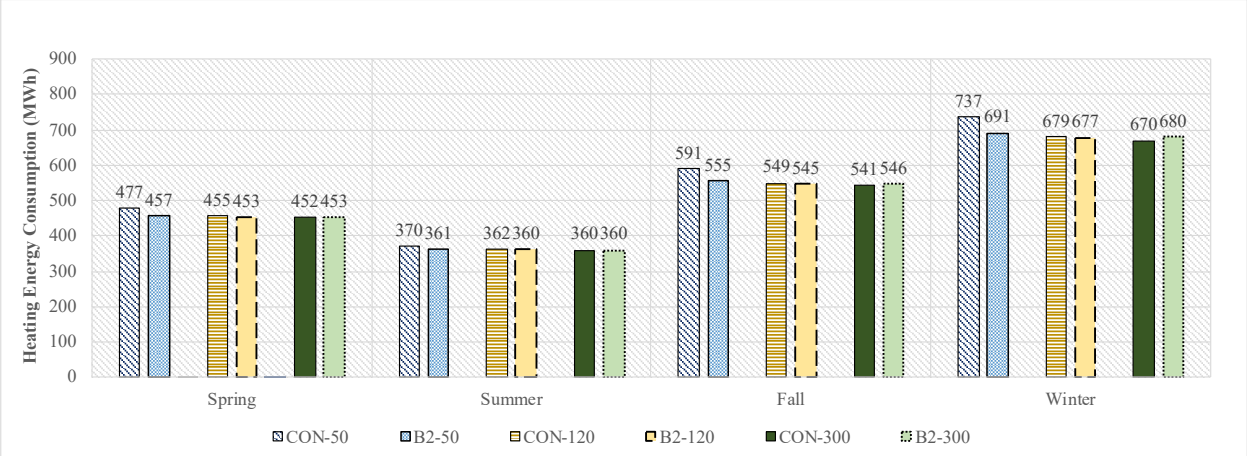

Figure E - 16: Seasonal heating loads for conventional roof and green roof with design of growing media of 150 mm and LAI of 2 for insulation thicknesses 50 mm, 120 mm and 300 mm – current climate (hospital building).

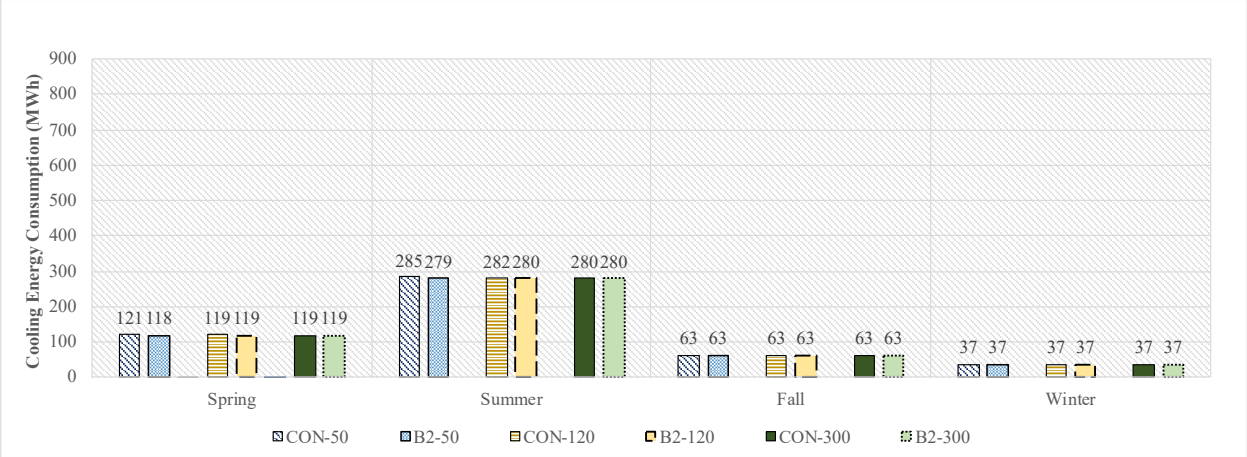

Figure E - 17: Seasonal cooling loads for conventional roof and green roof with design of growing media of 150 mm and LAI of 2 for insulation thicknesses 50 mm, 120 mm and 300 mm – current climate (hospital building).

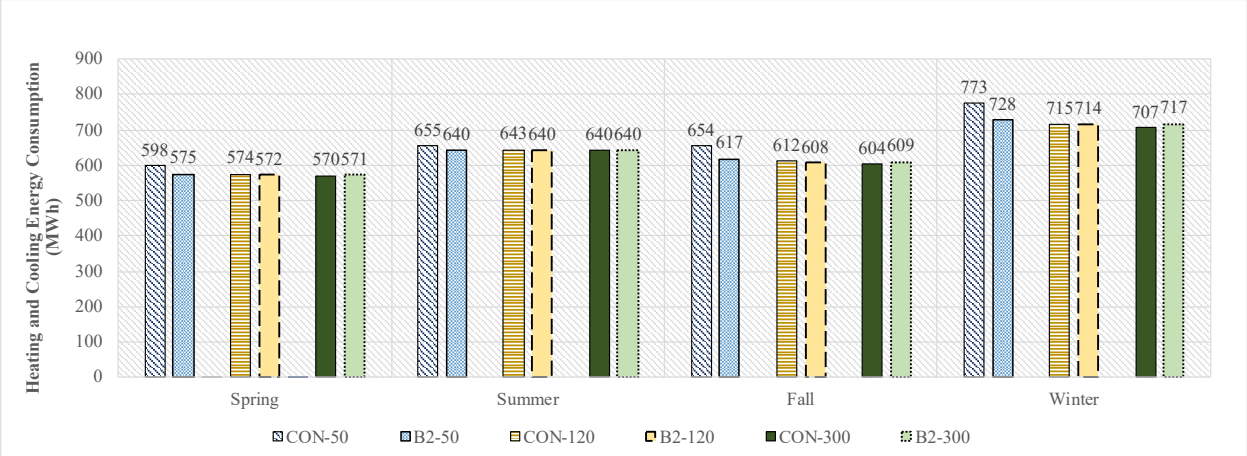

Figure E - 18: Seasonal total heating and cooling loads for conventional roof and green roof with design of growing media of 150 mm and LAI of 2 for insulation thicknesses 50 mm, 120 mm and 300 mm – current climate (hospital building).

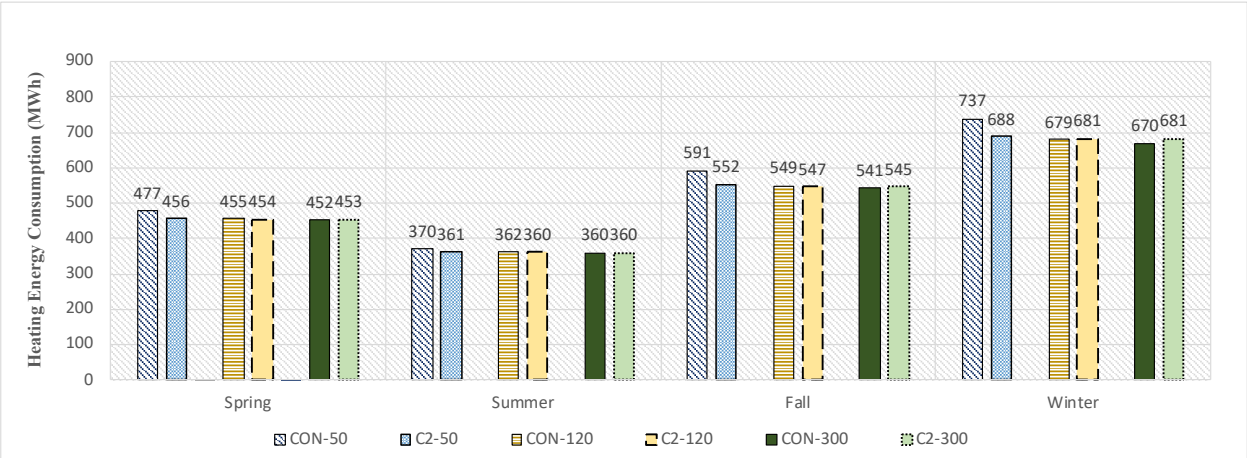

Figure E - 19: Seasonal heating loads for conventional roof and green roof with design of growing media of 200 mm and LAI of 2 for insulation thicknesses 50 mm, 120 mm and 300 mm – current climate (hospital building).

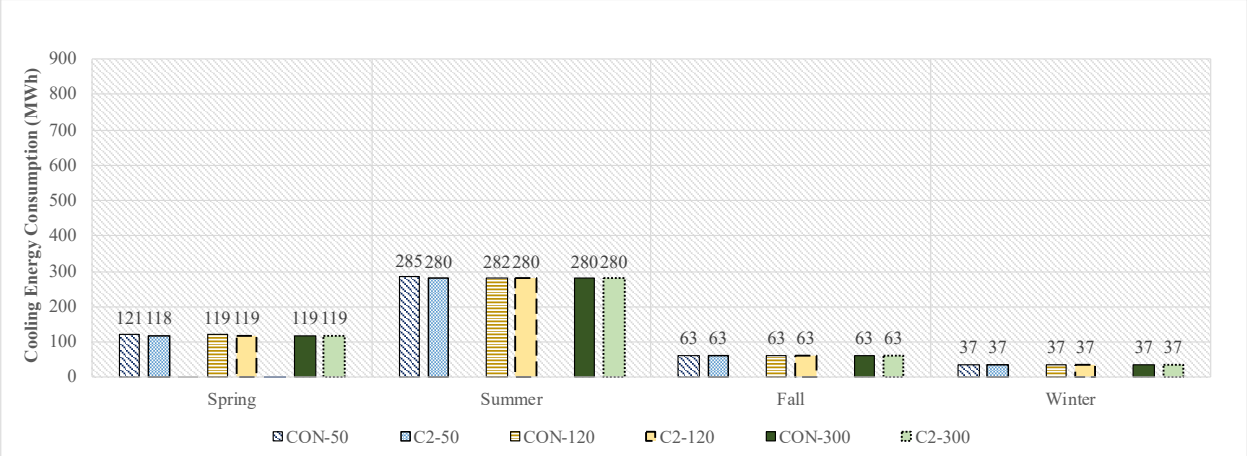

Figure E - 20: Seasonal cooling loads for conventional roof and green roof with design of growing media of 200 mm and LAI of 2 for insulation thicknesses 50 mm, 120 mm and 300 mm – current climate (hospital building).

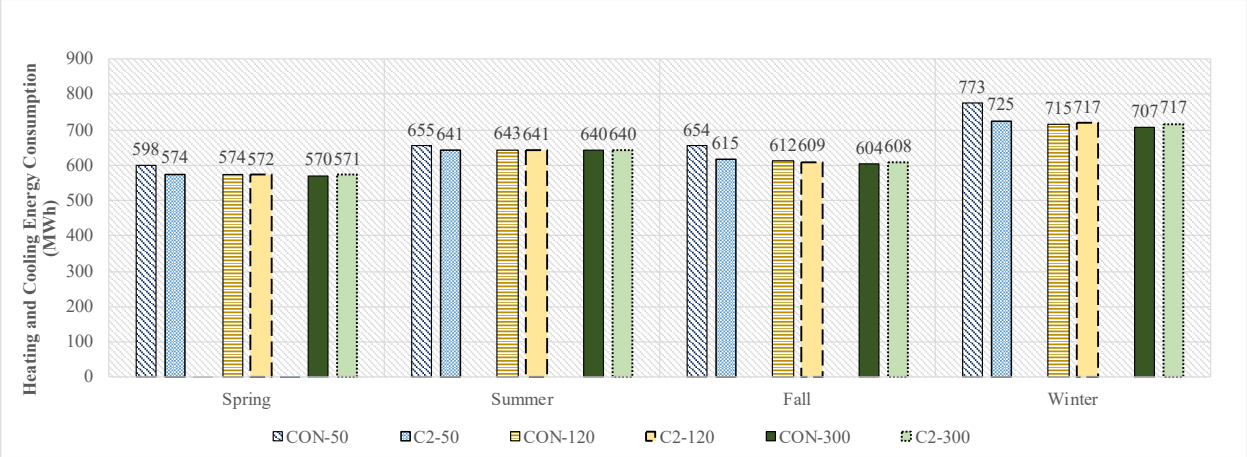

Figure E - 21: Seasonal total heating and cooling loads for conventional roof and green roof with design of growing media of 200 mm and LAI of 2 for insulation thicknesses 50 mm, 120 mm and 300 mm – current climate (hospital building).

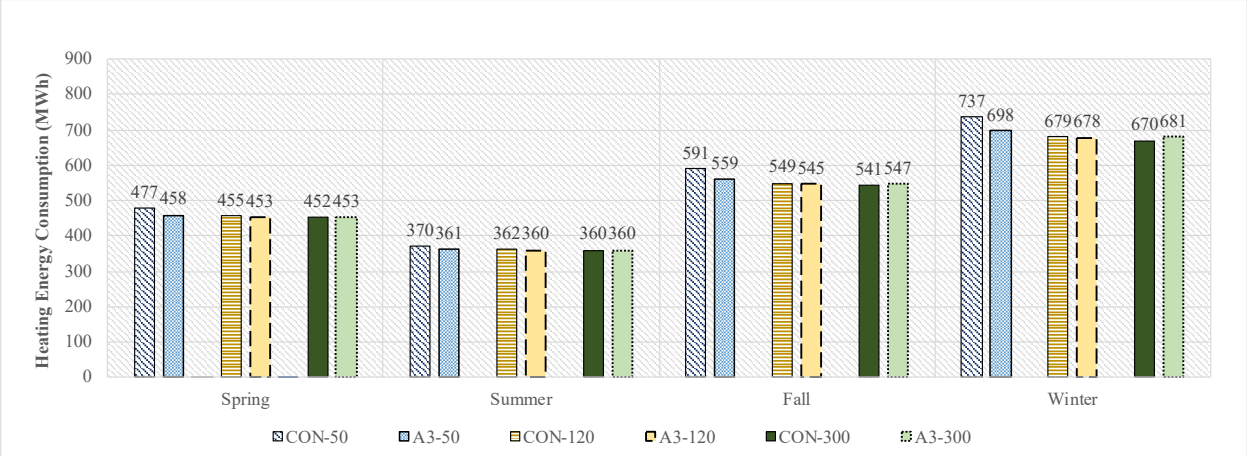

Figure E - 22: Seasonal heating loads for conventional roof and green roof with design of growing media of 100 mm and LAI of 3 for insulation thicknesses 50 mm, 120 mm and 300 mm – current climate (hospital building).

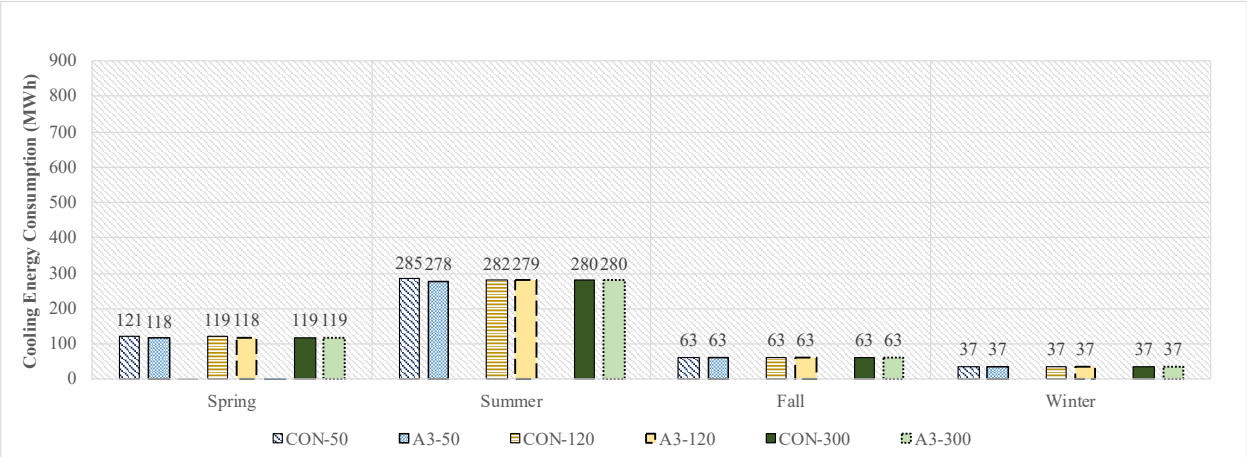

Figure E - 23: Seasonal cooling loads for conventional roof and green roof with design of growing media of 100 mm and LAI of 3 for insulation thicknesses 50 mm, 120 mm and 300 mm – current climate (hospital building).

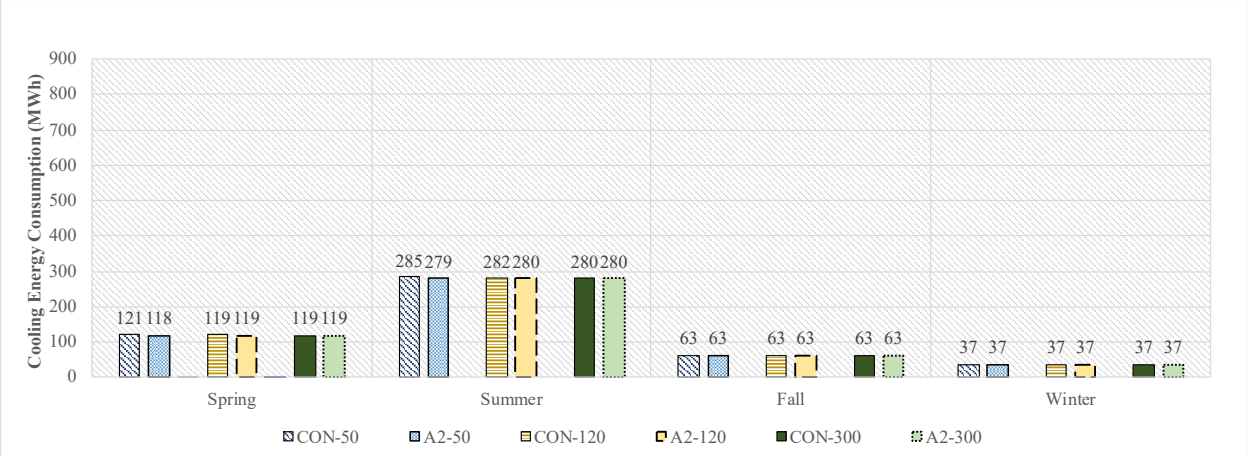

Figure E - 24: Seasonal cooling loads for conventional roof and green roof with design of growing media of 100 mm and LAI of 2 for insulation thicknesses 50 mm, 120 mm and 300 mm – current climate (hospital building).

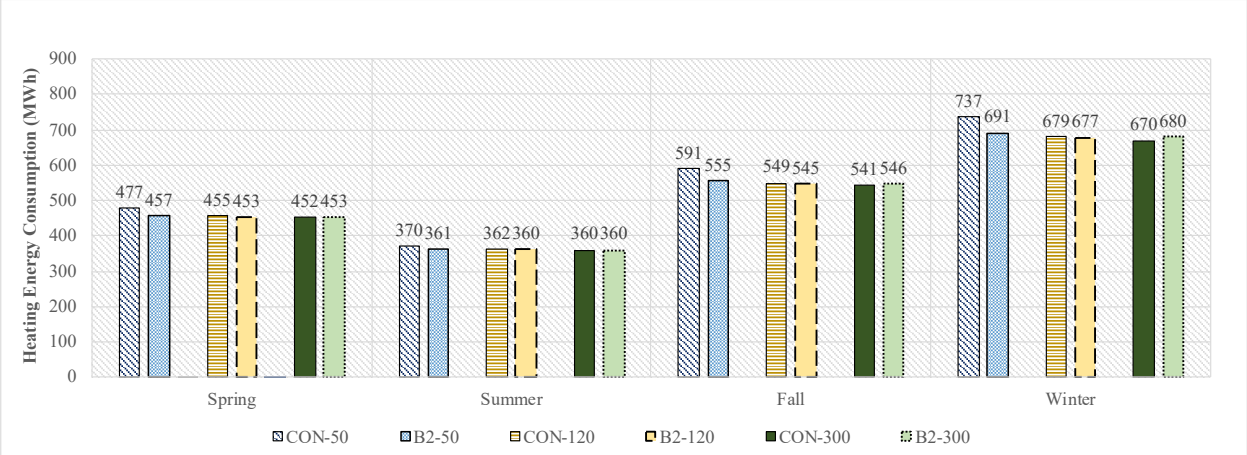

Figure E - 25: Seasonal heating loads for conventional roof and green roof with design of growing media of 150 mm and LAI of 2 for insulation thicknesses 50 mm, 120 mm and 300 mm – current climate (hospital building).

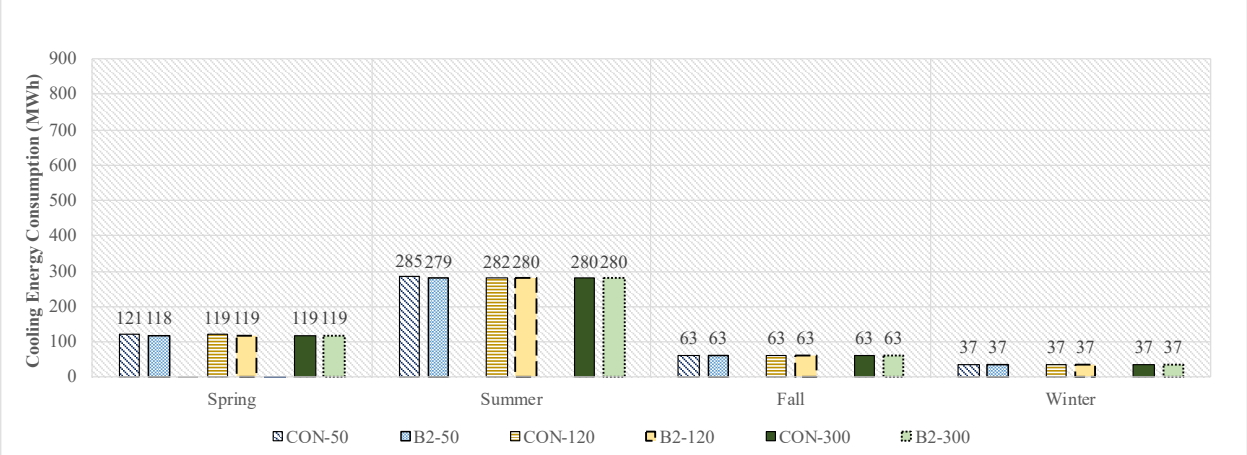

Figure E - 26: Seasonal cooling loads for conventional roof and green roof with design of growing media of 150 mm and LAI of 2 for insulation thicknesses 50 mm, 120 mm and 300 mm – current climate (hospital building).

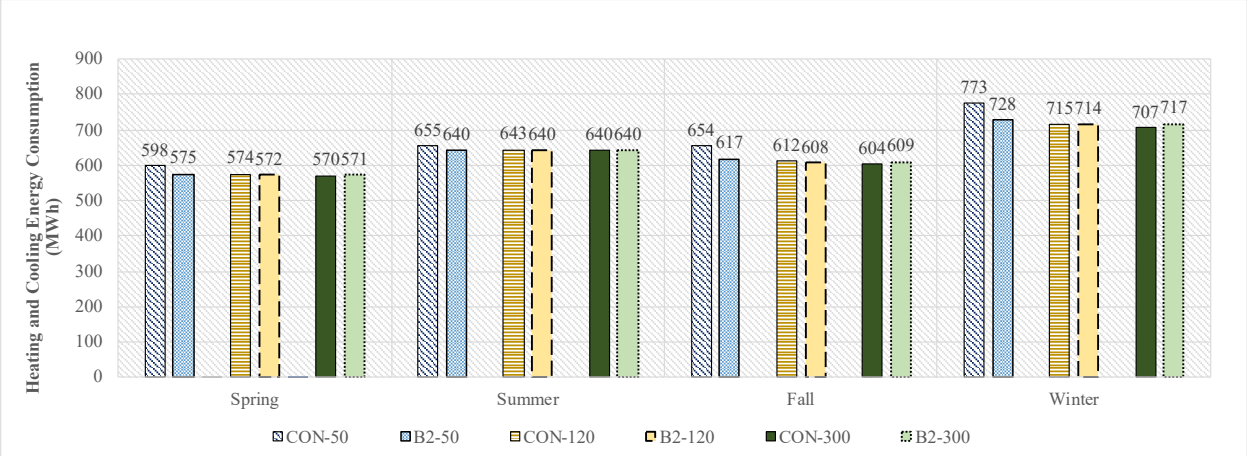

Figure E - 27: Seasonal total heating and cooling loads for conventional roof and green roof with design of growing media of 150 mm and LAI of 2 for insulation thicknesses 50 mm, 120 mm and 300 mm – current climate (hospital building).

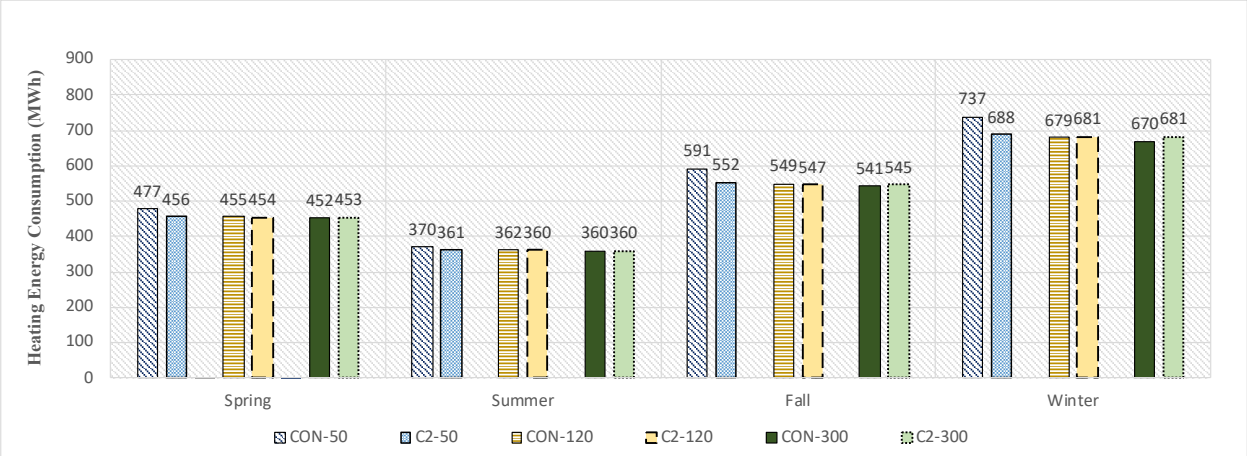

Figure E - 28: Seasonal heating loads for conventional roof and green roof with design of growing media of 200 mm and LAI of 2 for insulation thicknesses 50 mm, 120 mm and 300 mm – current climate (hospital building).

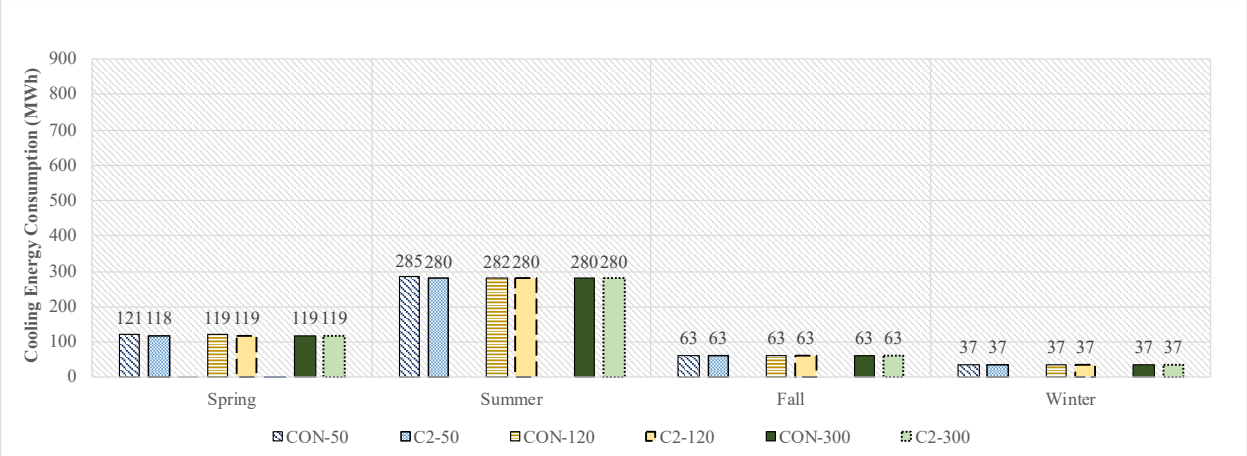

Figure E - 29: Seasonal cooling loads for conventional roof and green roof with design of growing media of 200 mm and LAI of 2 for insulation thicknesses 50 mm, 120 mm and 300 mm – current climate (hospital building).

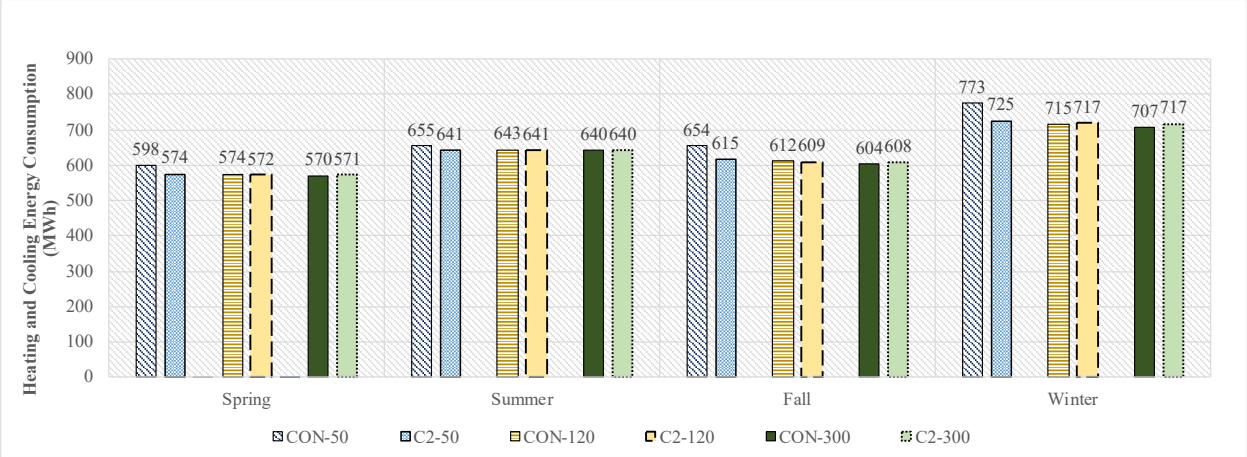

Figure E - 30: Seasonal total heating and cooling loads for conventional roof and green roof with design of growing media of 200 mm and LAI of 2 for insulation thicknesses 50 mm, 120 mm and 300 mm – current climate (hospital building).

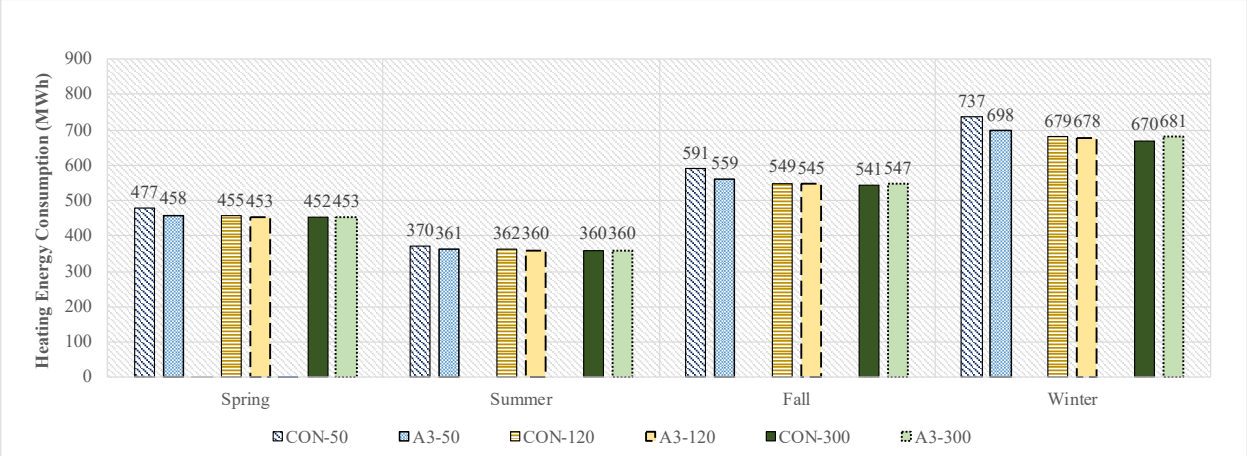

Figure E - 31: Seasonal heating loads for conventional roof and green roof with design of growing media of 100 mm and LAI of 3 for insulation thicknesses 50 mm, 120 mm and 300 mm – current climate (hospital building).

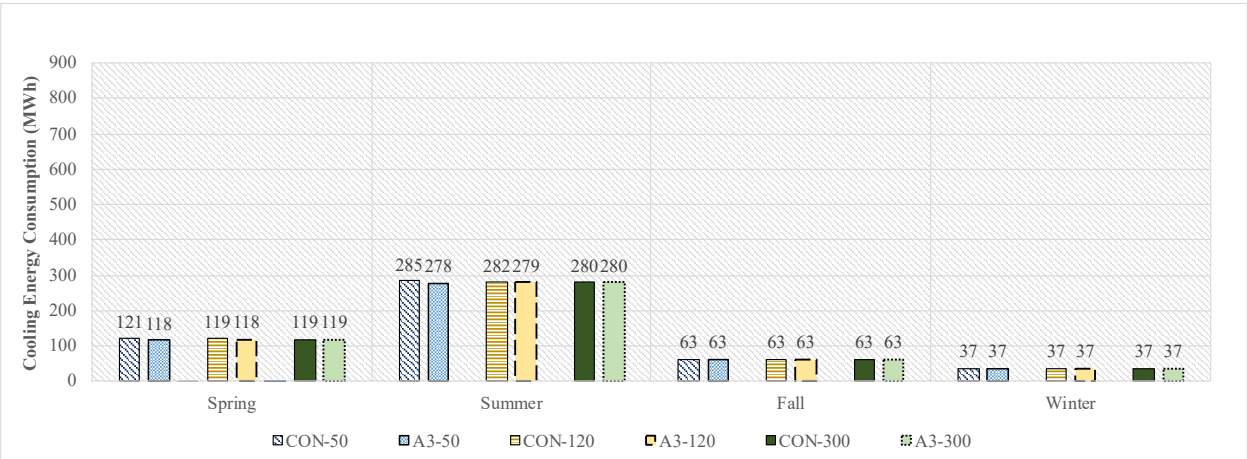

Figure E - 32: Seasonal cooling loads for conventional roof and green roof with design of growing media of 100 mm and LAI of 3 for insulation thicknesses 50 mm, 120 mm and 300 mm – current climate (hospital building).

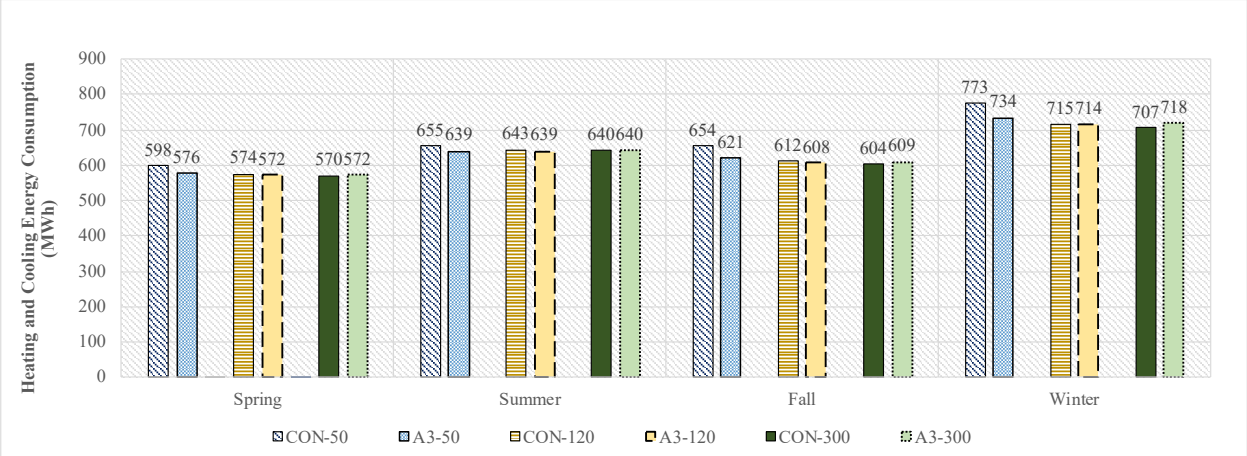

Figure E - 33: Seasonal total heating and cooling loads for conventional roof and green roof with design of growing media of 100 mm and LAI of 3 for insulation thicknesses 50 mm, 120 mm and 300 mm – current climate (hospital building).

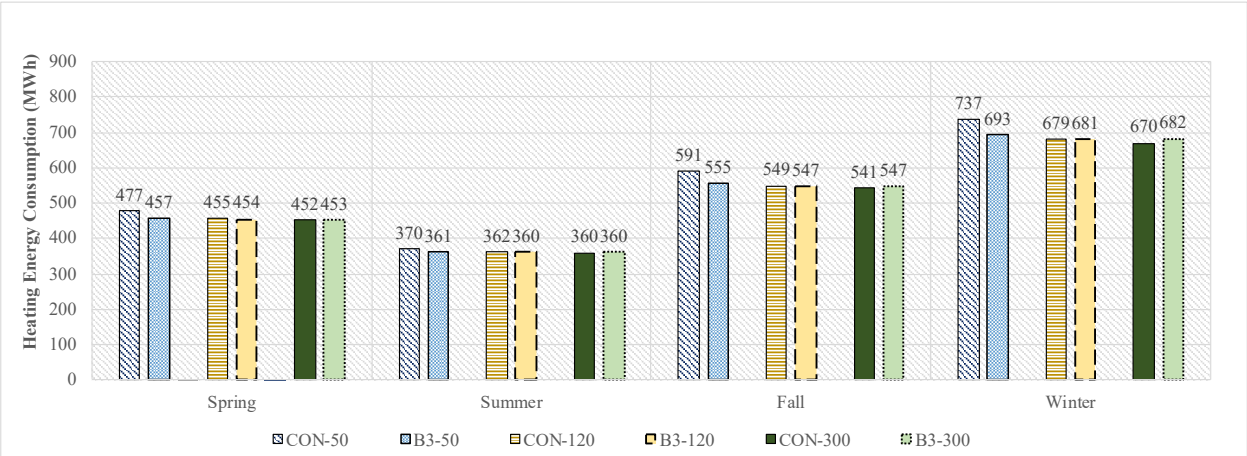

Figure E - 34: Seasonal heating loads for conventional roof and green roof with design of growing media of 150 mm and LAI of 3 for insulation thicknesses 50 mm, 120 mm and 300 mm – current climate (hospital building).

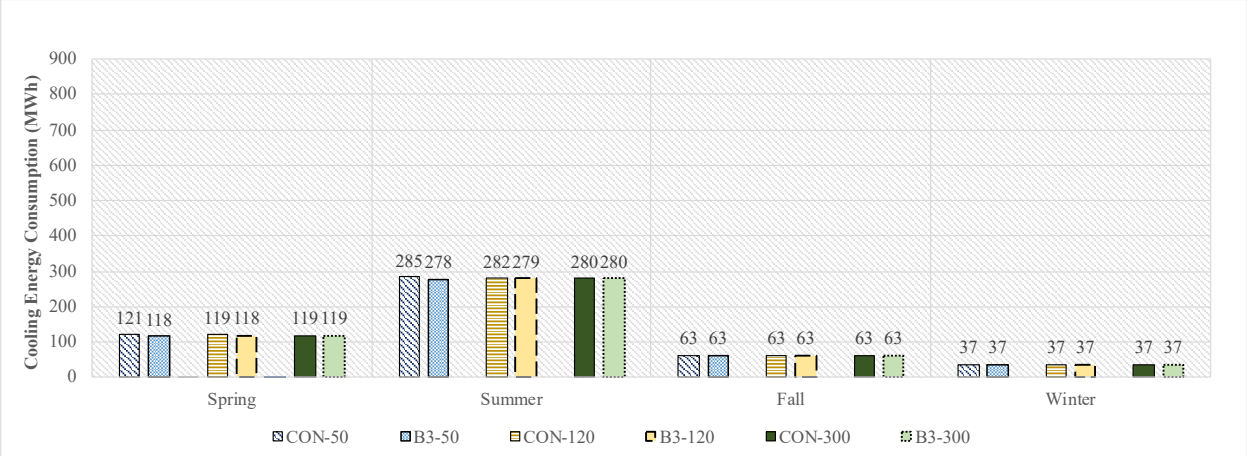

Figure E - 35: Seasonal cooling loads for conventional roof and green roof with design of growing media of 150 mm and LAI of 3 for insulation thicknesses 50 mm, 120 mm and 300 mm – current climate (hospital building).

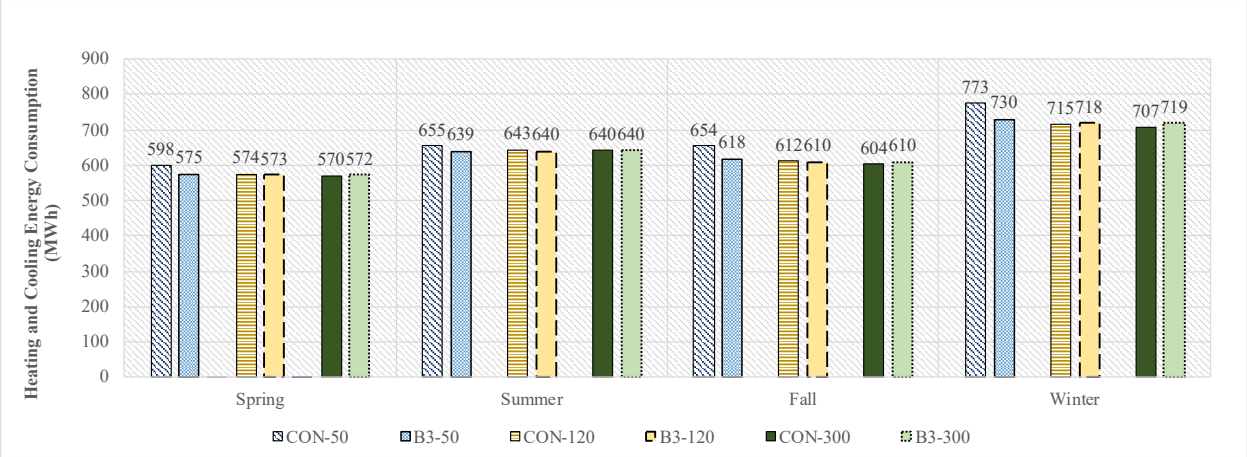

Figure E - 36: Seasonal total heating and cooling loads for conventional roof and green roof with design of growing media of 150 mm and LAI of 3 for insulation thicknesses 50 mm, 120 mm and 300 mm – current climate (hospital building).

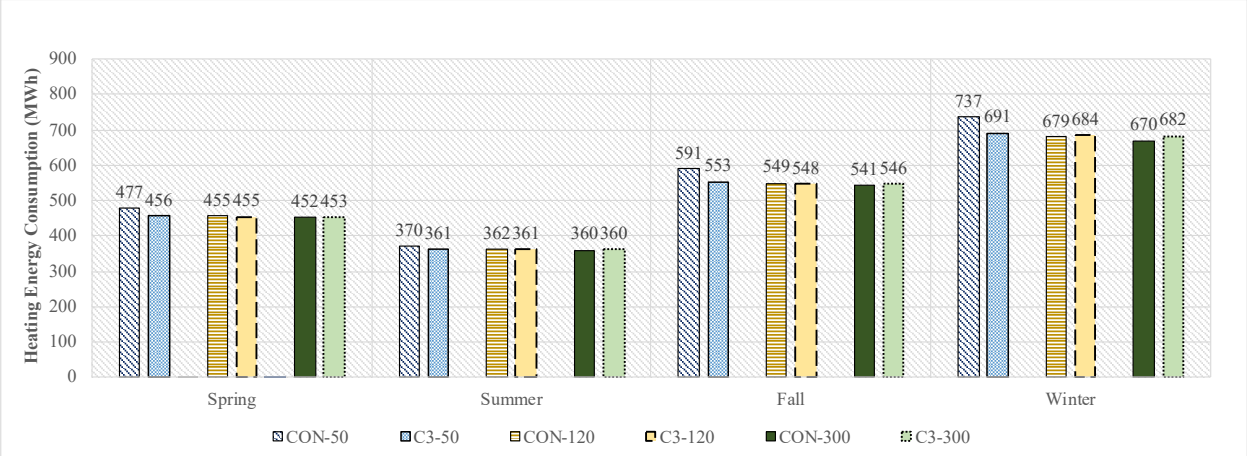

Figure E - 37: Seasonal heating loads for conventional roof and green roof with design of growing media of 200 mm and LAI of 3 for insulation thicknesses 50 mm, 120 mm and 300 mm – current climate (hospital building).

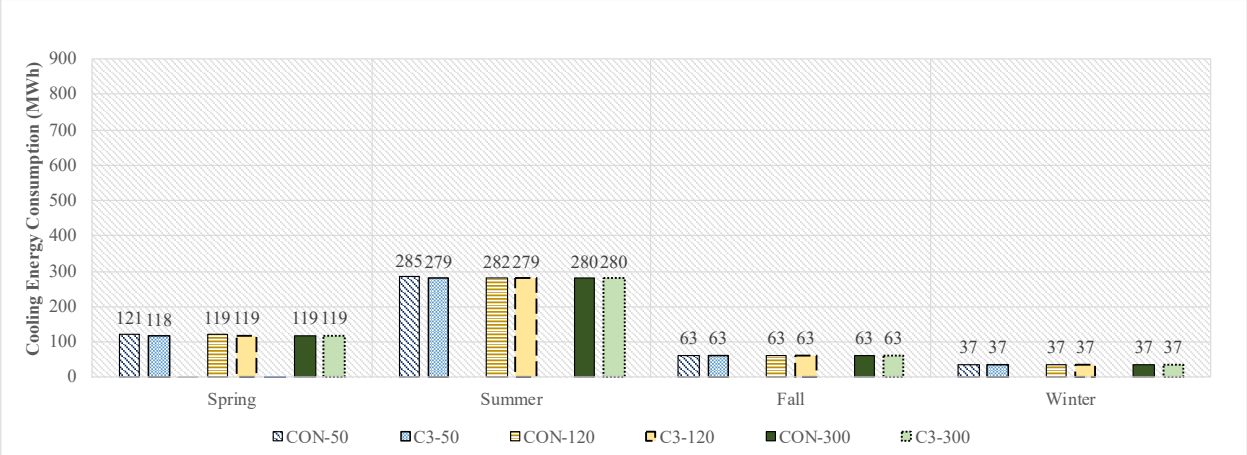

Figure E - 38: Seasonal cooling loads for conventional roof and green roof with design of growing media of 200 mm and LAI of 3 for insulation thicknesses 50 mm, 120 mm and 300 mm – current climate (hospital building).

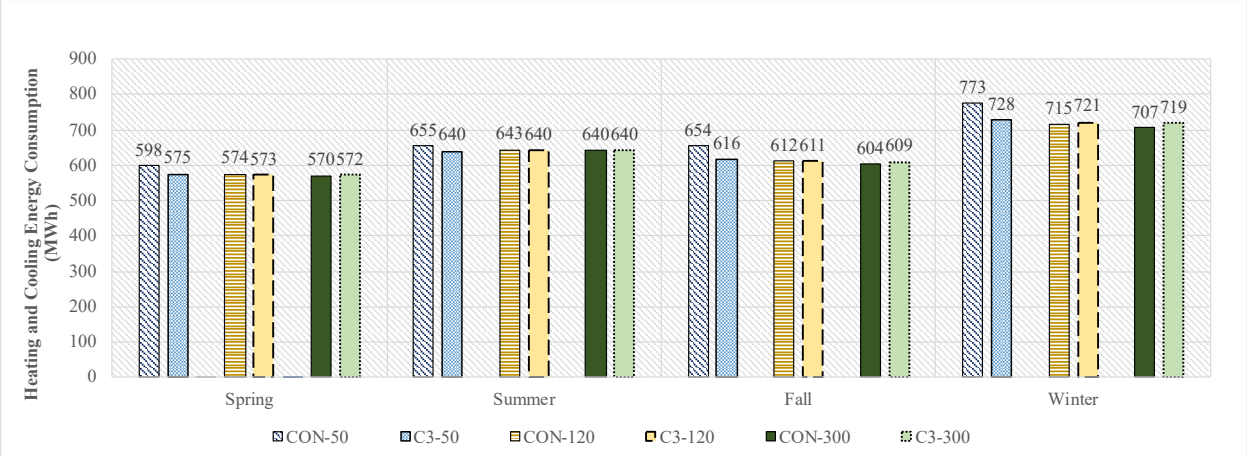

Figure E - 39: Seasonal total heating and cooling loads for conventional roof and green roof with design of growing media of 200 mm and LAI of 3 for insulation thicknesses 50 mm, 120 mm and 300 mm – current climate (hospital building).

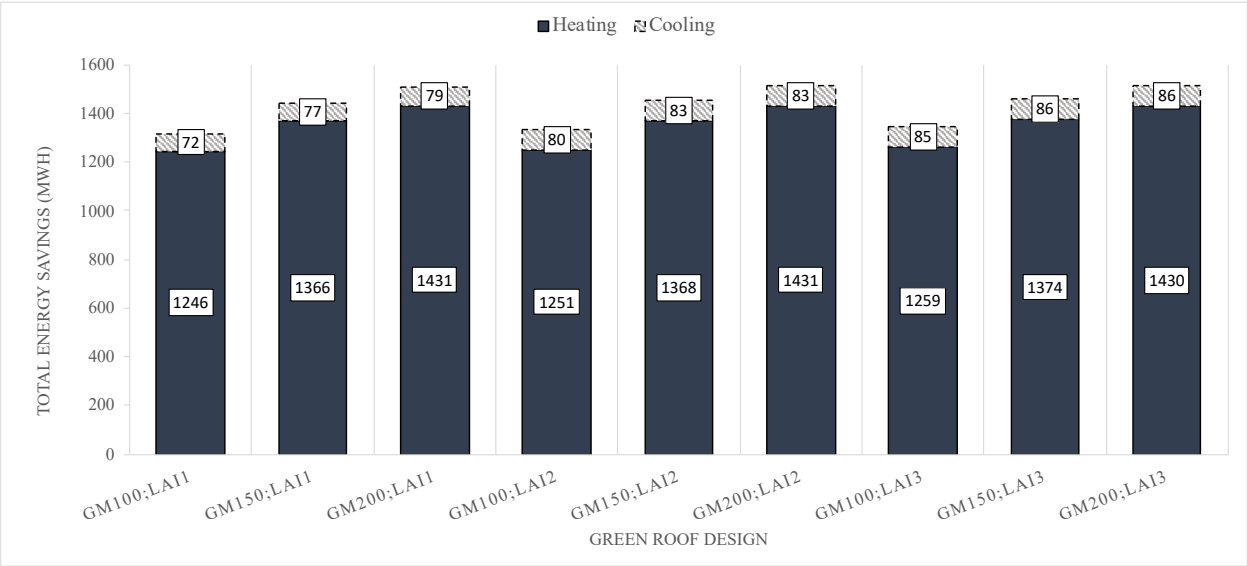

Figure E - 40: Total heating and cooling energy savings (MWh) of green roof compared to conventional roof for all growing media (GM) depths and LAIs; without insulation layer – current climate (hospital building).

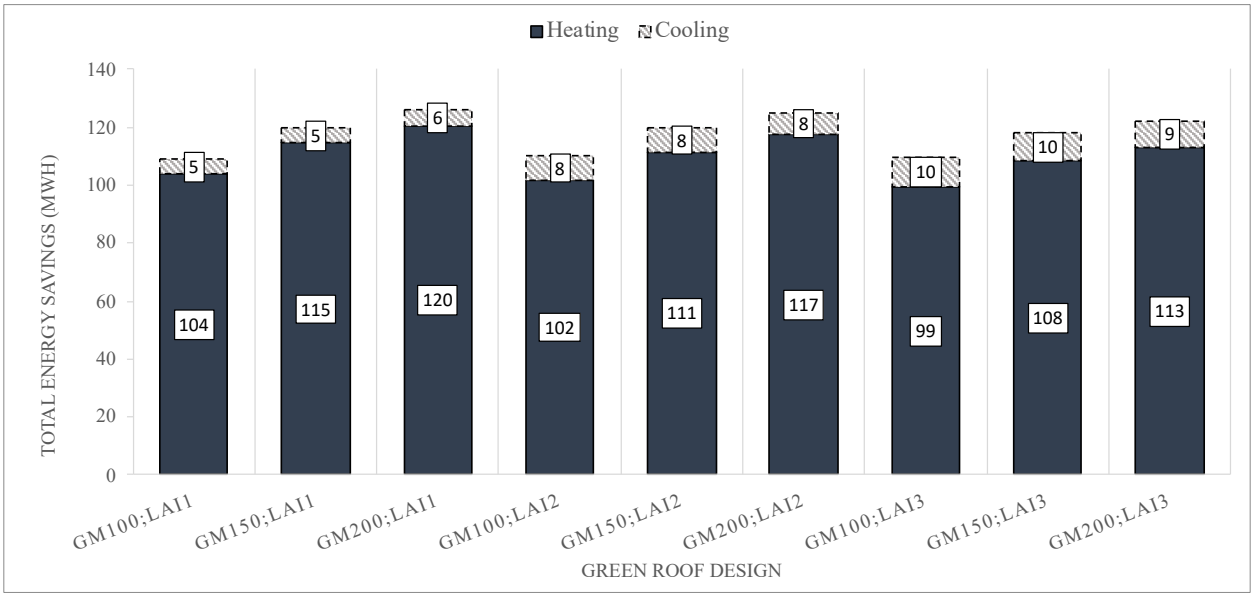

Figure E - 41: Total heating and cooling energy savings (MWh) of green roof compared to conventional roof for all growing media (GM) depths and LAIs; with 50 mm insulation layer – current climate (hospital building).

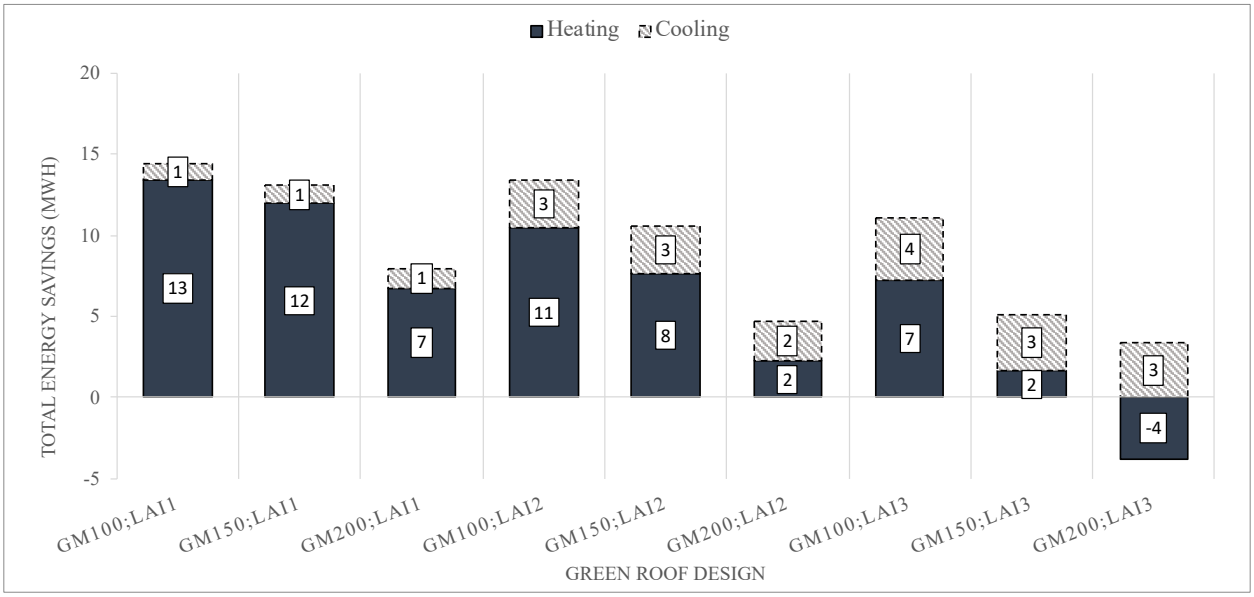

Figure E - 42: Total heating and cooling energy savings (MWh) of green roof compared to conventional roof for all growing media (GM) depths and LAIs; with 120 mm insulation layer – current climate (hospital building).

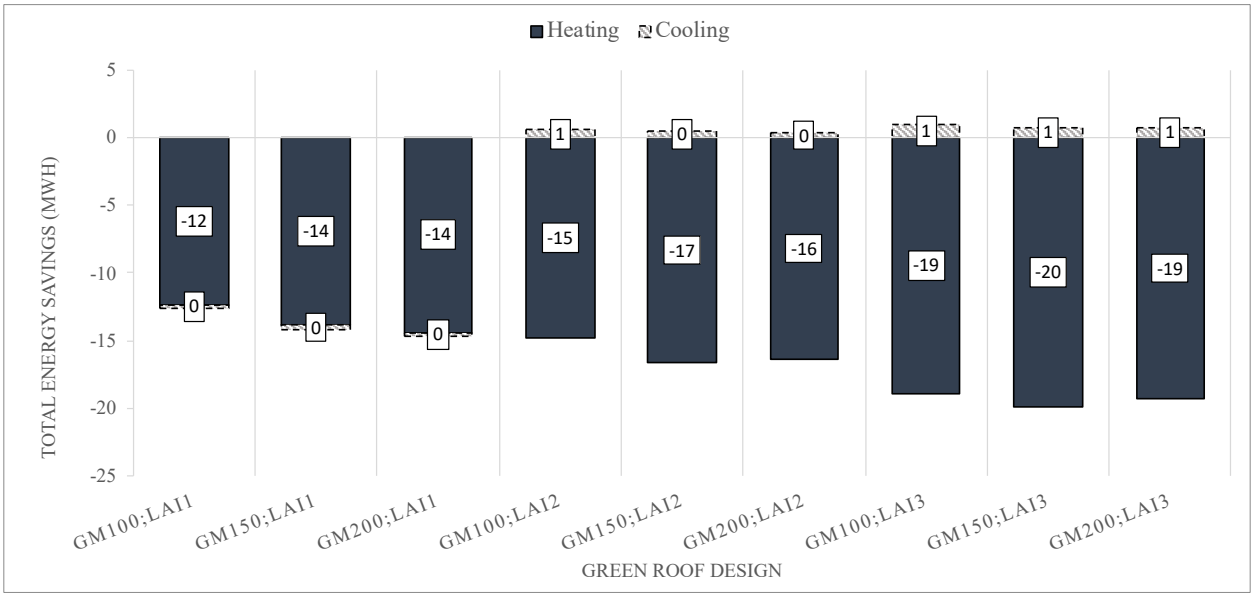

Figure E - 43: Total heating and cooling energy savings (MWh) of green roof compared to conventional roof for all growing media (GM) depths and LAIs; with 300 mm insulation layer – current climate (hospital building).

Appendix F: Annual Energy Consumption and Savings for Cooling/Heating Loads – Future Climate Conditions Hospital Building

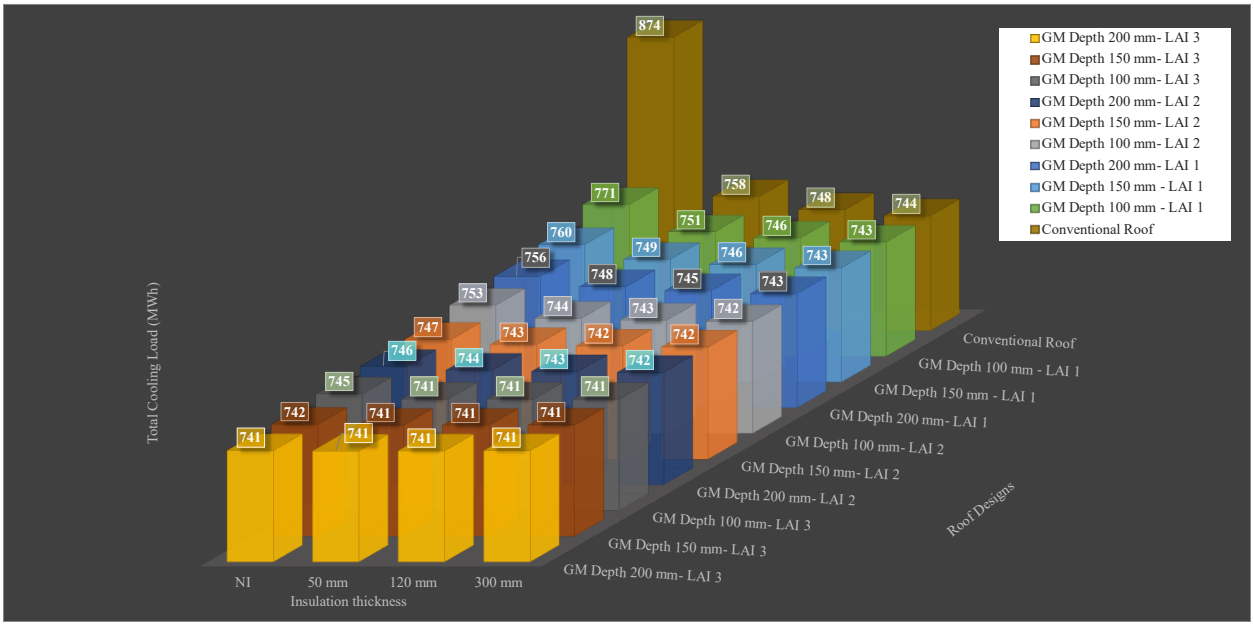

Figure F - 1: Total heating loads for all roof designs; all insulation thickness; LAIs; and growing media depths under future climate – hospital building.

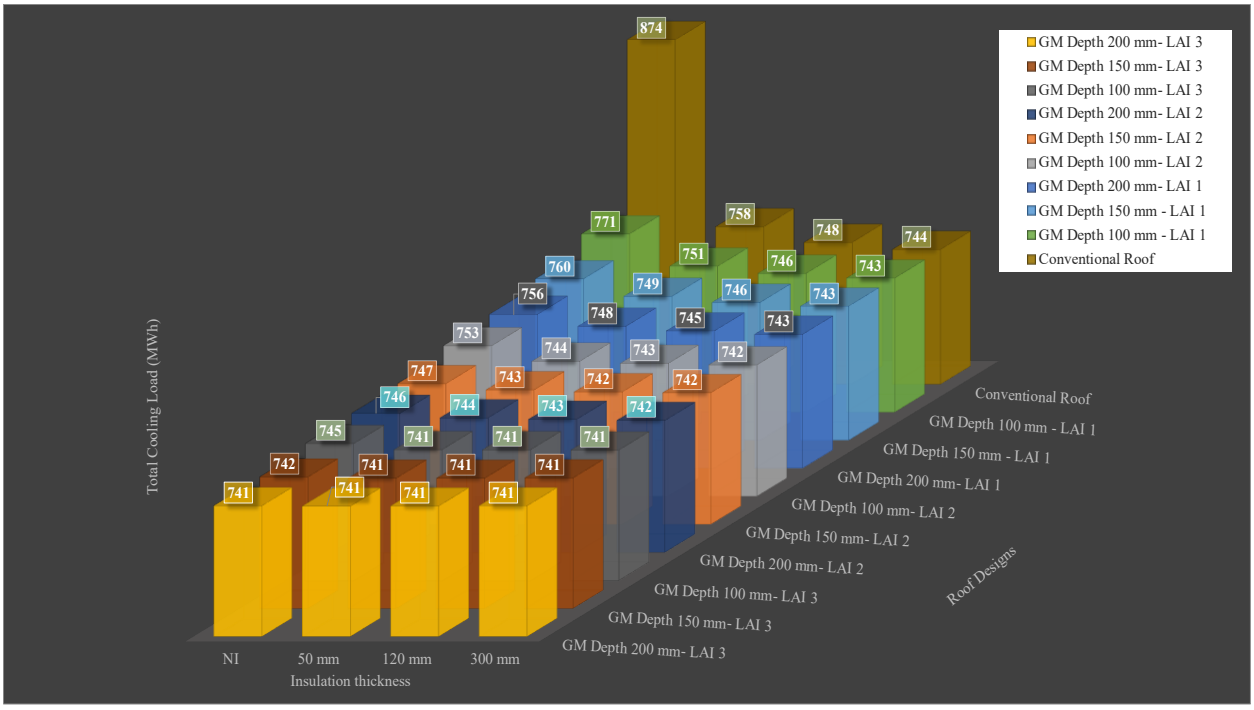

Figure F - 2: Total cooling loads for all roof designs; all insulation thickness; LAIs; and growing media depths under future climate – hospital building.

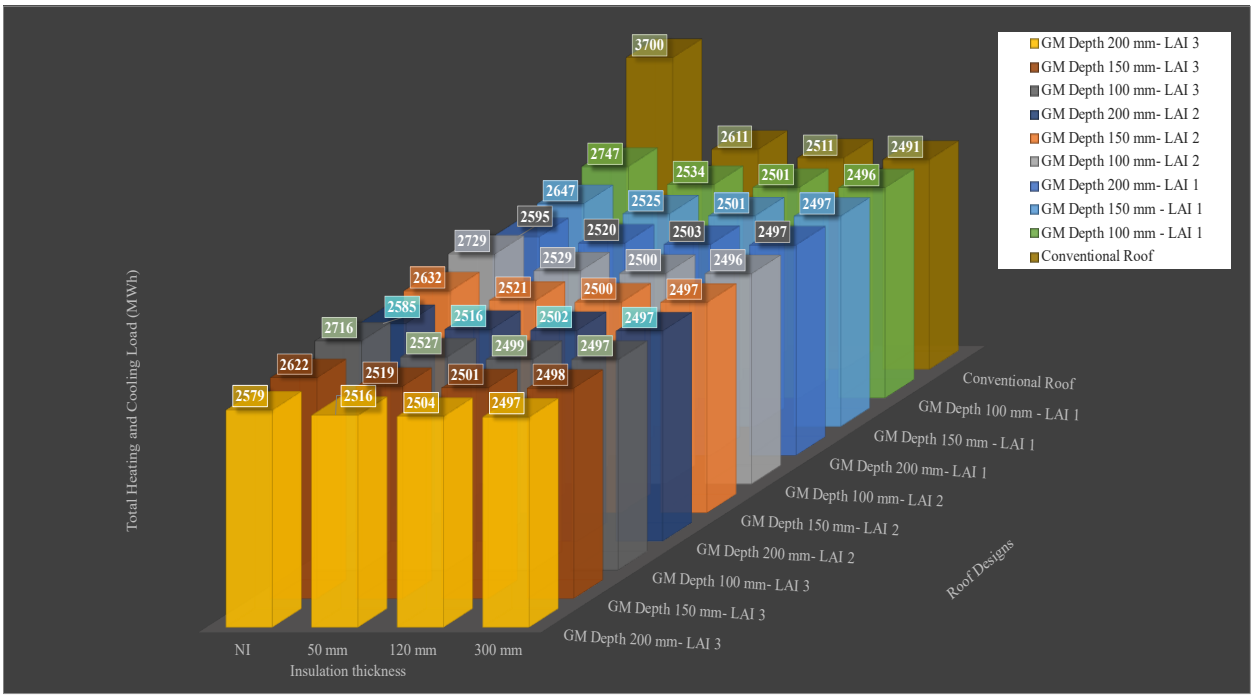

Figure F - 3: Total heating and cooling loads for all roof designs; all insulation thickness; LAIs; and growing media depths under future climate – hospital building.

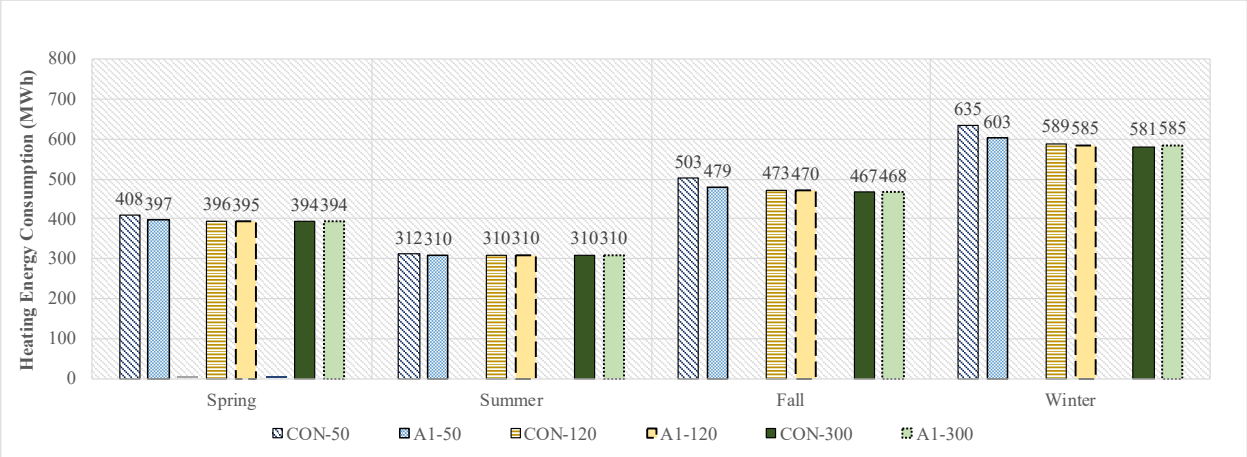

Figure F - 4: Seasonal heating loads for conventional roof and green roof with design of growing media of 100 mm and LAI of 1 for insulation thicknesses 50 mm, 120 mm and 300 mm – future climate (hospital building).

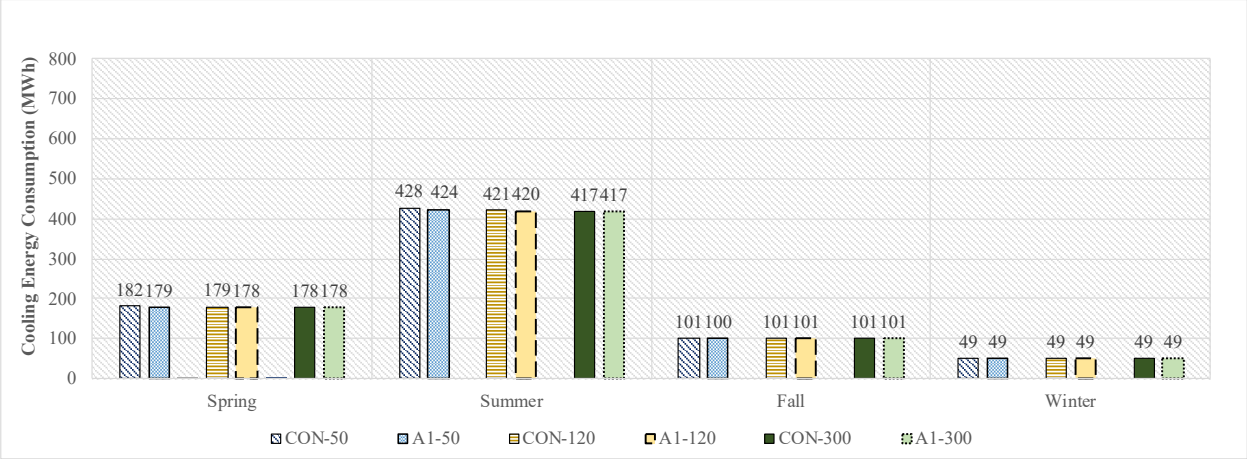

Figure F - 5: Seasonal cooling loads for conventional roof and green roof with design of growing media of 100 mm and LAI of 1 for insulation thicknesses 50 mm, 120 mm and 300 mm – future climate (hospital building).

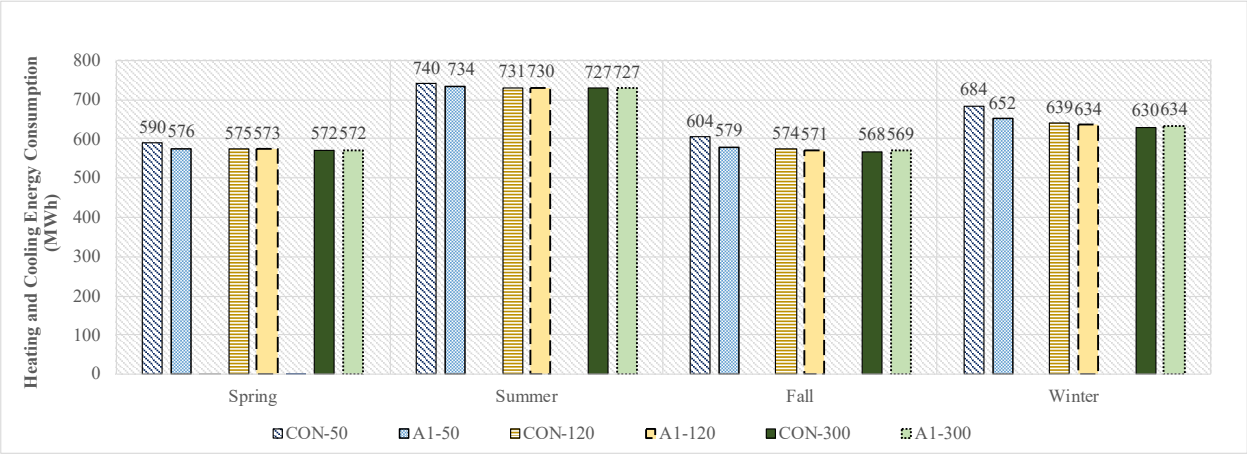

Figure F - 6: Seasonal total heating and cooling loads for conventional roof and green roof with design of growing media of 100 mm and LAI of 1 for insulation thicknesses 50 mm, 120 mm and 300 mm – future climate (hospital building).

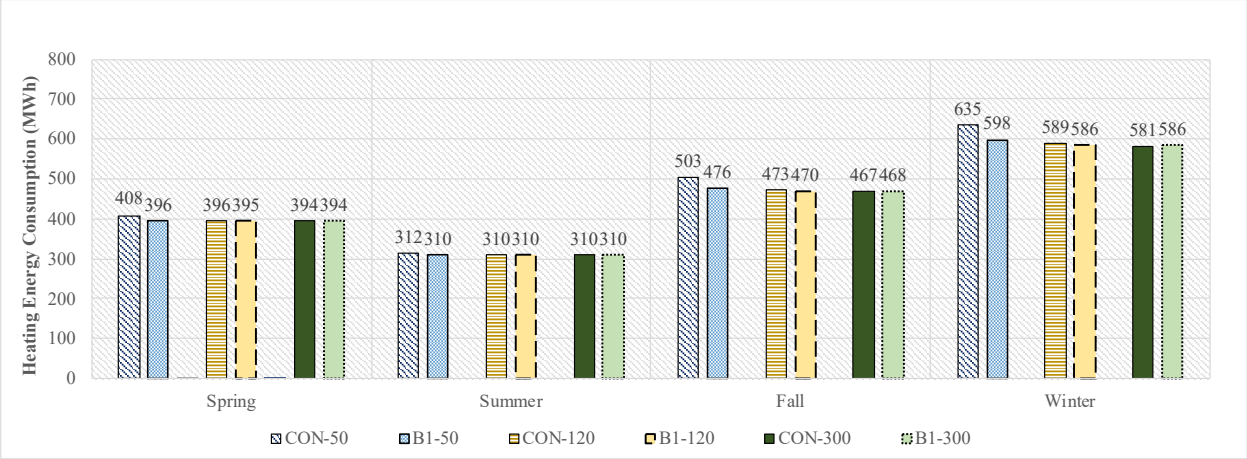

Figure F - 7: Seasonal heating loads for conventional roof and green roof with design of growing media of 150 mm and LAI of 1 for insulation thicknesses 50 mm, 120 mm and 300 mm – future climate (hospital building).

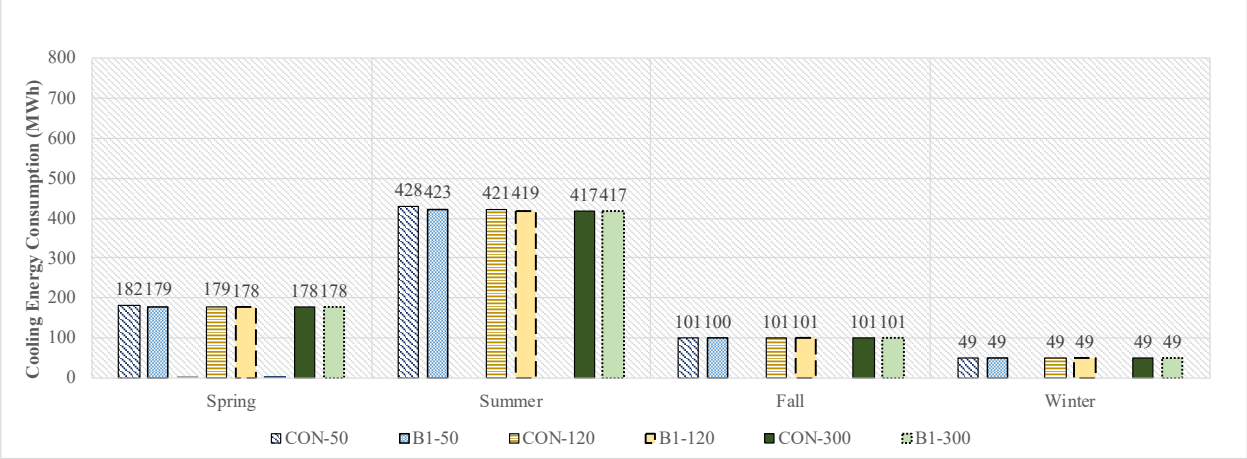

Figure F - 8:Seasonal cooling loads for conventional roof and green roof with design of growing media of 150 mm and LAI of 1 for insulation thicknesses 50 mm, 120 mm and 300 mm – future climate (hospital building).

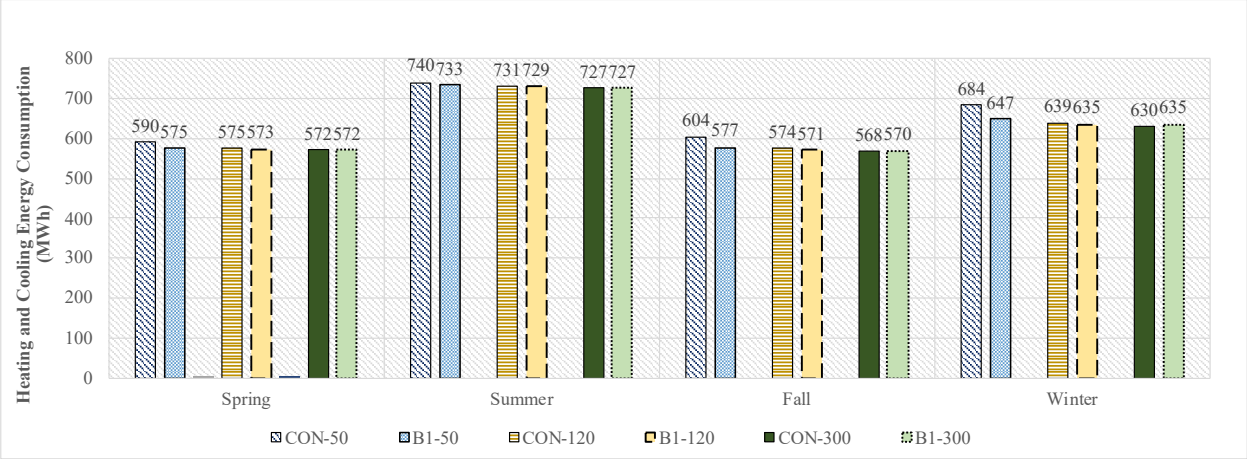

Figure F - 9: Seasonal total heating and cooling loads for conventional roof and green roof with design of growing media of 150 mm and LAI of 1 for insulation thicknesses 50 mm, 120 mm and 300 mm – future climate (hospital building).

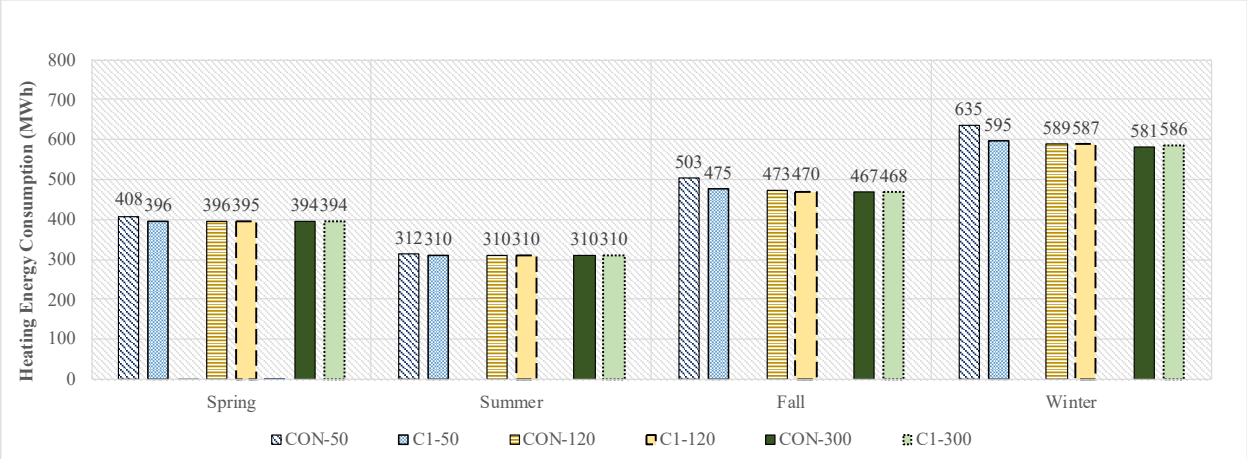

Figure F - 10: Seasonal heating loads for conventional roof and green roof with design of growing media of 200 mm and LAI of 1 for insulation thicknesses 50 mm, 120 mm and 300 mm – future climate (hospital building).

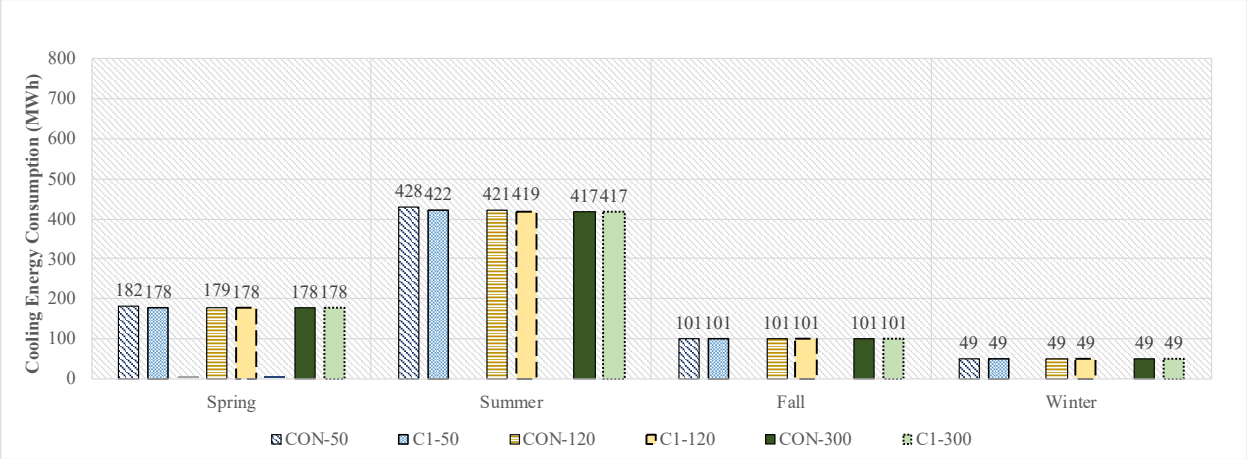

Figure F - 11: Seasonal cooling loads for conventional roof and green roof with design of growing media of 200 mm and LAI of 1 for insulation thicknesses 50 mm, 120 mm and 300 mm – future climate (hospital building).

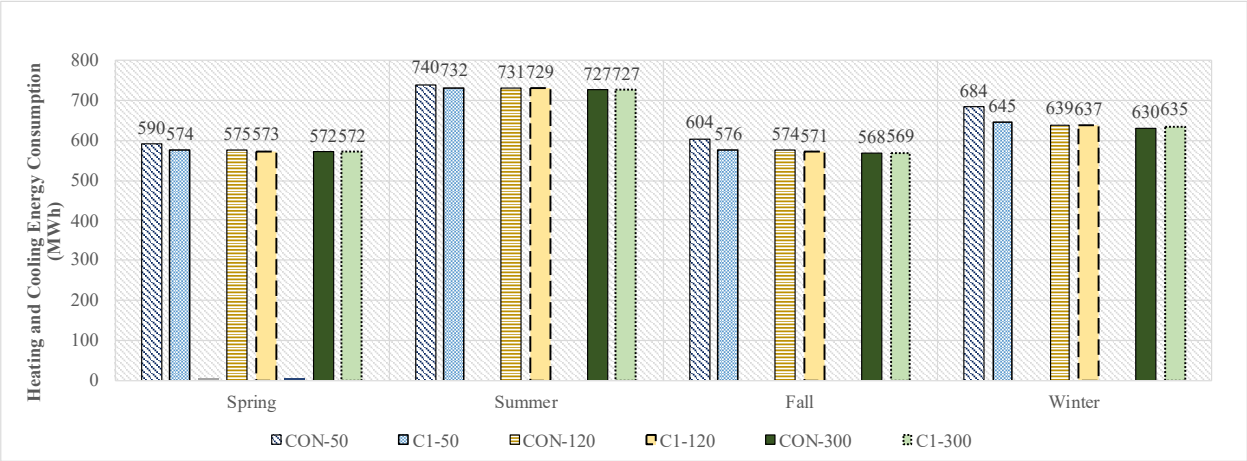

Figure F - 12: Seasonal total heating and cooling loads for conventional roof and green roof with design of growing media of 200 mm and LAI of 1 for insulation thicknesses 50 mm, 120 mm and 300 mm – future climate (hospital building).

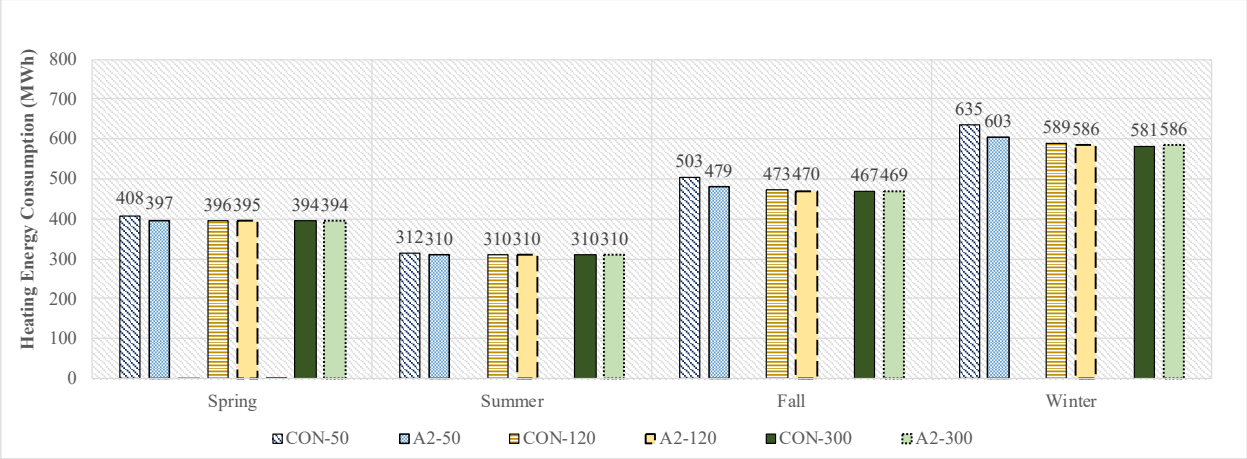

Figure F - 13: Seasonal heating loads for conventional roof and green roof with design of growing media of 100 mm and LAI of 2 for insulation thicknesses 50 mm, 120 mm and 300 mm – future climate (hospital building).

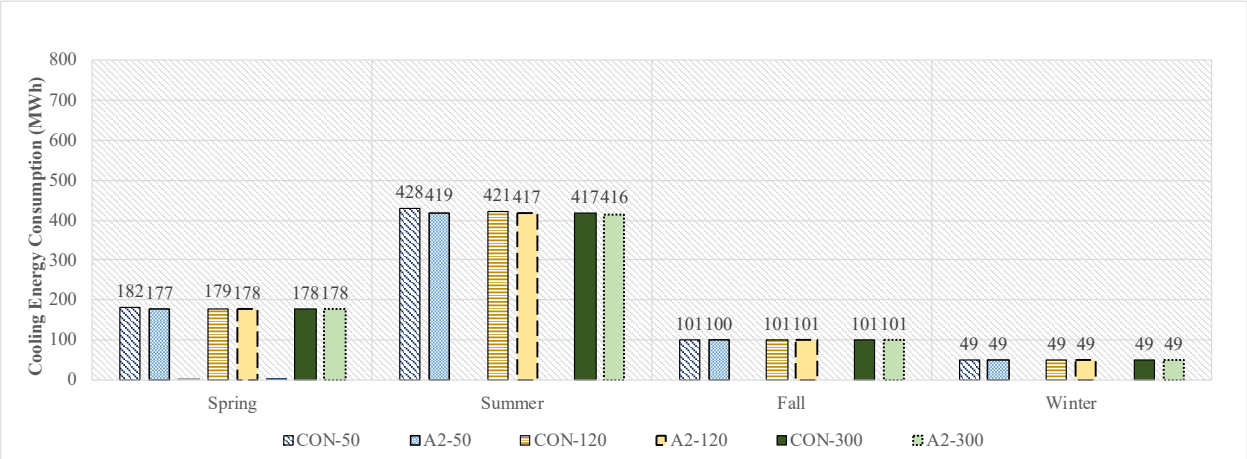

Figure F - 14: Seasonal cooling loads for conventional roof and green roof with design of growing media of 100 mm and LAI of 2 for insulation thicknesses 50 mm, 120 mm and 300 mm – future climate (hospital building).

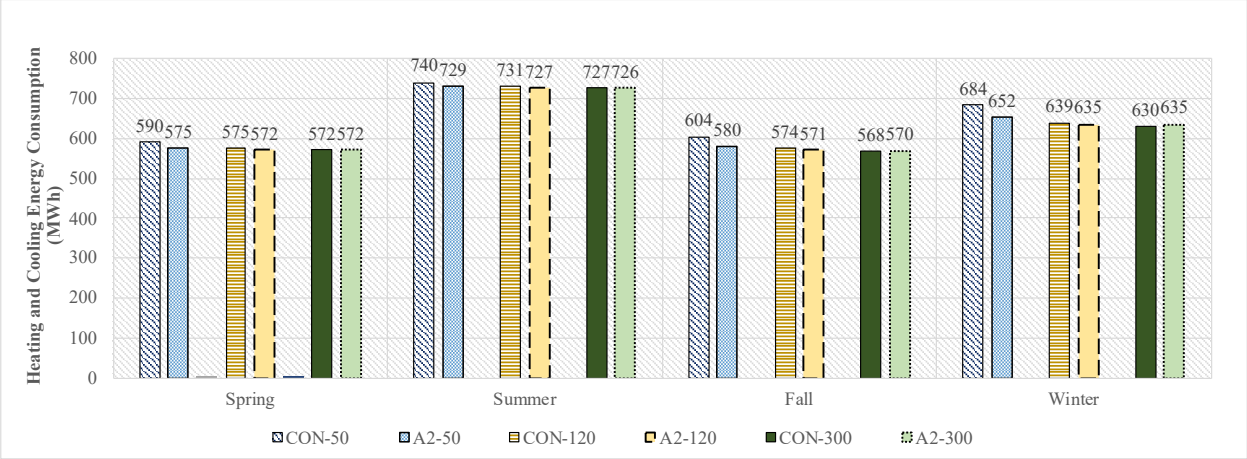

Figure F - 15: Seasonal total heating and cooling loads for conventional roof and green roof with design of growing media of 100 mm and LAI of 2 for insulation thicknesses 50 mm, 120 mm and 300 mm – future climate (hospital building).

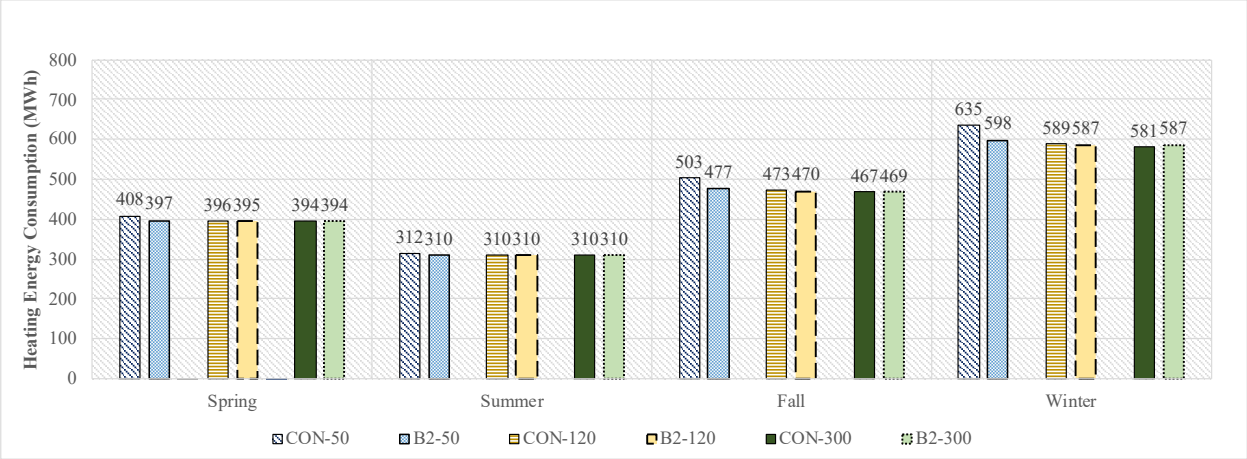

Figure F - 16: Seasonal heating loads for conventional roof and green roof with design of growing media of 150 mm and LAI of 2 for insulation thicknesses 50 mm, 120 mm and 300 mm – future climate (hospital building).

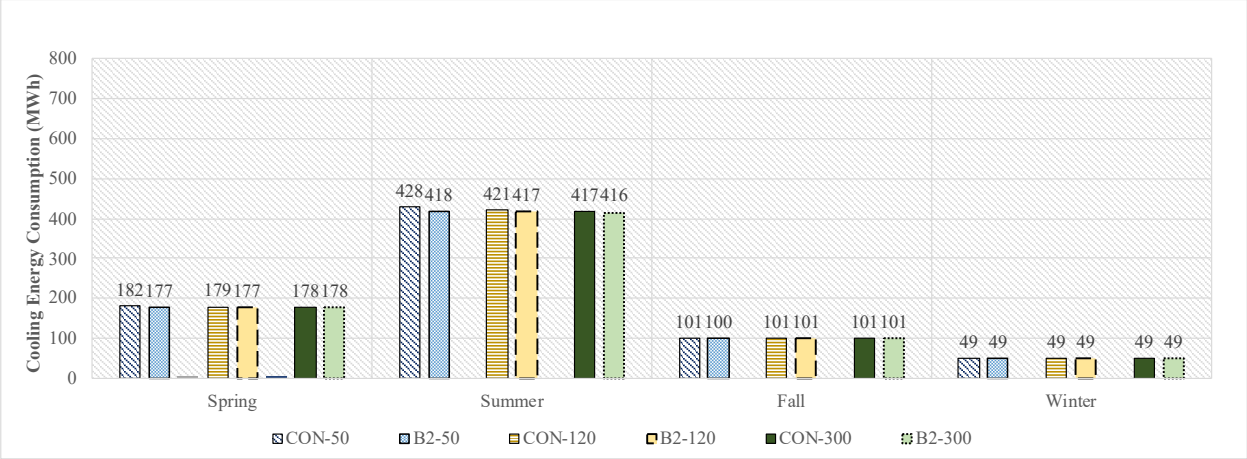

Figure F - 17: Seasonal cooling loads for conventional roof and green roof with design of growing media of 150 mm and LAI of 2 for insulation thicknesses 50 mm, 120 mm and 300 mm – future climate (hospital building).

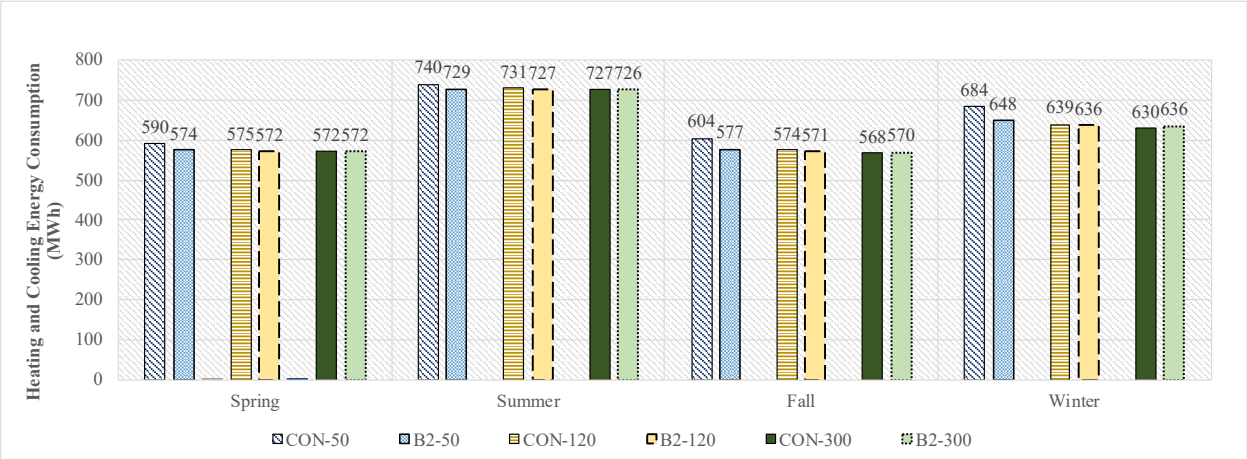

Figure F - 18: Seasonal total heating and cooling loads for conventional roof and green roof with design of growing media of 150 mm and LAI of 2 for insulation thicknesses 50 mm, 120 mm and 300 mm – future climate (hospital building).

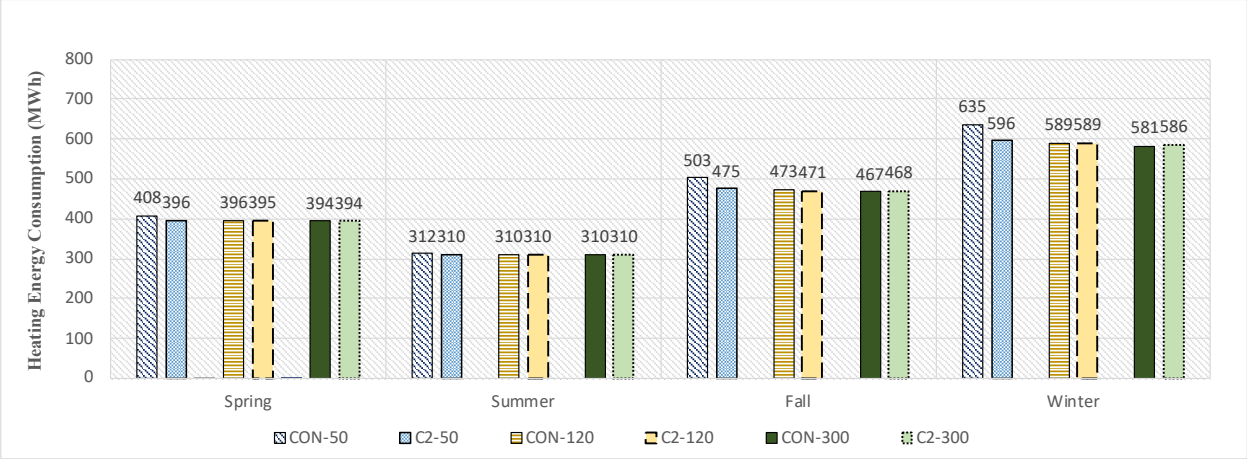

Figure F - 19: Seasonal heating loads for conventional roof and green roof with design of growing media of 200 mm and LAI of 2 for insulation thicknesses 50 mm, 120 mm and 300 mm – future climate (hospital building).

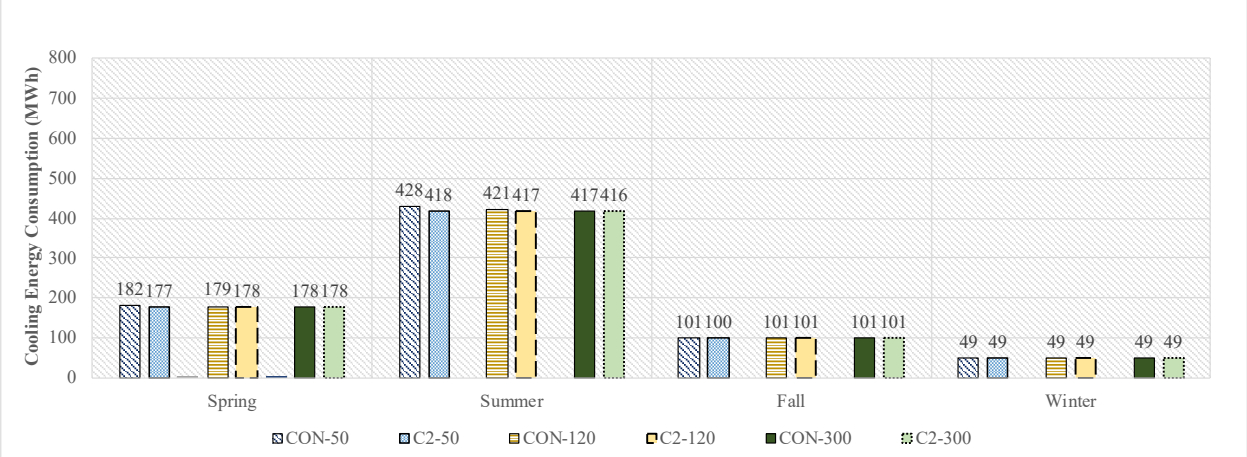

Figure F - 20: Seasonal cooling loads for conventional roof and green roof with design of growing media of 200 mm and LAI of 2 for insulation thicknesses 50 mm, 120 mm and 300 mm – future climate (hospital building).

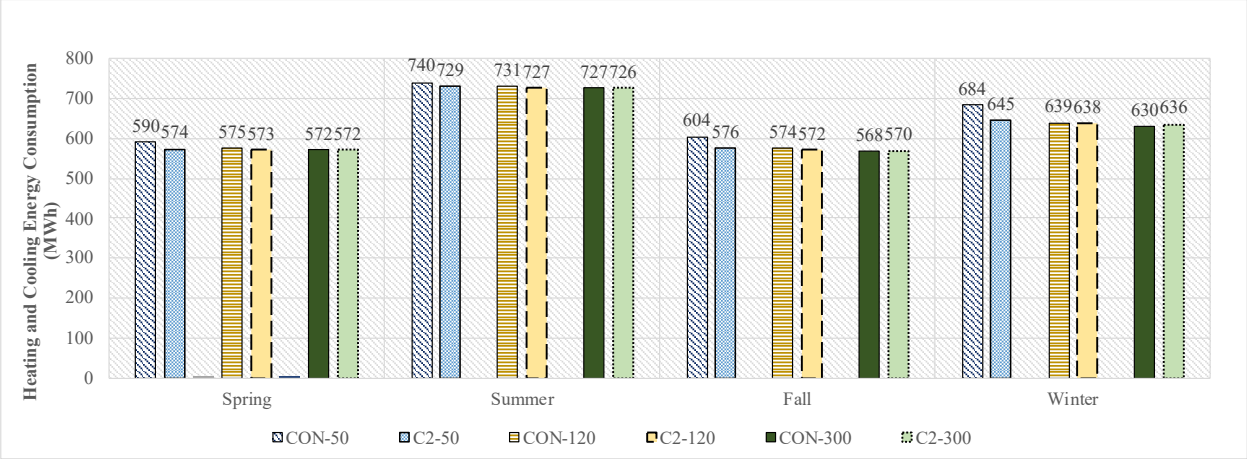

Figure F - 21: Seasonal total heating and cooling loads for conventional roof and green roof with design of growing media of 200 mm and LAI of 2 for insulation thicknesses 50 mm, 120 mm and 300 mm – future climate (hospital building).

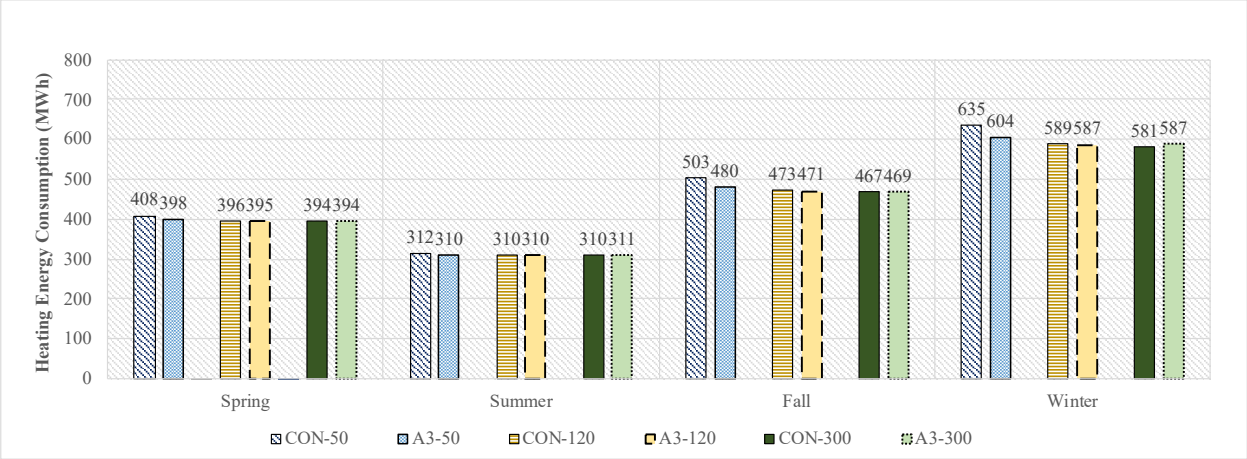

Figure F - 22: Seasonal heating loads for conventional roof and green roof with design of growing media of 100 mm and LAI of 3 for insulation thicknesses 50 mm, 120 mm and 300 mm – future climate (hospital building).

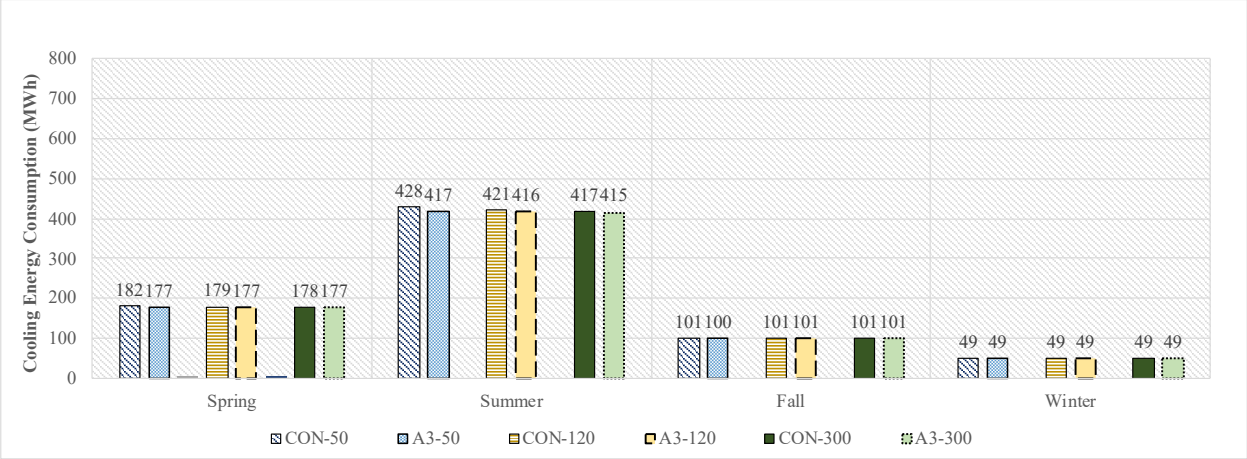

Figure F - 23: Seasonal cooling loads for conventional roof and green roof with design of growing media of 100 mm and LAI of 3 for insulation thicknesses 50 mm, 120 mm and 300 mm – future climate (hospital building).

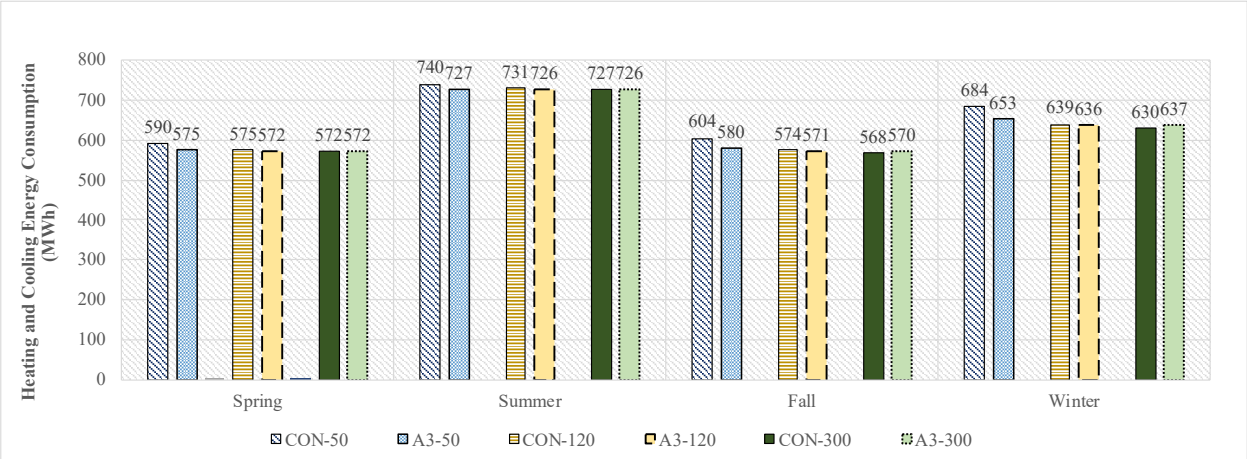

Figure F - 24: Seasonal total heating and cooling loads for conventional roof and green roof with design of growing media of 100 mm and LAI of 3 for insulation thicknesses 50 mm, 120 mm and 300 mm – future climate (hospital building).

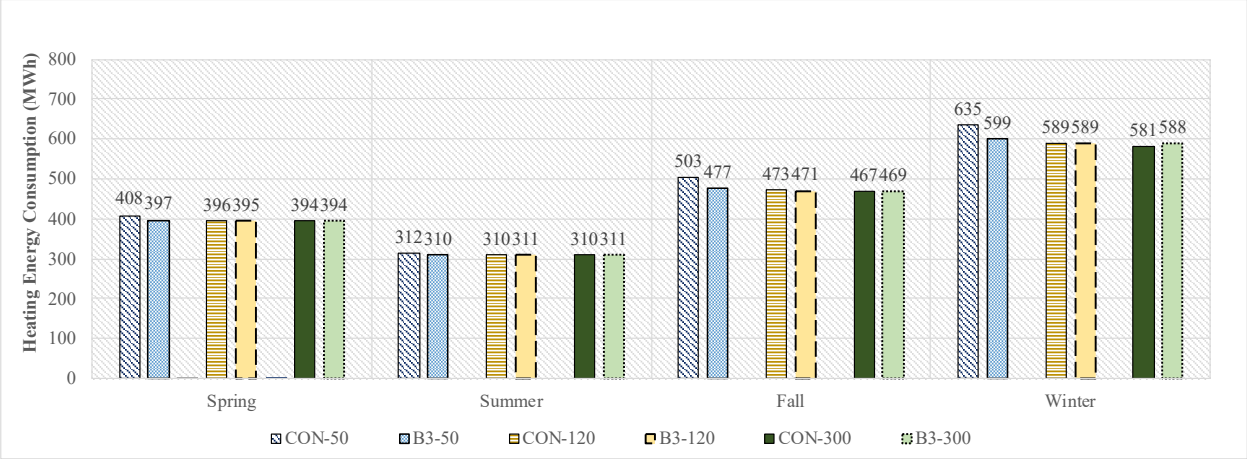

Figure F - 25: Seasonal heating loads for conventional roof and green roof with design of growing media of 150 mm and LAI of 3 for insulation thicknesses 50 mm, 120 mm and 300 mm – future climate (hospital building).

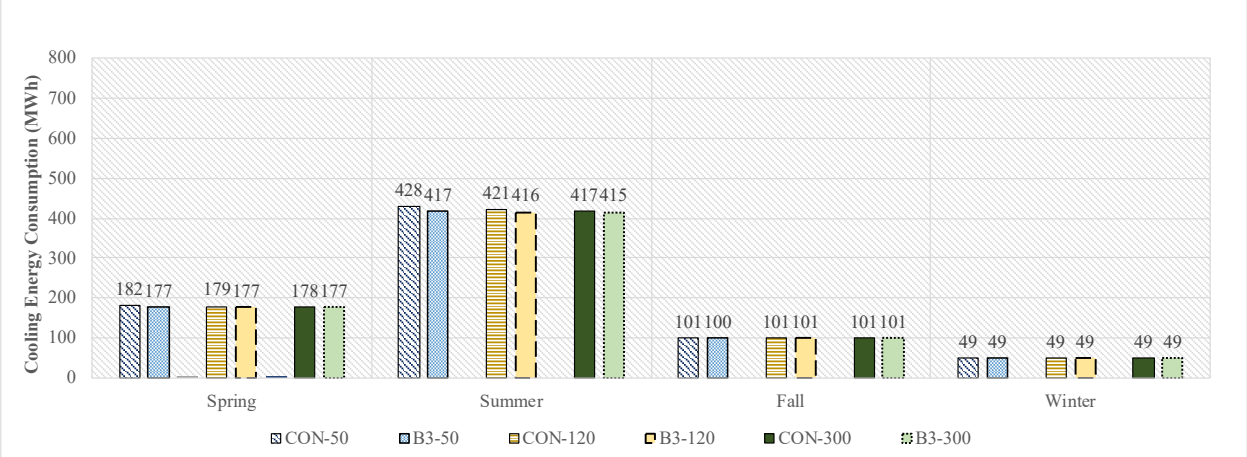

Figure F - 26: Seasonal cooling loads for conventional roof and green roof with design of growing media of 150 mm and LAI of 3 for insulation thicknesses 50 mm, 120 mm and 300 mm – future climate (hospital building).

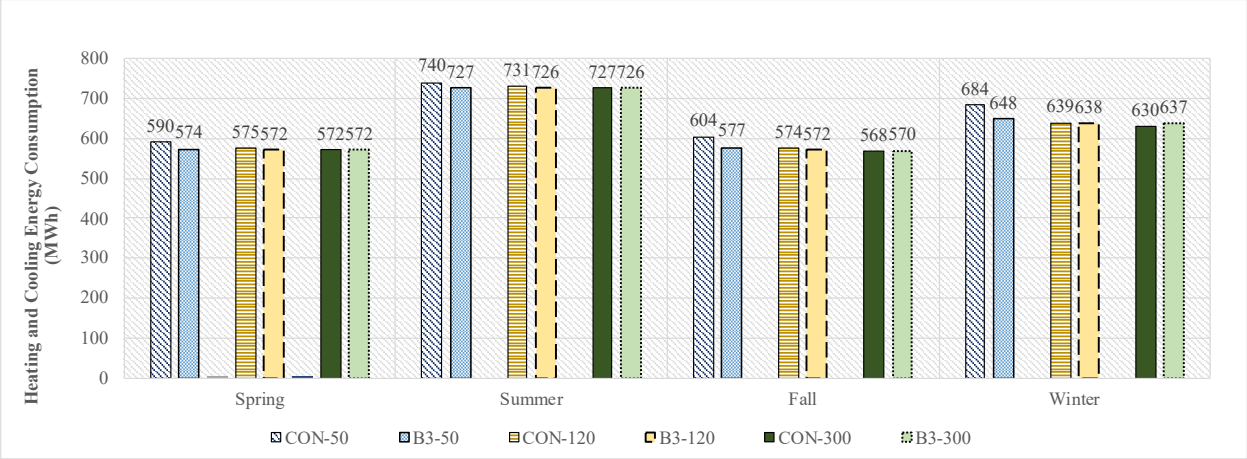

Figure F - 27: Seasonal total heating and cooling loads for conventional roof and green roof with design of growing media of 150 mm and LAI of 3 for insulation thicknesses 50 mm, 120 mm and 300 mm – future climate (hospital building).

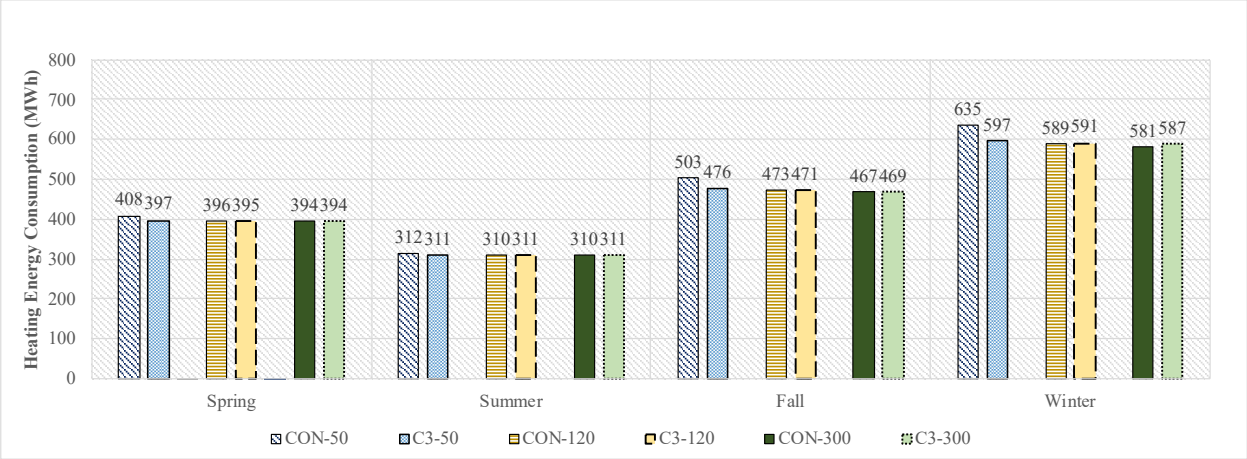

Figure F - 28: Seasonal heating loads for conventional roof and green roof with design of growing media of 200 mm and LAI of 3 for insulation thicknesses 50 mm, 120 mm and 300 mm – future climate (hospital building).

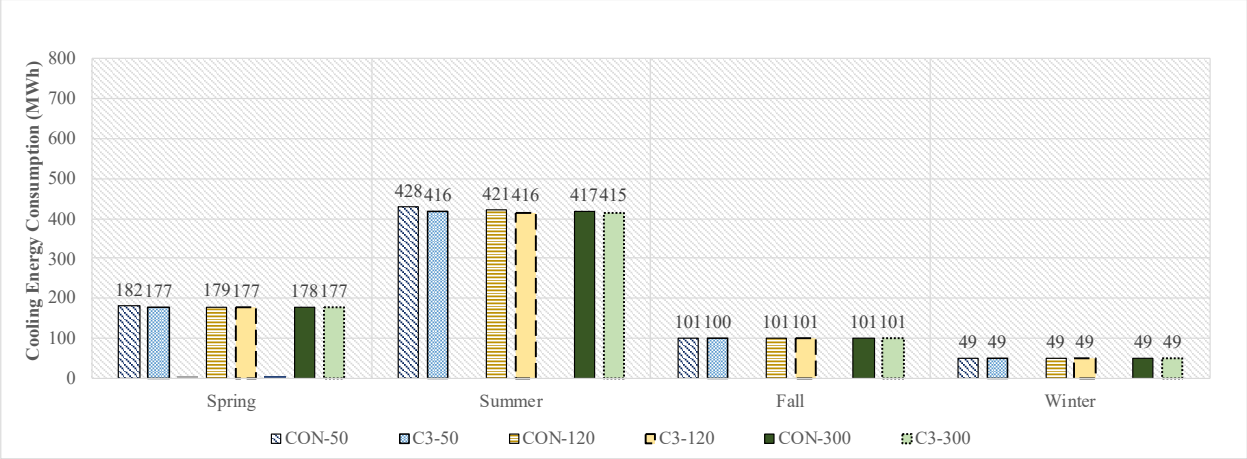

Figure F - 29: Seasonal cooling loads for conventional roof and green roof with design of growing media of 200 mm and LAI of 3 for insulation thicknesses 50 mm, 120 mm and 300 mm – future climate (hospital building).

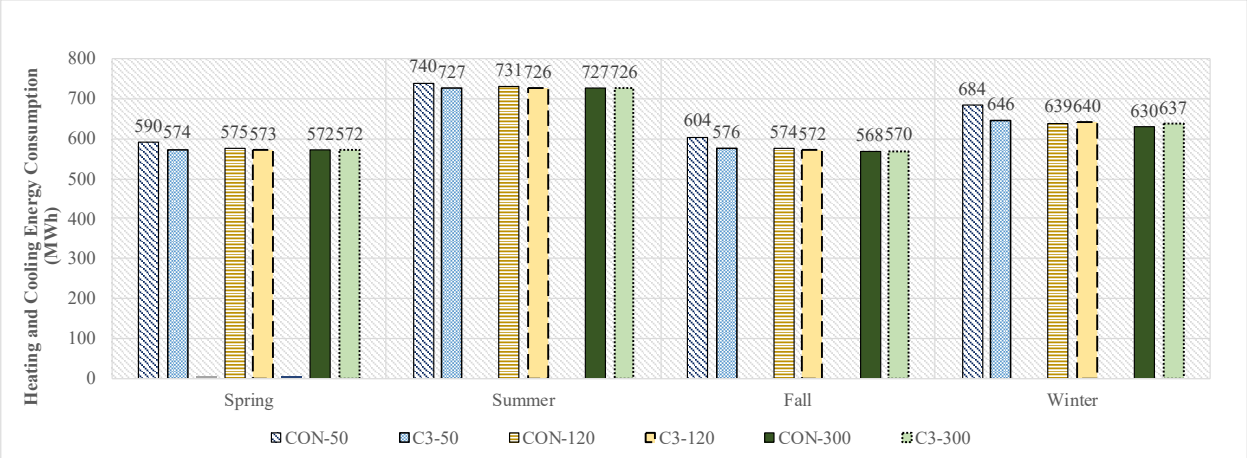

Figure F - 30: Seasonal total heating and cooling loads for conventional roof and green roof with design of growing media of 200 mm and LAI of 3 for insulation thicknesses 50 mm, 120 mm and 300 mm – future climate (hospital building).

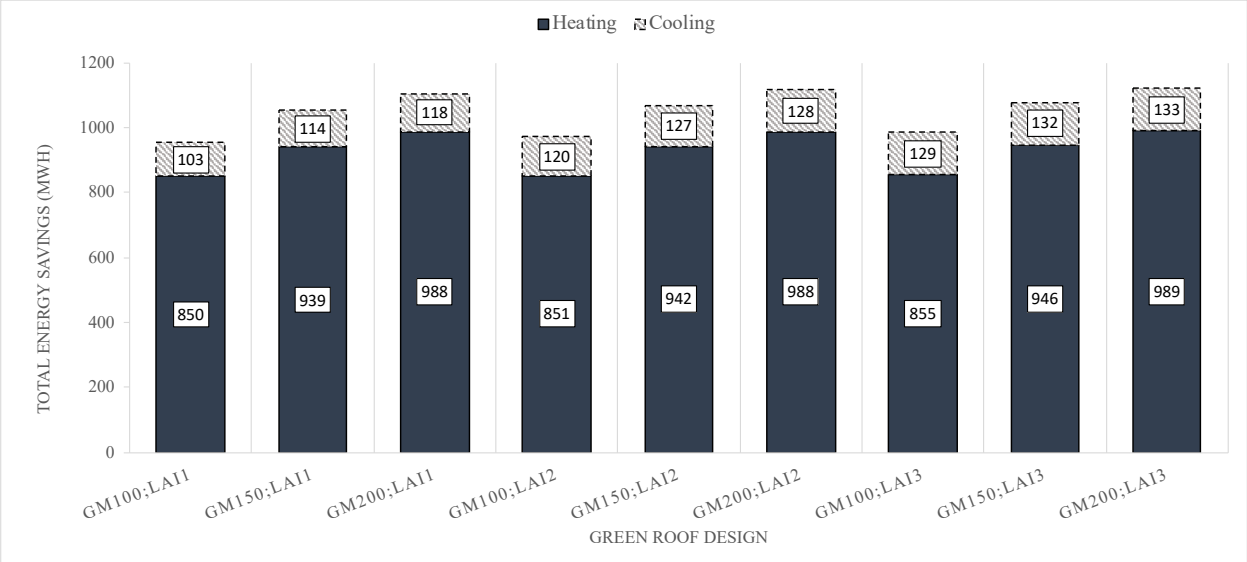

Figure F - 31: Total heating and cooling energy savings (MWh) of green roof compared to conventional roof for all growing media (GM) depths and LAIs; without insulation layer – future climate (hospital building).

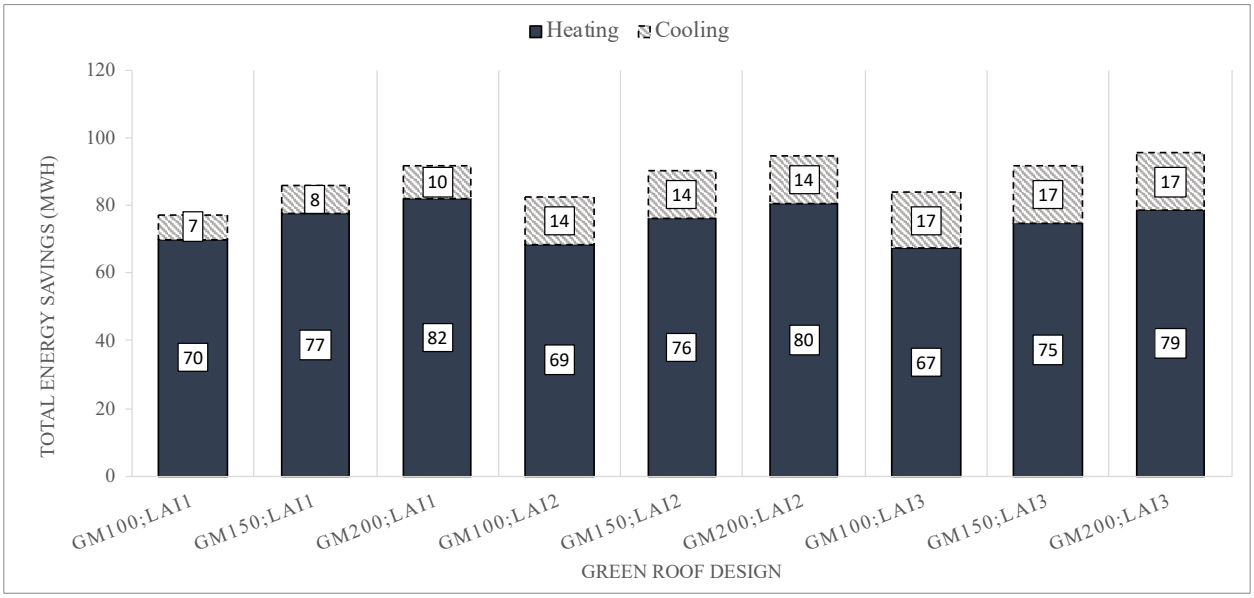

Figure F - 32: Total heating and cooling energy savings (MWh) of green roof compared to conventional roof for all growing media (GM) depths and LAIs; with 50 mm insulation layer – future climate (hospital building).

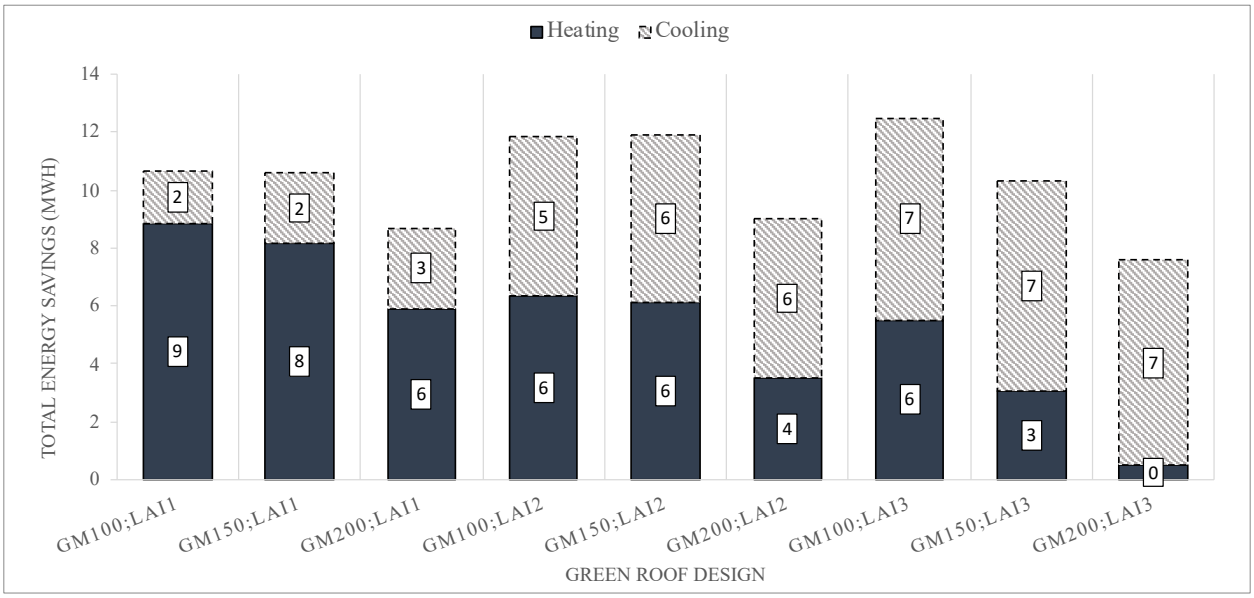

Figure F - 33: Total heating and cooling energy savings (MWh) of green roof compared to conventional roof for all growing media (GM) depths and LAIs; with 120 mm insulation layer – future climate (hospital building).

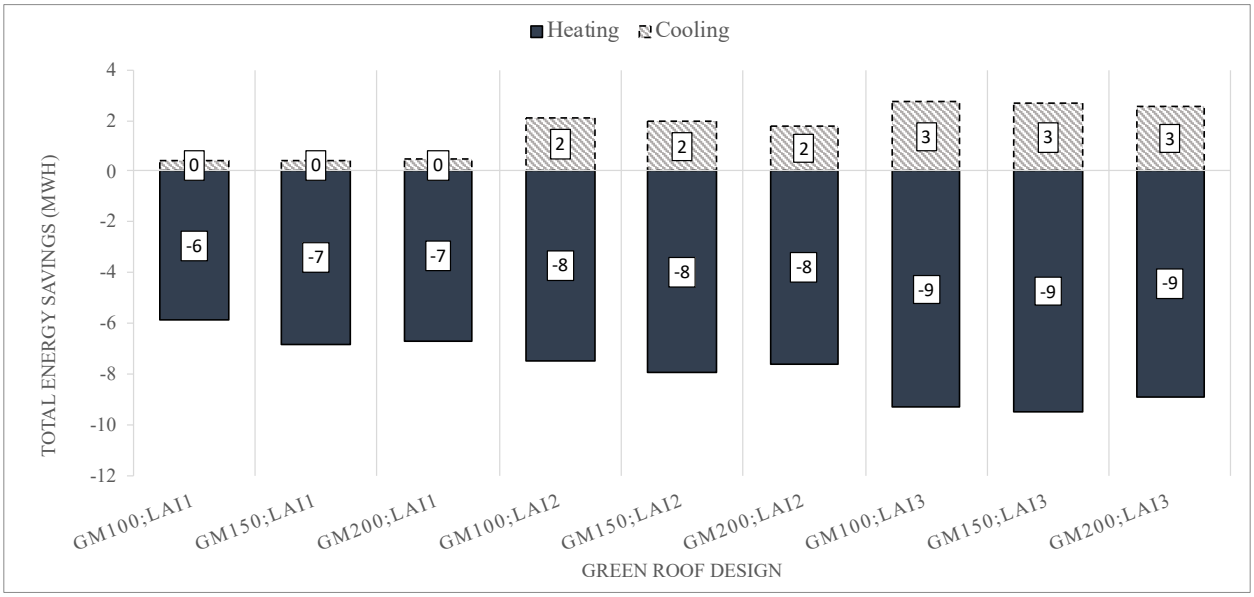

Figure F - 34: Total heating and cooling energy savings (MWh) of green roof compared to conventional roof for all growing media (GM) depths and LAIs; with 300 mm insulation layer – future climate (hospital building).